

Alternative Pathways for Olefin Treatment in Thermally Cracked Naphtha

by

Shirley Fong

A thesis submitted in partial fulfillment of the requirements for the degree of

Master of Science

in

Chemical Engineering

Department of Chemical and Materials Engineering

University of Alberta

© Shirley Fong, 2019

Abstract

During thermal cracking of bitumen, olefins are formed via free radical reactions and are mainly concentrated in the naphtha and distillate cut of the upgraded bitumen. Olefins are undesirable in the upgraded bitumen product because they are associated with equipment fouling. As a result, these compounds are commonly treated via hydrogenation in bitumen upgrader facilities. Hydrogenation is not a preferred technology for use in partial upgrading. Therefore, the purpose of this research is to study alternative pathways to treat the olefins in thermally cracked naphtha without the use of hydrogen.

Two alternatives were evaluated. The first alternative consists of using phosphoric acid to reactively absorb the olefins in the naphtha by forming alkyl phosphoric acid esters. The chemistry between olefins and phosphoric acid was studied by reacting model compounds namely olefins within the range of C₅-C₇ with phosphoric acid at 50 °C at different reaction times. The results indicated that the process for olefin removal using phosphoric acid is inefficient due to slow reaction rate at a temperature where the alkyl phosphoric acid esters would be stable. Furthermore, the alkyl phosphoric acid esters formed from C₆ and C₇ olefins were soluble in the naphtha. The low absorption rate and solubility of some alkyl phosphoric acids in the organic phase made it impractical to develop a temperature swing absorption process based on phosphoric acid.

The second alternative studied the use of asphaltenes to treat the olefins in the thermally cracked naphtha via hydrogen transfer. The study was divided into three sections: (i) a preliminary study using model compounds as hydrogen donor and acceptor. It was found that hydrogen transfer could be employed for saturation of olefins. (ii) The second section used asphaltenes as hydrogen donor

and model olefinic compound as hydrogen acceptor, the feed was reacted at different reaction conditions. It was found that asphaltenes were capable of transferring hydrogens to saturate the olefin. (iii) The third section used asphaltenes as hydrogen donor and thermally cracked naphtha as hydrogen acceptor. Asphaltenes were capable of hydrogenating the olefins in the cracked naphtha. The study indicated that hydrogen transfer could be considered as strategy for olefin treating. The results of the applied study using asphaltenes to treat thermally cracked naphtha were encouraging.

Keywords: olefin saturation, cracked naphtha, phosphoric acid, alkyl phosphoric acid esters, hydrogen transfer, asphaltenes.

Preface
(Mandatory due to collaborative work)

Chapter 3 of this thesis will be submitted for publication to the journal Energy & Fuels as “Fong, S.Y; Montoya Sánchez, N; De Klerk, A. “Reaction of pentenes, hexenes, and heptenes with phosphoric acid”. I was responsible for reactor construction, performance of experiments, data interpretation, and manuscript composition. Natalia Montoya Sánchez acted as co-supervisory author and was involved in data interpretation and manuscript composition. Arno de Klerk acted as co-supervisory author and was involved in the concept formation, data interpretation and manuscript composition. Mark Miskolzie from the University of Alberta performed the NMR analyses. Béla Reiz from the University of Alberta performed the HPLC-MS analyses.

Chapter 4 of this thesis received collaborative work from Natalia Montoya Sánchez who acted as co-supervisory author and was involved in data interpretation and thesis review. Arno de Klerk acted as co-supervisory author and was involved in concept formation, data interpretation and thesis review. Yuwei Yan, Graduate Student at the University Alberta, performed the SimDist Analyses.

Dedication

To my parents,

Thank you for everything you gave up so I could have a better chance in life.

Acknowledgments

I am truly grateful to Dr. Arno de Klerk. Thank you for giving me the chance to be part of your research group and to be such an inspiring supervisor. I am so grateful for all the support that you have given me, not just in research, but also about pursuing learning opportunities in other fields that are equally important in life. Thank you for reminding me “*you are a human being first, an engineer later*”.

To my co-supervisor and friend, Dr. Natalia Montoya Sánchez, thank you for all the constructive feedback and patience that you have given me. I am so glad to have shared this journey with my MSc. with your supervision. Thank you for opening your doors and letting me be a part of your little family in Edmonton.

I want to thank Riya for being such an amazing and supportive friend throughout this journey. Thank you for your patience and for always being there for me. Thank you, Joy, Cloribel, Isabel, Giselle, and Shruthi for your advice and help during the thesis. Your help and friendship are invaluable and truly appreciated. I want to express my gratitude to the incredible research group that I had the opportunity to share and learn. Not only are you people incredibly intelligent but also with the most fascinating backgrounds and personalities.

I am so thankful to my childhood friend Pedro and my sister Sara for always being there for me, even when we are so far apart. I love you, guys.

Thank you Vlada Blinova from the Department of Human Ecology for giving me the opportunity to learn about garment design and construction. I would have never imagined having this opportunity during my MSc. Furthermore, I would also like to thank Mark Miskolzie from Chemistry NMR Laboratory. Thank you for all the patience and for teaching me so much about NMR.

Finally, I want to express my gratitude to CNOOC International Limited for providing financial support for this project to happen.

TABLE OF CONTENTS

CHAPTER 1 – INTRODUCTION	1
1.1 Background	1
1.2 Objective	3
1.3 Scope of work	3
References (Chapter 1)	4
CHAPTER 2 – LITERATURE REVIEW	6
2.1 Background	6
2.1.1 Bitumen partial upgrading	6
2.1.2 CNOOC International BituMax™ partial upgrading technology	7
2.1.3 Olefins in Thermally Cracked Bitumen	8
2.1.3.1 Olefin Formation	8
2.1.3.2 Naphtha composition	9
2.1.3.3 Hydrogen production and olefin hydrotreating	15
2.2 Olefin treatment using phosphoric acid	16
2.2.1 Phosphoric acid	16
2.2.2 Reaction of phosphoric acid and olefins	17
2.2.2.1 Formation of phosphoric acid ester:	17
2.2.2.2 Reactivity of the olefins with phosphoric acid	18
2.2.2.3 Decomposition of alkyl phosphoric acid ester	18
2.2.2.4 Reaction between two molecules of phosphoric acid ester	19
2.2.2.5 Detection of alkyl phosphoric acid esters	19
2.2.3 Temperature-swing absorption process	21

2.3 Olefin treatment using asphaltenes	22
2.3.1 Asphaltenes.....	22
2.3.2 Solvent deasphalting.....	23
2.3.3 Chemistry between asphaltenes and olefins	24
2.3.3.1 Asphaltenes as hydrogen donors.....	24
2.3.3.2 Olefins as hydrogen acceptors	26
2.3.4 Relevant free radical reactions	28
2.3.4.1 Hydrogen abstraction reaction	28
2.3.4.2 Combination or coupling reaction	29
2.3.4.3 Hydrogen disproportionation	29
References (Chapter 2)	31
CHAPTER 3 – REACTION WITH PHOSPHORIC ACID: AN ALTERNATIVE APPROACH FOR TREATING THERMALLY CRACKED NAPHTHA	35
Abstract.....	35
3.1 Introduction.....	36
3.2 Experimental.....	38
3.2.1 Materials	38
3.2.2 Equipment and procedure.....	40
3.2.2.1 Olefin reactive absorption.....	40
3.2.2.2 Quantification of olefin removal rate.....	41
3.2.3 Analyses.....	42
3.2.3.1 Nuclear magnetic resonance (NMR) spectroscopy.....	42
3.2.3.2 Reverse Phase High-Performance Liquid Chromatography-Ultraviolet-Mass Spectrometry (RP-HPLC-UV-MS)	43

3.2.3.3	Gas Chromatography with Flame Ionization Detector (GC-FID) and Gas Chromatography with Mass Spectrometry (GC-MS).....	44
3.2.4	Calculations.....	45
3.3	Results.....	46
3.3.1	Detection of alkyl phosphoric acid esters with NMR Spectroscopy	46
3.3.2	Phase partitioning of alkyl phosphoric acid esters using NMR.....	51
3.3.3	Detection of alkyl phosphoric acid esters with HPLC-UV-MS	53
3.3.4	Identification of alkyl phosphoric acid esters with HPLC-UV-MS	54
3.5	Phase partitioning for alkyl phosphoric acid esters.....	59
3.6	Conversion of 1-hexene by phosphoric acid	60
3.4	Discussion	62
3.4.1	Chemistry of C ₅ -C ₇ olefins with phosphoric acid.....	62
3.4.1.1	Effect of α -carbon on stability of alkyl phosphoric acid ester.....	62
3.4.1.2	Effect of olefin hydrocarbon chain length on product distribution	63
3.4.1.3	Effect of olefin structure on product distribution	64
3.4.2	Phase partitioning.....	65
3.4.3	Process for olefin removal by reactive absorption with H ₃ PO ₄	66
3.4.3.1	Effect of olefin removal efficiency and reaction rate	66
3.4.3.2	Effect of phase partitioning and emulsion formation	67
3.5	Conclusions.....	68
	References (Chapter 3)	69
CHAPTER 4 – HYDROGEN TRANSFER OF ASPHALTENES TO OLEFINS: AN ALTERNATIVE APPROACH FOR TREATING THERMALLY CRACKED NAPHTHA.....		71
4.1	Introduction.....	72
4.2	Experimental	73

4.2.1	Materials	73
4.2.2	Equipment and procedure	77
4.2.2.2	Collection of recovered products	83
4.2.2.3	Extraction and filtration of liquid products.....	84
4.2.3	Analyses.....	85
4.2.3.1	Gas Chromatography with Mass Spectrometry (GC-MS) and Gas Chromatography- Flame Ionization Detector (GC-FID).....	85
4.2.3.2	Simulated Distillation Gas Chromatography (SimDist GC).....	86
4.2.3.3	Differential Scanning Calorimetry (DSC)	87
4.2.3.4	Fluorescence Spectroscopy	87
4.2.4	Calculations	88
4.2.4.1	Definitions.....	88
4.2.4.2	Reactions with 1-hexene: Calculations for olefin reduction using asphaltenes.....	89
4.2.4.3	Reactions with 1-hexene: Calculations for conversion of 1-hexene.....	92
4.2.4.4	Reactions with 1-hexene: Calculations for product selectivity.....	93
4.2.4.5	Reactions with spiked naphtha: Calculations for olefin reduction using asphaltenes 93	
4.2.4.6	Reactions with spiked naphtha: Calculations for conversion of 1-hexene	95
4.2.4.7	Reactions with spiked naphtha: Calculations for product formation.....	95
4.3	Results and discussion of the preliminary study: 1,2-Dihydronaphthalene as hydrogen donor 95	
4.3.1	Effect of time	95
4.3.2	Effect of temperature	99
4.3.3	Conversion and selectivity of reactions of 1-hexene and 1,2-dihydronaphthalene ..	102
4.4	Results of the study: Asphaltenes as hydrogen donor	104

4.4.1	Reactions of asphaltenes and 1-hexene.....	104
4.4.2	Reaction of asphaltenes and thermally cracked naphtha	113
4.5	Discussion	117
4.5.1	Effect of temperature on reactions of 1-hexene with asphaltenes	117
4.5.2	Effect of time on reactions of 1-hexene with asphaltenes	119
4.5.2.1	Effect of time at 250 °C	119
4.5.2.2	Effect of time at 350 °C	121
4.5.3	Effect of ratio of asphaltenes to 1-hexene	123
4.5.4	Effect of reactor walls and asphaltene contribution to reaction with 1-hexene.....	124
4.5.5	Chemistry for olefin reduction using asphaltenes	125
4.5.6	Thermally cracked naphtha treated with asphaltenes	130
4.5.6.1	1-Hexene representation in thermally cracked naphtha	130
4.5.6.2	Reactions of asphaltenes and thermally cracked naphtha	131
4.5.7	Industrial applications and cost evaluation	133
4.5.7.1	CNOOC BituMax: Olefins-aromatic alkylation	133
4.5.7.2	Olefins treating with asphaltenes at 250 °C	135
4.5.7.3	Olefins treating with asphaltenes at 350 °C	137
4.5.7.4	Comparison of the different processes.....	138
4.6	Conclusions.....	139
	References (Chapter 4)	141
	CHAPTER 5 – CONCLUSIONS	144
5.1	Introduction.....	144
5.2	Significance and major conclusions.....	144
5.2.1	Use of phosphoric acid	144
5.2.2	Use of asphaltenes	145

5.3	Suggested future work	146
5.3.1	Use of phosphoric acid	146
5.3.2	Use of asphaltenes	147
5.4	Presentations and publications.....	148
	References (Chapter 5)	149
	REFERENCES	150
	APPENDIX A.....	156
	APPENDIX B.....	159
	APPENDIX C	161
C.1	Chromatograms of recovered and filtered samples.....	161
C.2	Extraction efficiency of methanol	163
C.3	Calibration curve for quantification	166
	References (Appendix C).....	167
	APPENDIX D.....	169
	APPENDIX E	171
E.1	Boiling points of the linear paraffins in the standard	171
E.2	Determining the weight percentage of carbon number	172
	APPENDIX F.....	175
	APPENDIX G.....	177
G.1	Current and proposed processes for olefin reduction.....	177
G.1.1	CNOOC BituMax: Olefins-aromatic alkylation	177
G.1.2	Olefins treating with asphaltenes at 250 °C	178
G.1.3	Olefins treating with asphaltenes at 350 °C	178
G.2	Calculations for equipment sizing and cost estimation.....	179
G.2.1	Furnace.....	179

G.2.2 Heat exchanger.....	185
G.2.3 Reactor and flash separator (pressurized vessels).....	188

LIST OF TABLES

Table 2.2 Carbon number distribution for different types of naphtha from Mid-continent petroleum	10
Table 2.3 Distribution of hydrocarbon classes by carbon number of thermal coker naphtha from Mid-continent petroleum	11
Table 2.4 Identified olefins in visbroken naphtha from CNOOC International Long Lake upgrader facility by Páez Cárdenas.....	12
Table 2.5 Olefins in visbroken naphtha from CNOOC International Long Lake upgrader facility by Santiago and Subramanya.....	14
Table 2.6 Distribution of phosphoric acid species according to the hydration state of the phosphoric acid with water.....	16
Table 2.7 Decomposition temperature of alkyl phosphoric acid esters.....	19
Table 3.2 Materials employed for this experimental study.....	39
Table 3.3 Detection of alkyl phosphoric acid esters formation using NMR for C ₅ -C ₇ reactions with 85% phosphoric acid at 50 °C for 68 h	52
Table 3.4 Detection of alkyl phosphoric acid esters formation using HPLC-UV-MS for C ₅ -C ₇ reactions with 85% phosphoric acid at 50 °C for 68 h.....	54
Table 3.5 Organo-phosphorous products present in the organic phase recovered from reaction of C ₅ -C ₇ branched olefins with 85% phosphoric acid at 50 °C for 68 h	55
Table 3.6 Organo-phosphorous products present in the organic phase recovered from reaction of C ₅ olefins with 85% phosphoric acid at 50 °C for 68 h	58
Table 3.7 Conversion and selectivity for the reaction of 1-hexene with phosphoric acid at 50 °C and different reaction times	60

Table 3.8 Alkyl phosphoric acid esters identified by HPLC-MS analysis of the organic phase after reaction of 1-hexene with phosphoric acid at 50 °C for different reaction times	61
Table 4.1 Feed characterization of industrial asphaltenes from Long Lake upgrader of CNOOC (former Nexen Energy ULC)	74
Table 4.2 Chemicals employed in this experimental study	75
Table 4.3 Feed characterization of thermally cracked naphtha from Long Lake upgrader of CNOOC (former Nexen Energy ULC)	76
Table 4.4 Experimental conditions for the preliminary study reactions with 1,2-dihydronaphthalene as hydrogen donor and 1-hexene as hydrogen acceptor.....	81
Table 4.5 Experimental conditions for the reactions of asphaltenes as hydrogen donor and 1-hexene as hydrogen acceptor	82
Table 4.6 Experimental conditions for the reactions of asphaltenes as hydrogen donor and thermally cracked naphtha as hydrogen acceptor	83
Table 4.7 Conversion and product selectivity of reactions of 1-hexene and 1,2-dihydronaphthalene at different experimental conditions	103
Table 4.8 Summary of results of olefin reduction and 1-hexene conversion of reactions of asphaltenes and 1-hexene at different reaction conditions detectable by GC-FID.....	107
Table 4.9 Summary of results of product selectivity of reactions of asphaltenes and 1-hexene at different reaction conditions identified by GC-MS and quantified by GC-FID.....	108
Table 4.10 Product distribution by carbon number for reactions of asphaltenes and 1-hexene at different reaction conditions analyzed by SimDist.....	109
Table 4.11 Olefin reduction and 1-hexene conversion of reaction of asphaltenes and naphtha at 350 °C, 3 h, 4:1 asphaltenes to 1-hexene, 7 MPa, detectable by GC-FID	114
Table 4.12 Effect of asphaltene treatment on thermally cracked naphtha on product formation	115
Table 4.13 Gum content in the treated and untreated naphtha	116

Table 4.14 Comparison between ratios of linear alpha olefins to their corresponding hydrocarbon chain length linear alkane	132
Table 4.15 Summary of cost and design evaluation for Olefins-Aromatic Alkylation Process .	134
Table 4.16 Summary of cost and design evaluation for treatment plant using asphaltenes at 250 °C	136
Table 4.17 Summary of cost and design evaluation for treatment plant using asphaltenes at 350 °C	138
Table B.1 Experimental conditions for the reactions of asphaltenes as hydrogen donor and 1-hexene as hydrogen acceptor	159
Table C.1 Comparison between the concentrations of filtrate and recovered product of reaction of asphaltenes and 1-hexene at 350 °C, 0.5 h, 7 MPa, 1:1 weight ratio.....	163
Table C.2 Control experiments to determine product recovery by using methanol extraction ..	164
Table C.3 Results for control experiments for product recovery with methanol without heating	166
Table D.1 Peak areas from GC-FID analyses of reactions using 1,2-dihydronaphthalene as hydrogen donor	169
Table E.1 Boiling points of the linear paraffins in the calibration standard used for SimDist analyses	171
Table E.2 Boiling points of the linear paraffins in the calibration standard used for SimDist analyses	173
Table G.1 Correction factors used for calculations of the furnace	184
Table G. 2 Correction factors used for calculations of the heat exchanger	188
Table G.3 Correction factors and parameters used for calculations of the pressurized vessels .	194
Table G.4 Summary of cost and design evaluation for Olefins-Aromatic Alkylation Process ..	195

Table G.5 Summary of cost and design evaluation for treatment plant using asphaltenes at 250 °C
..... 195

LIST OF FIGURES

Figure 2.2 CNOOC International BituMax™ flow diagram	7
Figure 2.3 Formation of phosphoric acid ester from reaction of olefin and phosphoric acid.....	17
Figure 2.4 Formation of barium salt of ethyl phosphoric acid	20
Figure 2.5 Generic process flow diagram of H ₂ S gas removal by alcohol amine absorption	22
Figure 2.6 Process diagram of a typical solvent deasphalting process	24
Figure 2.7 Reaction of tetralin as hydrogen donor	25
Figure 2.8 Hydrogen transfer between α -methylstyrene and cumene	26
Figure 2.9 Energy-reaction coordinate diagram for olefin reaction with free radical	26
Figure 2.10 Possible termination steps for olefin reaction with free radical	27
Figure 2.11 Reaction mechanism of the hydrogenation of α -methylstyrene with 9,10-dihydroanthracene.....	28
Figure 2.12 Hydrogen abstraction reaction.....	29
Figure 2.13 Combination reaction vs disproportionation reaction	30
Figure 3.2 Proposed process to reduce olefin content in an olefin-containing feed without the use of hydrogen (pumps not shown)	37
Figure 3.3 Experimental set up for the reactions (a) pressurized batch reactor system with stirring for C ₅ olefins (b) ball flask with reflux system with stirring for C ₆ and C ₇ olefins.....	40
Figure 3.4 ³¹ P NMR spectrum of the aqueous phase recovered after reaction of cyclopentene with phosphoric acid. Reaction conditions: 50°C, 6MPa, and 68 h.....	47

Figure 3.5 ^1H NMR spectrum of the aqueous phase recovered after reaction of cyclopentene with phosphoric acid. Reaction conditions: 50°C, 6MPa, and 68 h.....	48
Figure 3.6 ^1H one-dimensional zTOCSY spectrum of the aqueous phase recovered after reaction of cyclopentene with phosphoric acid. Reaction conditions: 50°C, 6MPa, and 68 h	49
Figure 3.7 ^1H $\{^{31}\text{P}\}$ decoupling spectrum of the aqueous phase recovered after reaction of cyclopentene with 85% phosphoric acid. Reaction conditions: 50°C, 6MPa, and 68 h	50
Figure 3.8 ^1H - ^{31}P gHSQC spectrum of the aqueous phase cyclopentene reaction with 85% phosphoric acid in D_2O	51
Figure 3.9 Conversion of 1-hexene from reaction of 1-hexene and 85% phosphoric acid for 2 h, 5 h, 24 h, and 68 h.....	60
Figure 3.10 Alkyl phosphoric acid esters formed by 2-methyl-1-butene and 2-methyl-2-butene	63
Figure 4.1 Experimental set up for reactions performed in micro-batch reactors	78
Figure 4.2 Sample preparation for experiments using naphtha	79
Figure 4.3 Inside the reactor	83
Figure 4.4 Light product distribution from reactions of 1,2-dihydronaphthalene and 1-hexene at 250 °C and different reaction times (chromatogram obtained from GC-MS)	96
Figure 4.5 Heavy product distribution from reactions of 1,2-dihydronaphthalene and 1-hexene at 250 °C and different reaction times (chromatogram obtained from GC-MS)	97
Figure 4.6 Decomposition products of 1,2-dihydronaphthalene in the GC-MS column.....	99
Figure 4.7 Light product distribution from reactions of 1,2-dihydronaphthalene and 1-hexene at 2 h and different reaction temperatures (chromatogram obtained from GC-MS)	100
Figure 4.8 Heavy product distribution from reactions of 1,2-dihydronaphthalene and 1-hexene at 2 h and different reaction temperatures (chromatogram obtained from GC-MS)	101

Figure 4.9 Contour maps by fluorescence spectroscopy of reaction products of 1-hexene and asphaltenes at different experimental conditions	111
Figure 4.10 Comparison of SimDist analyses between untreated naphtha and naphtha treated with asphaltenes	115
Figure 4.11 Effect of temperature on olefin reduction at 2 h and 1:1 ratio of asphaltenes to 1-hexene	117
Figure 4.12 Effect of temperature on product distribution at 2 h and 1:1 ratio of asphaltenes to 1-hexene	118
Figure 4.13 Effect of time on olefin reduction at 250 °C and 1:1 ratio of asphaltenes to 1-hexene	120
Figure 4.14 Effect of time on product distribution at 250 °C and 1:1 ratio of asphaltenes to 1-hexene	121
Figure 4.15 Effect of time on olefin reduction at 350 °C and 1:1 weight ratio of asphaltenes to 1-hexene	122
Figure 4.16 Effect of weight ratio of asphaltenes to 1-hexene on olefin reduction at 300 °C and 2 h.....	123
Figure 4.17 Contribution of asphaltenes to product selectivity (decoupling the effect of the reactor walls).....	124
Figure 4.18 Reaction of 1,2-dihydronaphthalene and 1-hexene for <i>n</i> -hexane formation	125
Figure 4.19 Proposed reactions of olefin with asphaltenes.....	127
Figure 4.20 Mass spectra of compounds suggested as C ₁₀ and C ₁₁ alkane by GC-MS	128
Figure 4.21 Proposed pathway for formation of C ₁₀ and C ₁₁ alkanes	129
Figure 4.22 Process diagram of CNOOC olefin-aromatics alkylation plant	134

Figure 4.23 Process diagram for olefin treatment with asphaltenes at 250 °C	135
Figure 4.24 Process diagram for olefin treatment with asphaltenes at 350 °C	137
Figure A.1 Product distribution from reactions of 1,2-dihydronaphthalene and <i>n</i> -hexane at 300 °C, 2 h and 1:1 ratio (chromatogram obtained from GC-MS)	156
Figure A. 2 Product distribution from reactions of 1,2-dihydronaphthalene at 300 °C and 2 h (chromatogram obtained from GC-MS)	157
Figure A.3 Product distribution from reactions of <i>n</i> -hexane at 300 °C and 2 h (chromatogram obtained from GC-MS)	157
Figure C.1 Light product distribution from reactions of 1-hexene and asphaltenes at 350 °C, 0.5 h, 7 MPa, 1:1 weight ratio (chromatogram obtained from GC-MS)	161
Figure C.2 Heavier product distribution from reactions of 1-hexene and asphaltenes at 350 °C, 0.5 h, 7 MPa, 1:1 weight ratio (chromatogram obtained from GC-MS)	162
Figure C.3 Calibration curve for 1-hexene obtained from GC-FID by using biphenyl as internal standard.	167
Figure C.4 Calibration curve for <i>n</i> -hexane obtained from GC-FID by using biphenyl as internal standard.	167
Figure C.5 Calibration curve for <i>n</i> -dodecane obtained from GC-FID by using biphenyl as internal standard.	168
Figure G.1 Process diagram of CNOOC olefin alkylation plant	177
Figure G.2 Process diagram for olefin treatment with asphaltenes at 250 °C	178
Figure G.3 Process diagram for olefin treatment with asphaltenes at 350 °C	179
Figure G.4 Furnace prices	184

Figure G. 5 Price of tube-type exchangers.....	187
Figure G.6 Determination of surface area and weight for two bottoms	191
Figure G.7 Determination of base price for shell and bottoms.....	192
Figure G.8 Determination of thickness correction factor f_e	192
Figure G.9 Determination of prices of accessories for reactors, columns, and drums.....	192

CHAPTER 1 – INTRODUCTION

1.1 Background

Currently, in order to transport the bitumen from the extraction site to the refineries, it is required to blend the bitumen with diluent in order to improve its fluidity in the pipelines.¹ However, the addition of diluent is typically around 30% volume of the bitumen, meaning that the effective space for bitumen transportation in the pipelines is decreased.¹ As a result, this has been a bottleneck for the Canadian oil industry, as the available space of pipelines is limited. Partial upgrading technologies produce a lower density and viscosity bitumen that is *good enough* to flow through the pipelines without the use or a decreased amount of diluent.²

One of the common technologies used in partial upgrading for density and viscosity improvement of the bitumen is thermal cracking. Thermal cracking converts larger and complex molecules in the bitumen to smaller and lighter compounds.³ As a result of the conversion of the heavier molecules, fluidity of the bitumen is improved. However, when the bitumen is thermally cracked, olefins are formed.³ Depending on the source of the bitumen, cracking technology, and other relevant factors, the olefin content, and composition may vary.⁴ It has been found that the highest amount of olefins in the cracked product is in the naphtha and distillate fractions, i.e. material with normal boiling points < 360 °C.⁴

Olefins are reportedly associated with the formation of gums that can later cause fouling in the equipment downstream.⁵ As a result, in order to protect the integrity of the pipelines, a pipeline specification for the maximum amount of olefin content transportable in pipelines was created. According to the current Canadian pipeline specifications, the amount of olefins may not be more than 1 wt.% equivalent to 1-decene.⁶ Consequently, oil companies have been commonly turning towards hydrotreatment to saturate the olefins in the thermally cracked products.⁷

Hydrotreatment is energy and cost-intensive technology, which requires the production of hydrogen on-site.⁸ This implies that in order to hydrogenate the olefins, additional infrastructure to produce hydrogen is required in the facility, increasing the overall size of the facility. Because

the intent is for partial upgraders to be located in the fields near the extraction site, i.e. field upgraders, space and access to utilities and support infrastructure may be limited. This has resulted in a difficult step for partial upgraders to overcome, as the use of hydrogen will not only require large facility space, utilities, and support infrastructure but will also increase the overall capital and operational cost.

The present research work evaluates two alternative approaches to treat olefins present in the naphtha cut from thermally cracked bitumen without requiring the use of hydrogen.

The first alternative uses phosphoric acid to treat such olefins. From previous studies,^{9,10} it has been found that phosphoric acid can be used to determine whether oil contained thermally converted material, as phosphoric acid would react with these olefinic materials at 100-140 °C to form alkyl phosphoric acid esters. Therefore, it was postulated that phosphoric acid might be useful to remove the olefins from the naphtha. The phosphoric acid reaction with olefins was evaluated as an *absorption* and *desorption* process. In the proposed process, the acid could act as a reactive olefin absorbent to form alkyl phosphoric acid esters. After separating the alkyl phosphoric acid esters from the treated cracked naphtha, the absorbent can be regenerated. When these compounds are heated, they decompose to yield phosphoric acid and olefins,¹⁰ hence enabling the *desorption* of the olefins and regenerating the acid for further absorption.

The second alternative is based on a previous study performed by Naghizada, et al.¹¹ It was found that asphaltenes could act as hydrogen donors at 250 °C. The study demonstrated that asphaltenes could transfer hydrogen to α -methylstyrene, an olefinic compound, to form cumene. However, α -methylstyrene is a well-known hydrogen acceptor molecule, which means that it can easily accept a hydrogen from a hydrogen donor to form cumene.¹² Therefore, it was questioned whether asphaltenes can be used to saturate the olefins in the thermally cracked naphtha, which can potentially have olefins with lower reactivity than α -methylstyrene.¹³ The purpose of this study is to solve two common problems present in the heavy oil industry. Firstly, asphaltenes are considered one of the least valuable components of the crude oil; yet, asphaltenes are produced in large quantities as undesired side products.¹⁴ By employing the asphaltenes as a source of hydrogen to saturate the olefins by hydrogen transfer, some value is obtained from asphaltenes and the olefins are converted without the use of hydrogen or hydrotreating.

1.2 Objective

The main objective of this work is to evaluate unconventional alternatives to treat olefins present in thermally cracked naphtha without the use of hydrogen.

1.3 Scope of work

The study is divided into four sections. The first section is a literature review to gain a better insight into the problem and science behind the issues related to the presence of olefins in the treated bitumen (Chapter 2). The second section intends to gain a better understanding of the chemistry between phosphoric acid and olefins (Chapter 3). In order to achieve this purpose, the study employed olefin model compounds representative of the composition in the thermally cracked naphtha, rather than working with thermally cracked naphtha. The third section studied the possible use of asphaltenes to treat the olefins via hydrogen transfer (Chapter 4). This study also initially employed olefin model compounds to explore hydrogen transfer of asphaltenes to olefins, before evaluating the conversion of thermally cracked naphtha with asphaltenes. Finally, the study will be finalized by an overview of the conclusions and recommended work (Chapter 5)

References (Chapter 1)

- (1) Murray, G. R. *Upgrading Oilsands Bitumen and Heavy Oil*; University of Alberta Press: Edmonton, 2015.
- (2) Zachariah, A.; De Klerk, A. Partial Upgrading of Bitumen: Impact of Solvent Deasphalting and Visbreaking Sequence. *Energy and Fuels* **2017**, *31* (9), 9374–9380.
- (3) Gray, M. R.; Mccaffrey, W. C. Role of Chain Reactions and Olefin Formation in Cracking , Hydroconversion , and Coking of Petroleum and Bitumen Fractions. *Energy Fuels* **2002**, *16* (3), 756-766.
- (4) Cady, E.; Marschner, R. F. Composition of Virgin , Thermal , and Catalytic Naphthas from Mid-Continent Petroleum. *Ind. Eng. Chem.* **1952**, *44* (8), 1859-1864
- (5) Nagpal, J. M.; Joshi, G. C.; Singh, J.; Rastogi, S. N.; Joshi, G. C.; Singh, J.; Gum, S. N. R. Gum Formation Olefinic Precursors in Motor Gasoline, a Model Compound. *Fuel Sci. Technol. Intl.* **1994**, *12* (6), 873–894.
- (6) Enbridge. *Enbridge: Quality Pooling Specification Package*; Edmonton, 2018.
- (7) Xin, Q.; Alvarez-Majmutov, A.; Dettman, H.; Chen, J. Hydrogenation of Olefins in Bitumen-Derived Naphtha over a Commercial Hydrotreating Catalyst. *Energy & Fuels* **2018**, *32* (5), 6167-6175.
- (8) Häring, H.-W. *Industrial Gases Processing*; Wiley-VCH: Weinheim, 2008.
- (9) De Filippis, P. A Simple Test Method for Distinguishing Straight-Run from Thermal (Visbreaker) Residues or Bitumens. *Fuel* **1995**, *74* (10), 1537–1539.
- (10) Ipatieff, V. N. *Catalytic Reactions at High Pressures and Temperatures*; The Macmillan Company: New York, 1937.
- (11) Naghizada, N. Uncatalyzed Hydrogen Transfer during 100-250 ° C Conversion of Asphaltenes, Master of Science Thesis, University of Alberta, Edmonton, AB, **2017**.
- (12) Meille, V; Bellefon, C. De; Schweich, D. Kinetics of α -Methylstyrene Hydrogenation on Pd / Al₂O₃. *Ind. Eng. Chem. Res.* **2002**, *41* (7), 1711–1715.

- (13) Levitt, M.; Perutz, M. F. Aromatic Rings Act as Hydrogen Bond Acceptors. *J. Mol. Biol.* **1988**, *201* (4), 751–754.
- (14) Chilingarian, G. V.; Yen, T. F. Introduction to Asphaltenes and Asphalts. In *Asphaltenes and Asphalts, Volume 2*; 2000; pp 1–5.
- (15) Rylander, P. N. Platinum Metal Catalysts. In *Catalytic Hydrogenation over Platinum Metals*; Engelhard Industries: Newark, New Jersey, 1967; pp 3–29.

CHAPTER 2 – LITERATURE REVIEW

2.1 Background

In order to have a better understanding of the present research work, this chapter presents some fundamental aspects of olefin treatment. In this way, three main sections will be developed. The first section will describe the industrial background related to the purpose of this research, emphasizing the relationship with bitumen partial upgrading and thermally cracked naphtha. The second section will cover the use of phosphoric acid for olefin removal, which corresponds to the first unconventional process evaluated in this research work. It reviews the available literature in terms of the chemistry between olefins and phosphoric acid and its intended application as a temperature-swing absorption process. Finally, the last section supports the second unconventional process evaluated in this work, which involves the use of asphaltenes as a hydrogen source to treat olefins. Literature about asphaltenes, its properties, and chemistry as a hydrogen donor and its intended application in a treatment process similar to solvent deasphalting is reviewed.

It is intended that the findings of the present research work have application in bitumen partial upgrading; therefore, relevant information about the topic is provided.

2.1.1 Bitumen partial upgrading

Bitumen partial upgrading has the objective to reduce diluent addition and/ or processing steps of the bitumen for it to meet the pipeline specifications for transportation.^{1,2} Partial upgrading of bitumen started as an initiative to achieve a product that can avoid the current problems of bitumen transportation in Alberta to the market (mainly to the U.S), which has largely impacted the Albertan economy.¹ Current approaches to handling and delivering of bitumen to the market consist of railway or pipeline transportation by diluting the bitumen (dilbit) with approximately 30% of diluent that can significantly increase operating cost.^{1,3} It was reported that in the second quarter of 2017, the cost of diluent per barrel of bitumen was 14 USD.² Another approach is bitumen upgrading to produce synthetic crude oil (SCO), which involves a higher production cost

and has faced high competition in the market with the unconventional light crude oil produced in the U.S.¹

Because of the high density and viscosity of the Canadian bitumen, in order to achieve a transportable product via pipeline without, or with reduced amount of diluent, the bitumen requires further processing to remove and/ or reduce the solids, water, salts and heteroatoms.⁴ One of the pipeline specifications that are relevant to this project is the maximum amount of olefin content, which has to be less than 1 wt.% equivalent of 1-decene by ¹H NMR test method.⁵ The presence of olefin in the pipelines has been related to the oxidative stability of the product and gum formation, which can cause fouling downstream.^{3,6}

2.1.2 CNOOC International BituMax™ partial upgrading technology

CNOOC International (former Nexen Energy ULC) is one of the oil companies that has been working on bitumen partial upgrading with a process called BituMax™. This process is based on solvent deasphalting and visbreaking processes to produce partially upgraded bitumen, reducing or eliminating the need for diluent (see Figure 2.1).⁷

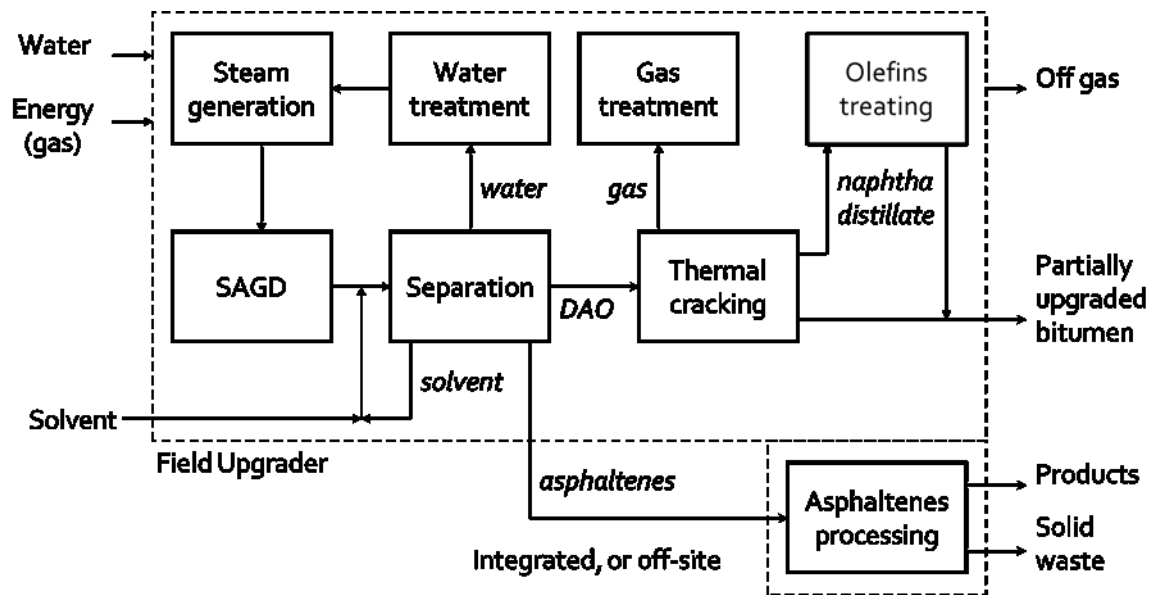


Figure 2.1 CNOOC International BituMax™ flow diagram

In the first step of the BituMax process, the bitumen goes to a solvent deasphalting process where it is mixed with a solvent to form deasphalted oil (DAO) and asphaltenes. The asphaltenes are rejected as an asphaltenes-and-water slurry product and ultimately becomes a solid waste. On the other hand, the DAO enters a thermal cracking process where it is mildly cracked at $> 400^{\circ}\text{C}$ via visbreaking to break down the large and complex molecules in the bitumen into smaller ones. This thermal process results in a decrease in density and viscosity of the bitumen. However, the application of high temperatures leads to the formation of olefins, which are mainly concentrated in the naphtha and distillate streams.^{8,9} Therefore, in order to fulfill pipeline specifications, the olefins have to be treated (decreased, removed or saturated) before blending all the streams to form partially upgraded bitumen. The process block for olefin treating shown in Figure 2.1 will be the main focus of this study.

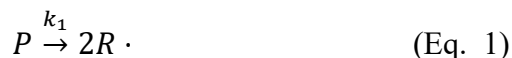
2.1.3 Olefins in Thermally Cracked Bitumen

When bitumen undergoes visbreaking, it results in the formation of olefins, and hence their presence in the thermally cracked bitumen. The next section will describe how these olefins are formed in the presence of high temperatures. In addition, because one of the product fractions from visbreaking, which is rich in olefins, corresponds to the naphtha fraction, some comments in terms of its olefins composition and the current way of treatment will be made.

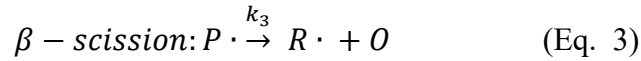
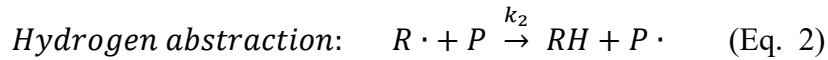
2.1.3.1 Olefin Formation

When enough heat is applied to the organic molecules, it can lead to thermolysis of relatively weak bonds to initiate the free radical reaction (usually bonds containing a heteroatom).³ The thermally induced homolytic bond dissociation of the molecules forms radical precursors that further participate in propagation reactions such as hydrogen abstraction and β -scission. In the case of β -scission propagation, an olefin and a new radical are produced.^{8,10} A simplified illustration³ of the cracking of an n -alkane in solvent can be observed in the following steps:

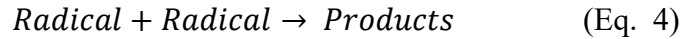
Initiation:



Propagation:

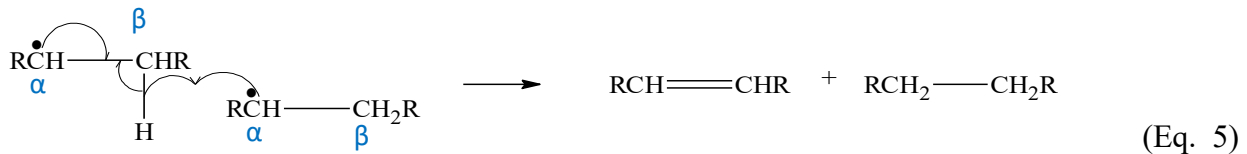


Termination:



Where P and P• correspond to the parent alkane and the parent radical, respectively; R• and RH are lower alkyl radicals and their corresponding alkanes, and O represents an olefin.

After propagation, free radicals undergo termination reactions. Different types of termination reactions are possible, such as combination reactions and hydrogen disproportionation (Eq. 5). In hydrogen disproportionation of radicals, one of the termination products is an olefin.¹⁰ The presence of olefins in thermally cracked bitumen is expected and yet undesirable.



2.1.3.2 Naphtha composition

Naphtha refers to material in the distillation range that is employed to produce gasoline, which is typically petroleum liquids with normal boiling points <175 °C. Naphtha composition may vary depending on the petroleum source, boiling range, and if the naphtha was obtained by straight-run distillation or produced by catalytic or thermal cracking of heavier oil fractions.¹¹ The hydrocarbons can be present as paraffins, naphthenes, cyclic olefins, olefins, diolefins, and aromatic hydrocarbons with carbon chains in the C₄ to C₁₂ range^{11,12} (Table 2.1). When the naphtha is obtained from processes involving thermal cracking, the complexity of the hydrocarbon mixture increases compared to straight run (virgin) petroleum naphtha, especially in terms of the

olefin content,¹³ because new olefins are produced due to the free radical chemistry that took place in the thermal conversion step.

Table 2.1 Carbon number distribution for different types of naphtha from Mid-continent petroleum¹³

Carbon Number Distribution	Virgin Distillate (Liq. Vol. %)	Thermal Coker (Liq. Vol. %)	Fluid Catalytic Cracking (Liq. Vol. %)
4	2.3	4.7	2.8
5	10.2	45.4	38.5
6	19.9	25.9	35.2
7	26.7	12 ^a	18.3
8	23.5	5 ^a	4.5
9	14.4	3 ^a	0.3
10+	3.0	4 ^a	0.4
Total	100.0	100.0	100.0

^a Estimated from ASTM distillation

Table 2.1 gives insight into the carbon number distribution for naphtha obtained from different processes. In the case of thermally cracked coker naphtha, most hydrocarbons are found in the C₅ - C₇ range. Table 2.2 presents the distribution of hydrocarbon classes within C₅ to C₆, where the olefins are present as the second major hydrocarbon class that is less abundant than only the paraffins.

Table 2.2 Distribution of hydrocarbon classes by carbon number of thermal coker naphtha from Mid-continent petroleum ¹²

Carbon number	Hydrocarbon class	Thermal Coker (%) ^a
5	Paraffins	55.7
	Naphthenes	2.4
	Cyclo-olefins	2.4
	Olefins	39.5
	Diolfins	0.0
	Total	100.0
6	Paraffins	42.8
	Naphthenes	10.7
	Cyclo-olefins	8.8
	Olefins	36.3
	Diolfins	0.1
	Aromatics	1.3
Total	100.0	

^a Percentage may be determined by multiplying its value by the appropriate group percentage listed in Table 2.1.

In the case of visbroken naphtha, an attempt to identify some of the olefins present in the naphtha was done by Páez Cárdenas,⁴ where the naphtha was spiked with model compounds to determine their identification by various gas chromatography techniques. A summary of the olefins identified within the C₅ to C₇ range is presented in Table 2.3:

Table 2.3 Identified olefins in visbroken naphtha from CNOOC International Long Lake upgrader facility by Páez Cárdenas⁴

Carbon Number	Olefin Structure	Identified Compounds
C ₅	Linear	pentene <i>trans</i> -2-pentene <i>cis</i> -2-pentene
	Branched	2-methyl-1-butene 2-methyl-2-butene 3-Methyl-1-butene
	Cyclic	Methylenecyclobutane Cyclopentene
	Diolefins	1,4-pentadiene 2-methyl-1,3-butadiene <i>trans</i> 1,3-Pentadiene
C ₆	Linear	hexene <i>trans</i> -3-hexene <i>trans</i> -2-hexene <i>cis</i> -3-hexene <i>cis</i> -2-hexene
	Branched	3,3-dimethylpentene-1 2-methylpentene-2
	Cyclic	methyl-cyclopentene cyclohexene
	Diolefins	1,5-hexadiene <i>trans</i> -1,4-hexadiene 2,3-dimethyl-1,3-butadiene 1,3-hexadiene 2,4-hexadiene 3-methyl-1,3-pentadiene 2-methyl-1,5-hexadiene
C ₇	Linear	heptene <i>cis</i> -2-heptene <i>trans</i> -2-heptene <i>trans</i> -3-heptene <i>cis</i> -3-heptene
	Branched	<i>cis</i> -3-methyl-3-hexene
	Cyclic	1-methyl-cyclohexene
	Diolefins	3-methyl-2,4-hexadiene

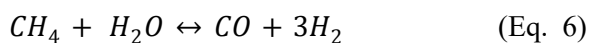
Another study was performed by Santiago and Subramanya¹⁴ to determine the concentration of the olefins in the visbroken naphtha from CNOOC International Long Lake upgrader facility. This study involves the distillation of the naphtha into smaller boiling fractions in order to perform characterization studies, and various gas chromatographic techniques to identify and quantify the olefins. The olefins identified in this study are shown in Table 2.4.

Table 2.4 Olefins in visbroken naphtha from CNOOC International Long Lake upgrader facility
by Santiago and Subramanya¹⁴

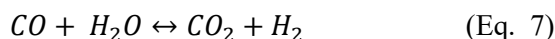
Carbon Number	Compound	Weight %
C₄	2-butene	0.51
	Total C₄ olefins	0.51
C₅	3-methyl-1-butene	0.09
	2-methyl-1-butene	0.37
	2-pentene	0.99
	Cyclopentene	0.13
	Total C₅ olefins	1.58
C₆	4-methyl-1-pentene	0.25
	3-methyl-1-pentene	0.11
	4-methyl-2-pentene	0.07
	2-methyl-1-pentene	0.30
	1-hexene	0.68
	2-methyl-2-pentene	0.70
	3-methyl-cyclopentene	0.12
	3-methyl-2-pentene	0.52
	3-hexene	1.03
	3-methyl-cyclopentene	0.60
	Ethylidenecyclobutane	0.11
	Total C₆ olefins	4.49
	C₇	2,4-dimethyl-1-pentene
3-methyl-1-hexene		0.07
5-methyl-1-hexene		0.06
2-methyl-3-hexene		0.06
4-methyl-1-hexene		0.18
4-methyl-2-hexene		0.18
1-heptene		0.58
3-methyl-3-hexene		0.23
2-methyl-2-hexene		0.22
2-heptene		0.40
3-ethyl-cyclopentene	0.04	
Ethylidene-cyclopentene	0.31	
Total C₇ olefins	2.27	
C₈	4-methyl-2-heptene	0.04
	6-methyl-2-heptene	0.11
	1-ethyl-5-methyl-cyclopentene	0.24
	2,6-dimethyl-1-heptene	0.17
	2,6-dimethyl-3-heptene	0.14
Total C₈ olefins	0.71	
C₉	3-(1-methylethyl)-cyclohexene	0.07
	1-nonene	0.34
	4-nonene	0.14
Total C₉ olefins	0.55	

2.1.3.3 Hydrogen production and olefin hydrotreating

Presently, one of the most common technologies used in the oil industry for olefin treating is hydrogenation due to its effectiveness in saturating the olefinic double bonds.³ However, in order to obtain hydrogen in a bitumen upgrader, it is necessary to produce the hydrogen on-site.³ The most common hydrogen production process is via steam methane reforming and it is produced from direct synthesis. The reaction occurs in two stages, which will be explained in a simplified way. The first step requires reaction of methane and steam at high temperatures (800-870 °C) and pressure (2.2-2.9 MPa) over a nickel catalyst.³



The second stage processes the mixture of carbon monoxide and hydrogen to form additional hydrogen via water-gas shift reaction:



Finally, the removal of CO₂ requires specialized solvents or pressure-swing absorption processes. However, it is important to mention that this approach is energy-intensive, due to its high operational conditions, therefore increasing the overall production and operational cost. Furthermore, production of hydrogen on-site requires large facility spaces.¹⁵ Both factors are not desirable for the purpose of a partial upgrader because the intent is to locate the partial upgraders in remote locations near the extraction site and to produce an economically feasible product.¹⁶

Once the hydrogen is produced on-site, the olefins are then treated with the hydrogen with the assistance of a sulfided base metal catalyst, such as NiMo/ Al₂O₃. Typical naphtha hydrogenation conditions are at the operational range of 250-360 °C and 1-3 MPa.⁹

2.2 Olefin treatment using phosphoric acid

Because the first strategy evaluated in the present research work consists of the use of phosphoric acid for olefin removal, the following section presents pertinent information about the topic. In other words, the use of phosphoric acid to form alkyl phosphoric esters, their analytical detection as well as the basics of temperature-swing absorption processes will be discussed.

2.2.1 Phosphoric acid

Phosphoric acid is a viscous, transparent and polar compound that is highly soluble in water. Phosphoric acid is a term used to denote a class of compounds that are within the general formula of $H_{2+n}P_nO_{3n+1}$. The hydration state of phosphoric acid refers to the amount of water that is in the solution with relation to the pure orthophosphoric acid (H_3PO_4) content.¹⁷ Therefore, the species present in the solution may vary depending on the water content (Table 2.5). This is an important factor to consider in the use of phosphoric acid as a catalyst, as the hydration state affects whether the acid sites are weaker or stronger depending on the acid concentration. As a result, this impacts the activity of the phosphoric acid as a catalyst, its selectivity, and conversion in the reaction.¹⁷ In the case of 85% hydration state of phosphoric acid, the species are present in the solution as H_3PO_4 .¹⁷

Table 2.5 Distribution of phosphoric acid species according to the hydration state of the phosphoric acid with water

Species	Phosphoric acid hydration state (% H_3PO_4)				
	85	100	104	108	115
H_3PO_4	100	76.6	58.9	33.4	5.2
$H_4P_2O_7$		22.6	38.0	50.5	21.0
$H_5P_3O_{10}$		0.8	2.8	13.0	22.3
$H_6P_4O_{13}$			0.3	2.6	17.9
$H_7P_5O_{16}$				0.5	12.7 ^a

^a Remainder constituted by P_6 - P_{14} species. With P indicating the number of phosphorus atoms present in the species.

For the purpose of this study, to simplify the chemistry, the use of 85% hydration state of phosphoric acid will be ideal, as the acid will only be present as H₃PO₄.

2.2.2 Reaction of phosphoric acid and olefins

Liquid phosphoric acid has long been used in the industry as an effective catalyst for oligomerization of light olefins after the discoveries of Ipatieff.¹⁸ The oligomerization mechanism of olefin via two esters proposed by Ipatieff is presented in the following.^{19,20}

2.2.2.1 Formation of phosphoric acid ester:

The oligomerization of olefins, when reacted with phosphoric acid, does not involve a true acid-derived carbocation, but it rather goes through the formation of an unstable alkyl phosphoric acid ester, the alkyl phosphoric acid ester is formed by the interaction of a cationic protonated olefin and anionic phosphate as described in

Figure 2.2^{21,22}:

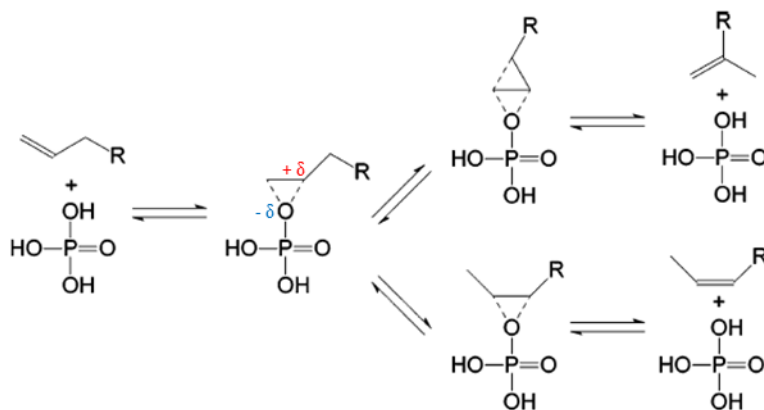


Figure 2.2 Formation of phosphoric acid ester from reaction of olefin and phosphoric acid

The formation of the intermediate alkyl phosphoric acid ester is particularly important for this study. Because the intended application of this research is to form alkyl phosphoric acid esters from the phosphoric acid and the olefins in the thermally cracked naphtha.

2.2.2.2 Reactivity of the olefins with phosphoric acid

As the purpose of this study is to form the alkyl phosphoric acid esters, it is important to understand the factors that affect the reactivity of the olefins with phosphoric acid. The reactivity of the olefins with phosphoric acid is dependent on the strength of the alkyl phosphoric acid ester and the stability of the carbocation intermediate.²² The stability of the carbocation intermediate depends on the time that the phosphoric acid can polarize the olefin; this means the strength of the ester. If the interaction between the olefin and the phosphoric acid is too weak, then the period of interaction between these compounds will be short, therefore, leading to an unstable carbocation intermediate and low reactivity to olefin oligomerization. It has been found that the stability of the carbocation intermediate is similar to the stability of a classic carbocation, following the order tertiary > secondary > primary carbocation.²³ As a result, the more stable the carbocation intermediate the more reactive the alkyl phosphoric acid ester. When the purpose is to form a stable phosphoric acid ester, it is anticipated that the opposite would be true. A less stable carbocation intermediate would lead to slower reaction, but also to a more temperature stable phosphoric acid ester. However, another factor to take into consideration is the length of the hydrocarbon chain of the olefin. The phosphoric acid is a highly polar compound, which means that the chances of interaction between the acid and the apolar organic molecule will be decreased.¹⁷

2.2.2.3 Decomposition of alkyl phosphoric acid ester

Alkyl phosphoric acid esters can be thermally degraded.²⁴ The stronger the ester, the higher the temperature for thermal degradation. However, there is not a straightforward trend with respect to the decomposition temperature. The shorter the alkyl chain does not implicate a lower decomposition temperature, as can be seen in the case of isopropyl phosphoric acid ester (Table 2.6).¹⁷ The decomposition of the alkyl phosphoric acid esters depends on the stability of the ester and so takes place at different temperatures. Once the ester is degraded, the resulting products of thermal degradation consist of the elimination of phosphoric acid and a potentially isomerized olefin.²⁴

Table 2.6 Decomposition temperature of alkyl phosphoric acid esters

Alkyl phosphoric acid ester	Formula	Decomposition temperature (°C)
Methyl phosphoric acid ester	CH ₃ (H ₂ PO ₄)	169-173
Ethyl phosphoric acid ester	CH ₃ CH ₂ (H ₂ PO ₄)	165-170
Propyl phosphoric acid ester	CH ₃ (CH ₂) ₂ (H ₂ PO ₄)	122-128
Isopropyl phosphoric acid ester	(CH ₃) ₂ CH(H ₂ PO ₄)	74-80
Butyl phosphoric acid ester	CH ₃ (CH ₂) ₃ (H ₂ PO ₄)	105-110
Octyl phosphoric acid ester	CH ₃ (CH ₂) ₇ (H ₂ PO ₄)	170-175

2.2.2.4 Reaction between two molecules of phosphoric acid ester

In addition to the formation of the intermediate alkyl phosphoric acid ester, additional products may be formed. When the reaction temperature is further increased from the decomposition temperature, the alkyl phosphoric acid esters may undergo true polymerization or conjunct polymerization.²⁰ True polymerization consists of olefins having molecular weights that are integral multiples of the monomer olefin. Conjunct polymerization, on the other hand, occurs when a complex mixture of alkanes, alkenes, alkadienes, cycloalkanes, cycloalkenes, cycloalkadienes, and even aromatic hydrocarbons are formed. These products do not necessarily have a number of carbon atoms corresponding to an integral multiple of the monomer.²⁰ The type of polymerization that takes place depends on the reaction temperature. Conjunct polymerization over phosphoric acid usually occurs at temperatures above 250-300°C.²⁰

2.2.2.5 Detection of alkyl phosphoric acid esters

An important aspect when dealing with alkyl phosphoric acid esters is analytical detection. Their detection is challenging due to their natural characteristics. In the case of gas chromatography, these compounds cannot migrate through the gas column as they have low volatility and tendency to be destroyed by thermal decomposition.²⁵ Therefore, this technique cannot be used for the direct analysis of phosphoric acid esters. Furthermore, the detection of alkyl phosphoric acid esters in

concentrated phosphoric acid represents another challenge, as the direct injection of acidic samples can damage certain instruments.²⁶

However, prior to the development of more advanced analytical methods, researchers used to follow a time-consuming and complex experimental method for alkyl phosphoric acid esters detection. The following method was used to detect the presence of alkyl phosphoric acid esters in the aqueous phase of ethylene and propylene reaction separately.^{19,27} This was achieved by diluting the aqueous phase with water in a volumetric ratio of 1:12 of phosphoric acid to water. This step was then followed by the addition of barium carbonate and barium hydroxide to the solution at 60°C until it was neutralized to phenolphthalein as acid-base indicator. These conditions enabled the precipitation of barium phosphate while keeping the barium salt of the alkyl phosphoric acid esters in solution. Furthermore, the solution goes through filtration while adding alcohol in order to precipitate the barium salt of the alkyl phosphoric acid esters (Figure 2.3). The characteristics of the barium salt of the alkyl phosphoric acid esters are well-defined needle-like crystals that are soluble in water but not in alcohol. Therefore, based on the information in the literature, the detection of alkyl phosphoric acid esters is expected to be challenging for the experimental work planned in this thesis.

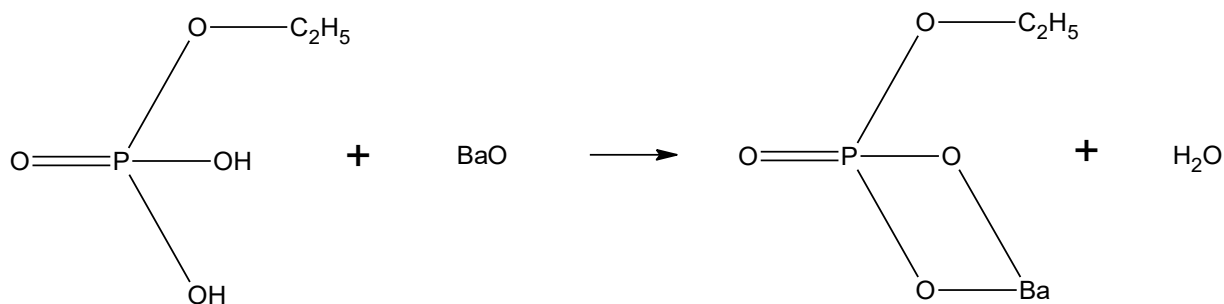


Figure 2.3 Formation of barium salt of ethyl phosphoric acid

2.2.3 Temperature-swing absorption process

The intended industrial application of phosphoric acid treatment of the olefins in the thermally cracked naphtha is a temperature-swing absorption (TSA) process. The basics of this type of process are described in this chapter because it will be later mentioned in Chapter 3.

TSA is a process based on temperature variation to shift equilibrium reactions to achieve absorption and desorption of species. A common example of the TSA process used in the oil industry is the amine-treatment for sour gas removal by using chemical solvents. The process can be seen as a two-staged process where it first starts with the absorption of the absorbate, such as H₂S in the case of amine-based H₂S absorption process. The absorption reaction is promoted by high pressure and low-temperature conditions to achieve chemisorption of the species to the absorbent.²⁸ Once the absorbent is loaded and reaches breakthrough or saturation, the solution is then delivered to the second stage for desorption. In the second stage, the temperature is increased while the pressure is decreased. These conditions will allow the regeneration of the absorbent that can be recycled back into the absorption stage while recovering, on the other hand, the absorbate in a separate stream.^{3,28}

An example of a process flow diagram of removal of H₂S by alcohol amine absorption is shown in Figure 2.4. A stream of gas containing H₂S is placed in contact with a solution of *lean* amine (amine with a low concentration of H₂S). The conditions of the absorption stage enable the chemisorption of the H₂S with the amine solution. Once the amine solution is loaded and *rich* in H₂S, the content is sent to the desorption stage where the increase in temperature will allow the separation of the H₂S from the amine solution. This will allow the regeneration of the amine solution and it can be recirculated into the absorber.

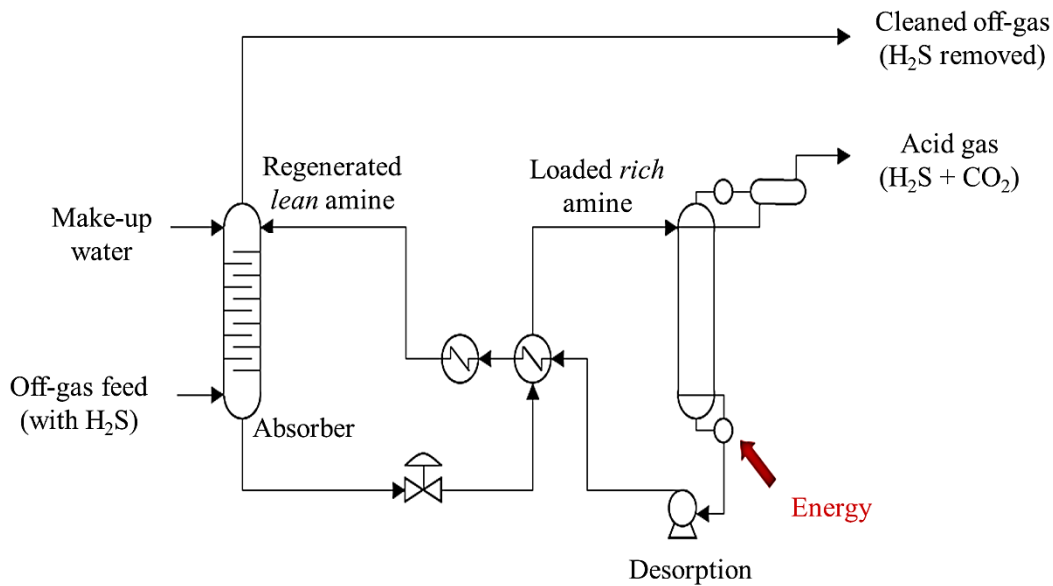


Figure 2.4 Generic process flow diagram of H₂S gas removal by alcohol amine absorption²⁹

2.3 Olefin treatment using asphaltenes

The second strategy for olefin removal evaluated in this research work involves the use of industrial asphaltenes; therefore, their definition, origin and main characteristics will be discussed.

2.3.1 Asphaltenes

Asphaltene is a component of the bitumen. It is defined as a solubility class. Asphaltenes can be defined as the insoluble fraction in linear alkanes, such as *n*-heptane or *n*-pentane, and soluble in toluene.³⁰ It is important to understand that the molecular mass, composition, functionality, polarity and any other property is different depending on the asphaltenes, and the only property in common is the insolubility in the *n*-heptane (or *n*-pentane).³¹

Asphaltenes are considered the least valuable component of the bitumen as their presence is related to the increase in viscosity of the oil. As asphaltenes are a solubility class, their presence can create instability in the oil and in some instances, any small change in pressure and temperature can cause the asphaltenes in the oil to form bulk solids, which means fouling.³²

2.3.2 Solvent deasphalting

This topic is covered in this chapter because solvent deasphalting is the process where the asphaltenes are produced in the BituMax partial upgrading process (see Figure 2.1). In addition, the approach of this process is used to describe the industrial application, which forms the basis of the proposal for the use of asphaltenes to treat the olefins in the thermally cracked naphtha.

Solvent deasphalting is a method to upgrade the feed, to form deasphalted (DAO), by phase separating the asphaltenes and removing the mineral solids, coke and solid salts from the bitumen.³ The removal of the asphaltenes will enable a substantial reduction in oil viscosity in the bitumen. The solvent deasphalting process consists of mixing the bitumen with a solvent from ratios of 3:1 up to 10:1 depending on the solvent of choice and desired yield of asphaltenes to DAO. The precipitate is then removed from the mixture and the solvent is recovered by flash. A typical solvent deasphalting process diagram is shown in Figure 2.5.³³ The solvent deasphalting process employed in the BituMax process is somewhat different, because it is integrated with the rest of the process. The process flow diagram in Figure 2.5 is therefore only for illustrative purposes.

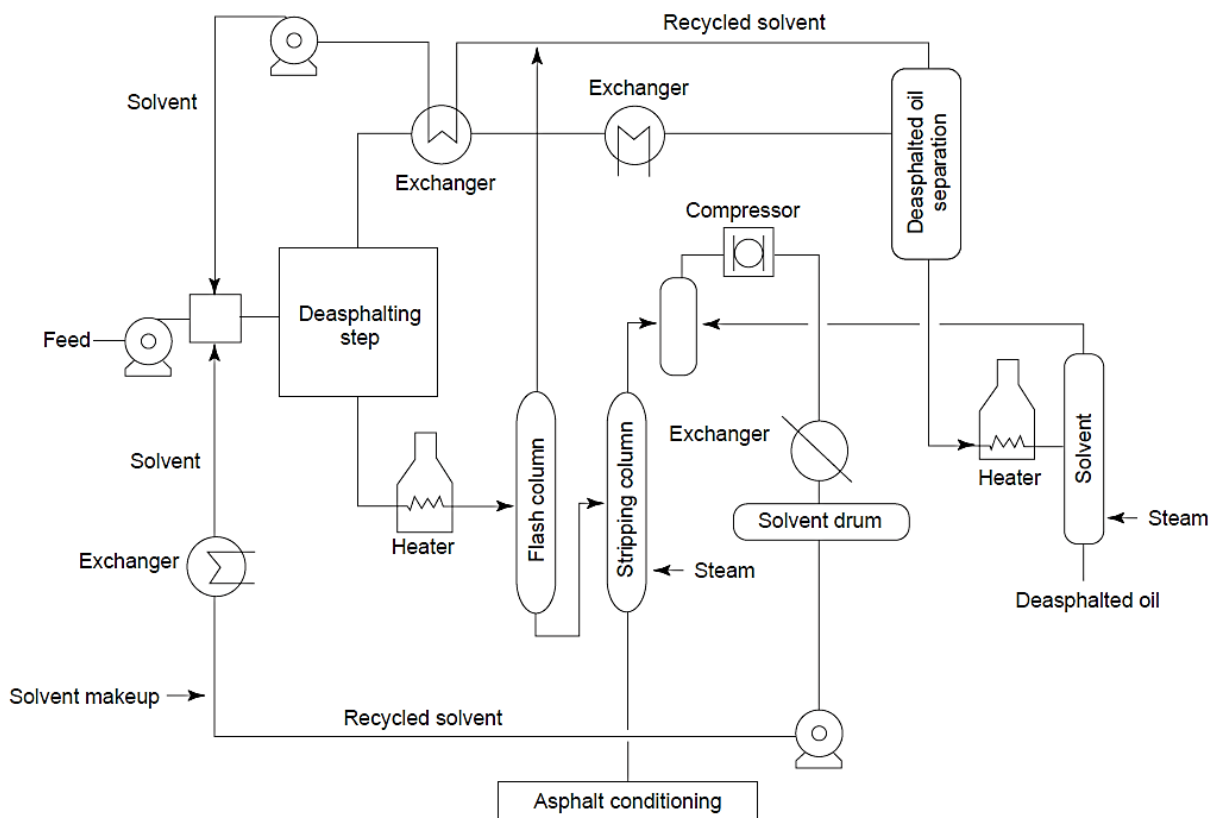


Figure 2.5 Process diagram of a typical solvent deasphalting process

2.3.3 Chemistry between asphaltenes and olefins

The intended application of using asphaltenes to treat the olefins is by using the hydrogen donating properties of the asphaltenes. This occurs via free radical reactions. Therefore, the next sections will involve relevant concepts related to the chemistry between the asphaltenes and the olefins.

2.3.3.1 Asphaltenes as hydrogen donors

A good hydrogen donor has low oxidation potential that enables the transfer of hydrogen from the donor to the acceptor under mild reaction conditions.³⁴ In the case of applications in the oil industry, good hydrogen donors usually contain naphthenic groups, partially hydrogenated aromatic compounds that can dehydrogenate to form aromatics and donate the hydrogen to a hydrogen

acceptor.³ An example is 1,2,3,4-tetrahydronaphthalene (tetralin), which can react in two steps to form naphthalene, which is a fully aromatic compound (See Figure 2.6).³

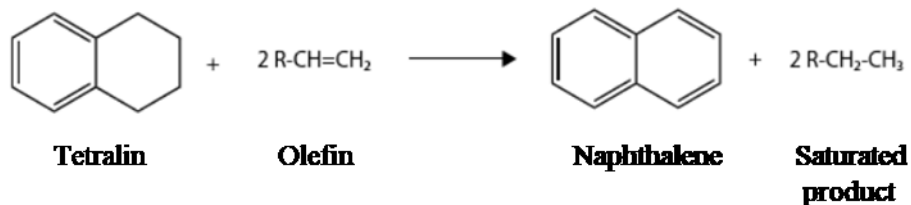


Figure 2.6 Reaction of tetralin as hydrogen donor

However, as with all reactions, it has been found that the hydrogen transfer reaction is temperature-dependent. When the temperature is decreased, tetralin has been found to be ineffective as a hydrogen donor. According to Payan et al.,³⁵ it can be explained as followed: first, when the reaction temperature is decreased, the energy available for homolytic bond dissociation is decreased. Secondly, when the temperature is decreased, there is also a decrease in the thermodynamic driving force for the cyclic hydrogen donors to become aromatic structures.

On the other hand, in the case of asphaltenes as hydrogen donors, a study performed by Gould and Wiehe,³⁶ found that petroleum residues contains high concentrations of natural hydrogen donors, and especially in the asphaltenes fraction. The hydrogen donors in the asphaltenes fraction were reported as the most reactive in comparison to the other fractions of the resid. Taking this knowledge into account, Naghizada, et al.,³⁷ performed research on uncatalyzed hydrogen transfer reactions between asphaltenes and α -methylstyrene. In this study, it was observed that asphaltenes can transfer hydrogen to α -methylstyrene at 250°C due to the resulting production of cumene. In addition, it was observed that the reverse reaction of cumene transferring hydrogen to asphaltenes did not occur (See Figure 2.7).³⁷ Therefore, indicating that the asphaltenes can be used as effective hydrogen donors.

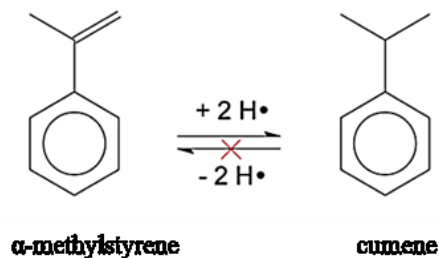


Figure 2.7 Hydrogen transfer between α -methylstyrene and cumene

2.3.3.2 Olefins as hydrogen acceptors

The carbon-carbon π bond of an olefin is more reactive than a carbon-carbon σ bond. Therefore, addition reactions of radical to an olefin are not uncommon. The intermolecular addition of a radical to an olefin is usually energetically favored because it leads to the formation of a new strong carbon-carbon σ bond (≈ 370 kJ/mol) at the expense of a weaker carbon-carbon π bond (≈ 235 kJ/mol).¹⁰

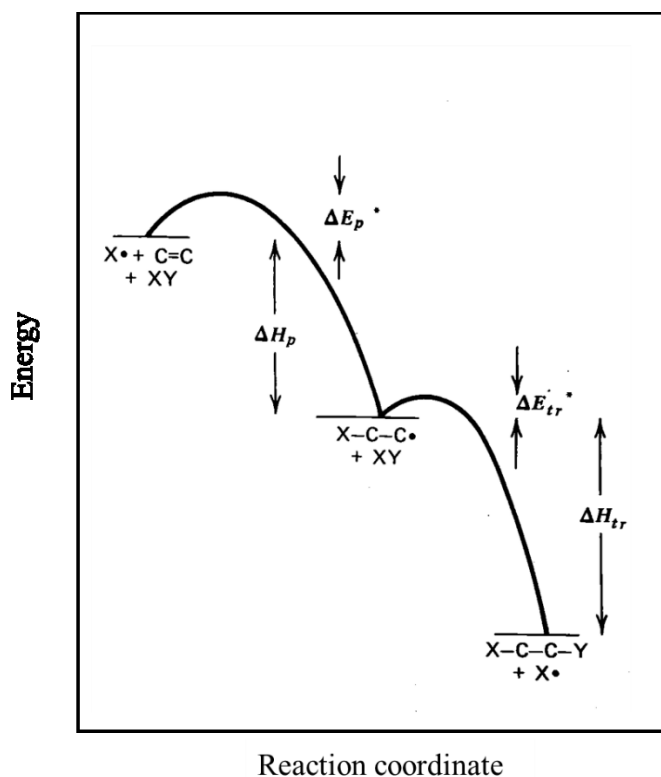


Figure 2.8 Energy-reaction coordinate diagram for olefin reaction with free radical³⁸

As a matter of illustration to understand an addition reaction, Figure 2.8 shows that the addition of a radical X (such as a proton radical) to an olefin will produce radical X-C-C•. The new radical will contain all the energy generated from the C-X bond. If this energy cannot be effectively dissipated (ΔH_p) from the structure of the intermediate radical, then the C-X bond will dissociate and return to the formation of X and olefin. Depending on the structure of the olefin, the addition of X to the double bond can be highly reversible or not at all. Certain olefins can form a considerably stable intermediate X-C-C•, such as the stabilization by resonance, these intermediates will then increase in concentration, therefore increasing its chance to participate in the termination step of the chain process by dimerization or disproportionation (Figure 2.9) and releasing ΔH_{tr} .³⁸

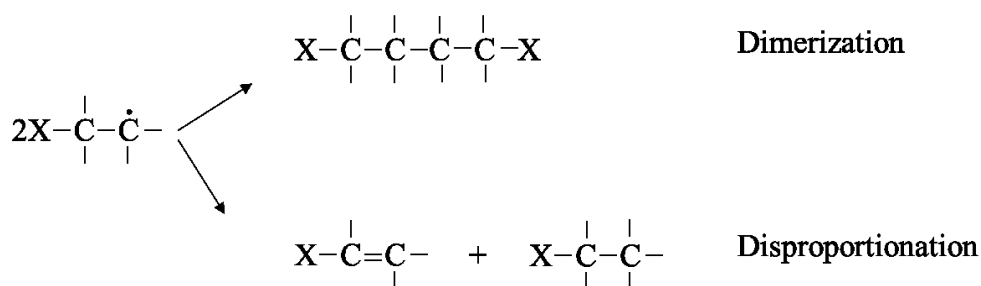


Figure 2.9 Possible termination steps for olefin reaction with free radical³⁸

Studies have been made of uncatalyzed hydrogen transfer reactions, such as the research conducted by Rüchardt et al.³⁹ In this study, they analyzed the reactions between model compound hydrogen donor dihydroanthracene and xanthene with the olefin α -methylstyrene. Obtaining, as a result, the hydrogenation of α -methylstyrene by forming cumene, without the need of catalysts (Figure 2.10).⁴⁰ α -Methylstyrene is an excellent hydrogen acceptor, as it forms a highly stable free radical intermediate, prior to the formation of cumene. This stability is given by the delocalization of the unpaired electron.⁴¹ However, this information is not necessarily true for other olefins such as linear and branched olefins, as they can only form alkyl radicals, which have lower stability than a benzyl radical.⁴¹

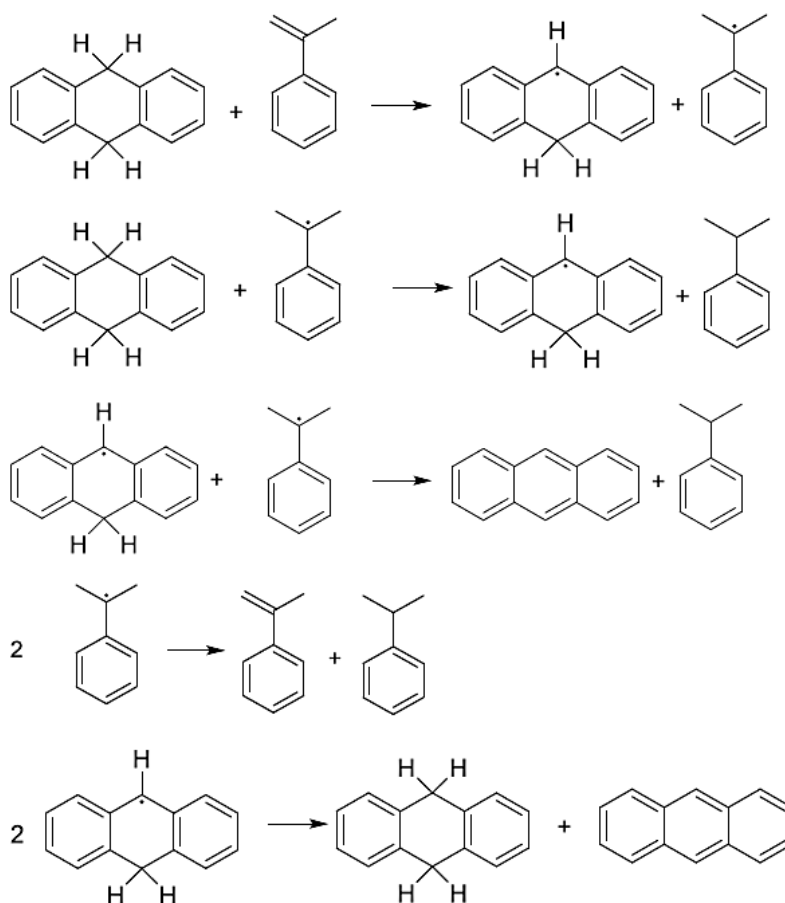


Figure 2.10 Reaction mechanism of the hydrogenation of α -methylstyrene with 9,10-dihydroanthracene

2.3.4 Relevant free radical reactions

In the case that asphaltenes can donate hydrogen to the olefins, several free radical reactions can be relevant to describe this chemistry.

2.3.4.1 Hydrogen abstraction reaction

Hydrogen abstraction reaction is a free radical propagation reaction where a free radical removes a hydrogen atom from a non-radical precursor.¹⁰ As a matter of illustration of the abstraction of a

hydrogen atom, a radical ($R^1\cdot$) attacks the σ bond of the hydrogen to form a new and more stable product radical ($R^2\cdot$). Radical abstraction reactions are favorable when the hydrogen attached to the σ bond is weak, therefore, enabling the formation of a more stable product radical ($R^2\cdot$) and a stronger σ bond in the product ($R^1\text{--}H$).

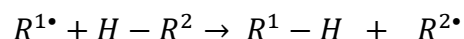


Figure 2.11 Hydrogen abstraction reaction

2.3.4.2 Combination or coupling reaction

It is a type of termination reaction between radicals. Combination reaction involves the coupling of two radicals.^{10,42} When the combination reaction occurs between two identical radicals ($R\cdot$), a dimer is formed and this is called homocoupling. On the other hand, when two different radicals combine, it is known as heterocoupling reaction.

Combination reactions are diffusion-controlled and to achieve an efficient combination reaction, a high concentration of radicals is required in order to ensure collision between the radicals.¹⁰ Steric hindrance is also an important factor to consider, as hindered carbon centers can represent an obstacle to forming a combined product.⁴³

2.3.4.3 Hydrogen disproportionation

Disproportionation is a free radical termination reaction, where one of the two encountering radicals has a hydrogen atom β to the radical center and the abstraction of this hydrogen by the other radical forms two stable molecules.^{10,44} The resulting products are the formation of an unsaturated and saturated product. The unsaturated product is formed by the abstraction of the hydrogen and the saturated product is formed from the new σ C-H bond. This reaction is in competition with combination reaction and both reactions have similar diffusion-controlled reaction rates (see Figure 2.12).¹⁰ Disproportionation is favored when there is a high concentration of radicals with β -hydrogens.¹⁰

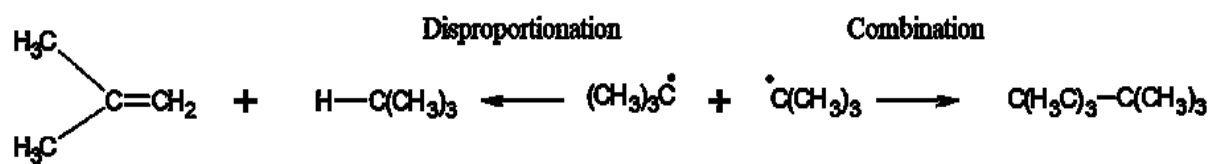


Figure 2.12 Combination reaction vs disproportionation reaction

References (Chapter 2)

- (1) Fellows, G. K.; Mansell, R.; Schlenker, R.; Winter, J. *Public-Interest Benefit Evaluation of Partial-Upgrading Technology*; Calgary, 2017; Vol. 10.
- (2) Gieseman, J.; Brasier, R. S. *Bitumen Partial Upgrading 2018 Whitepaper*; Jacobs Consultancy, Edmonton, AB, 2018.
- (3) Murray, G. R. *Upgrading Oilsands Bitumen and Heavy Oil*; University of Alberta Press: Edmonton, 2015.
- (4) Paez, N. Identification, Conversion and Reactivity of Diolefins in Thermally Cracked Naphtha, Master of Science Thesis, University of Alberta, Edmonton, AB, 2016.
- (5) Enbridge Quality Pooling. *Enbridge: Quality Pooling Specification Package*; Edmonton, 2018.
- (6) Nagpal, J. M.; Joshi, G. C.; Singh, J.; Rastogi, S. N.; Joshi, G. C.; Singh, J.; Gum, S. N. R. Gum Formation Olefinic Precursors in Motor Gasoline, a Model Compound. *Fuel Sci. Technol. Intl.* **1994**, *12* (6), 873–894.
- (7) De Klerk, A. *Annual Report 2016-2017 (Year 1), Progress Report on Industrial Research Chair Program Issued to NSERC, Nexen Energy ULC, and Alberta Innovates*; Edmonton, 2017.
- (8) Gray, M. R.; McCaffrey, W. C. Role of Chain Reactions and Olefin Formation in Cracking, Hydroconversion, and Coking of Petroleum and Bitumen Fractions. *Energy Fuels* **2002**, *16* (3), 756–766.
- (9) Xin, Q.; Alvarez-Majmutov, A.; Dettman, H.; Chen, J. Hydrogenation of Olefins in Bitumen-Derived Naphtha over a Commercial Hydrotreating Catalyst. *Energy & Fuels* **2018**, *32* (5), 6167–6175.
- (10) Parsons, A. F. *An Introduction to Free Radical Chemistry*; Blackwell Science: Oxford, 2000.
- (11) Elsayed, H. A.; Menoufy, M. F.; Shaban, S. A.; Ahmed, H. S.; Heakal, B. H. Optimization of the Reaction Parameters of Heavy Naphtha Reforming Process Using Pt-Re / Al₂O₃ Catalyst System. *Egypt. J. Pet.* **2017**, *26* (4), 885–893.
- (12) Ramnas, O.; Ostermark U.; Petersson, G. Characterization of Sixty Alkenes in a Cat-Cracked Gasoline Naphtha by Gas Chromatography. *Intl. J. Sep. Sci.* **1994**, *38* (3), 222–226.
- (13) E. Cady, W.; F. Marschner, R.; P. Cropper, W. Composition of Virgin, Thermal, and Catalytic Naphthas from Mid-Continent Petroleum. *Ind. Eng. Chem.* **1952**, *44* (8), 1859–

- 1864.
- (14) Santiago, C.; Subramanya, A. S. *Olefin Characterization of Thermally Cracked Naphtha*; Edmonton, AB, unpublished work, 2019.
 - (15) Nimana, B.; Canter, C.; Kumar, A. Energy Consumption and Greenhouse Gas Emissions in Upgrading and Refining of Canada's Oil Sands Products. *Energy* **2015**, *83* (1), 65–79.
 - (16) Zachariah, A.; De Klerk, A. Partial Upgrading of Bitumen: Impact of Solvent Deasphalting and Visbreaking Sequence. *Energy and Fuels* **2017**, *31* (9), 9374–9380.
 - (17) de Klerk, A. Key Catalyst Types for the Efficient Refining of Fischer-Tropsch Syncrude: Alumina and Phosphoric Acid. In *Catalysis: Volume 23*; 2011; pp 1–49.
 - (18) Ipatieff, V. N. Catalytic Polymerization of Gaseous Olefins by Liquid Phosphoric Acid: I. Propylene. *Ind. Eng. Chem.* **1935**, *27* (9), 1067–1069.
 - (19) Ipatieff, V. N. *Catalytic Reactions at High Pressures and Temperatures*; The Macmillan Company: New York, 1937.
 - (20) Schmerling, L.; Ipatieff, V. N. The Mechanism of the Polymerization of Alkenes. *Adv. Catal.* **1950**, *2*, 21–80.
 - (21) Nicholas, C. P. Applications of Light Olefin Oligomerization to the Production of Fuels and Chemicals. *Appl. Catal. A Gen.* **2017**, *543* (3), 82–97.
 - (22) De Klerk, A. Reactivity Differences of Octenes over Solid Phosphoric Acid. *Ind. Eng. Chem. Res.* **2006**, *45* (2), 578–584.
 - (23) March, J. *Advanced Organic Chemistry*, 3rd ed.; Wiley: New York, 1985.
 - (24) Howell, B. A.; Daniel, Y. G. Thermal Degradation of Phosphorus Esters Derived from Isosorbide and 10-Undecenoic Acid. *J. Therm. Anal. Calorim.* **2015**, *121* (1), 411–419.
 - (25) Hardy, C. J. Analysis of Alkyl Esters of Phosphoric Acid by Gas Chromatography. *J. Chromatogr. A* **1964**, *13*, 372–376.
 - (26) Buglass, A. J.; Lee, S. H. Sequential Analysis of Malic Acid and Both Enantiomers of Lactic Acid in Wine Using a High-Performance Liquid Chromatographic Column-Switching Procedure. *Journ. Chrom. Sci.* **2001**, *39* (11), 453–458.
 - (27) Müller, A. Über Die Absorption Des Äthylens Durch Ortho', Pyro' Und Metaphosphorsäure. *Eur. J. Inorg. Chem.* **1925**, *58* (9), 2105–2110.
 - (28) Leprince, P. *Petroleum Refining Vol. 3 Conversion Processes*; Editions Technip: Paris, 2001.

- (29) De Klerk, A. CHE 522 Lecture on Utilities Part I: Off-gas treating. Presented at University of Alberta, Edmonton, AB, 2018.
- (30) Sheu, E. Y.; Mullins, O. C. *Asphaltenes Fundamentals and Applications*; Plenum Press: New York, 1995.
- (31) Masliyah, J. H.; Czarnecki, J.; Xu, Z. *Handbook on Theory and Practice of Bitumen Recovery from Athasbasca Oil Sands. Volume I: Theoretical Basis*; Kingsley Knowledge Publishing: Canada, 2011.
- (32) Gross, L.; Mullins, O. C.; Schuler, B.; Meyer, G.; Peña, D. Unraveling the Molecular Structures of Asphaltenes by Atomic Force Microscopy. *J. Am. Chem. Soc.* **2015**, *137* (31), 9870–9876.
- (33) Aitani, A. M. Oil Refining and Products. In *Encyclopedia of Energy*, El Sevier, 2004, pp. 715–729.
- (34) Alemán-Vázquez, L. O.; Torres-Mancera, P.; Ancheyta, J.; Ramírez-Salgado, J. Use of Hydrogen Donors for Partial Upgrading of Heavy Petroleum. *Energy and Fuels* **2016**, *30* (11), 9050–9060.
- (35) Payan, F.; De Klerk, A. Hydrogen Transfer in Asphaltenes and Bitumen at 250 °C. *Energy and Fuels* **2018**, *32* (9), 9340–9348.
- (36) Gould, K. A.; Wiehe, I. A.; Briarwood, W.; Dri, V.; Heights, B.; Solutions, S.; Lane, L. Natural Hydrogen Donors in Petroleum Resids. *Energy Fuels* **2007**, *21* (3), 1199–1204.
- (37) Naghizada, N.; Prado, G. H. C.; de Klerk, A. Uncatalyzed Hydrogen Transfer during 100–250 ° C Conversion of Asphaltenes. *Energy & Fuels* **2017**, *31* (7), 6800–6811.
- (38) Abell, P. I.; Benson, S. W.; Fischer, H.; Howard, A. J.; Kaplan, L.; Kice, J. L.; Kochi, J. K.; Martin, J. C.; Nelsen, S. F.; O’Neal, E. H.; et al. *Free Radicals: Volume II*; Wiley-Interscience Publication: New York, 1973.
- (39) Ruchardt, C.; Gerst, M.; Nolke, M. The Uncatalyzed Transfer Hydrogenation of α -Methylstyrene by Dihydroanthracene or Xanthene - a Radical Reaction. *Angew. Chem. Int. Ed. Engl.* **1992**, *31* (11), 1523–1525.
- (40) Naghizada, N. Uncatalyzed Hydrogen Transfer during 100–250 ° C Conversion of Asphaltenes, Master of Science Thesis, University of Alberta, Edmonton, AB, 2017.
- (41) Nonhebel, D. C.; Walton, J. C. *Free-Radical Chemistry*; Cambridge University Press: London, 1974.

- (42) Moad, G.; Solomon, D. H. *The Chemistry of Radical Polymerization*, 1st ed.; El Sevier: Oxford, 2006.
- (43) Tempesti, T. C.; Pierini, A. B.; Baumgartner, M. T. Steric Effects of Nucleophile-Radical Coupling Reaction. Determination of Rate Constants for the Reaction of Aryl Radicals with 2-Naphthoxide Anion. *New J. Chem.* **2009**, 33 (7), 1523–1528.
- (44) Gibian, M. J.; Corley, R. C. Organic Radical-Radical Reactions. Disproportionation vs. Combination. *Chem. Rev.* **1973**, 73 (5), 441–464.

CHAPTER 3 – REACTION WITH PHOSPHORIC ACID: AN ALTERNATIVE APPROACH FOR TREATING THERMALLY CRACKED NAPHTHA

Abstract

This work investigated the feasibility of using phosphoric acid to remove the olefins in the thermally cracked naphtha to decrease its olefin content. Hence, phosphoric acid and different model compounds, namely olefins within the range of C₅-C₇ were reacted at 50°C varying the reaction time. Nuclear Magnetic Resonance (NMR) and High-Performance Liquid Chromatography coupled with Mass Spectrometry (HPLC-MS) were used to detect the presence of alkyl phosphoric acid esters in the reaction products. Results indicated that olefin removal is inefficient due to the slow reaction rate. Additionally, it was found that alkyl phosphoric acid esters in the C₆-C₇ range could be soluble in the naphtha. This phase partitioning behavior raises challenges for the usage of phosphoric acid for olefin removal in thermally cracked naphtha.

Keywords: Phosphoric acid, olefin, alkyl phosphoric acid ester, naphtha, NMR, HPLC

3.1 Introduction

The fluidity of bitumen, which is obtained from the Canadian oilsands, is poor. One of the reasons for this poor fluidity is the absence, or near absence of naphtha and kerosene range material,¹ which is commonly present in most conventional crude oils. Deficient fluidity can be addressed by dilution with lighter lower viscosity material, or by conversion to generate lighter lower viscosity material. Ideally, fluidity should be improved as close as practical to the site of production, which may be in remote locations, and at low cost.

When the bitumen is converted to generate a lower viscosity product, one of the lowest cost methods of upgrading is by mild thermal conversion, i.e. visbreaking.² In a visbreaking process, thermal cracking produces lighter products, some of which are olefins. However, fear of fouling during pipeline transport places a limit on the maximum olefin content of oil that is considered acceptable for pipeline transport.

The conventional way of decreasing the olefin content in oil is by hydroprocessing, but hydroprocessing is expensive and requires considerable infrastructure beyond what is needed for the hydroprocessing unit itself. In this way, a process that could be implemented at low cost and potentially in a remote location is desired. This raised the question, what alternative processes could be considered to reduce the olefin content in oil if hydroprocessing could not be considered?

An alternative to reduce the olefin content in oil is to employ selective olefin removal by phosphoric acid. De Filippis, et al.³ proposed a simple test method to determine whether bitumen contained thermally converted material, which was based on reaction with phosphoric acid at 100-140 °C. The addition reaction between phosphoric acid and thermally converted bitumen likely formed alkyl phosphoric acid esters, as described by Ipatieff.⁴ From this work it is known that the thermal stability of the alkyl phosphoric acid esters depends on the nature of the alkyl group.⁵

It was reasoned that ester formation by reaction at lower temperature, followed by ester decomposition at higher temperature could be employed to remove reactive olefins from thermally cracked bitumen in a temperature-swing process, as illustrated in Figure 3.1.

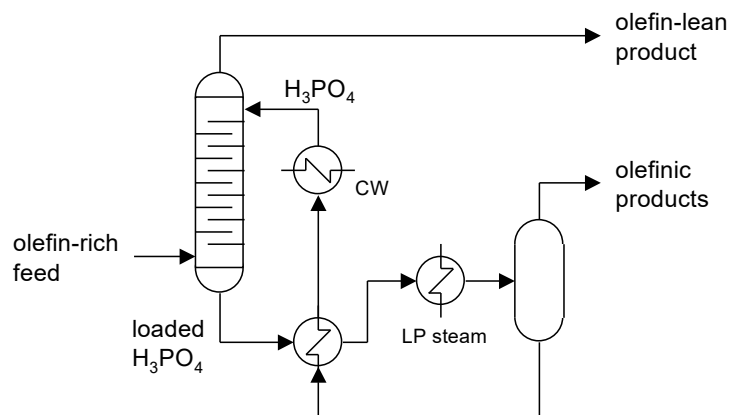


Figure 3.1 Proposed process to reduce olefin content in an olefin-containing feed without the use of hydrogen (pumps not shown)

In the proposed process (Figure 3.1), the olefin-rich material is contacted with the phosphoric acid in an appropriate vessel, such as a counter-current liquid-liquid extraction column. The olefins react with the phosphoric acid to form alkyl phosphoric acid esters that are retained in the polar phase during reactive removal. After reactive removal, the loaded phosphoric acid is heated up to regenerate the phosphoric acid. The alkyl phosphoric acid esters are decomposed, with the olefins separating as an olefinic product containing olefin monomers and heavier oligomers.

The bulk of the olefins formed by thermal cracking of bitumen are concentrated in the lighter product fractions. It is therefore not necessary to treat the thermally cracked bitumen as a whole, but only the lighter fractions. The material in the lighter product fraction is also less polar and less viscous compared to bitumen. However, some of the lighter olefins react with phosphoric acid to form alkyl phosphoric acid esters with lower decomposition temperatures.

It was suspected that the proposed process would require reaction at a low enough temperature to prevent alkyl phosphoric acid ester decomposition, imposing a limitation on the reaction rate. It was also suspected that the proposed process would face mass transport limitations related to the polarity difference between the phosphoric acid and organic phases. In these respects, the literature was of limited assistance.

The purpose of the present investigation was to experimentally evaluate the reactive absorption step of the process shown in Figure 3.1. The reactivity of C₅-C₇ naphtha range olefins with phosphoric acid at < 100 °C was determined, as well as the phase partitioning of the alkyl phosphoric acid esters of different types of olefins, i.e. linear, branched, and cyclic.

3.2 Experimental

3.2.1 Materials

Olefins in the C₅-C₇ carbon number range were selected as model compounds. In all cases, linear, branch, and cyclic structures were selected to evaluate the effect of the olefin structure on the reactivity with phosphoric acid at low temperature. The materials used for the experimental work are listed in Table 3.1.

Table 3.1 Materials employed for this experimental study

Compound	Formula	CASRN ^a	Mass fraction purity ^b	Supplier
<i>Materials used for reactions</i>				
1-pentene	C ₅ H ₁₀	109-67-1	0.98	Sigma-Aldrich
2-methyl-1-butene	C ₅ H ₁₀	563-46-2	0.98	Sigma-Aldrich
2-methyl-2-butene	C ₅ H ₁₀	563-35-9	≥0.95	Sigma-Aldrich
cyclopentene	C ₅ H ₈	142-29-0	0.96	Sigma-Aldrich
1-hexene	C ₆ H ₁₂	592-41-6	0.97	Sigma-Aldrich
2-methyl-1-pentene	C ₆ H ₁₂	763-29-1	≥0.99 (GC)	Sigma-Aldrich
cyclohexene	C ₆ H ₁₀	110-83-8	0.99	Sigma-Aldrich
1-heptene	C ₇ H ₁₄	592-76-7	0.97	Sigma-Aldrich
2-methyl-1-hexene	C ₇ H ₁₄	6094-02-6	0.96	Sigma-Aldrich
4-methylcyclohexene	C ₇ H ₁₂	591-47-9	0.99	Sigma-Aldrich
phosphoric acid	H ₃ PO ₄	7664-38-2	0.85	Fisher Scientific
<i>Materials used for identification</i>				
<i>cis</i> -2-hexene	C ₆ H ₁₂	7688-21-3	0.97	Fluka Chemika
<i>trans</i> -2-hexene	C ₆ H ₁₂	4050-45-7	0.99	Alfa Aesar
<i>cis</i> -3-hexene	C ₆ H ₁₂	7642-09-3	0.96	Sigma Aldrich
<i>trans</i> -3-hexene	C ₆ H ₁₂	13269-52-8	0.98	Alfa Aesar
<i>Solvent for NMR</i>				
chloroform-d	CDCl ₃	865-49-6	0.998	Acros Organic
deuterium oxide	D ₂ O	7789-20-0	0.999	Sigma- Aldrich
dimethyl sulfoxide-d ₆	(CD ₃) ₂ SO	2206-27-1	0.9999	Sigma-Aldrich
<i>Cylinder gases</i>				
nitrogen	N ₂	7727-37-9	0.99 ^c	Praxair

^a CASRN = Chemical Abstracts Services Registry Number

^b This is the purity of the material guaranteed by the supplier; material was not further purified.

^c Mole fraction purity.

3.2.2 Equipment and procedure

3.2.2.1 Olefin reactive absorption

Each olefin was mixed with 85% phosphoric acid (molar ratio 1:1) and reacted at 50 °C for 68 h. The decision to evaluate the process with 85 % phosphoric acid, was to avoid the more complicated chemistry when more than one phosphoric acid species is present.⁶ Experiments dealing with C₅ olefins, namely 1-pentene, 2-methyl-2-butene, and cyclopentene, were carried out in Swagelok stainless steel batch reactors. In all cases, an equimolar amount of C₅ olefin and 85% phosphoric acid (0.08 moles) and a magnetic stirrer were placed in a clear glass test tube inside the reactor. The reactor was then closed and pressurized with nitrogen to 6MPa in order to ensure reaction in liquid phase. Heating was achieved by placing the reactor inside an oil bath (Julabo Bath Fluid Thermal C50S) set on top of a magnetic hot plate stirrer (Fisher Scientific Isotemp Hote Plate Stirrer) equipped with temperature control. Stirring was at kept 1500 rpm. A schematic of the experimental set up is presented in Figure 3.2 (a).

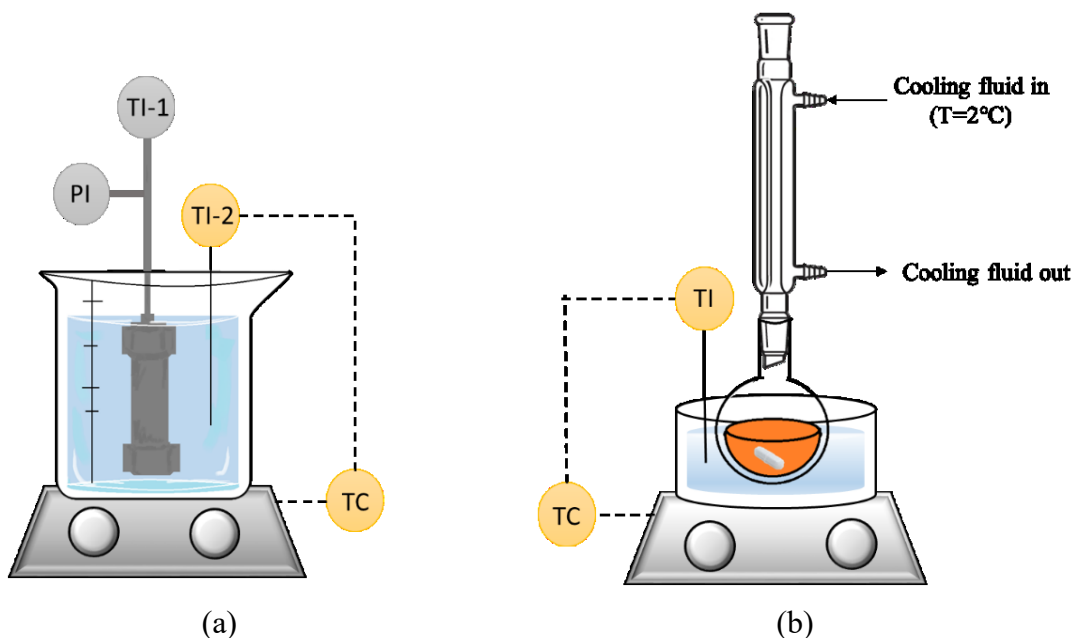


Figure 3.2 Experimental set up for the reactions (a) pressurized batch reactor system with stirring for C₅ olefins (b) ball flask with reflux system with stirring for C₆ and C₇ olefins

As C₆ and C₇ olefins have higher boiling points, it was not necessary to conduct the experiments under pressurized conditions for liquid phase reaction. Therefore, the experiments with C₆ and C₇ olefins were conducted at 50 °C under atmospheric pressure for 68 h in a standard reflux setup consisting of a round bottom flask and a condenser kept at 2 °C (Figure 3.2 (b)). An equimolar amount of C₆ or C₇ olefin and 85% phosphoric acid (0.08 moles) were placed inside the flask with a magnetic stirrer. The flask was then placed in an oil bath set on top of a magnetic hot plate stirrer equipped with temperature control. Because of the change in setup geometry, it was found that a lower stirring speed was more effective in this case. Stirring was kept between 200-500 rpm. In addition, a blank experiment in which 85% phosphoric acid was heated at reaction conditions was also performed to verify that the acid would not self-react under these conditions.

After reaction, two immiscible layers, namely aqueous and organic phases, were observed. Each phase was recovered by using a separation funnel and stored for further analyses. Reactions for cyclohexene and 4-methylcyclohexene produced an emulsion layer. Emulsions were not broken and are considered as a third phase in the present study.

All weight measurements were performed on an analytical balance (Mettler Toledo, Model XP1203S) with a maximum capacity of 1210 g and readability to 0.001 g. Mass balance for all experiments was between 97-99 %.

3.2.2.2 Quantification of olefin removal rate

Olefin removal rate by chemical absorption with phosphoric acid was evaluated. Reaction of 1-hexene with phosphoric acid was used, as an example, to quantify the effectiveness of this strategy. 1-Hexene was reacted with 85% phosphoric acid (1:1 molar ratio) at 50°C and atmospheric pressure for 2, 5, 24, and 68 h. The experimental setup was similar to the one presented in Figure 3.2 (a) as the reaction of 1-hexene with phosphoric acid does not require high pressures to maintain a liquid phase reaction under the temperature studied.

After reaction, *n*-hexane was added to the sample in an equal amount as 1-hexene; the sample was later topped up with 20g of *n*-heptane. By doing so, two immiscible liquid phases were formed

and recovered using a separation funnel. In this case, *n*-heptane was added to decrease the loss of material in the organic layer during phase recovery. On the other hand, as *n*-hexane has a similar structure to 1-hexene, it was added to the product to simulate and track the behavior of 1-hexene, in case the addition of *n*-heptane affects its phase partitioning between the organic and aqueous layer. A blank sample was also prepared by mixing the same amount of 1-hexene and *n*-hexane with 20 g of *n*-heptane for determining how much of each compound should be present if no reaction with phosphoric acid occurred.

The organic layer recovered in each case was further analyzed by gas chromatography with flame ionization detector (GC-FID) for quantification of the olefins as well as reverse-phase high-performance liquid chromatography-ultraviolet-mass spectrometry (RP-HPLC-UV-MS) for identification of alkyl phosphoric acid esters. In the case of GC-FID, a calibration curve was prepared. *n*-Octane was used as an internal standard and *n*-heptane was used as the solvent.

3.2.3 Analyses

3.2.3.1 Nuclear magnetic resonance (NMR) spectroscopy

Samples analyzed by nuclear magnetic resonance (NMR) spectroscopy were prepared in Norell XR-55-7 standard series NMR tubes (7 inch long NMR tubes with a 5 mm outer diameter). In all cases, approximately 100 μ L of sample was diluted with approximately 0.7 mL of deuterated NMR solvent. The organic phase was diluted with CDCl_3 and the aqueous phase was diluted with D_2O . In addition, DMSO-d_6 was used for dilution of emulsion layers.

Agilent/Varian 400, 500 and 600 MHz spectrometers were used to acquire proton and phosphorous spectra. The Inova 400 and 500 MHz instruments were equipped with a broadband Z-gradient probe. The VNMRS 600 MHz instrument used a Z-gradient indirect detection HCN triple resonance probe to acquire ^1H data on dilute samples. All samples were measured at 27 $^\circ\text{C}$. Parameters for one-dimensional data sets were adjusted in order to improve the signal to noise ratio as needed. The sweep width for ^1H was 11 to -1 ppm and 150 to -150 ppm for ^{31}P . The acquisition time was 5 s for ^1H and 1s for ^{31}P , with a relaxation delay of 0.1 s and 30 $^\circ$ flip angle.

A total of 16 scans were acquired for ^1H . ^{31}P spectra were recorded with ^1H decoupling at all times during the pulse sequence and as many as 3000 scans were used depending on the signal to noise ratio of the spectrum is acquired. Data processing was carried out using the spectrometer acquisition software, VNMRJ 4.2A.

Additional NMR experiments were performed to detect and elucidate organophosphorus compounds, namely ^1H $\{^{31}\text{P}\}$ decoupling and one-dimensional Total Correlation Spectroscopy which employed a zero-quantum filter (zTOCSY) and 100 ms spin lock mixing time. Two-dimensional experiments such as ^1H - ^{31}P gradient selected heteronuclear single quantum coherence (gHSQC) and gradient selected double quantum filtered correlation spectroscopy (gDQF-COSY) were also carried out. Samples were referenced depending on the type of experiment and the nature of the sample. For ^1H NMR, aqueous samples were referenced to external DSS (4,4-dimethyl-4-silapentane-1-sulfonic acid). Organic samples were referenced to the residual protonated component of the deuterated solvent used to make the sample, i.e. the CHCl_3 resonance in CDCl_3 set to be 7.26 ppm downfield from TMS. For ^{31}P NMR, aqueous samples were referenced to the residual phosphoric acid in the sample; while, organic samples were referenced to external 85% phosphoric acid.

3.2.3.2 Reverse Phase High-Performance Liquid Chromatography-Ultraviolet-Mass Spectrometry (RP-HPLC-UV-MS)

RP-HPLC-UV-MS was performed using an Agilent 1200 SL HPLC System with a Phenomenex Kinetex C8 reverse-phase analytical column (2.1x50mm) with guard (Phenomenex, Torrance, CA, USA), thermostated at 50 °C followed UV and mass spectrometric detection. An aliquot of 5 μL was loaded onto the column at a flow rate of 0.50 mL/min and an initial buffer composition of 98 % of 0.1 % formic acid as mobile phase A and 2 % of 0.1 % acetonitrile as mobile phase B. The column was washed at the initial condition for 1 minute to effectively remove the salts followed by the elution of the analytes using a linear gradient from 2 % to 98 % mobile phase B over a period of 7 minutes, held at 98 % mobile phase B for 3 minutes to remove all analytes from the column and 98 % to 2 % mobile phase B over a period of 1.0 minute.

Mass spectra were acquired in negative mode ionization using an Agilent 6220 Accurate-Mass TOF HPLC/MS system (Santa Clara, CA, USA) equipped with a dual sprayer electrospray ionization source with the second sprayer providing a reference mass solution. Mass spectrometric conditions were drying gas 9 L/min at 325 °C, nebulizer 140 kPa, mass range 100-1100 Da, acquisition rate of ~1.03 spectra/sec, fragmentor 110V, skimmer 65V, capillary 3500V, instrument state 4GHz High Resolution. Mass correction was performed for every individual spectrum using peaks at m/z 112.98558 and 1033.98811 from the reference solution. Data acquisition was performed using the Mass Hunter software package (ver. B.04.00.). Analysis of the HPLC-UV-MS data was done using the Agilent Mass Hunter Qualitative Analysis software (ver. B.07.00).

Possible molecular formulas for the reaction products were obtained from the HPLC-UV-MS data analysis. Because of the overall complexity of the mass spectra data, the peak selection and molecular formula generation process was limited to molecules with no more than 2 phosphorous, 100 carbon, 100 hydrogen, and 8 oxygen atoms. The number of reported matches of molecular formula to each peak in the corresponding mass spectrum was set to two, limiting the detection to a maximum of two isomers per molecular formula.

3.2.3.3 Gas Chromatography with Flame Ionization Detector (GC-FID) and Gas Chromatography with Mass Spectrometry (GC-MS)

GC-FID was used to quantify the olefin conversion and GC-MS was used to identify the side reaction products that were formed in the organic phase. Reacted samples were dissolved in *n*-heptane for analysis in the GC-FID and GC-MS. Analyses for quantification were carried out using an Agilent Model 7890A gas chromatography (GC) equipped with a flame ionization detector (FID). The separation was performed on an Agilent 19091S-001 HP-PONA capillary column of 50 m x 0.20 mm x 0.50 μm . The carrier gas was a constant flow rate of helium at 1 mL/min. The oven temperature program was set to start at 35 °C and held for 30 minutes; then, the temperature was increased to reach 75 °C at a rate of 2 °C/min; a second temperature ramp was added to reach 100 °C at 5 °C/min and finally, 325 °C at 20 °C/min.

Analyses for identification were performed with an Agilent Model 7820A gas chromatography (GC) coupled with an Agilent Model 5977E MSD mass spectrometry (MS) detector. Separation was carried out in the same column model as the GC-FID, and all parameters were the same as well. Product identification was done by comparing the mass spectra of the products with the database of the National Institute of Standards and Technology (NIST) through the NIST MS Search 2.0 – Mass Spectra Library.

As the GC-MS could not provide accurate identification of the C₆ olefin isomers, the model compounds were injected into the GC-FID and using the same method to identify the corresponding C₆ isomers.

3.2.4 Calculations

The following calculations were performed to obtain the results regarding relative abundance, conversion, and selectivity for better comparison between the experimental data.

- Relative abundance of compound i:

The relative abundance is defined as the abundance of each compound relative to the abundance of the relevant compounds. Relevant compounds were defined as products with a formula score of more than 70 % and more than 1000 units in abundance from the results obtained from HPLC-UV-MS analyses.

$$\text{Relative abundance}_i = \frac{\text{Abundance of compound}_i}{\sum \text{abundance of all relevant compounds}}$$

(Eq. 8)

- Conversion of 1-hexene at a determined reaction time:

The conversion of 1-hexene was determined by taking into consideration, based on the experimental results, that little 1-hexene was removed from the organic layer. Therefore, the conversion of 1-hexene was mainly towards the production of C₆ olefin isomers.

$$\text{Conversion} = 1 - \frac{\text{Area of 1-hexene}}{\sum \text{Areas of 1-hexene and C}_6 \text{ isomers}}$$

(Eq. 9)

- Selectivity towards compound i:

The following equation was used to determine the selectivity of the reaction of 1-hexene and H₃PO₄ towards the formation of each C₆ olefin isomer:

$$\text{Selectivity for compound}_i = \frac{\text{Area of isomer}_i}{\sum \text{Areas of all C}_6 \text{ isomers}}$$

(Eq. 10)

3.3 Results

3.3.1 Detection of alkyl phosphoric acid esters with NMR Spectroscopy

The first step in the process shown in Figure 3.1 is the reactive absorption of the olefins in the cracked naphtha. This step involves the formation of an alkyl phosphoric acid ester through the reaction of H₃PO₄ with an olefin in the aqueous phase. It was consequently important to confirm that alkyl phosphoric acid esters were formed and were present in the aqueous phase.

Formation of alkyl phosphoric acid esters was confirmed through NMR spectroscopy. Both phosphorous nuclear magnetic resonance (³¹P NMR) and proton nuclear magnetic resonance (¹H

NMR) spectra were obtained. The presence of organic phosphorus, as well as the presence of hydrogen on the carbon attached to the alkyl phosphoric acid ester group, was investigated in all cases.

Results from the analysis of the aqueous phase recovered after reacting cyclopentene with phosphoric acid are presented in the following to illustrate the detection process for alkyl phosphoric acid esters. First, a ^{31}P NMR spectrum of the sample was acquired to detect the presence of phosphorous compounds. The corresponding spectrum (Figure 3.3) showed two clear resonances at 0.0 ppm and -0.77 ppm. The signal at 0.0 ppm reflects unreacted phosphoric acid in the sample; whereas, the signal at -0.77 ppm indicates the presence of a second phosphorus-containing compound in the sample. Chemical shifts for phosphate monoesters have been reported to occur in a wide range, 0 to -10 ppm.⁷ Moreover, chemical shifts are influenced by environmental conditions such as pH, temperature, concentration, as well as torsional angles and neighboring groups around the nucleus.⁸⁻¹⁰ Therefore, even though the presence of a phosphoric acid ester is likely in this case, further analysis was carried out to elucidate the nature of the second phosphorus-containing compound.

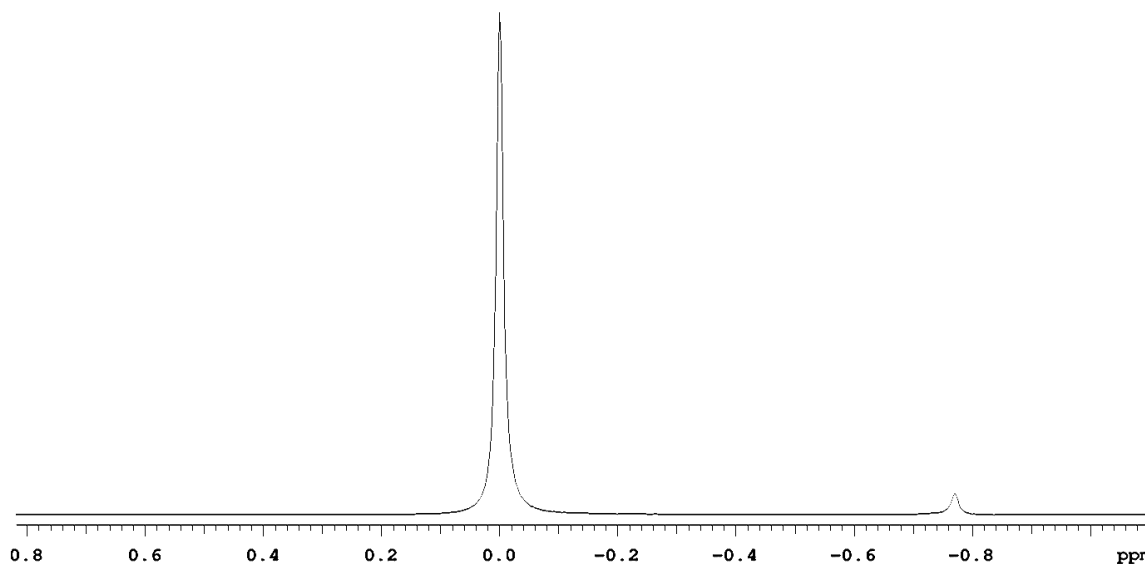


Figure 3.3 ^{31}P NMR spectrum of the aqueous phase recovered after reaction of cyclopentene with phosphoric acid. Reaction conditions: 50°C, 6MPa, and 68 h

A ^1H NMR spectrum of the same sample was also acquired (Figure 3.4). Even though the spectrum is complex, the peaks present in the 4.0-4.6 ppm region suggested the presence of an ester group. Chemical shifts of methyl esters have been reported to occur in the 3.7-3.9 ppm range and ethyl esters in the 4.0-4.8 ppm range.¹¹ In addition, chemical shifts for alpha-monosubstituted aliphatic compounds typically occur around 2.0-5.0 ppm.¹² It is worth to mention that the chemical shifts observed in the 1.0-2.0 ppm region of the spectrum (peak 3) are associated with aliphatic acyclic protons of the cyclopentane, which is attached to the phosphoric acid ester.¹²

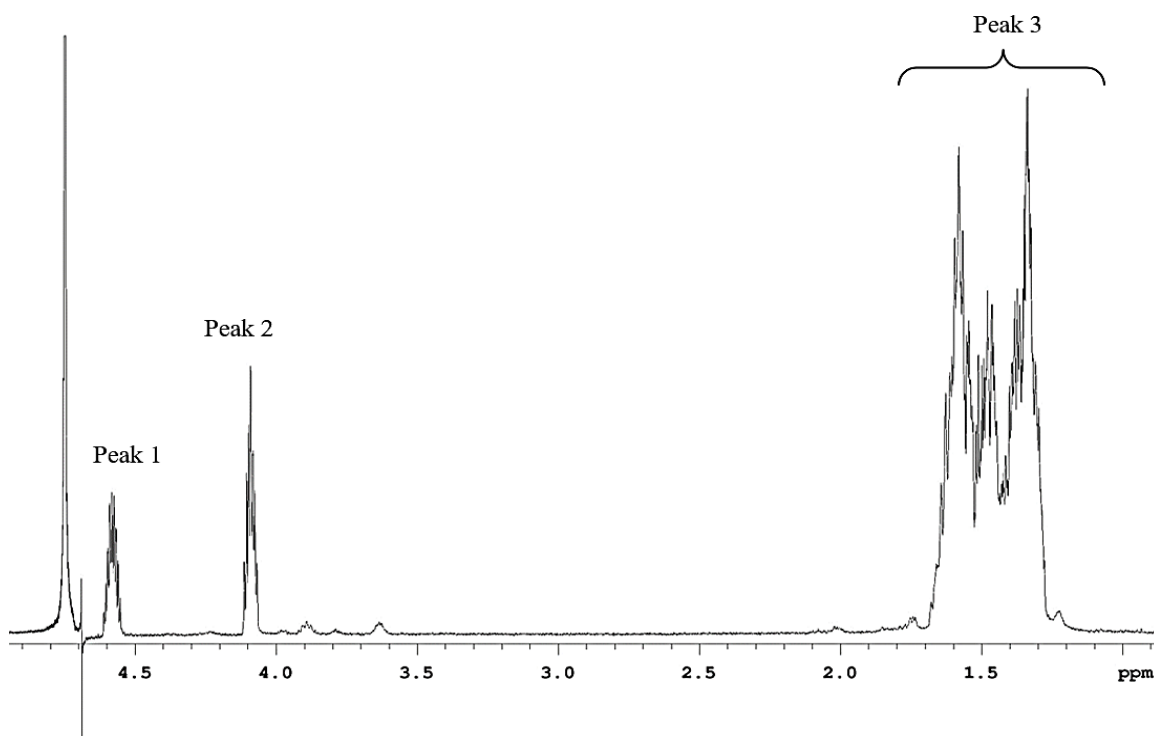


Figure 3.4 ^1H NMR spectrum of the aqueous phase recovered after reaction of cyclopentene with phosphoric acid. Reaction conditions: 50°C, 6MPa, and 68 h

Peaks in Figure 3.4, specifically the apparent nonet (peak 1) and apparent septet (peak 2), were further analyzed. Because of the uncommon presence of a nonet, ^1H $\{^{31}\text{P}\}$ decoupling and one-dimensional ^1H zTOCSY experiments were conducted to simplify the ^1H NMR spectrum. The proton associated with peak 1 was selectively excited for the one-dimensional ^1H zTOCSY. This experiment allowed the simplification of the ^1H NMR spectrum by removing the components that

are not within the same spin system as peak 1 (Figure 3.5). The ^1H zTOCSY results indicated that peaks 1 and 2 are not associated (peak 2 disappeared from ^1H NMR the spectrum). In contrast, peak 1 was observed to be associated with the aliphatic alicyclic protons of the cyclopentane (peak 3 did not disappear from ^1H NMR the spectrum).

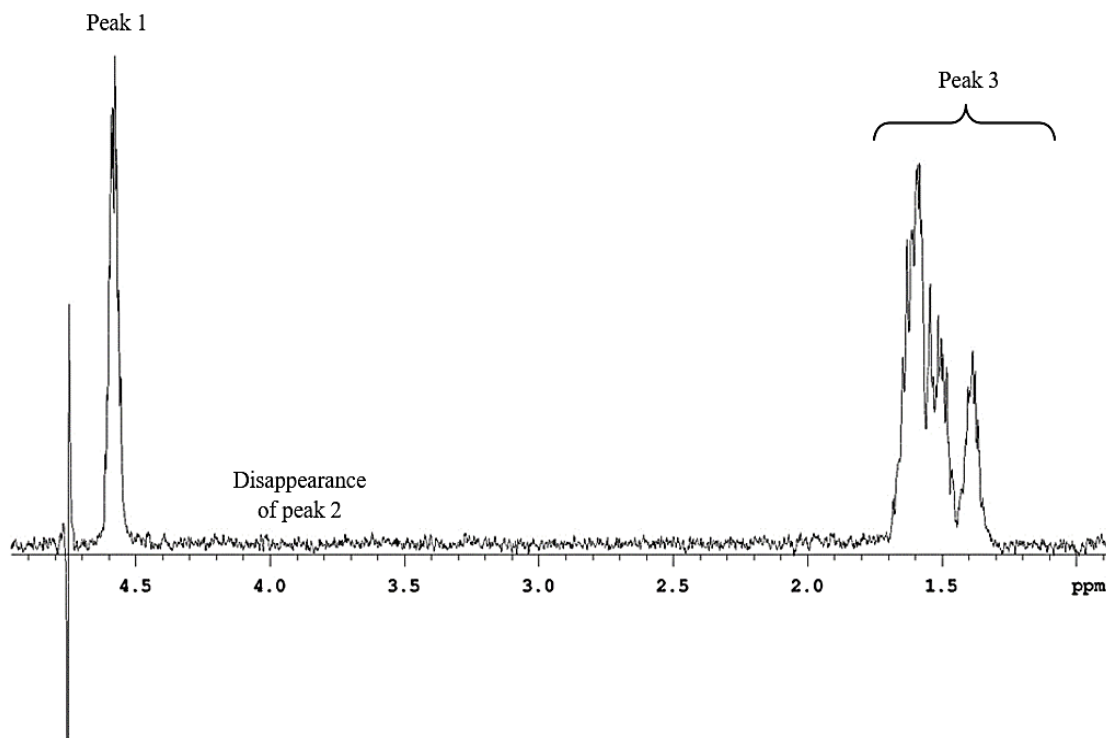


Figure 3.5 ^1H one-dimensional zTOCSY spectrum of the aqueous phase recovered after reaction of cyclopentene with phosphoric acid. Reaction conditions: 50°C, 6MPa, and 68 h

In combination with the information obtained from the one-dimensional ^1H zTOCSY experiment, the ^1H $\{^{31}\text{P}\}$ decoupling experiment indicated that peak 1 is actually a septet once the scalar coupling of phosphorus was removed (Figure 3.6). The septet can be interpreted as a triplet of triplets, indicating the two different sets of neighboring hydrogens scalar coupling with the proton that is also coupled to phosphorous. As a result, the detected proton corresponds to the alpha hydrogen that is associated with a carbon bonded to the phosphoric acid ester group (indicated proton in Figure 3.6).

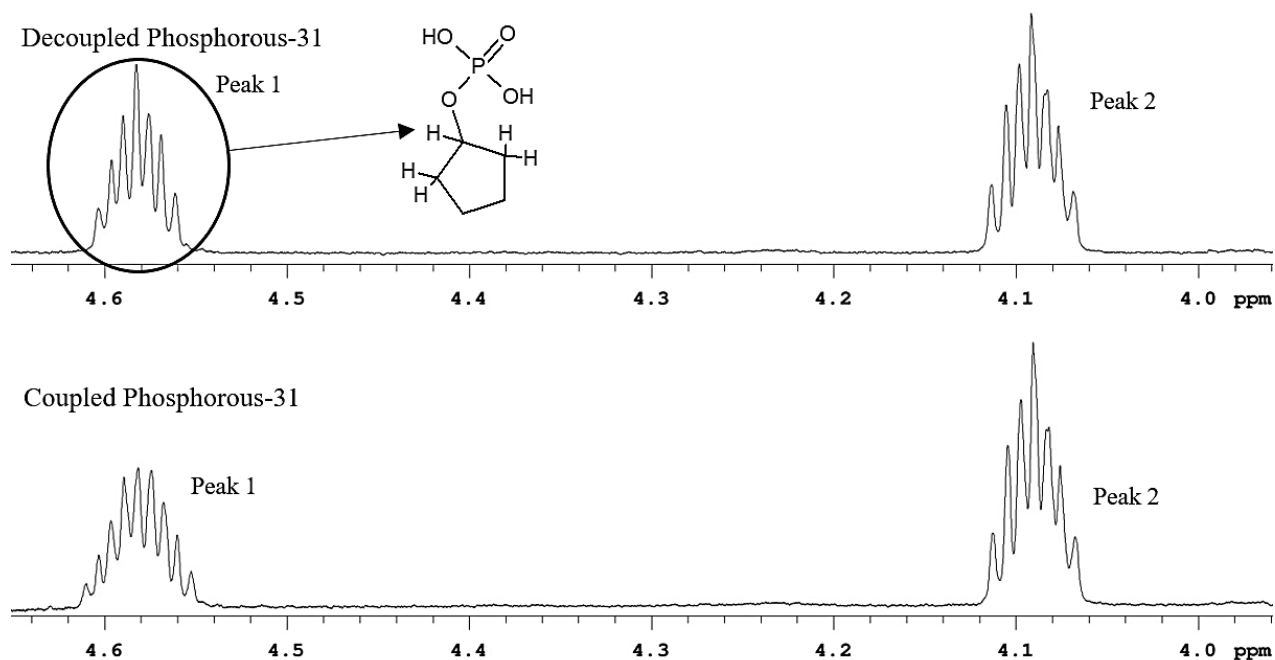


Figure 3.6 $^1\text{H} \{^{31}\text{P}\}$ decoupling spectrum of the aqueous phase recovered after reaction of cyclopentene with 85% phosphoric acid. Reaction conditions: 50°C, 6MPa, and 68 h

A two-dimensional ^1H - ^{31}P gHSQC experiment was performed to verify the bond between the aliphatic group and the phosphate group and identify the specific phosphorus resonance (Figure 3.7). This 2D experiment indicated that ^1H resonance referred to as peak one at 4.57 ppm is attached to the ^{31}P resonance at -0.77 ppm.

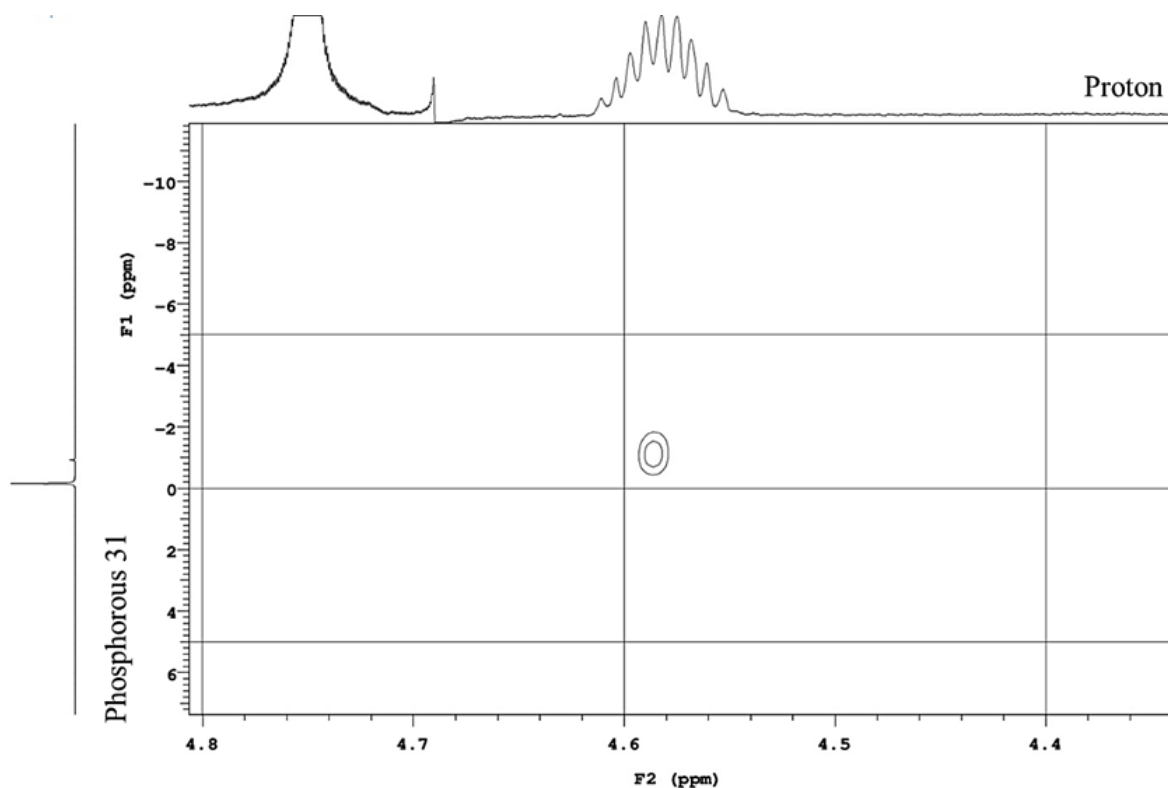

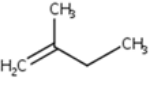
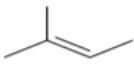

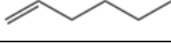
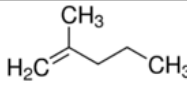
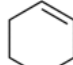

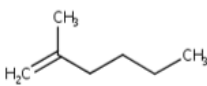
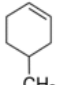


Figure 3.7 ^1H - ^{31}P gHSQC spectrum of the aqueous phase cyclopentene reaction with 85% phosphoric acid in D_2O

3.3.2 Phase partitioning of alkyl phosphoric acid esters using NMR

Although the primary aim was to confirm the presence of alkyl phosphoric acid esters in the aqueous phase, it was also important to check whether any alkyl phosphoric acid esters were present in organic phase and emulsion phase, when such a phase was present. Detection of alkyl phosphoric acid esters in all reacted samples followed a similar procedure. ^{31}P NMR and ^1H NMR experiments were common experiments and depending on the initial results, samples were further analyzed, if necessary, with ^1H $\{^{31}\text{P}\}$ decoupling, one-dimension ^1H zTOCSY and/or two-dimension ^1H - ^{31}P gHSQC. The outcome of the analyses is presented in Table 3.2.

Table 3.2 Detection of alkyl phosphoric acid esters formation using NMR for C₅-C₇ reactions with 85% phosphoric acid at 50 °C for 68 h

Chain length	Compound	Structure	Aqueous	Organic	Emulsion
C ₅	1-pentene		✓	X	- ^a
	2-methyl-1-butene		✓	X	- ^a
	2-methyl-2-butene		X	X	- ^a
	cyclopentene		✓	✓	- ^a
C ₆	1-hexene		✓	✓	- ^a
	2-methyl-1-pentene		✓	X	- ^a
	cyclohexene		✓	- ^b	✓
C ₇	1-heptene		✓	✓	- ^a
	2-methyl-1-hexene		X	X	- ^a
	4-methylcyclohexene		✓	✓	✓

^a No emulsion phase was formed

^b No separate organic phase, all of the organic phase was emulsified

It was surprising not to find evidence of the alkyl phosphoric acid ester of 2-methyl-2-butene in the aqueous phase product. Likewise, there was no evidence of the alkyl phosphoric acid ester of 2-methyl-1-hexene either. In some instances where alkyl phosphoric acid esters were detected in the aqueous phase, they were also detected in the other phases. However, the absence of the alkyl phosphoric acid ester of 2-methyl-2-butene, which should have been detected based on its

reactivity during phosphoric acid catalysis,¹³ raised the question: was it present but below the detection limit of NMR?

3.3.3 Detection of alkyl phosphoric acid esters with HPLC-UV-MS

Detection of alkyl phosphoric acid esters at low concentration required separation before detection. For this purpose, chromatographic techniques were considered. On one hand, the alkyl phosphoric acid esters are sensitive to decomposition and release phosphoric acid when subject to high temperatures, which disqualifies gas chromatography as analytical technique for separation and analysis of alkyl phosphoric acid esters.⁴ Detection of alkyl phosphoric acid esters in concentrated phosphoric acid is complex as the direct injection of acidic samples can damage certain instruments.¹⁴ For instance, detection of alkyl phosphoric acid esters through chromatographic analysis is limited due to the stability of the column towards the acid. Analytical procedures involving several systematic reactions have been reported in the literature; however, they tend to be time-consuming and not sensitive to detect small quantities of alkyl phosphoric acid esters.⁴

High-performance liquid chromatography has been used with success for analysis of phosphoric acid species.¹⁵ Therefore, samples for which the presence of phosphoric acid esters could not be confirmed through NMR analysis were further analyzed by HPLC-UV-MS. In several instances where no alkyl phosphoric acid esters were detected by NMR analysis, HPLC analysis was able to confirm their presence (Table 3.3). The only instance where no alkyl phosphoric acid esters were detected was the aqueous phase product from reaction with 2-methyl-1-hexene.

Table 3.3 Detection of alkyl phosphoric acid esters formation using HPLC-UV-MS for C₅-C₇ reactions with 85% phosphoric acid at 50 °C for 68 h

Chain length	Compound	Structure	Aq.	Org.	Em.
C ₅	1-pentene		✓	✓ ^a	- ^b
	2-methyl-1-butene		✓	✓ ^a	- ^b
	2-methyl-2-butene		✓ ^a	✓ ^a	- ^b
	cyclopentene		✓	✓	- ^b
C ₆	1-hexene		✓	✓	- ^b
	2-methyl-1-pentene		✓	✓ ^a	- ^b
	Cyclohexene		✓	- ^c	✓
C ₇	1-heptene		✓	✓	- ^b
	2-methyl-1-hexene		X	✓ ^a	- ^b
	4-methylcyclohexene		✓	✓	✓

^a Not observed by NMR (Table 3.2), concentration too low.

^b No emulsion phase was formed.

^c No separate organic phase, all of the organic phase was emulsified.

3.3.4 Identification of alkyl phosphoric acid esters with HPLC-UV-MS

The presence of alkyl phosphoric acid esters in the organic phase meant that the ester-forming reaction between the olefins and phosphoric acid caused a sufficient change in polarity that the alkyl phosphoric

acid esters were soluble in the organic phase. It was decided to look in more detail at the species that were present in the organic phase to better understand the nature of the alkyl phosphoric acid esters that dissolved in the organic phase.

Table 3.4 Organo-phosphorous products present in the organic phase recovered from reaction of C₅-C₇ branched olefins with 85% phosphoric acid at 50 °C for 68 h

	Retention time (min)	Suggested molecular formula	Relative abundance (%)
C ₅ 2-methyl-1-butene	1.27-1.49	C ₅ H ₁₃ O ₄ P	60
	4.09-4.28	C ₅ H ₁₃ O ₄ P	1
	4.09-4.29	C ₁₀ H ₂₃ O ₄ P	35
	4.28-4.58	C ₁₁ H ₂₅ O ₄ P	1
	5.44-5.82	C ₁₇ H ₃₅ O ₄ P	1
	5.63-6.07	C ₁₈ H ₃₇ O ₄ P	1
	5.85-6.10	C ₁₉ H ₃₉ O ₄ P	1
C ₆ 2-methyl-1-pentene	1.41-1.62	C ₆ H ₁₃ O ₄ P	- ^a
	3.18-3.35	C ₆ H ₁₅ O ₄ P	4
	3.38-3.54	C ₆ H ₁₅ O ₄ P	30
	5.39-5.63	C ₁₂ H ₂₅ O ₄ P	31
	5.74-6.03	C ₁₃ H ₂₇ O ₄ P	- ^a
	5.92-6.06	C ₁₂ H ₂₇ O ₄ P	- ^a
	6.29-6.54	C ₁₂ H ₂₇ O ₄ P	10
	6.75-7.06	C ₁₆ H ₃₃ O ₄ P	5
	7.47-7.99	C ₂₀ H ₃₉ O ₄ P	1
	8.00-8.16	C ₁₈ H ₃₇ O ₄ P	16
	8.16-8.58	C ₁₈ H ₃₉ O ₄ P	1
	8.21-8.53	C ₂₂ H ₄₅ O ₄ P	- ^a
8.76-9.00	C ₂₂ H ₄₅ O ₄ P	2	
C ₇ 2-methyl-1-hexene	2.28-2.49	C ₇ H ₁₅ O ₄ P	68
	3.28-3.56	C ₇ H ₁₇ O ₄ P	21
	5.74-5.95	C ₁₄ H ₃₁ O ₄ P	11

^a Detectable, but very low abundance

The first group of compounds that was evaluated was the alkyl phosphoric acid esters in the organic phase product after reactive absorption of 2-methyl-1-butene, 2-methyl-1-pentene, and 2-methyl-1-hexene. These species appeared to be more soluble in the organic phase because 2-methyl-1-hexene was the only olefin formed with no products that were soluble in the aqueous phase. The species identified by HPLC-MS analysis are shown in Table 3.4 and the product distribution varied in all cases.

The reaction product from 2-methyl-1-butene contained mainly C₅-alkyl phosphoric acid esters (61 %) and C₁₀-alkyl phosphoric acid esters (35 %). In the case of the C₁₀-alkyl phosphoric acid esters, mass spectrometry was not useful to differentiate between a di-C₅-alkyl and mono-C₁₀-alkyl attached to the phosphoric acid. It was likely that the products were monoesters because the dissociation constant of the second hydrogen in H₃PO₄ is low and unlikely to yield an appreciable amount of di-ester formation.¹⁶ The amount of heavier products was minor and based on the molecular formula suggested by mass spectrometry there were also alkyl groups with an alkyl chain length that were not integer multiples of the alkyl chain length of C₅.

The organic phase product from the reaction of 2-methyl-1-pentene contained C₆-, C₁₂- and C₁₈-alkyl phosphoric esters with a relative abundance of around 34 %, 41%, and 17% respectively. As in the case of the reaction of 2-methyl-1-butene, mass spectrometry was not useful to differentiate between alkyl groups that were oligomers and multiple alkyl groups. Some heavier products and products with an alkyl chain length that was not an integer multiple of C₆ were detected. The formation of heavier than C₁₈-alkyl esters can only be explained when olefin oligomerization takes place and cannot be explained just in terms of multiple alkyl groups.

One other noteworthy observation was that the molecular formula that was suggested for some of the alkyl phosphoric acid esters by mass spectrometry was hydrogen deficient, for example, C₆H₁₃O₄P and C₆H₁₅O₄P, C₁₂H₂₅O₄P and C₁₂H₂₇O₄P, and C₁₈H₃₇O₄P and C₁₈H₃₉O₄P. Considering the high abundance of some of the hydrogen deficient species, it appears unlikely that the suggested molecular formula reflected a molecule that was actually hydrogen deficient, but the possibility of hydrogen deficiency could not be ruled out.

The least complicated reaction product was obtained from the reaction of 2-methyl-1-hexene. According to the molecular formula suggested by mass spectrometry, the reaction products consisted only of C₇-alkyl (89 %) and C₁₄-alkyl (11 %) phosphoric acid esters.

The study was expanded to look in more detail at the alkyl phosphoric acid esters formed by different olefins with the same carbon number, which would also provide information on the species formed by reaction with linear and cyclic olefins. The C₅ olefins were selected for this purpose. The alkyl phosphoric acid esters identified in the organic phase reaction products from reaction with 1-pentene, 2-methyl-2-butene, and cyclopentene are presented in Table 3.5.

Table 3.5 Organo-phosphorous products present in the organic phase recovered from reaction of C₅ olefins with 85% phosphoric acid at 50 °C for 68 h

	Retention time	Suggested molecular formula	Relative Abundance (%)
1-pentene	1.13-1.42	C ₅ H ₁₃ O ₄ P	54
	1.16-1.38	C ₁₀ H ₂₆ O ₈ P ₂	16
	3.82-3.95	C ₁₀ H ₂₁ O ₄ P	- ^a
	3.96-4.15	C ₁₁ H ₂₃ O ₄ P	- ^a
	4.07-4.33	C ₁₀ H ₂₃ O ₄ P	26
	4.14-4.34	C ₅ H ₁₃ O ₄ P	- ^a
	4.17-4.52	C ₁₂ H ₂₅ O ₄ P	1
	4.42-4.59	C ₁₃ H ₂₇ O ₄ P	1
	5.07-5.55	C ₁₅ H ₃₁ O ₄ P	- ^a
	5.24-5.71	C ₁₆ H ₃₃ O ₄ P	- ^a
	5.25-5.43	C ₁₅ H ₃₃ O ₄ P	- ^a
	5.35-5.82	C ₁₇ H ₃₅ O ₄ P	- ^a
	5.49-5.70	C ₁₅ H ₃₃ O ₄ P	- ^a
2-methyl-1-butene	1.27-1.49	C ₅ H ₁₃ O ₄ P	60
	4.09-4.28	C ₅ H ₁₃ O ₄ P	1
	4.09-4.29	C ₁₀ H ₂₃ O ₄ P	35
	4.28-4.58	C ₁₁ H ₂₅ O ₄ P	1
	5.44-5.82	C ₁₇ H ₃₅ O ₄ P	1
	5.63-6.07	C ₁₈ H ₃₇ O ₄ P	1
	5.85-6.10	C ₁₉ H ₃₉ O ₄ P	1
2-methyl-2-butene ^b	1.25-1.40	C ₅ H ₁₃ O ₄ P	82
	4.00-4.08	C ₁₀ H ₂₃ O ₄ P	18
Cyclopentene	0.72-0.91	C ₅ H ₁₁ O ₄ P	75
	3.41-3.61	C ₁₀ H ₁₇ O ₄ P	4
	3.55-3.79	C ₁₀ H ₁₉ O ₄ P	20
	4.84-5.19	C ₁₅ H ₂₇ O ₄ P	1

^a Detectable, but very low abundance

^b The abundance of the alkyl phosphoric acid esters was very low (<0.1%) compared to the other C₅ olefins

In the reaction products from 1-pentene, there appeared to be two C₅-alkyl phosphoric acid esters, with near similar retention time around 1.1–1.4 min. Based on the mass spectrum, one of the products appeared dimeric (C₁₀H₂₆O₈P₂), but the retention time indicates that this was likely not present as the dimeric product in the liquid phase. The opposite was observed at retention times around 4.1–4.5 min, where a partial decomposition product (C₅H₁₃O₄P) among the C₁₀-alkyl phosphoric acid esters. The main products were C₅-alkyl (70 %) and C₁₀-alkyl (26 %) phosphoric acid esters. Small amounts of heavier products were observed, including products with alkyl chain lengths that were not integer multiples of the chain length of the feed.

Reaction of 2-methyl-2-butene with H₃PO₄ resulted in a low abundance of alkyl phosphoric acid esters in the organic phase. The relative abundance of products was of the order 0.1% of that of the products from 1-pentene and cyclopentene. Only two reaction products were detected, a C₅-alkyl phosphoric acid ester (82 %) and a C₁₀-alkyl phosphoric acid ester (18 %).

Cyclopentene reaction products comprised of C₅-alkyl (75 %), C₁₀-alkyl (24 %) and C₁₅-alkyl (1 %) phosphoric acid esters.

3.5 Phase partitioning for alkyl phosphoric acid esters

All reacted olefins produced alkyl phosphoric acid esters (Table 3.3). All samples reported presence of alkyl phosphoric acid esters in the organic phase, indicating the solubility of alkyl phosphoric acid esters in the organic layer. The presence of alkyl phosphoric acid esters in the organic phase of the branched olefins (2-methyl-1-hexene, 2-methyl-1-pentene, and 2-methyl-1-butene) and 1-pentene were only detectable by HPLC, indicating that the amount of alkyl phosphoric acid esters formed and soluble in the organic phase was very little in comparison to the aqueous phase. Emulsion formation appears to be related to the presence of a six-membered cyclic olefin, and not only due to the cyclic characteristics of the olefin, as cyclopentene did not report formation of emulsion.

3.6 Conversion of 1-hexene by phosphoric acid

The reaction rate of olefins with phosphoric acid at 50 °C was anticipated to be slow. To provide some indication of the reaction rate, the conversion of 1-hexene was determined at different reaction times by analysis of the organic phase by gas chromatography. The alkyl phosphoric acid esters were sufficiently labile at 50 °C to result in double bond isomerization (Table 3.6). The total content of hexene isomers in the reaction product was near similar to that of the feed and GC-FID analysis indicated that little hexene was removed from the organic (Figure 3.8).

Table 3.6 Conversion and selectivity for the reaction of 1-hexene with phosphoric acid at 50 °C and different reaction times

Reaction time (h)	Conversion (%)	Selectivity (%)			
		<i>cis</i> -2-hexene	<i>trans</i> -2-hexene	<i>cis</i> -3-hexene	<i>trans</i> -3-hexene
2	0.1	26	74	_a	_a
5	0.2	30	70	_a	_a
24	9.5	30	50	17	3
68	83.2	25	53	19	3

^a Not detected by GC-FID

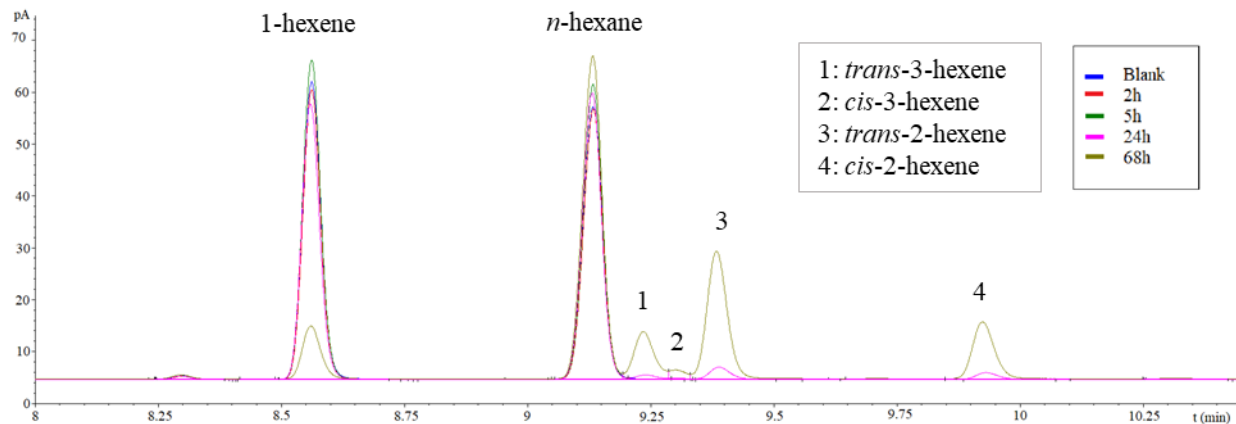


Figure 3.8 Conversion of 1-hexene from reaction of 1-hexene and 85% phosphoric acid for 2 h, 5 h, 24 h, and 68 h

The samples were analyzed by HPLC-MS (See results in Table 3.7), and for all reaction times, there was detectable formation of alkyl phosphoric acid esters. For all cases, oligomerization followed by cracking does not occur. After 24 hours, the abundance of dimers was higher than the monoester. Further oligomerization occurred with the resulting formation of trimers and a different dimer with saturation.

The alkyl phosphoric acid esters detected in the organic liquid at different reaction times are listed in Table 3.7. Analogous observations about the identification of the molecular formula of the products could be made as in Section 3.3.4. At 2 h reaction time, 96 % was present as C₆-alkyl phosphoric acid ester. With increasing reaction time, the amount of C₁₂-alkyl and C₁₈-alkyl phosphoric acid esters increased.

Table 3.7 Alkyl phosphoric acid esters identified by HPLC-MS analysis of the organic phase after reaction of 1-hexene with phosphoric acid at 50 °C for different reaction times

Retention time (min)	Suggested molecular formula	Relative abundance (%)			
		2 h	5 h	24 h	68 h
2.65-2.76	C ₆ H ₁₅ O ₄ P	-	80	-	-
2.76-2.87	C ₆ H ₁₅ O ₄ P	96	-	-	-
2.90-3.16	C ₆ H ₁₅ O ₄ P	-	-	48	43
4.82-5.22	C ₁₂ H ₂₅ O ₄ P	-	-	- ^a	- ^a
4.97-5.17	C ₁₂ H ₂₇ O ₄ P	- ^a	1	-	-
5.18-5.39	C ₆ H ₁₅ O ₄ P	-	- ^a	4	11
5.22-5.58	C ₁₂ H ₂₇ O ₄ P	4	19	48	45
6.36-6.67	C ₁₈ H ₃₇ O ₄ P	-	-	-	- ^a
6.85-7.15	C ₁₈ H ₃₉ O ₄ P	-	-	-	1

^a Detectable, but very low abundance

3.4 Discussion

3.4.1 Chemistry of C₅-C₇ olefins with phosphoric acid

The reaction of olefins with phosphoric acid is Brønsted acid-catalyzed.⁴ The transfer of a proton from the phosphoric acid to the olefin leads to the formation of an alkyl phosphoric acid ester (as demonstrated in Section 3.3.1) and not a carbocation. This reaction is reversible and it forms the basis for phosphoric acid-catalyzed olefin oligomerization, such as solid phosphoric acid-catalyzed olefin oligomerization employed industrially.^{16,17}

3.4.1.1 Effect of α -carbon on stability of alkyl phosphoric acid ester

Only the alkyl phosphoric acid esters that were thermally stable and present in sufficient quantity to be detected were reported in Tables 3.5, 3.6 and 3.7. Based on published decomposition data for short-chain alkyl phosphoric acid esters, it is known that *n*-alkyl esters are more stable than *iso*-alkyl esters. For example, *n*-propyl phosphoric acid ester has a decomposition temperature of 125 °C, whereas that for the *iso*-propyl phosphoric acid ester is 75 °C.¹⁸ A bond between the phosphoric acid and the α -carbon of an olefin improves stability of the alkyl phosphoric acid ester.

In this study evidence of stability of ester bonding to the α -carbon can be seen from Table 3.2 when comparing the reaction products of 2-methyl-1-butene and 2-methyl-2-butene. Only 2-methyl-1-butene formed a detectable amount of alkyl phosphoric acid ester. Of the two compounds, only 2-methyl-1-butene could form an α -carbon bonded alkyl phosphoric acid ester, as illustrated by Figure 3.9.

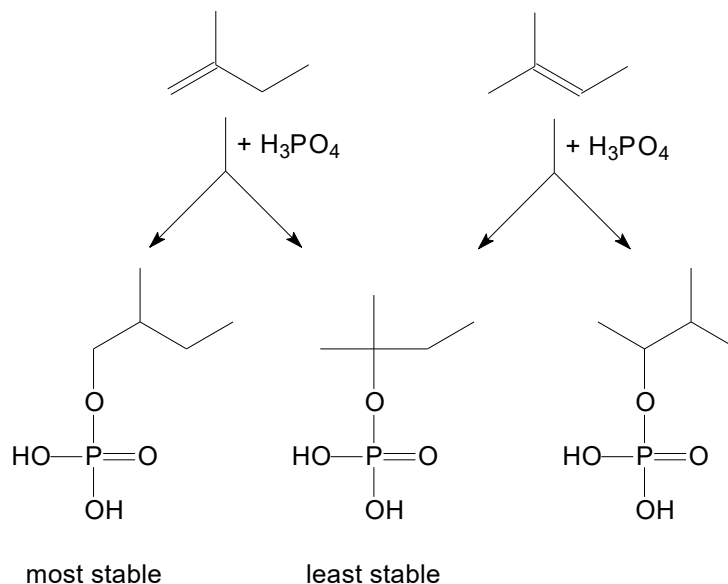


Figure 3.9 Alkyl phosphoric acid esters formed by 2-methyl-1-butene and 2-methyl-2-butene

The difference in thermal stability of the different alkyl phosphoric acid esters affects their reactivity. When an alkyl phosphoric acid ester is not observed, it does not imply that it is not formed. More labile alkyl phosphoric acid esters are formed and decomposed as part of a dynamic process, which results in a low concentration of those alkyl phosphoric acid esters.

3.4.1.2 Effect of olefin hydrocarbon chain length on product distribution

The following will compare the effect of hydrocarbon chain length of the product distribution. For comparison, the branched olefins from C_5 - C_7 (2-methyl-1-butene, 2-methyl-1-pentene, and 2-methyl-1-hexene, respectively) are evaluated. The results in Table 3.4 indicate the different product distribution from the HPLC-MS analyses in the organic phase.

The product distribution appears to be affected by the length of the olefin hydrocarbon chain. The ratios of relative abundance of the dimeric/monomeric alkyl phosphoric acid esters (C_{2n}/C_n) were calculated from Table 3.4. These values resulted in 0.57, 1.20 and 0.12 for 2-methyl-1-butene, 2-methyl-1-pentene and 2-methyl-1-hexene, respectively.

It has been proposed by Ipatieff¹⁹ that dimerization mechanism occurs by the reaction between two phosphoric acid esters. Therefore, for dimerization to occur, the C_n alkyl phosphoric acid ester has to be stable enough for it to react with another ester and form a C_{2n} -alkyl phosphoric acid ester. Therefore, the ratios of C_{2n}/C_n alkyl phosphoric acid esters can be interpreted as indicative of the stability of the ester. The C_6 branched olefin, 2-methyl-1-pentene resulted in the highest ratio of C_{2n}/C_n alkyl phosphoric acid esters, with 1.20. This can be an indication that 2-methyl-1-pentene formed the most stable mono-substituted alkyl phosphoric acid ester intermediate, therefore, enabling the successive formation of more C_{2n} -alkyl phosphoric acid esters.

However, in the case of 2-methyl-1-hexene, the ratio of C_{2n}/C_n alkyl phosphoric acid esters resulted in the lowest, at 0.12. Additionally, from Table 3.2, 2-methyl-1-hexene did not form detectable alkyl phosphoric acid esters by NMR in the organic or aqueous phase. Which could suggest that the concentration of alkyl phosphoric acid esters was so low that they were not detectable by NMR. A plausible explanation is due to the low reactivity of 2-methyl-1-hexene with the phosphoric acid, therefore, forming less monomeric alkyl phosphoric acid ester. As a result, it decreases the chance to form C_{14} -alkyl phosphoric acid esters in comparison to the other cases. No further studies were performed to conclude about the reactivity of 2-methyl-1-hexene.

3.4.1.3 Effect of olefin structure on product distribution

The presence of cyclic structured olefins, regardless of the hydrocarbon chain length from C_5 - C_7 , resulted in the formation of alkyl phosphoric acid esters soluble in the organic and aqueous phase (see Table 3.2 for more information). Additionally, because NMR has a lower detection level than HPLC-MS, compounds detectable by NMR can be seen as higher product concentration than compounds detectable by HPLC-MS and not by NMR. From Table 3.2, the results show that all alkyl phosphoric acid esters formed from cyclic olefins are detectable by NMR in the aqueous and organic phase. Therefore, indicating that cyclic olefins can react with the phosphoric acid and produces alkyl phosphoric acid esters in relatively high concentrations. A similar trend was observed for the linear olefins, where NMR detected products in the aqueous and organic phase, except in the case of 1-pentene where it did not form detectable alkyl phosphoric acid esters by NMR.

On the other hand, the results in Table 3.5 show the product distribution of different structures of C₅ olefins. The ratios of dimeric/ monomeric (C_{2n}-/C_n) alkyl phosphoric acid esters were calculated from Table 3.5. The values resulted in 0.78, 0.57 and 0.32 for 1-pentene, 2-methyl-1-butene and cyclopentene, respectively. Similar to the comparison made previously in Section 3.4.1.2, 1-pentene resulted in the highest ratio of C_{2n}-/C_n alkyl phosphoric acid esters, with 0.78. Therefore, indicating that 1-pentene formed the most stable C₅-alkyl phosphoric acid esters, as it resulted in the highest formation of C₁₀-alkyl phosphoric acid esters. However, in the case of cyclopentene, it resulted in the lowest ratio of C_{2n}-/C_n alkyl phosphoric acid esters, with 0.32. In this case, the low formation of C_{2n} is not due to the instability of the C_n alkyl phosphoric acid esters, as these were present in high concentrations as shown in the results from NMR. A possible explanation of the low formation of C₁₀-alkyl phosphoric acid esters from the cyclohexene is likely due to the steric hindrance of the natural configuration of the cyclic compound in comparison to the branched and linear olefin.

3.4.2 Phase partitioning

The alkyl phosphoric acid esters formed from C₅–C₇ olefins changed in solubility from predominantly water-soluble for C₅ olefins to solubility in both phases (Table 3.2). If one considers also results from HPLC-MS analysis (Table 3.3), all of the alkyl phosphoric acid esters were soluble to some extent in both aqueous and organic phases. This makes sense if one considers that the alkyl phosphoric acid esters contain a polar –O–PO(OH)₂ ‘head’ and a non-polar hydrocarbon ‘tail’, which should, in principle, provide them with amphiphilic properties. Furthermore, the increase in chain length of the hydrocarbon “tail” increases the hydrophobicity of the alkyl phosphoric acid ester,¹⁶ therefore, resulting in the solubility of the esters in the organic phase.

Furthermore, a noticeable formation of emulsion occurred in presence of a six-membered cyclic hydrocarbon as alkyl group. Both cyclohexyl phosphoric acid esters evaluated in this work resulted in the formation of stable emulsions. The same was not observed with the cyclopentyl phosphoric acid esters. Although emulsion formation was not further studied, it is not unknown that phosphoric acid esters can act as emulsifiers. The phosphoric acid esters, especially the trialkyl-

phosphoric acid esters, have been known to be used as emulsifiers and forming stable emulsions even during product storage.²⁰

3.4.3 Process for olefin removal by reactive absorption with H₃PO₄

The use of phosphoric acid for the reactive absorption of olefins was investigated as potential process to remove olefins from cracked naphtha (Figure 3.1) without hydrotreating. However, the results obtained from the experimental work highlighted issues that would make such a process impractical. The main issues are explained below.

3.4.3.1 Effect of olefin removal efficiency and reaction rate

Alkyl phosphoric acid esters formed by reactive absorption of olefins with phosphoric acid were thermally labile. At 50 °C, the alkyl phosphoric acid esters of the C₅–C₇ olefins were sufficiently stable to be detected by NMR (Table 3.2) and HPLC-MS (Table 3.3). Yet, in some instances, the concentrations after 68 h reaction time were still so low that detection was possible only by HPLC-MS and not by NMR. The reason for such low production of phosphoric acid esters was later apparent when the organic product was analyzed. There was an increase in double bond isomerized products with time (Table 3.6), which indicated that at 50 °C alkyl phosphoric acid esters were sufficiently thermally labile to decompose and yield hexene isomerization. If formation and decomposition of alkyl phosphoric acid esters occurred dynamically at 50 °C and to the extent where the “equilibrium” concentration of the alkyl phosphoric acid esters remained low. As a result, the reactive absorption step in the process has a very low efficiency, therefore, making it impractical.

Furthermore, the rate of reactive absorption of olefins by phosphoric acid at 50 °C was slow. This was to some extent anticipated because the process required transport across the liquid-liquid interface. In the experiments with 1-hexene (Section 3.3.6) that were used to evaluate the rate of reactive olefin absorption, the concentration of the hexenes in the organic phase remained near similar to time. Although an increased abundance of alkyl phosphoric acid esters was found based on HPLC-MS analysis, the rate of reactive olefin absorption was too slow to be practical.

The impact of these findings signifies that the olefin removal efficiency from the proposed system in Figure 3.1 is low even when long residence time is provided. Therefore, the process will require extremely large reaction vessels for the long residence time and has low olefin removal efficiency.

3.4.3.2 Effect of phase partitioning and emulsion formation

Alkyl phosphoric acid esters were present in both aqueous and organic phases (Table 3.2 and Table 3.3). In the case of cyclohexene and methylcyclohexene, the reactive absorption caused the formation of a stable emulsion. To achieve olefin removal according to the swing process proposed in Figure 3.1, it was necessary for the alkyl phosphoric acid esters to remain in the aqueous phase, which was not the case and emulsion made the separation inefficient and impractical.

As a result, the formation of stable emulsions and alkyl phosphoric acid esters soluble in the organic phase would require further separation processes that could lead to an increase in the overall operational cost. Additionally, the presence of alkyl phosphoric acid esters in the organic phase is not desirable because the final objective of this work is to remove the olefins in the thermally cracked naphtha. The experimental results indicate that if the naphtha was treated with phosphoric acid, an amount of alkyl phosphoric acid esters will be soluble in the naphtha. The treated naphtha would likely encounter high operational temperatures downstream that can result in the decomposition of the alkyl phosphoric acid esters. Consequently, releasing phosphoric acid into the system, which can lead to corrosion.²¹

The reactive absorption process was proposed based on what was known from the reaction of C₂-C₄ olefins with phosphoric acid,^{4,16} but on several accounts, different behavior was found for the reaction of C₅-C₇ olefins with phosphoric acid. Therefore, the research work conclusively demonstrates that the reactive olefin absorption process in Figure 3.1 is not a viable process.

3.5 Conclusions

Based on the literature, it is known that certain olefins with C₂-C₄ hydrocarbon chain length could react with phosphoric acid. Therefore, it was investigated whether phosphoric acid can be used to reactively absorb the olefins from the thermally cracked naphtha to reduce its olefin content. The following observations were made based on the performed research work:

- Phosphoric acid can react with the selected model compound olefins of C₅ – C₇ to form alkyl phosphoric acid esters at 50 °C.
- NMR and its different techniques (¹H NMR, ³¹P NMR, zTOCSY, gHSQC) are useful for detection of alkyl phosphoric acid esters in the aqueous and organic phase. HPLC-MS can be used to detect and identify the molecular formula of the alkyl phosphoric acid esters in the organic phase.
- Alkyl phosphoric acid esters formed from C₅ olefins are mainly soluble in the aqueous phase. While alkyl phosphoric acid esters formed from C₆-C₇ olefins had were soluble to some extent in both aqueous and organic phases.
- The presence of six-membered cyclic hydrocarbon as alkyl group of phosphoric acid esters was associated with the formation of a stable emulsion, which complicated the separation between the aqueous and organic phases.
- The proposed process for olefin removal via reactive absorption with phosphoric acid is not a viable process due to low removal efficiency, slow reaction rate, emulsion formation with the presence of six-membered cyclic compounds and the solubility of the phosphoric alkyl esters in the organic phase.

References (Chapter 3)

- (1) Strausz, O.; Lown, E. *The Chemistry of Alberta Oil Sands, Bitumen and Heavy Oils*; Alberta Energy Research Institute: Calgary, 2003.
- (2) Maples, R. *Petroleum Refinery Process Economics*; PennWell: Tulsa, 1993.
- (3) De Filippis, P. A Simple Test Method for Distinguishing Straight-Run from Thermal (Visbreaker) Residues or Bitumens. *Fuel* **1995**, *74* (10), 1537–1539.
- (4) Ipatieff, V. N. *Catalytic Reactions at High Pressures and Temperatures*; The Macmillan Company: New York, 1937.
- (5) Woodstock, A. H. The Alkyl Esters of Phosphoric Acid. *Chem. Ind.* **1942**, *51*, 516–521, 557.
- (6) Jameson, R. F. The Composition of the “Strong” Phosphoric Acids. *J. Chem. Soc.* **1959**, *0*, 752–759.
- (7) Hupfer, M.; Ru, B.; Berlin, D.-; Schmieder, P. Origin and Diagenesis of Polyphosphate in Lake Sediments : A ³¹P-NMR Study. *Limnol. Oceanogr.* **2004**, *49* (1), 1–10.
- (8) Gorenstein, D. G. Phosphorus-31 Chemical Shifts: Principles and Empirical Observations. In *Phosphorus 31 NMR: Principles and Applications*; Academic Press Inc., Publishers: Orlando, 1984; pp 7–36.
- (9) Farrar, T. C.; Schwartz, J. L.; Rodriguez, S. pH , Temperature , and Concentration Dependence of the Chemical Shift and Scalar Coupling Constants in disodium hydrogen phosphite and disodium fluorophosphate. **1993**, *97* (28), 7201–7207.
- (10) Chen, T.; Hsiao, C.; Huang, S.; Huang, J. The Nearest-Neighbor Effect on Random-Coil NMR Chemical Shifts Demonstrated Using a Low-Complexity Amino-Acid Sequence. *Pro. & Pept. Let.* **2016**, *23* (11), 967–975.
- (11) Pretsch, E.; Clerc, T.; Seibl, J.; Simon, W. ¹H-NMR. In *Tables of Spectral Data for Structure Determination of Organic Compounds*; Berlin: Springer-Verlag: Berlin, 1983; pp 104–177.
- (12) Silverstein, R. M.; Webster, F. X. *Spectrometric Identification of Organic Compounds*, Sixth.; John Wiley & Sons, Inc.: New York, 1998.
- (13) De Klerk, A. Reactivity Differences of Octenes over Solid Phosphoric Acid. *Ind. Eng. Chem. Res.* **2006**, *45* (2), 578–584.

- (14) Buglass, A. J.; Lee, S. H. Sequential Analysis of Malic Acid and Both Enantiomers of Lactic Acid in Wine Using a High-Performance Liquid Chromatographic Column-Switching Procedure. *J. Chromatogr. Sci.* **2001**, *39* (11), 453–458.
- (15) Quintana, J. B.; Rodil, R.; Reemtsma, T. Determination of Phosphoric Acid Mono- and Diesters in Municipal Wastewater by Solid-Phase Extraction and Ion-Pair Liquid Chromatography-Tandem Mass Spectrometry. *Anal. Chem.* **2006**, *78* (5), 1644–1650.
- (16) de Klerk, A. Key Catalyst Types for the Efficient Refining of Fischer-Tropsch Syncrude: Alumina and Phosphoric Acid. In *Catalysis: Volume 23*; 2011; pp 1–49.
- (17) Nicholas, C. P. Applications of Light Olefin Oligomerization to the Production of Fuels and Chemicals. *Appl. Catal. A Gen.* **2017**, *543* (3), 82–97.
- (18) Waggaman, W. H. *Phosphoric Acid, Phosphates, and Phosphatic Fertilizers*, 2ed ed.; Reinhold: New York, 1952.
- (19) Schmerling, L.; Ipatieff, V. N. The Mechanism of the Polymerization of Alkenes. *Adv. Catal.* **1950**, *2*, 21–80.
- (20) Zabrocki, K.; Schaupp, K. Emulsifier Composition. U.S. Patent 4,360,452, Nov. 23, 1982.
- (21) Kosting, P. R.; Heins, C. Corrosion of Metals by Phosphoric Acid. *Ind. Eng. Chem.* **1930**, *23* (2), 140–150.

CHAPTER 4 – HYDROGEN TRANSFER OF ASPHALTENES TO OLEFINS: AN ALTERNATIVE APPROACH FOR TREATING THERMALLY CRACKED NAPHTHA

Abstract

From previous research, it has been found that asphaltenes have hydrogen-donating properties via hydrogen transfer reactions at 250 °C. Therefore, the present work studied the possibility of using asphaltenes to hydrogenate olefins in the thermally cracked naphtha. The preliminary study involves model compounds 1,2-dihydronaphthalene and 1-hexene, to verify the possibility of 1-hexene hydrogenation via hydrogen transfer. 1-Hexene was found to be representative of the olefins in the cracked naphtha and it was capable of receiving hydrogens via hydrogen transfer. Therefore, the system asphaltenes- naphtha was researched and different experimental conditions were evaluated. Temperature, reaction time and weight of asphaltenes were varied. Gas Chromatography-Mass Spectroscopy (GC-MS), Gas Chromatography- Flame Ionization Detector (GC-FID), Simulated Distillation (SimDist), and Fluorescence Spectroscopy were used for product analyses. Results indicated that asphaltenes were capable of hydrogenating 1-hexene to form *n*-hexane. The research also found that asphaltenes could hydrogenate olefins in thermally cracked naphtha. The findings can lead to potential application of asphaltenes for olefin treatment.

Keywords: Asphaltenes, olefin, naphtha, hydrogen transfer, hydrogenation

4.1 Introduction

In the previous chapter (Chapter 3), it was pointed out that olefins were formed in the bitumen during thermal cracking, and hydrotreatment is commonly used for olefin treating. Alternative pathways to treat the olefins were evaluated, to substitute potentially the need for hydrogenation. For the CNOOC International Ltd., BituMax partial upgrader, asphaltenes are rejected as part of the upgrading process. It was therefore evaluated if asphaltenes could be used to treat the olefins in the cracked bitumen.

In the case of Canadian bitumen, *n*-pentane insoluble asphaltenes are present at around 17-20 wt.% of the bitumen,¹ therefore, representing a considerable quantity of material. Due to the large volume of asphaltenes in relation to the size of the market for asphaltenes, e.g. road paving, researchers have been and continue to seek alternative applications of asphaltenes in order to increase its economic value.

One of the interesting characteristics of asphaltenes is its ability to transfer hydrogen. Gould and Wiehe² have detected reactive hydrogen donors present in industrial asphaltenes by reacting asphaltenes with 2,3-dichloro-5,6-dicyano-*p*-benzoquinone (DDQ), which is a known hydrogen acceptor. Similarly, Naghizada et al.,³ saturated α -methylstyrene into cumene via hydrogen disproportionation, by reacting α -methylstyrene with industrial asphaltenes obtained from Athabasca bitumen at 250 °C. In both cases, those olefins were selected as model compounds, because they were very good hydrogen acceptors.

As a result, the question of whether asphaltenes could be used to saturate the olefins present in thermally cracked naphtha arose. It was not obvious that this would be possible because the olefins in cracked naphtha originated from conditions where hydrogen transfer was possible and were not saturated. Therefore, the olefins in cracked naphtha were likely to be poor hydrogen acceptors.

If the proposed process results successful, it addresses olefin conversion without the use of hydrogen, therefore, making beneficial use of asphaltenes and offering a potential solution for olefin treatment. Other prospecting applications from this process can be the use of the hydrogen-

depleted asphaltenes as feed for the production of carbon fiber. The technology of carbon fiber production with asphaltenes involves a step that requires the removal of hydrogen from the asphaltenes during carbonization to achieve carbon bound carbon fiber composite.⁴ Therefore, the hydrogen depleted asphaltenes could potentially be useful for this technology.

In the present study, 1-hexene was reacted with industrial asphaltenes, namely *n*-pentane insoluble material obtained from Athabasca bitumen. 1-Hexene was selected as a model compound representative of the olefins present in thermally cracked naphtha. 1-Hexene is not a good hydrogen acceptor, because the intermediate free radical product would be either a primary or a secondary radical with no resonance stabilization. Furthermore, the effect of reaction time, temperature and ratio of asphaltenes to olefins were studied.

4.2 Experimental

4.2.1 Materials

Asphaltenes feed was obtained from the solvent deasphalting unit at the Long Lake upgrader facility of CNOOC (former Nexen Energy ULC) in Alberta, Canada. This unit utilizes *n*-pentane hydrocarbon deasphalting of Athabasca oilsands bitumen that is recovered subsurface by steam-assisted gravity drainage (SAGD). Characterization of asphaltenes was done in previous works^{5,6} and the details are summarized in Table 4.1. The chemicals and gases used to perform the experimental study are summarized in Table 4.2.

Table 4.1 Feed characterization of industrial asphaltenes from Long Lake upgrader of CNOOC
(former Nexen Energy ULC)

Description	Industrial asphaltenes feed ^a	
	Average	Std. deviation
C ₇ - asphaltenes (wt%) ^b	66.8	1.7
Maltenes ^b	32.5	1.5
Elemental analysis ^c		
Carbon (wt%)	80.3	0.1
Hydrogen (wt%)	8.0	0.1
Nitrogen (wt%)	1.1	0.0
Sulfur (wt%)	7.7	0.1
¹ H-NMR ^c		
Aliphatic hydrogen	86.5	0.5
Aromatic hydrogen	13.5	0.5
TGA ^c		
Micro carbon residue (wt%)	36.0	

^a average and standard deviation of triplicates

^b extracted from Naghizada⁵

^c extracted from Styles and De Klerk⁶

Table 4.2 Chemicals employed in this experimental study

Compound	Formula	CASRN ^a	Mass fraction purity ^b	Supplier
<i>Reactants</i>				
1,2-dihydronaphthalene	C ₁₀ H ₁₀	447-53-0	0.98	Sigma Aldrich
1-hexene	C ₆ H ₁₂	592-41-6	0.97	Sigma Aldrich
<i>n</i> -dodecane	C ₁₂ H ₂₆	112-40-3	0.99	Sigma Aldrich
<i>n</i> -hexane	C ₆ H ₁₄	110-54-3	>0.99	Sigma Aldrich
<i>Solvents</i>				
Carbon disulfide	CS ₂	75-15-0	0.9999	Fisher Scientific
Methanol	MeOH	67-56-1	0.999	Fisher Scientific
Toluene	C ₇ H ₈	108-88-3	0.999	Fisher Scientific
<i>Cylinder gases</i>				
Nitrogen	N ₂	7727-37-9	0.99999 ^c	Praxair

^a CASRN = Chemical Abstracts Services Registry Number

^b This is the purity of the material guaranteed by the supplier; material was not further purified.

^c Mole fraction purity.

Thermally cracked naphtha was obtained from the same upgrader facility as the asphaltenes. The naphtha was properly stored in a sealed sample container to avoid storage degradation. A summary of its characterization was collected from previous studies,⁷⁻⁹ and it is presented in Table 4.3.

Table 4.3 Feed characterization of thermally cracked naphtha from Long Lake upgrader of CNOOC (former Nexen Energy ULC)

<i>Property</i>	<i>Units</i>	<i>Naphtha</i>
Density	kg/m ³ @ 20 °C	762.7
API Gravity	-	53.5
<i>Elemental analysis</i>		
Sulfur	wt. %	0.90
Nitrogen	wt. %	0.09
Carbon	wt. %	84.34
Hydrogen	wt. %	13.76
Oxygen	wt. %	0.25
Viscosity	cSt @ 25 °C	0.85
<i>¹H NMR analysis</i>		
Aliphatic saturate	mol %	96.42
Aliphatic olefin	mol %	1.26
Aromatic	mol %	2.32
Olefin content	wt. % 1-decene eq.	4.7
Diene number	g I ₂ / 100g	0.62
Bromine number	g Br ₂ / 100g	27.84
CCR	wt. %	45.12 ± 2.55
Acid number	mg KOH/ g	0.123 ± 0.003
<i>Distillation profile</i>		
IBP	°C	30
T10	°C	68
T30	°C	100
T50	°C	133
T70	°C	173
T90	°C	239
FBP	°C	265

4.2.2 Equipment and procedure

The study and the corresponding experimental work were separated into three sections:

- First, a preliminary study using model compounds to investigate the reaction between a good hydrogen donor, 1,2-dihydronaphthalene and 1-hexene as hydrogen acceptor. The purpose of this study was to understand whether 1-hexene can be saturated via hydrogen transfer.
- Second, using the learnings from the preliminary study, the reaction of industrial asphaltenes, as hydrogen donor and 1-hexene, as a hydrogen acceptor was investigated. The purpose of this second study was to evaluate the olefin reduction, conversion, and product distribution at different operational conditions. Additionally, the use of a model compound as hydrogen acceptor simplifies the analytical process when compared to the use of real feed, i.e., cracked naphtha.
- Third, the reaction of real feed materials, namely industrial asphaltenes as hydrogen donor and thermally cracked naphtha as the hydrogen acceptor, was investigated. The aim of this third study was to determine whether the asphaltenes could be used to decrease the olefin content of thermally cracked naphtha.

The equipment and procedure are similar for all three cases and will be described for a typical experiment. Firstly, a known amount of hydrogen donor and acceptor were placed inside a glass vial. Approximately a total of 3 g for reactions using 1:1 and 2:1 weight ratio of hydrogen donor: hydrogen acceptor, and 9 g for reactions using 4:1 and 8:1 weight ratio of hydrogen donor: hydrogen acceptor. Mass was varied between experiments to have enough sample of treated hydrogen acceptor for further analysis (~ 1 g). The samples were manually shaken to ensure contact between the reactants. When using asphaltenes as hydrogen donor, the asphaltenes were finely ground with a ceramic mortar and pestle before adding the ground asphaltenes into the vial.

Furthermore, the glass vial containing the reactants was later inserted into a Swagelok stainless steel batch reactor and purged three times with nitrogen. The reactor was later pressurized to 6 or 7 MPa depending on the reaction temperature. For reactions at 250 – 300 °C, the initial pressure was 6 MPa and increased to ~ 10-11 MPa at reaction temperature. For reactions at 350 °C, the initial pressure was at 7 MPa and increased to ~ 11-12 MPa at reaction temperature. The change in pressure allowed maintaining a dense fluid phase reaction between the reactants. The batch reactor was not equipped with any form of agitation.

The pressurized batch reactor was later placed inside an Omega fluidized sand bath heater set at the corresponding experimental temperature (See Figure 4.1). A thermocouple installed in the batch reactor measured the temperature of the reaction mixture. Heat-up time of the reactor to reach the reaction temperature varied between 5-15 minutes depending on the dimensions of the reactor and the experimental temperature set point. Reaction time reported, is the time period that started once the reactor reached the temperature set point.

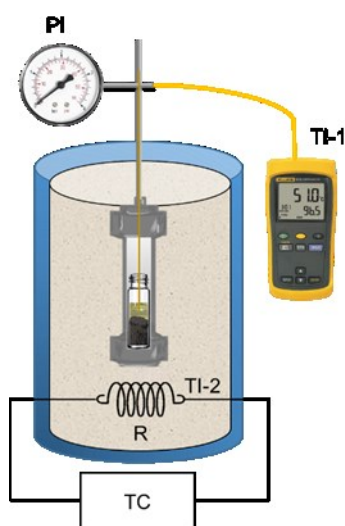


Figure 4.1 Experimental set up for reactions performed in micro-batch reactors

After the corresponding reaction time, the reactor was removed from the sand bath and quenched with air until it reached room temperature. Quenching time was between 5-10 minutes depending on the dimensions of the reactor and the experimental temperature. Mass balance for all experiments was between 99-100 %.

Experiments with naphtha:

For the experiments using naphtha as hydrogen acceptor, the following procedure was followed for the sample preparation prior to reaction (See Figure 4.2). The naphtha was spiked with a solution A. Solution A contained 10 wt. % of 1-hexene in *n*-hexane (1:9 weight ratio respectively) to provide comparative analysis that could be related to the model compound studies of olefin reduction. The 1:9 ratio of 1-hexene/*n*-hexane was selected because the characterization studies performed by Santiago and Subramanya⁹ determined that the olefin content of the cracked naphtha used in this work was ~ 10 wt. %.* Therefore, by adding this solution, the spiking of the naphtha will not alter the original matrix of the naphtha.

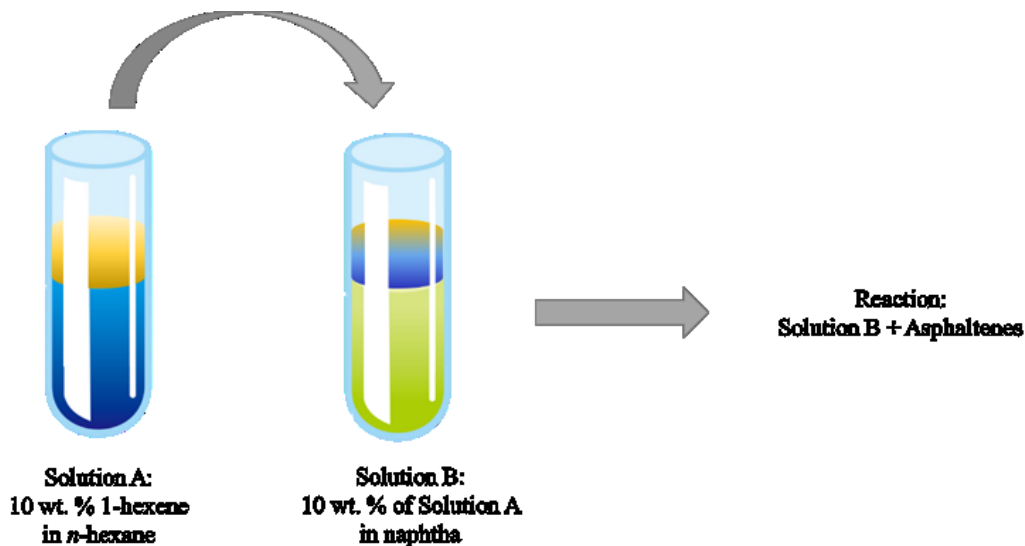


Figure 4.2 Sample preparation for experiments using naphtha

The naphtha was then spiked with 10 wt. % of solution A because at this concentration, the peak corresponding to 1-hexene (detected by GC-FID) was noticeably larger than the peak of 1-hexene

* The 10 wt. % olefin content determined by Santiago and Subramanya¹³ is not directly comparable with the "1-decene equivalent" measure reported in Table 4.3. The wt. % indicates the weight percentage of olefin in the naphtha while the 1-decene equivalent is determined from a ¹H NMR method. The method requires two spectra per sample, the first spectrum is from the actual material and the second one is spiked with 1-decene. The wt. % of olefins is then determined as 1-decene equivalent.²⁹

in the original naphtha. For simplification, this solution is called Solution B and this was used for the reactions with asphaltenes.

For comparison purposes, another experiment was performed. In this case, using Solution A as hydrogen acceptor, to simulate the naphtha mixture. This experiment allows the comparison between the olefin reduction values obtained from the model compound reactions with 1-hexene and asphaltenes with the experiments using naphtha and asphaltenes.

Finally, an additional experiment using naphtha feed and asphaltenes, without spiking the naphtha (Exp. 22 from Table 4.6), was performed to determine the gum content before and after treating the naphtha with the asphaltenes.

4.2.2.1 Experimental conditions

The experiments were carried out under different experimental conditions by varying the hydrogen donor, the hydrogen acceptor, temperature, reaction time and/or weight ratio of hydrogen donor to hydrogen acceptor. Tables 4.4 – 4.6 present a summary of the experimental conditions investigated in each stage of the work.

Table 4.4 Experimental conditions for the preliminary study reactions with 1,2-dihydronaphthalene as hydrogen donor and 1-hexene as hydrogen acceptor

Exp.	Reactants	Weight ratio of reactants	Temperature [°C]	Time [h]
0.1	1,2-dihydronaphthalene: 1-hexene	1:1	250	1
0.2	1,2-dihydronaphthalene: 1-hexene	1:1	250	2
0.3	1,2-dihydronaphthalene: 1-hexene	1:1	300	2
<i>Control experiments^a</i>				
0.4 ^b	1,2-dihydronaphthalene: <i>n</i> -hexane	1:1	300	2
0.5 ^c	1,2-dihydronaphthalene	-	300	2
0.6 ^d	<i>n</i> -hexane	-	300	2
0.7 ^e	1-hexene	-	300	2

^a The chromatograms obtained by GC-MS analysis of the reaction products from the control experiments can be found in Appendix A

^b Control experiment was performed to verify that *n*-hexane is not capable of donating its hydrogen to 1,2-dihydronaphthalene. Therefore, if 1-hexene was converted into *n*-hexane by hydrogen transfer from 1,2-dihydronaphthalene, the reverse reaction is not possible.

^c Control experiment was performed to determine the products obtained from the self-reaction of 1,2-dihydronaphthalene under the experimental conditions. This will provide information of which products were formed due to self-reaction of 1,2-dihydronaphthalene and not from the reaction of 1,2-dihydronaphthalene and other reactants.

^d Control experiment was performed to verify that *n*-hexane did not self-react under the experimental conditions.

^e Control experiment was performed to determine the products obtained from the self-reaction of 1-hexene under the experimental conditions. The experiment is the same as Exp. 10 in Table 4.5.

Table 4.5 Experimental conditions for the reactions of asphaltenes as hydrogen donor and 1-hexene as hydrogen acceptor

Experiment	Weight ratio of reactants (asphaltenes: 1-hexene) ^a	Temperature [°C]	Time [h]
1	1:1	250	1
2	1:1	250	2
3	1:1	250	4
4	1:1	250	24
5	0:1 ^b	250	24
6	1:1	300	2
7	2:1	300	2
8	4:1	300	2
9	8:1	300	2
10	0:1 ^b	300	2
11	2:1	300	4
12	1:1	300	4
13	0:1 ^b	300	4
14	1:1	325	2
15	1:1	350	0.5
16	1:1	350	1
17	1:1	350	2
18	1:1	350	3
19	0:1 ^b	350	3

^a The total actual measured masses for each experiment is shown in Appendix B

^b Control experiments. The control experiments were performed to determine which products are formed from 1-hexene under the experimental conditions without the presence of asphaltenes.

Table 4.6 Experimental conditions for the reactions of asphaltenes as hydrogen donor and thermally cracked naphtha as hydrogen acceptor

Exp.	Weight ratio of reactants	Temperature [°C]	Time [h]
20	4:1 (asphaltenes: spiked naphtha ^a)	350	3
21	4:1 (asphaltenes: solution of 1-hexene/ <i>n</i> -hexane)	350	3
22	4:1 (asphaltenes: naphtha)	350	3

^a Thermally cracked naphtha spiked with 10 wt. % of a solution of 1-hexene in *n*-hexane (1:10 weight ratio)

4.2.2.2 Collection of recovered products

After reaction, in all cases, part of the liquid product ended outside of the glass vial that was placed inside the reactor and was in direct contact with the metal walls of the reactor (See Figure 4.2). This liquid product was collected with a glass pipette, transferred into a glass vial with lid and labeled as “recovered product”.

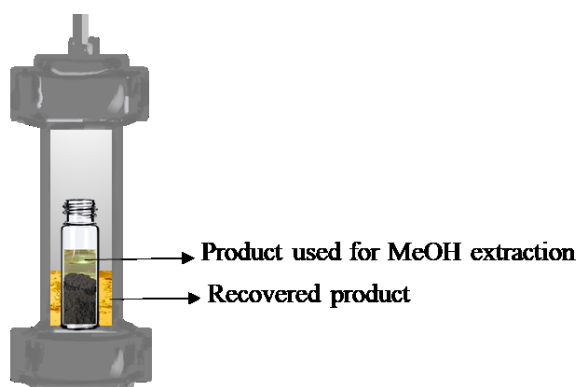


Figure 4.3 Inside the reactor

To facilitate the calculations and experimental procedure, the product remaining in the vial and absorbed on the asphaltenes was extracted for analyses and comparison. In this case, the purpose was to determine whether the concentration of the products was the same inside and outside the

glass vial. If it was the same, then the calculations and experimental procedure could be simplified by only analyzing the recovered product.

4.2.2.3 Extraction and filtration of liquid products

In the case of experiments using asphaltenes as hydrogen donor, the product inside the glass vial consisted of asphaltenes and liquid product absorbed into them. In order to analyze the products absorbed into the asphaltenes, an extraction process was required. For the extraction, a weight ratio of 40:1 (methanol to olefin) was used. Methanol was selected as solvent, as it does not dissolve the asphaltenes and is capable of extracting the products of interest (C₆ and C₁₂ hydrocarbons) when large quantities are used.

The product inside the glass vial was transferred to a larger lidded glass vial and was thoroughly stirred with the methanol for 30 minutes at 1000 rpm at room temperature (stirring was performed on a Fisher Scientific Isotemp Hot Plate Stirrer). The product was later filtered under vacuum to separate the solids from the liquid products. The extracted product was labeled as “filtrate product”.

This experiment was performed for several experiments to verify that the concentration of the products was the same inside and outside the vial (See Appendix C for more information). Additionally, a separate set of experiment was performed to determine the extraction efficiency of methanol (See Appendix C for more information)

All weight measurements were performed on an analytical balance (Mettler Toledo, Model XP1203S) with a maximum capacity of 1210 g and readability to 0.001g.

4.2.3 Analyses

4.2.3.1 Gas Chromatography with Mass Spectrometry (GC-MS) and Gas Chromatography- Flame Ionization Detector (GC-FID)

GC-MS was used to identify the reaction products that were formed in the recovered product and GC-FID was used to quantify the olefin reduction. The recovered product and samples obtained from reactions with 1,2-dihydronaphthalene were analyzed by adding 0.1g of sample and topped with methanol in a 10 mL volumetric flask. The filtrate product was directly used for analysis. Methanol was selected as solvent of choice because the products were soluble in methanol (when large amount of methanol is used) and it is not naturally present in any of the materials of interest.

Analyses to identify the nature of the reaction products were performed with an Agilent Model 7820A gas chromatography (GC) coupled with an Agilent Model 5977E MSD mass spectrometry (MS) detector. The separation was performed on an Agilent 19091S-001 HP-PONA capillary column of 50 m x 0.20 mm x 0.50 μm . In the case of experiments using 1-hexene as hydrogen acceptor; the injection volume was 1 μL and a split ratio of 100:1. The carrier gas was a constant flow rate of helium at 1 mL/min. the oven temperature program was set to start at 36 $^{\circ}\text{C}$ and held for 30 minutes; then, the temperature was increased to reach 75 $^{\circ}\text{C}$ at a rate of 2 $^{\circ}\text{C}/\text{min}$; a second temperature ramp was added to reach 100 $^{\circ}\text{C}$ at 5 $^{\circ}\text{C}/\text{min}$ and finally, 325 $^{\circ}\text{C}$ at 20 $^{\circ}\text{C}/\text{min}$ and held for 10 minutes.

The method for GC-MS analysis of the naphtha samples was modified as follows. The recovered products were directly injected into the instrument. The injection volume was 0.1 μL with a 100:1 split ratio. The carrier gas was a constant flow rate of helium at 1 mL/min. The oven temperature program started at 35 $^{\circ}\text{C}$ with hold up time of 30 minutes. The first ramp was 2 $^{\circ}\text{C}/\text{min}$ until 200 $^{\circ}\text{C}$, followed by a second temperature ramp of 10 $^{\circ}\text{C}/\text{min}$ until 300 $^{\circ}\text{C}$ with a holdup time of 7.5 minutes.

In all cases, product identification with GC-MS was done by comparing the mass spectra of the products with the database of the National Institute of Standards and Technology (NIST) through the NIST MS Search 2.0 – Mass Spectra Library.

Analyses for quantification were carried out using an Agilent Model 7890A gas chromatography (GC) equipped with a flame ionization detector (FID). Separation was carried out in the same column model as the GC-MS, and all parameters were kept the same for each type of experiment. It was assumed that all compounds of interest had an FID relative response factor of 1 because all compounds of interest were either paraffin or an olefin and their response factors are ~1.^{9,10}

All weight measurements for sample preparation were performed on an analytical balance (Mettler Toledo, Model ME204) with a maximum capacity of 220 g and readability to 0.0001g.

4.2.3.2 Simulated Distillation Gas Chromatography (SimDist GC)

Simulated distillation analysis was performed following the ASTM D 7169-11 standard procedure.¹¹ The analysis was done using an Agilent 7890B high-temperature gas chromatograph with a flame ionization detector and DB-HT-SIMDIST column (5 m × 0.53 mm × 0.15 μm). The injection volume was 0.5 μL with helium as carrier gas. The temperature program started at 50 °C and had a temperature ramp of 15 °C/min to 425 °C for which it remained constant for 10 minutes. The samples were prepared by adding 0.1 g of the recovered product in a 10 mL volumetric flask and topped with carbon disulfide.

In order to obtain the data of boiling point distribution, a two-step calibration mixture was necessary. First, the injection of dissolved polywax 655 in carbon disulfide followed by the injection of a Boiling Point Calibration Sample #1 kit, part number 5080-8716 by Agilent Technologies. The latter is a mixture of known concentrations of linear paraffins that enables the determination of the boiling points distribution by comparing the sample against these standards.

It is worth mentioning that because the amount of recovered product samples was limited, they were not filtered before analysis in the SimDist. Thus, the presence of traces amounts of asphaltenes or heavy materials is likely.

The weight of the products and CS₂ was measured with an analytical balance (Mettler Toledo, Model ME204) with a maximum capacity of 220 g and readability to 0.0001 g.

4.2.3.3 Differential Scanning Calorimetry (DSC)

Differential Scanning Calorimetry was used to determine the gum content in the naphtha feed and treated naphtha. In this study, gum considered is known as *existent gum*. Existent gum is defined as the evaporation residue of the fuels, without any further treatment.¹² To obtain the gum content, the samples of naphtha treated with asphaltenes and the naphtha feed without any treatment were placed in standard aluminum 100 µL sealed crucibles with perforated lids as reactors. Then, the samples were thermally treated using a DSC from Mettler Toledo, DSC 1 STARe system coupled with a GC10 gas controller. Samples were heated from 10 °C to 165 °C at 1 °C/ min under nitrogen flow of 50 mL/min. Temperature was then dropped from 165 °C to 10 °C at -10 °C/min rate. The weight difference of the sample before and after the thermal treatment with the DSC is considered as the existent gum content in the naphtha.

All weight measurements were performed on an analytical balance (Mettler Toledo, Model XS105) with a maximum capacity of 120 g and readability to 0.1 mg.

4.2.3.4 Fluorescence Spectroscopy

The following samples were analyzed by Fluorescence Spectroscopy:

- To verify the presence of traces of asphaltenes that could have affected the results from SimDist analysis, fluorescence spectroscopy was performed on the samples that showed the presence of hydrocarbons with a chain length of C₉₈ (Products from experiments 2, 6, 16, 17, and 18).

- In order to compare the reaction products with asphaltene feed and 1-hexene, separately, blank samples of each reactant were performed to determine their response.
- To verify that the response of samples containing asphaltenes was different from the thermally treated 1-hexene products, the blank reactions Exp. 10 and 19 were analyzed.
- For comparison, a sample without the presence of C₉₈ hydrocarbon in the SimDist analysis was analyzed. The selected sample was Exp. 4.

The analyses were carried out with a Horiba Scientific Aqualog Compact Steady State Spectrofluorometer. The parameters were set with 0.1 s integration time, excitation wavelength was set to 240 – 800 nm at 3 nm increment and emission coverage was set from 246.58 – 828.43 nm with 8.65 nm increment and medium CCD gain.

Toluene was selected as blank and solvent, as it can dissolve the traces of asphaltenes if present in the samples. The samples (recovered product and blank asphaltene) for analyses were prepared by adding ~ 1 mg of sample in 10 g of toluene. The samples for blank 1-hexene analysis were prepared by adding ~ 10 mg of sample in 10 g of toluene, as the signal was very weak for detection. The blank and samples were placed in a Horiba quartz cuvette for analyses. The cuvette has a 4 mL volume, 10 mm x 10 mm cross-section and a Teflon stopper to decrease sample evaporation.

All weight measurements were performed on an analytical balance (Mettler Toledo, Model XS105) with a maximum capacity of 120 g and readability to 0.1 mg.

4.2.4 Calculations

4.2.4.1 Definitions

In order to have a better understanding of the different calculations performed in the present study, some definitions are presented:

- *Olefin reduction*: Amount of olefin that was removed from the feed after reaction. Olefin reduction is expressed in terms of the moles of olefins in the product relative to the moles of olefins in the feed. The removal of olefin can be due to the formation of saturated compounds due to hydrogen transfer or by forming dimers of the olefins. For instance, when two olefins react to form one olefinic dimer, the moles of olefins went from two to one, reducing the olefin content by half.
- *Conversion of 1-hexene*: Amount of 1-hexene that was reacted and converted to products of different nature.
- *Selectivity*: Amount produced of one particular product per amount produced of all the products including the component itself.

4.2.4.2 Reactions with 1-hexene: Calculations for olefin reduction using asphaltenes

This section explains the procedure to determine the olefin reduction for reactions involving 1-hexene with asphaltenes:

- Equation for olefin reduction:

To calculate the olefin reduction, Equation 1 was used:

$$\% \text{ Molar concentration of olefin reduction} = \frac{C_{\text{olefin before rxn}} - C_{\text{olefin after rxn}}}{C_{\text{olefin before rxn}}} \times 100$$

(Eq. 11)

The previous equation can also be re-written in terms of weight percentage:

$$\text{wt\% of olefin reduction} = \frac{\text{wt\% olefin before rxn} - \text{wt\% olefin after rxn}}{\text{wt\% olefin before rxn}} \times 100$$

(Eq. 12)

Concentration or weight percentage was used to determine the olefin reduction because it was used as assumption that the amount of liquid in the feed remained approximately the same after reaction. Therefore, for simplification, the calculations may be performed in molar concentration or weight percentage rather than by total mass.

- Determination of mole percentage of olefins before reaction:

Since there was only 1-hexene initially in the feed, the weight percentage of olefin before reaction corresponds to 100 wt. %.

$$wt. \% olefin\ before\ rxn = 100\ wt. \%$$

(Eq. 13)

This expression can be converted in terms of moles by using the molecular weight of 1-hexene:

$$\% moles\ olefin\ before\ rxn \left[\frac{mol\ 1 - hexene}{g\ feed} \right] = \frac{100\ wt. \%}{84\ g/mol}$$

(Eq. 14)

- Determination of mole percentage of olefins after reaction:

The weight percentage of olefin after reaction would correspond to the weight percentage of olefin in the recovered product:

$$wt. \% olefin\ after\ rxn = \sum wt. \% olefinic\ compounds\ in\ rec.\ product$$

(Eq. 15)

In order to calculate the weight percentage of olefinic compounds in the recovered product, the compounds were classified into different groups. Based on the results obtained from GS-MS

analyses, the compounds can be classified as reactant: 1-hexene, and as products: C₆ isomers different from 1-hexene, *n*-hexane, C₁₀ alkane, C₁₁ alkane, C₁₂ alkane, and C₁₂ olefins.

Therefore,

$$\sum (wt.\% \text{ of } 1 - \text{hexene, } C_6 \text{ olefin isomers, } C_{12} \text{ olefins}) \text{ in rec. product} = \sum wt.\% \text{ olefinic compounds in rec. product} =$$

(Eq. 16)

To calculate the weight percentage of each compound:

$$wt.\% (\text{olefin compound class})_i = \frac{\sum \text{Areas that belongs to compound group } i}{\sum \text{Areas of products and reactants}}$$

(Eq. 17)

The weight percentage of each olefin compound class can be converted into moles by using the molecular weights. The molecular weight used for C₁₀ alkane was approximated as *n*-decane, C₁₁ alkane as *n*-undecane, C₁₂ alkane as *n*-dodecane, and C₁₂ olefin as 1-dodecene.

$$\% \text{ moles } (\text{olefin compound class})_i \left[\frac{\text{mol}}{\text{g feed}} \right] = \frac{wt.\% (\text{olefin compound class})_i}{\text{Molecular weight of } i}$$

(Eq. 18)

Once having all these values, Equation 1 can be used to calculate the olefin reduction in terms of moles and the g of feed in the denominator will cancel out.

4.2.4.3 Reactions with 1-hexene: Calculations for conversion of 1-hexene

- Equation for conversion of 1-hexene:

The conversion of 1-hexene was calculated with the following equation:

$$\text{wt}\% \text{ Conversion of 1-hexene} = \frac{(\text{wt}\% \text{ 1-hexene before rxn}) - (\text{wt}\% \text{ 1-hexene after rxn})}{\text{wt}\% \text{ 1-hexene before rxn}} \times 100$$

(Eq. 19)

The conversion of 1-hexene can be represented in terms of weight or molar percentage. For both cases, the value is the same because the molecular weight of 1-hexene will cancel out.

- Determination of weight percentage of 1-hexene before reaction:

$$\text{wt.}\% \text{ 1-hexene before rxn} = 100 \text{ wt.}\%$$

(Eq. 20)

- Determination of weight percentage of 1-hexene after reaction:

$$\text{wt.}\% \text{ 1-hexene after rxn} = \text{wt.}\% \text{ 1-hexene in rec. product}$$

(Eq. 21)

Where:

$$\text{wt.}\% \text{ 1-hexene in rec. product} = \frac{\text{Area of 1-hexene in rec. product}}{\sum \text{Areas of products and reactants}}$$

(Eq. 22)

4.2.4.4 Reactions with 1-hexene: Calculations for product selectivity

Product selectivity was only calculated for reactions using 1-hexene and asphaltenes as feed. Product selectivity was calculated for each compound group by using the following equation:

$$\%Selectivity_{compound\ group\ i} = \frac{(Area\ of\ compound\ group\ i)_{Rec.\ product}}{\sum Areas\ in\ products_{Rec.\ Product}}$$

(Eq. 23)

4.2.4.5 Reactions with spiked naphtha: Calculations for olefin reduction using asphaltenes

Olefin reduction was calculated using (Eq. 11).

- Determination of mole percentage of olefins before reaction:

For simplification, the olefin reduction was determined with respect to 1-hexene, this means, the amount of 1-hexene reduced in the feed. As a result, only the products known to be associated with 1-hexene were tracked in the naphtha. GC-FID chromatogram for untreated spiked naphtha was obtained. The peak of 1-hexene and the peaks of the reaction products associated with 1-hexene (*n*-hexane, C₆ olefins, C₁₀, C₁₁ and C₁₂ alkanes, C₁₂ olefins) were identified. The area of the peaks was normalized with respect to the area of the peak corresponding to toluene (internal standard). Toluene is naturally present in the naphtha and it is expected to be unreactive to the asphaltenes due to its aromatic structure. Therefore, the area of the peak of toluene was assumed to be constant before and after reaction. By doing so, direct comparison between area ratios with other chromatograms is possible.

The mole percentage of olefins before reaction can be calculated as follow:

Calculate the area ratios with respect to area of toluene:

$$\text{Area ratio of compound}_i \text{ and toluene} = \frac{\text{Area of compound}_i}{\text{Area of toluene}}$$

(Eq. 24)

Calculate the weight percentage of each compound:

$$\text{wt. \% compound}_i = \frac{\text{Area ratio of compound}_i \text{ and toluene}}{\sum \text{All area of compound}_i \text{ and toluene}}$$

(Eq. 25)

Calculate the mole percentage of each compound group similar to the procedure in (Eq. 18).

Calculate the mole percentage of olefins before reaction:

$$\text{moles \% of olefins before rxn} = \sum \text{moles \% olefins in untreated spiked naphtha}$$

(Eq. 26)

- Determination of mole percentage of olefins after reaction:

Mole percentage of olefins after reaction can be calculated similarly to the previously explained procedure. However, the values will be obtained from the GC-FID chromatogram of the treated naphtha with asphaltenes at the experimental conditions in Table 4.6.

$$\begin{aligned} \text{moles \% of olefins after rxn} \\ = \sum \text{moles \% olefins in treated spiked naphtha with asphaltenes} \end{aligned}$$

(Eq. 27)

4.2.4.6 Reactions with spiked naphtha: Calculations for conversion of 1-hexene

The conversion of 1-hexene was calculated with (Eq. 19) with the % values of 1-hexene before and after treatment with asphaltenes.

4.2.4.7 Reactions with spiked naphtha: Calculations for product formation

Selectivity was not calculated for the experiments using naphtha as hydrogen acceptor. It was not possible to track all the products that can be formed after reaction with asphaltenes, due to the complexity of the feed. However, comparison before and after the treatment of the naphtha with the asphaltenes was made, by identifying the peaks from the GC-FID chromatogram of the untreated and treated naphtha, to find the corresponding peaks associated to the products of interest. The values for comparison were calculated from (Eq. 25) after converting into moles.

4.3 Results and discussion of the preliminary study: 1,2-Dihydronaphthalene as hydrogen donor

The purpose of the preliminary study was to obtain proof of concept that a hydrogen donor (model compound) can hydrogenate a poor hydrogen acceptor (such as a mono-olefin). The conversion chemistry of a model compound system was expected to be easier to test and interpret before moving on to reaction with complex materials, as is the case of asphaltenes.

4.3.1 Effect of time

Based on the studies performed by Naghizada et al.,³ it was found that at 250 °C, asphaltenes can transfer hydrogen to α -methylstyrene to form cumene. Therefore, 250 °C was selected as temperature starting point for the experimental work. The first set of experiments (Exp 0.1 and 0.2 from Table 4.4) was performed to study the effect of time at 250 °C.

GC-MS analysis of the products obtained in Exp 0.1, (reaction of 1,2-dihydronaphthalene and 1-hexene at 250 °C, for 1 h and using a weight ratio of 1:1) showed that there was no formation of *n*-hexane. The *n*-hexane detected in the reaction products comes from the impurities present in the 1-hexene reagent (See Figure 4.3). The impurities in the 1-hexene reagent were identified and verified with model compounds and correspond to *n*-hexane (chromatogram peak named as P-2), *trans*-3-hexene (P-3), *trans*-2-hexene (P-4) and *cis*-2-hexene (P-5). Quantification by GC-FID resulted in 0.47 wt. % of *trans*-2-hexene and 99.53 wt. % of 1-hexene, while other components were at concentrations below detection level of the instrument.

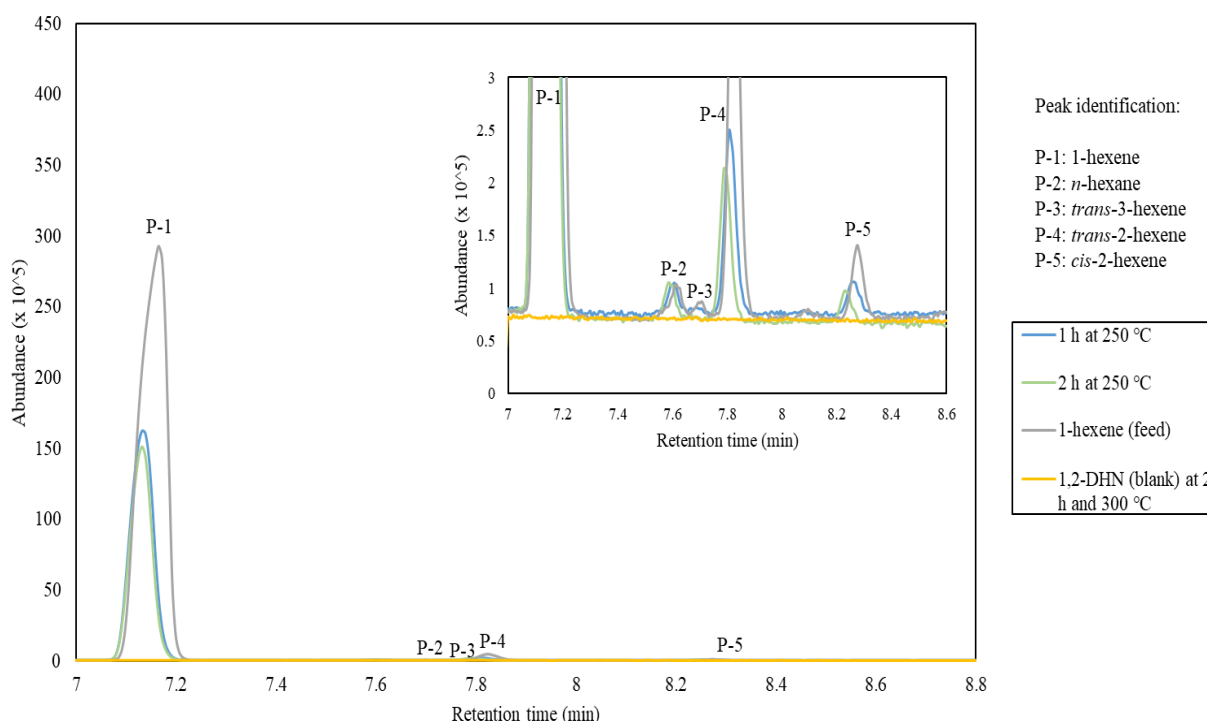


Figure 4.4 Light product distribution from reactions of 1,2-dihydronaphthalene and 1-hexene at 250 °C and different reaction times (chromatogram obtained from GC-MS)

As shown in Figure 4.4, the GC-MS chromatogram of the products obtained from Exp 0.1 and the 1-hexene reagent indicate that the desired reaction of 1-hexene to form *n*-hexane did not occur. As a result, Exp. 0.2 (reaction of 1,2-dihydronaphthalene and 1-hexene at 250 °C, for 2 h and using a weight ratio of 1:1) was performed, to evaluate if an increase in reaction time from 1 h to 2 h would result in the formation of *n*-hexane. However, based on the results shown in Figure 4.3, the light

products formed at 2 h reaction time are similar to the light products obtained from 1 h reaction time. For both cases, *n*-hexane was not formed and P-2 observed for all cases correspond to the presence of impurities in the 1-hexene reactant.

Although the light products did not indicate the formation of *n*-hexane, Figure 4.5 shows that heavier products were formed. The chromatograms of the heavier products from Exp. 0.1 and Exp. 0.2 were compared with the chromatograms of 1-hexene (reagent) and Exp. 0.5 (control experiment of 1,2-dihydronaphthalene at 300 °C and 2 h reaction time).

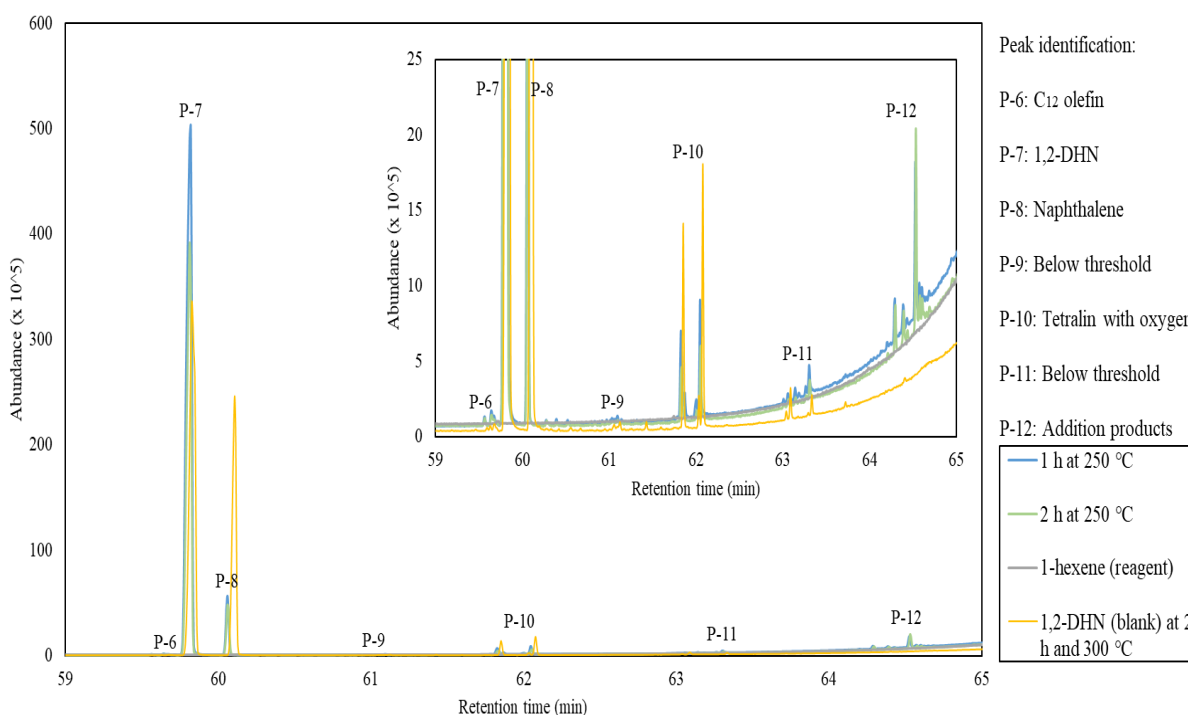


Figure 4.5 Heavy product distribution from reactions of 1,2-dihydronaphthalene and 1-hexene at 250 °C and different reaction times (chromatogram obtained from GC-MS)

The various peaks were divided into groups. A small peak (P-6) was identified as a C₁₂ olefin. P-8 was identified as naphthalene. According to the literature,¹³ 1,2-dihydronaphthalene can self-react to form naphthalene. Reaction products corresponding to the peaks of P-8 to P-11 are associated to the self-reaction of 1,2-dihydronaphthalene. The identity of the compounds with a

relative abundance of less than $2 \cdot 10^5$, namely peaks P-9 and P-11, could not be determined by the GC-MS. The peak corresponding to P-10 was identified as an aromatic (tetralin) compound with oxygen. The mass spectrum has a relevant 18 m/z mass fragment indicating the presence of oxygen in the structure and 91 m/z indicating alkyl substituted benzene.¹⁴ The molecular ion suggests a molecular formula of $C_{10}H_{10}O$.

Due to the unexpected formation of an oxygenated compound, an analysis of the reactant 1,2-dihydronaphthalene was performed by GC-MS for further comparison. In Figure 4.6, the chromatogram of 1,2-dihydronaphthalene reactant is plotted with the chromatogram of 1,2-dihydronaphthalene self-reaction at 300 °C and 2 h reaction time. According to Figure 4.6, the analysis of 1,2-dihydronaphthalene in the GC-MS was affected by potential decomposition of the compound during its elution through the capillary column under the analytical conditions.¹⁵ It has been found by previous research work¹⁶ that 1,2-dihydronaphthalene is thermally unstable. 1,2-Dihydronaphthalene can disproportionate to tetralin and naphthalene and dehydrogenate to naphthalene. Therefore, P-6, -8, -9, -10 and -11 are mainly associated with decomposition products of the reactant 1,2-dihydronaphthalene. Although, it is not known if the presence of 1-hexene in the reaction could affect the formation of these products. No further studies were performed to analyze the decomposition products.

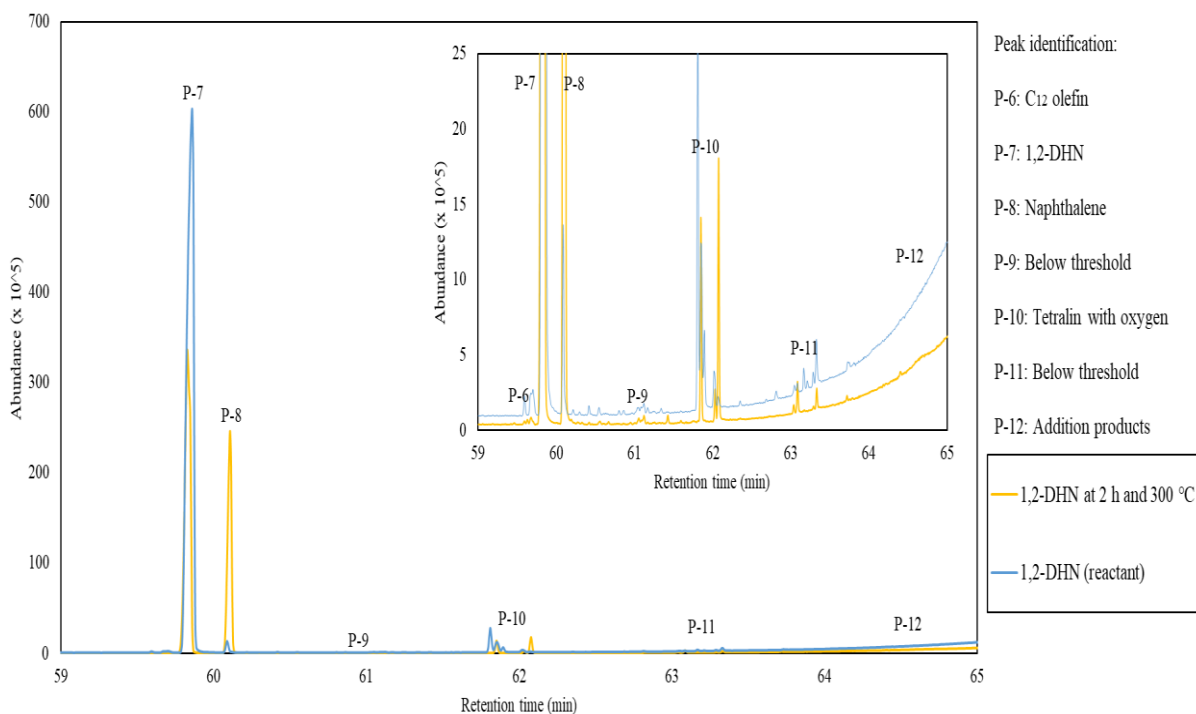


Figure 4.6 Decomposition products of 1,2-dihydronaphthalene in the GC-MS column

Only the products associated with P-12, which were identified as addition products of the reactants, were formed specifically due to the reaction of 1-hexene and 1,2-dihydronaphthalene at 250 °C. The mass spectrum of P-12 suggests a prominent 91 m/z mass fragment which indicates the presence of alkyl-substituted benzenes.¹⁴ No further studies were performed to analyze P-12.

Because no production of *n*-hexane was observed when reacting 1-hexene and 1,2-dihydronaphthalene *n*-hexane at 250 °C, a further attempt was proposed. An increase in reaction temperature was evaluated and the results are presented in the following section.

4.3.2 Effect of temperature

As the reaction of 1-hexene and 1,2-dihydronaphthalene at 1 and 2 h reaction time did not lead to the formation of *n*-hexane, an increase in the reaction temperature was studied. Temperature was manipulated as it could kinetically favor the possible formation of *n*-hexane and provide sufficient

energy to overcome the energy barrier to saturate 1-hexene. In Exp. 0.3, 1-hexene and 1,2-dihydronaphthalene at 1:1 weight ratio, were reacted at 300 °C for 2 h. Comparison of the chromatograms obtained from the reaction products of Exp. 0.1 (qualitatively similar products as Exp. 0.2) and 0.3 showed that the increase in temperature resulted in the formation of *n*-hexane (See Figure 4.7). There was a noticeable increase in the area of the peak P-2 (*n*-hexane) from the results obtained by GC-FID, in comparison to the one obtained from the experiment at 250 °C and 1 h reaction time.

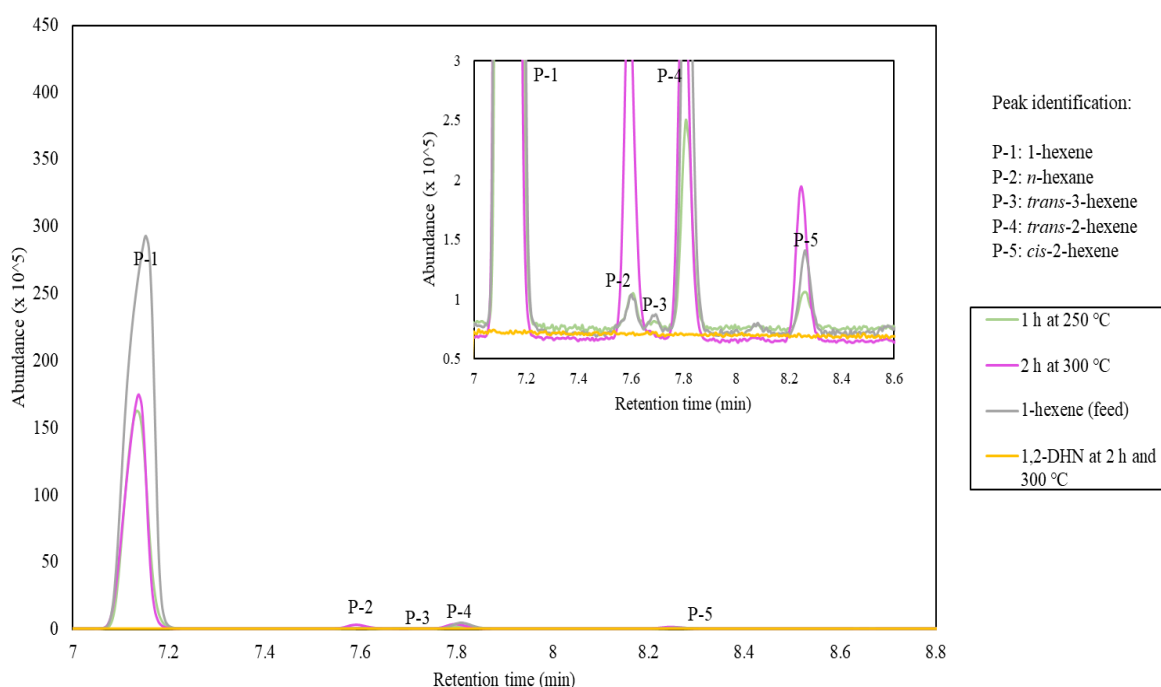


Figure 4.7 Light product distribution from reactions of 1,2-dihydronaphthalene and 1-hexene at 2 h and different reaction temperatures (chromatogram obtained from GC-MS)

Before obtaining these results, it was not evident that 1-hexene could be hydrogenated even by a good hydrogen donor such as 1,2-dihydronaphthalene. During hydrogen transfer reaction, 1-hexene would have to be converted into a hexyl radical intermediate, which is either a highly unstable primary or a secondary radical, prior to hydrogenation. The unstable intermediate can be a thermodynamic obstacle for 1-hexene hydrogenation to occur. However, the results obtained

from the experiment of 1-hexene and 1,2-dihydronaphthalene at 300 °C indicate that 1-hexene is capable of saturation to form *n*-hexane. The results demonstrate that this conversion chemistry is possible, providing important information for future study of olefin saturation with hydrogen donors.

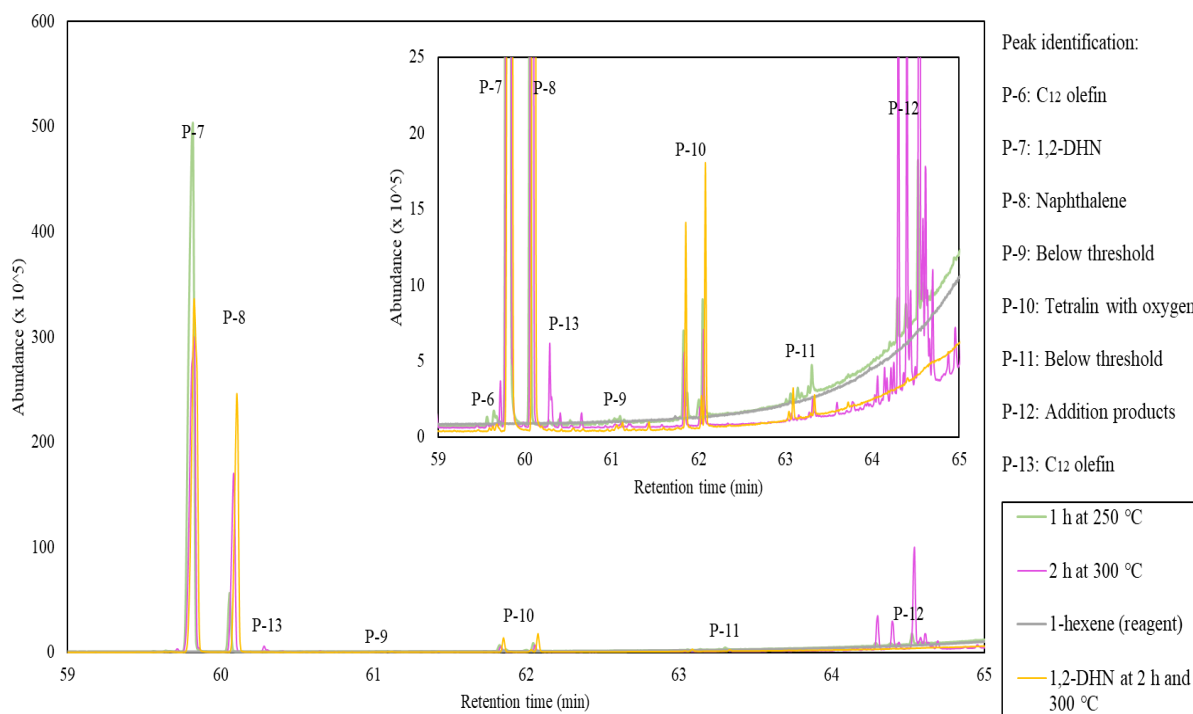


Figure 4.8 Heavy product distribution from reactions of 1,2-dihydronaphthalene and 1-hexene at 2 h and different reaction temperatures (chromatogram obtained from GC-MS)

On the other hand, it was evaluated whether the increase in temperature would affect the formation of heavier compounds. Figure 4.8 shows that reaction at 300 °C resulted in the increased formation of addition products (P-12). In addition, a new group of products labeled as P-13 was formed. These compounds were identified as C₁₂ olefins and they are products from the reaction of 1-hexene and 1,2-dihydronaphthalene because they are not present in the blank experiments or in Exp. 0.1 or Exp. 0.2. Production of C₁₂ olefins was unexpected; however, it can be viewed as

beneficial for the purpose of olefin reduction, as two moles of C₆ olefins are decreased into one mole of C₁₂ olefin.

4.3.3 Conversion and selectivity of reactions of 1-hexene and 1,2-dihydronaphthalene

Table 4.7 compares conversion and product selectivity for experiments Exp. 0.1 and Exp. 0.3 (reactions of 1-hexene and 1,2-dihydronaphthalene at 250 °C and 300 °C, respectively). Calculations from GC-FID analysis are presented in Appendix D. The products shown in Table 4.7 are combined peaks that were identified by GC-MS as similar compounds. Therefore, the selectivity can be interpreted as how much of the reactants transformed into those compounds.

From Table 4.7, the increase in time and temperature, from 250 °C and 1 h reaction time to 300 °C and 2 h, led to a considerable increase in conversion of 1-hexene and 1,2-dihydronaphthalene. The conversion of 1-hexene at 250 °C and 1 h reaction time was mainly selective towards the formation of hexene isomers, namely *trans*-2-hexene and *cis*-2-hexene. However, at 300 °C and 2 h reaction time, the conditions resulted in the formation of *n*-hexane with 2.7% selectivity and a decrease towards hexene isomers.

Products associated with P-6 to P-11 appear to be associated with thermal decomposition of 1,2-dihydronaphthalene in the gas chromatography column or by the reaction temperature of the experiment. P-6 was initially present in the reactant 1,2-dihydronaphthalene (see Figure 4.6) and was associated as a possible decomposition product in the GC-MS column during analysis. This peak disappeared when the experimental temperature increased from 250 °C to 300 °C (see Table 4.7). A similar trend was observed for compounds associated with peaks P-9, 10 and 11, which resulted in a lower selectivity after increasing the reaction time and temperature. However, the opposite trend was observed in the case of the naphthalene (P-8). An increase in temperature and time led to an increase in its selectivity.

When comparing the results of Exp. 0.3 and Exp. 0.5 in Table 4.7, the presence of 1-hexene also appears to affect the selectivity towards the products associated with P-8 to P-11. There was a decrease in selectivity towards naphthalene (P-8) when 1-hexene was present in the reaction (93%

in blank and 63% with 1-hexene). Similarly, the presence of 1-hexene suppressed the selectivity towards P-9 but favored the selectivity for P-10 and P-11. Therefore, the conversion of 1-hexene for each case considers the products of P-7 to P-11 as part of the products.

Table 4.7 Conversion and product selectivity of reactions of 1-hexene and 1,2-dihydronaphthalene at different experimental conditions

Experimental conditions	Experiments with: 1,2-dihydronaphthalene + 1-hexene ^a		Control Experiments
	Exp. 0.1: 250 °C, 1 h	Exp. 0.3: 300 °C, 2 h	Exp. 0.5: 1,2-DHN 300 °C, 2 h
Conversion of 1-hexene (%)	4.8%	27.6%	N/A
Conversion of 1,2-DHN (%)	5.6%	33.9%	30.7%
Compound identified by GC-MS	Selectivity (%)		
P-2: <i>n</i> -hexane	0.0% ^b	2.7%	0.0%
P-3: <i>trans</i> -3-hexene	0.0% ^b	0.0% ^b	0.0%
P-4: <i>trans</i> -2-hexene	10.2%	2.6%	0.0%
P-5: <i>cis</i> -2-hexene	10.4%	1.0%	0.0%
P-6 ^c : C ₁₂ olefin	4.5%	0.0%	0.0% ^b
P-8 ^d : naphthalene	39.7%	62.6%	92.7%
P-9 ^c : not identified	11.3%	0.0% ^b	3.1%
P-10 ^c : tetralin + oxygen	15.0%	5.5%	4.2%
P-11 ^c : not identified	9.0%	1.6%	0.0% ^b
P-12: addition products	0.0% ^b	24.0%	0.0%
P-13: C ₁₂ olefin	0.0%	1.2%	0.0%

^a Experiment of 1,2-dihydronaphthalene + 1-hexene at 250 °C, 2 h, 1:1 at 6 MPa was not analyzed by GC-FID

^b Detected by GC-MS but below detection level of the GC-FID

^c Decomposition products of 1,2-dihydronaphthalene in the GC-MS column under the analytical conditions

^d Side product of the reaction and decomposition products of 1,2-dihydronaphthalene in the GC-MS column under the analytical conditions

On the other hand, an increase in time and temperature also led to a higher selectivity towards the formation of P-12, which were directly associated with the reaction between 1-hexene and 1,2-dihydronaphthalene. The selectivity towards addition products increased from 0 % at 250 °C, 1 h reaction time to 24.0 % at 300 °C and 2 h reaction time. Additionally, the increase in time and temperature also resulted in the formation of C₁₂ olefins (P-13), which were not detected from previous experiments. The selectivity of C₁₂ olefins (P-13) at 300 °C and 2 h reaction time resulted in 1.2 %.

Therefore, the increase in reaction temperature from 250 °C to 300 °C not only resulted in an increase in conversion of the reactants but also led to the formation of *n*-hexane and C₁₂ olefins. The formation of these products was encouraging for the purpose of this study, which is to find alternative pathways to reduce olefin content without the use of hydrogen. The results from this preliminary study opened a research gate to investigate further the potential of 1-hexene saturation via hydrogen transfer. Once it was determined that 1-hexene is capable of receiving hydrogens via hydrogen transfer from a good hydrogen donor like 1,2-dihydronaphthalene; the next step was to study the reaction of hydrogenation of 1-hexene but using asphaltenes as the hydrogen donor.

4.4 Results of the study: Asphaltenes as hydrogen donor

4.4.1 Reactions of asphaltenes and 1-hexene

After verifying that 1-hexene, a poor hydrogen acceptor, is capable of receiving hydrogen from a good hydrogen donor like 1,2-dihydronaphthalene at 300 °C. The second part of the study involved replacing 1,2-dihydronaphthalene for industrial asphaltenes as hydrogen donor while keeping 1-hexene as hydrogen acceptor. Previous research³ have demonstrated hydrogen transfer abilities in the asphaltenes, hence, this was used as premise for this study.

1-Hexene and industrially obtained asphaltenes were reacted at different conditions (Table 4.8). As in the preliminary study, the effect of time and temperature were investigated. Studies performed by Naghizada et al.,³ determined that the variation of weight ratio of asphaltenes to

olefin can play a role in the amount of hydrogen available for transfer. Hence, effect of weight ratio was also considered.

In all cases, the reaction products were analyzed by GC-MS for compound identification and then by GC-FID for quantification. Based on the results, the olefin reduction, conversion of 1-hexene (Table 4.8) and product selectivity (Table 4.9) were calculated. In general terms, an increase in olefin reduction was observed when there was an increase in reaction time, temperature and weight ratio of asphaltenes to 1-hexene (in the evaluated range). In all cases, conversion of 1-hexene had a similar trend as the olefin reduction, there was an increase in 1-hexene conversion when reaction time, temperature and weight ratio of asphaltenes to 1-hexene were increased. Selectivity was distributed towards various products. These products were classified per compound groups as *n*-hexane, C₆ olefins (hexene isomers different from 1-hexene), C₁₀ alkane, C₁₁ alkane, C₁₂ alkane, and C₁₂ olefins. *n*-Hexane was formed in almost all the experiments involving asphaltenes in the reaction. Blank reactions of 1-hexene at different experimental conditions resulted in the formation of C₆ and C₁₂ olefins.

In summary, results from Tables 4.8 and 4.9 showed that 1-hexene was successfully hydrogenated or dimerized by the addition of asphaltenes. It was proven that asphaltenes are capable of hydrogenating a poor hydrogen acceptor such as 1-hexene to form *n*-hexane.

Comments on possible heavy product formation:

As GC-MS and GC-FID analyses were limited to the detection of a maximum of compounds with a C₁₂ hydrocarbon chain length, SimDist analyses were performed to investigate the formation of heavier compounds (> C₁₂ hydrocarbon chain length). The results obtained by SimDist are shown in Table 4.10. On average, most of the experiments involving asphaltenes resulted in products with a maximum of C₂₂ hydrocarbon chain length. For certain experiments (recovered liquid products from Exp. 2, 6, 16, 17 and 18), the presence of compounds with a C₉₈ hydrocarbon chain length was detected.

To assess the nature of the heavy material represented by C₉₈, fluorescence spectroscopy was used to determine if these heavy compounds were traces of asphaltenes or actual reaction products. The resulting contour maps are shown in Figure 4.9.

Table 4.8 Summary of results of olefin reduction and 1-hexene conversion of reactions of asphaltenes and 1-hexene at different reaction conditions detectable by GC-FID

Exp.	T (°C)	t (h)	Weight ratio Asph: Olefin	% Olefin reduction		% Conversion of 1-hexene	
				Average	Std. Deviation	Average	Std. deviation
1	250	1	1:1	0.4%	- ^a	0.7%	- ^a
2	250	2	1:1	0.8%	- ^a	1.6%	- ^a
3	250	4	1:1	2.6%	- ^a	3.4%	- ^a
4	250	24	1:1	4.3%	- ^a	6.1%	- ^a
5	250	24	0:1 ^d	1.0%	- ^b	1.9%	- ^b
6	300	2	1:1	3.7%	0.3% ^c	5.6%	1.4% ^c
7	300	2	2:1	6.1%	- ^b	8.7%	- ^b
8	300	2	4:1	7.8%	0.1% ^c	11.5%	0.1% ^c
9	300	2	8:1	10.4%	- ^a	14.9%	- ^a
10	300	2	0:1 ^d	1.4%	- ^b	2.1%	- ^b
11	300	4	1:1	8.3%	- ^b	15.0%	- ^b
12	300	4	2:1	11.9%	0.4% ^a	16.4%	0.5% ^a
13	300	4	0:1 ^d	2.7%	- ^b	4.7%	- ^b
14	325	2	1:1	7.0%	1.8% ^c	10.8%	3.2% ^c
15	350	0.5	1:1	5.7%	- ^a	11.4%	- ^a
16	350	1	1:1	14.9%	- ^a	19.8%	- ^a
17	350	2	1:1	24.0%	- ^a	33.8%	- ^a
18	350	3	1:1	38.1%	- ^a	49.3%	- ^a
19	350	3	0:1 ^d	8.8%	1.9 ^c	10.6%	2.3% ^c

^a Experiment was performed in duplicate

^b Experiment was only performed once

^c Standard deviation was calculated for experiments in triplicate

^d Control experiments

Table 4.9 Summary of results of product selectivity of reactions of asphaltenes and 1-hexene at different reaction conditions identified by GC-MS and quantified by GC-FID

Exp.	T (°C)	t (h)	weight ratio asph: olefin	% Selectivity					
				<i>n</i> -hexane	C ₆ olefins	C ₁₀ alkane	C ₁₁ alkane	C ₁₂ alkane	C ₁₂ olefin
1 ^a	250	1	1:1	0.0%	41.5%	0.0%	0.0%	0.0%	58.5%
2 ^a	250	2	1:1	5.9%	50.1%	0.0%	0.0%	0.0%	44.1%
3 ^a	250	4	1:1	11.4%	25.7%	0.0%	0.0%	2.6%	60.2%
4 ^a	250	24	1:1	33.1%	30.5%	0.0%	0.0%	10.1%	26.4%
5 ^b	250	24	0:1 ^d	0.0%	45.0%	0.0%	0.0%	0.0%	55.0%
6 ^c	300	2	1:1	30.2%	25.5%	0.0%	0.0%	9.7%	34.7%
7 ^b	300	2	2:1	34.4%	29.8%	0.0%	0.0%	8.7%	27.1%
8 ^a	300	2	4:1	50.9%	32.0%	0.6%	0.0%	5.4%	11.1%
9 ^b	300	2	8:1	51.1%	30.4%	0.5%	0.0%	6.4%	11.6%
10 ^b	300	2	0:1 ^d	0.0%	32.5%	0.0%	0.0%	0.0%	67.5%
11 ^c	300	4	1:1	30.5%	34.6%	0.3%	0.0%	8.3%	26.3%
12 ^b	300	4	2:1	39.0%	27.5%	0.5%	0.0%	10.9%	22.1%
13 ^b	300	4	0:1 ^d	0.0%	42.3%	0.0%	0.0%	0.0%	57.7%
14 ^c	325	2	1:1	25.4%	45.8%	0.2%	0.0%	6.7%	21.9%
15 ^a	350	0.5	1:1	23.6%	47.1%	0.0%	0.8%	2.6%	25.9%
16 ^a	350	1	1:1	35.5%	24.9%	1.3%	1.3%	7.8%	29.1%
17 ^a	350	2	1:1	39.0%	29.3%	0.7%	0.8%	7.8%	22.3%
18 ^a	350	3	1:1	44.6%	22.7%	0.8%	0.8%	11.3%	19.8%
19 ^b	350	3	0:1 ^d	0.62% ^e	16.71%	0.0%	0.0%	0.0%	82.67%

^a Experiment was performed in duplicate

^b Experiment was only performed once

^c Experiment was performed in triplicate

^d Control experiments

^e Only one of the three experiments resulted with a small peak of *n*-hexane

Table 4.10 Product distribution by carbon number for reactions of asphaltenes and 1-hexene at different reaction conditions analyzed by SimDist

wt.%																									
Exp.	C6	C7	C8	C9	C10	C11	C12	C14	C16	C17	C18	C20	C22	C24	C26	C32	C36	C42	C44	C52	C48	C66	C76	C86	C98
1	100																								
2	95																								5
3	87						13																		
4	89				1		10																		
5	89			1			10																		
6	95						1										1								3
7	86					1		1		12															
8	87						13																		
9	97			1			2																		
10	86						2			1			11												
11	83	2					2		1	12															
12	93		1				2		1						1					2					
13	83						2			1			14												
14	79		3		1		4		1				1					11							
15	83					1	1	1		1		13													
16	77			1			5	1		1		1		1		1					1	1		1	9
17	74		1		1	1	7	1	2	1	1		1	1		1		1					1		6
18	67	1	1	1		2	11	1	3	1	1		2		1		1							1	6
19	50			1	1	3	3	1	1	1	1	2	1		35										

The results presented in Table 4.10 rather than displaying the boiling curves of each sample, it provides the weight percentage of each carbon number present in the sample for easier comparison between experiments. The calculations to transform the distillation curve into weight percentage of carbon number in the sample are explained in Appendix E. It is important to mention that the results obtained by SimDist are calibrated with a standard of linear paraffins. Therefore, the results are dependent on the retention time of compounds relative to linear paraffins. In the case of certain branched paraffin isomers and some olefinic isomers, the boiling point temperatures may be more than 25 °C lower than that of the corresponding linear paraffin compounds. Hence, overlapping between boiling points of different compounds may occur; this would cause the C_n compounds to be reported as C_{n-1} or C_{n-2} . As a result, the information provided in Table 4.10 can only be seen as an indication of the possible carbon number distribution of the compounds in the sample based on the results obtained by boiling point.

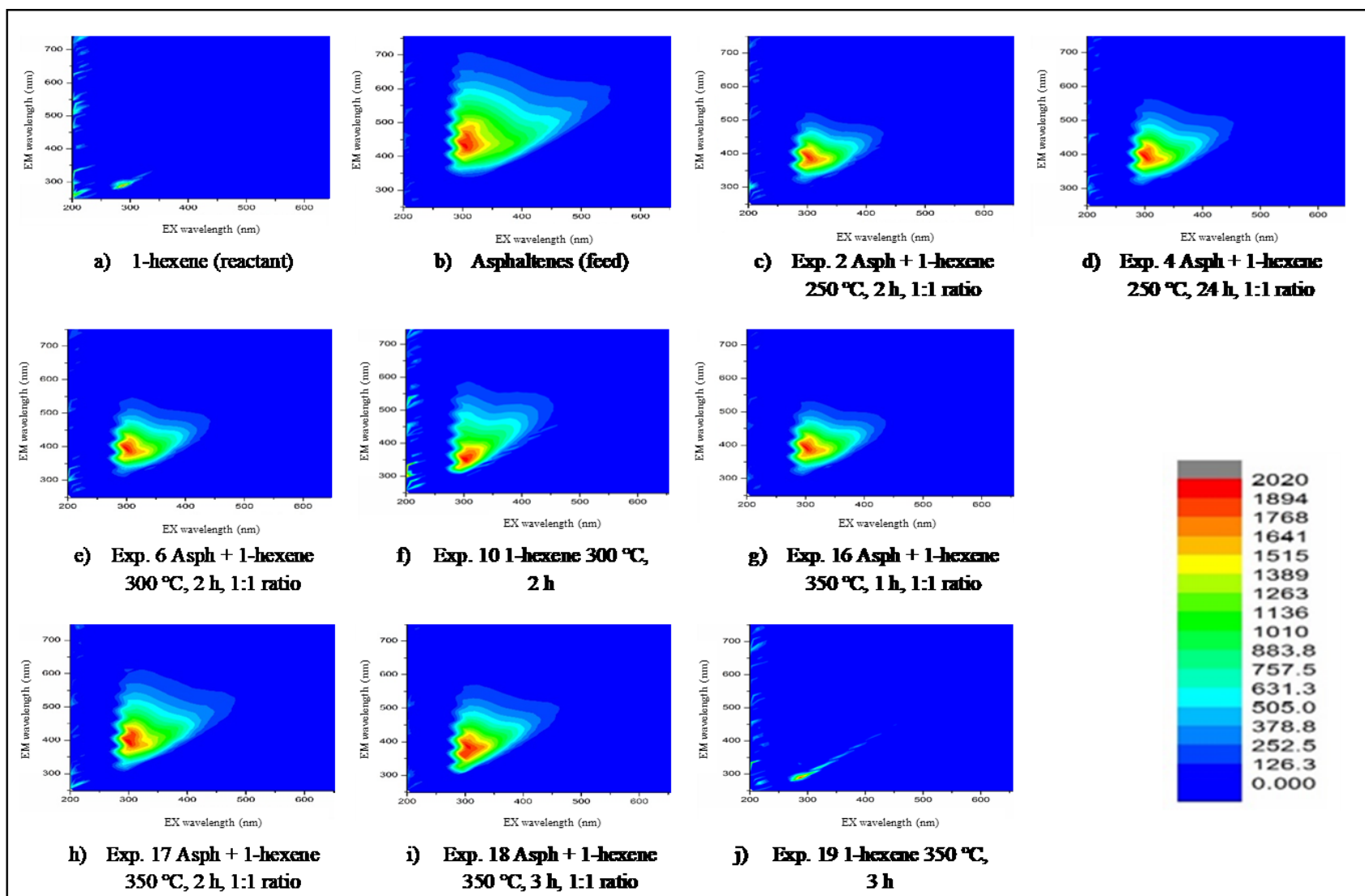


Figure 4.9 Contour maps by fluorescence spectroscopy of reaction products of 1-hexene and asphaltenes at different experimental conditions

Fluorescence spectroscopy was selected to detect the presence of asphaltenes in the sample because asphaltenes naturally have various chemical species that are fluorescent. According to the contour maps shown in Figure 4.9 (b), it can be seen that the fluorophores present in the asphaltenes feed, under the analytical conditions, fluoresce is a maximum at an emission wavelength of 420 nm and excitation wavelength of 310 nm. On the other hand, 1-hexene had almost no fluorescent emission.

All the samples that resulted in the presence of C₉₈ hydrocarbons in Table 4.10 (Exp. 2, 6, 16, 17 and 18) appear to have presence of asphaltenes. All the reaction products resulted in fluorophores fluorescing in similar emission and excitation wavelength as the asphaltene feed. This can be observed by comparing the fluorescence spectra of the reaction products (Figure 4.9 (c, e, g, h and i)) compared to the asphaltenes feed (Figure 4.9 (b)).

Based on the identified products by GC-MS, the liquid reaction products are conformed by mono-olefins and alkanes. Alkanes are not likely to fluoresce because the electrons in the sigma bonds have a high probability of remaining in the space between the two atoms. Therefore, these compounds would not emit light when stimulated by radiation. Mono-olefins, on the other hand, could emit light due to the presence of a double bond in its molecular structure. However, the fluorescence is usually weak as can be seen in Figure 4.9 (a) and according to the literature.¹⁷ As a result, the strong fluorescent component of the samples can most likely be associated with the presence of traces of asphaltenes.

For Exp. 4 (Figure 4.9 (d)), although the SimDist analysis did not result in detectable C₉₈ hydrocarbons, the sample fluoresces. The products from Exp. 4 contain fluorophores that fluoresce at an emission wavelength of 400 nm and excitation wavelength of 300 nm. The fluorescent emission is similar to the asphaltenes; as a result, it can be mostly associated with the presence of asphaltenes in the sample. It is possible that due to the detection limitations of the SimDist, the traces of asphaltenes were not detectable in the analysis.

When comparing the blank reactions of thermally treated 1-hexene (Exp. 10 and 19 in Figure 4.9 (f) and Figure 4.9 (j), respectively) the products from Exp. 10 fluoresce at a maximum of 350 nm emission wavelength and 300-excitation wavelength. On the other hand, the products formed from

Exp. 19 had almost no fluorescent emission, and the spectrum is similar to the 1-hexene feed in Figure 4.9 (a). It is unknown why the products from Exp. 10 fluoresce, while the products from Exp. 19 did not. However, no further studies were performed.

4.4.2 Reaction of asphaltenes and thermally cracked naphtha

After the successful hydrogenation of 1-hexene by asphaltenes at different experimental conditions, it was finally attempted to apply this knowledge on treating the olefins in the thermally cracked naphtha. Because thermally cracked naphtha is a complex mixture, it is not known if the reaction with asphaltenes would lead to olefin reduction. The presence of other compounds could interfere with the hydrogen transfer reactions between the olefins and the asphaltenes.

Reaction at 350 °C, 3 h reaction time, 7 MPa at 4:1 ratio of asphaltenes to naphtha was carried out. Two separate phases were observed. After opening the batch reactor for product collection, the treated naphtha was found outside of the glass vial, leaving behind the asphaltenes in the glass vial. The treated naphtha was collected with a glass pipet and transferred to a lidded glass vial for further analyses. Therefore, separation was not a concern for this application.

Olefin reduction was calculated with respect to 1-hexene due to the complexity of the naphtha. In Table 4.11, the olefin reduction and conversion of 1-hexene are calculated for each experiment. As previously defined in Section 4.2.4.1, olefin reduction looks at the nature of the products, while conversion of 1-hexene looks at the disappearance of 1-hexene in the reaction.

Two experiments were performed for comparison. The first experiment was the reaction of asphaltenes and naphtha spiked with 10 wt. % of a 1:9 ratio solution of 1-hexene to *n*-hexane to analyze the effect of asphaltenes on olefin reduction of the naphtha. The second experiment involves performing the same experiment, but with a solution of 10 wt.% of 1-hexene in *n*-hexane rather than naphtha. According to the results (Table 4.11), the conversion of 1-hexene is comparable for both cases, indicating that regardless of the other components present in the naphtha, the conversion of 1-hexene is not much affected. On the other hand, olefin reduction with respect to 1-hexene (Exp. 20) was ~ 14% for naphtha treated with asphaltenes. While the reaction of 1-hexene

under the same conditions (Exp. 21) was ~ 30 %. However, olefin reduction between both experiments cannot be compared directly, as the olefin reduction calculated from the experiments with naphtha does not consider the other compounds, such as other olefins, that are most likely participating in the competitive reaction for hydrogen provided by the asphaltenes.

Table 4.11 Olefin reduction and 1-hexene conversion of reaction of asphaltenes and naphtha at 350 °C, 3 h, 4:1 asphaltenes to 1-hexene, 7 MPa, detectable by GC-FID

Weight ratio of reactants	% Olefin reduction (with respect to 1-hexene) ^a	% Conversion of 1-hexene ^a
Exp. 20: 4:1 (asphaltenes: spiked naphtha)	13.6	78.9
Exp. 21: 4:1 (asphaltenes: solution of 1-hexene/ <i>n</i> -hexane)	30.4	73.2

^a Experiments performed in duplicates

In order to have more information about the olefin reduction and conversion of 1-hexene after the treatment with the asphaltenes, Table 4.12 presents a comparison between the mole percentage of the untreated and treated spiked naphtha. The moles of 1-hexene, C₁₂ alkanes and C₁₂ olefins in the naphtha decreased after treatment with the asphaltenes. While, the moles of *n*-hexane, C₆ olefins, and C₁₀ and C₁₁ alkanes increased.

Table 4.12 Effect of asphaltene treatment on thermally cracked naphtha on product formation

Compound group	mol %			Effect after treatment
	Untreated spiked naphtha	Treated spiked naphtha ^a	Difference (Untreated-Treated)	
1-hexene	0.121%	0.025%	0.095%	↓
<i>n</i> -hexane	0.825%	0.856%	-0.030%	↑
C ₆ olefins	0.054%	0.132%	-0.079%	↑
C ₁₀ alkanes	0.035%	0.039%	-0.004%	↑
C ₁₁ alkanes	0.019%	0.020%	-0.001%	↑
C ₁₂ alkanes	0.017%	0.015%	0.002%	↓
C ₁₂ olefins	0.020%	0.010%	0.010%	↓

^a Average value of experiments in duplicates

To evaluate whether the asphaltenes treatment affects the boiling curve of the thermally cracked naphtha, SimDist analyses were performed on the untreated and treated naphtha (Figure 4.10). However, not much difference between the boiling curve of the untreated and treated naphtha was observed. For all samples, 100 % recovery was achieved. Approximately 6 wt. % of material in samples were recovered isothermally. According to the result, the 6 wt. % of the treated naphtha distills at a relatively lower temperature (~ 260 °C) than the untreated naphtha (~ 270 °C).

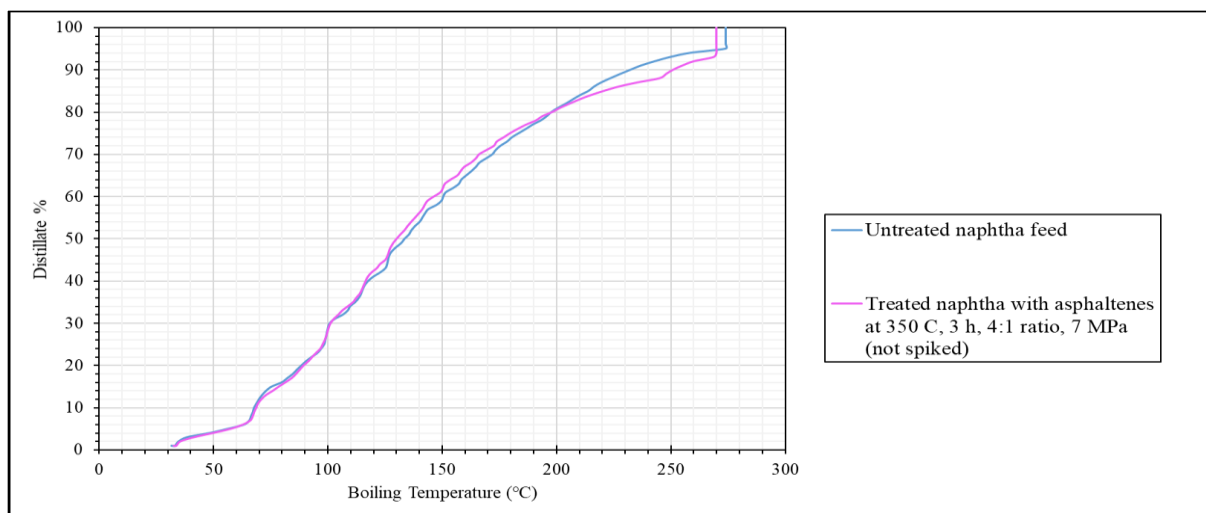


Figure 4.10 Comparison of SimDist analyses between untreated naphtha and naphtha treated with asphaltenes

However, after revising the chromatograms obtained from the SimDist and GC-MS, there were no peaks eluting at 270-275 °C. Therefore, it is likely that the heavy compounds boiling isothermally at 270-275 °C shown in the SimDist chromatogram is an artefact of the software when it transforms the chromatograms into a boiling curve.

The gum content in the treated and untreated naphtha was determined (Table 4. 13). However, the repeatability of the experiments was low. The gum content for each sample resulted in high variability. As a result, it cannot be concluded if the use of asphaltenes can decrease the gum content in the naphtha. However, the use of asphaltenes does not contribute to an increase in the gum content in the naphtha. The analyses of the treated naphtha resulted mainly with a lower or similar gum content as the naphtha. More studies have to be performed in order to conclude about the gum content in the treated naphtha.

Table 4. 13 Gum content in the treated and untreated naphtha

	Gum content (wt. % of g gum/ g sample)				Std. Deviation
	Analysis 1	Analysis 2	Analysis 3	Average	
Naphtha (feed)	0.080 %	0.062%	0.011%	0.051%	0.036%
Exp. 22.1: Asphaltenes + naphtha 4:1, 350 °C and 3 h	0.013 %	0.086 %	- ^a	0.049%	- ^a
Exp. 22.2: Asphaltenes + naphtha 4:1, 350 °C and 3 h	0.007 %	0.031%	-a	0.019%	-a

^a Experiments were performed in duplicates

4.5 Discussion

4.5.1 Effect of temperature on reactions of 1-hexene with asphaltenes

Based on the results of the preliminary study, the increase in temperature from 250 °C to 300 °C lead to the detectable formation of *n*-hexane and C₁₂ olefins as reaction products. Therefore, the effect of temperature in the range 250-350 °C was evaluated for reactions of 1-hexene and asphaltenes (experiments 2, 6, 14 and 17 listed in Table 4.5). Figure 4.11 presents the olefin reduction at different reaction temperatures at 2 h reaction time and 1:1 weight ratio of asphaltenes to 1-hexene.

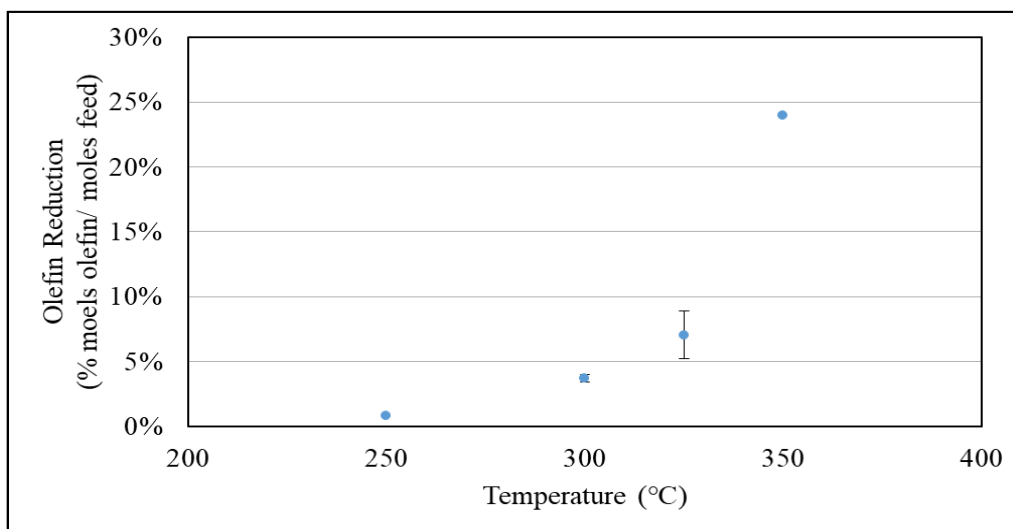


Figure 4.11 Effect of temperature on olefin reduction at 2 h and 1:1 ratio of asphaltenes to 1-hexene

It was not known that asphaltenes were capable of hydrogenating the olefins rather than leading other conversion reactions. However, when experimental temperature was increased, the olefin reduction increased. The highest temperature of study (350 °C) led to the highest olefin reduction (~25 % molar reduction). From a kinetic point of view, this seems logical. An increase in the reaction temperature accelerates the reaction kinetics. However, the temperature increase not only

affected the reaction rate but also played a role enabling the hydrogen transfer. Ultimately, this would result in the formation of products that reduced the olefin content.

The product distribution is presented in Figure 4.12. Hydrogenation to produce *n*-hexane is the main reaction contributing towards olefin reduction at temperatures higher than 300 °C; whereas, dimerization to form C₁₂ olefins is the main reaction pathway at temperatures lower than 300 °C. Directionally, the increase in temperature decreases the production of C₆ isomer olefins, which are an undesirable side product that does not contribute towards the olefin reduction.

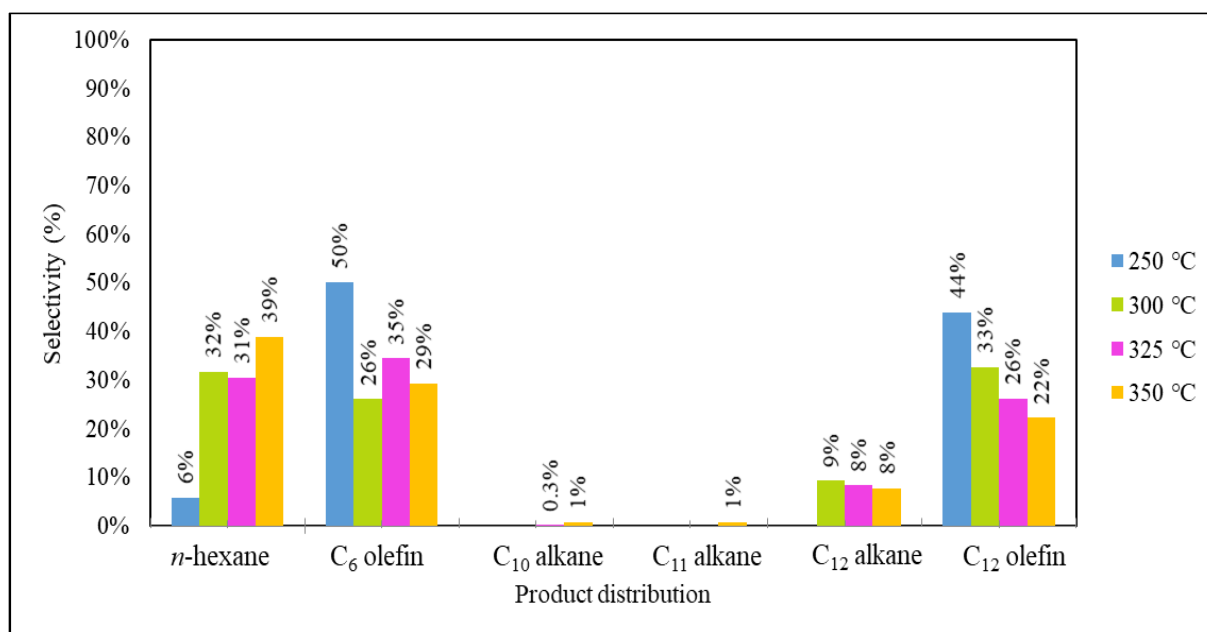


Figure 4.12 Effect of temperature on product distribution at 2 h and 1:1 ratio of asphaltenes to 1-hexene

Table 4.10 provides information on the heavier products formed at the different experimental conditions. At temperatures < 300 °C, most of the products (~ 95 wt. %) corresponded with a boiling point of C₆ hydrocarbon chain length and with a small percentage of C₁₂ hydrocarbons. However, when the temperature is raised to the range of 325- 350 °C, the product distribution resulted in an increase in the number of species than at lower temperatures. The total weight percentage of C₆

hydrocarbons was on average ~ 76 wt. %. There was a higher formation of heavier compounds such as C₁₄ to C₇₆. The presence of C₉₈ was verified by fluorescence spectroscopy as traces of asphaltenes in the sample.

4.5.2 Effect of time on reactions of 1-hexene with asphaltenes

4.5.2.1 Effect of time at 250 °C

As operational costs may increase considerably at higher reaction temperature due to higher energy consumptions and equipment limitations, i.e., the cost of a furnace ($T_{\text{out}} > 250\text{ °C}$) in comparison to the cost of a heat exchanger ($T_{\text{out}} < 250\text{ °C}$), it is important to contemplate operations at lower temperatures.

Based on the preliminary studies, at 250 °C and 1-2 h reaction time, *n*-hexane was not formed. However, it was questioned whether *n*-hexane could be formed if using asphaltenes as hydrogen donors or if a longer residence time could result in the formation of *n*-hexane at 250 °C. Therefore, 250 °C was evaluated as potential operational temperature. In this way, the reaction time was varied from 2 to 24 h using a 1:1 weight ratio of asphaltenes to 1-hexene. Figure 4.13 shows the results from the corresponding set of experiments (entries 1, 2, 3, 4 and 5 in Table 4.5). It can be observed that the increase in reaction time resulted in an increase in olefin reduction. Nevertheless, the olefin reduction is still low at the longest reaction time (24 h) with only a ~ 4.5 % molar reduction.

The blank reaction also resulted in a relatively high olefin reduction capacity. From Table 4.9, the blank experiment (Exp. 5, 1-hexene self-reaction at 250 °C, 6 MPa, and 24 h) resulted in 45 % selectivity towards hexene isomers and 55 % of C₁₂ olefins. From the experimental conditions, it was unlikely that 1-hexene self-reacted and resulted in thermal oligomerization. According to the literature,¹⁸ thermal polymerization of C₆ olefins required operational conditions as extreme as 370-400 MPa at 290 °C. Additionally, the occurrence of true thermal oligomerization is improbable due to possible impurities in the reactant or the use of metallic reactors that can result as the actual initiator of the olefin oligomerization.¹⁹ Therefore, based on the results obtained from the blank reactions, the products of hexene isomers and C₁₂ olefins might not be true thermal oligomerization

products but products formed from the catalytic effect of the reactor walls. This matter will be further discussed in Section 4.5.4.

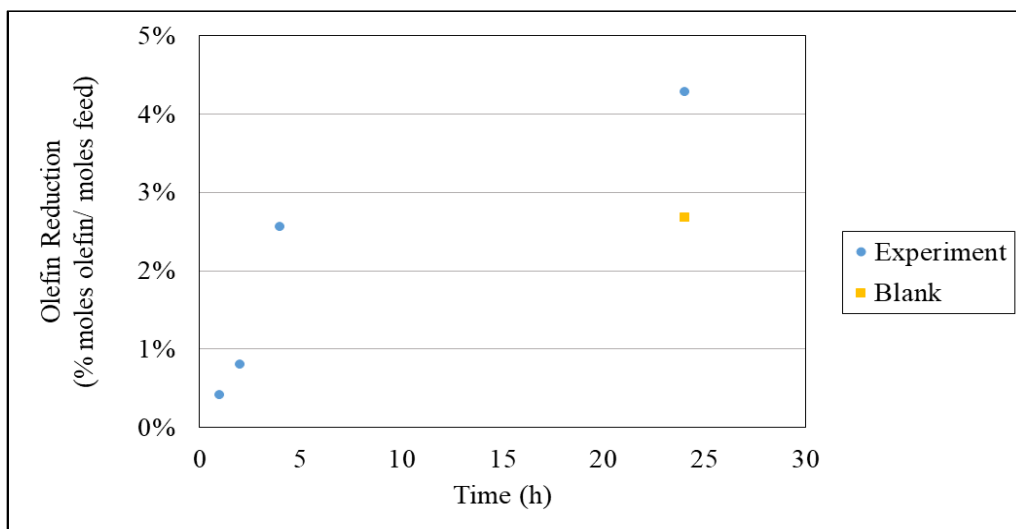


Figure 4.13 Effect of time on olefin reduction at 250 °C and 1:1 ratio of asphaltenes to 1-hexene

In order to understand the type of reactions undergone by 1-hexene at the studied experimental conditions, the product distribution was analyzed (Figure 4.14). At 250 °C, regardless of the reaction time, the main reaction pathway for olefin reduction is associated with the formation of C₁₂ olefins (dimerization). However, the longer reaction times, especially at 24 h, made possible the formation of saturated compounds such as *n*-hexane and C₁₂ alkanes. The formation of alkanes has a higher contribution towards olefin reduction than the formation of C₁₂ olefins, as the dimerization of the olefins can reduce the olefin content by half, while the saturation of an olefin can eliminate the unsaturation. The experimental data indicates that a poor hydrogen acceptor such as 1-hexene can accept hydrogen from the asphaltenes to form *n*-hexane.

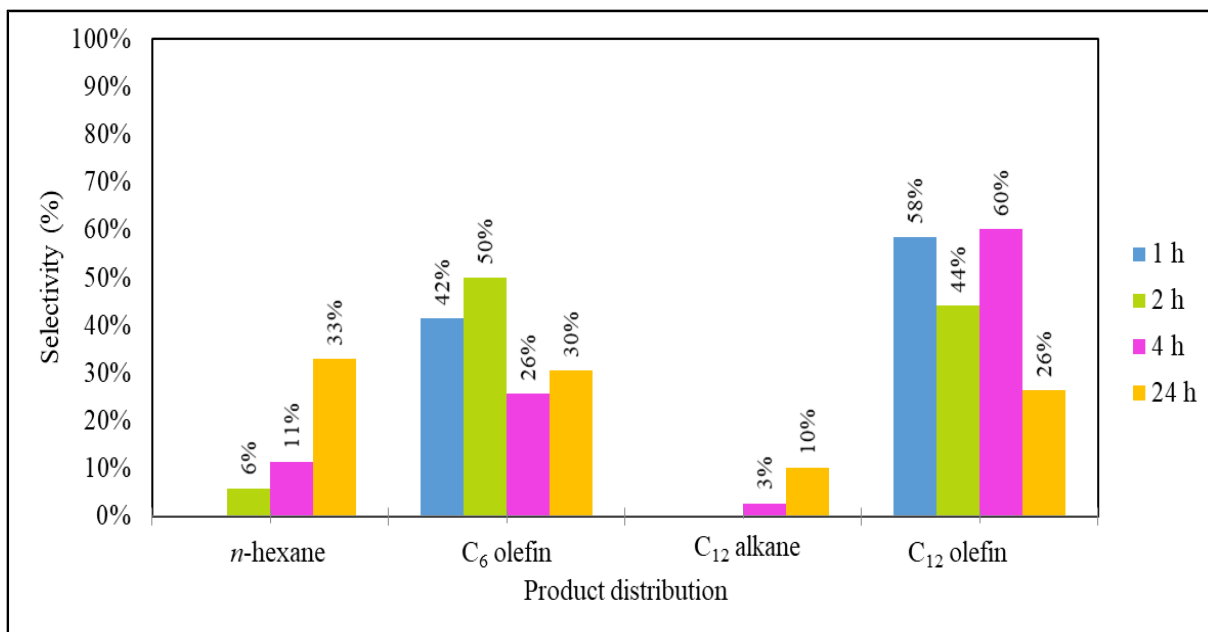


Figure 4.14 Effect of time on product distribution at 250 °C and 1:1 ratio of asphaltenes to 1-hexene

4.5.2.2 Effect of time at 350 °C

To achieve higher olefin reduction, the effect of reaction time at 350 °C was studied (experiments 15, 16, 17, 18 and 19 in Table 4.5). This temperature was selected because it resulted in the highest olefin reduction from temperature range evaluated (Section 4.3.2). The weight ratio of asphaltenes to 1-hexene was fixed at 1:1 in all experiments. Figure 4.15 presents a summary of the calculated olefin reduction.

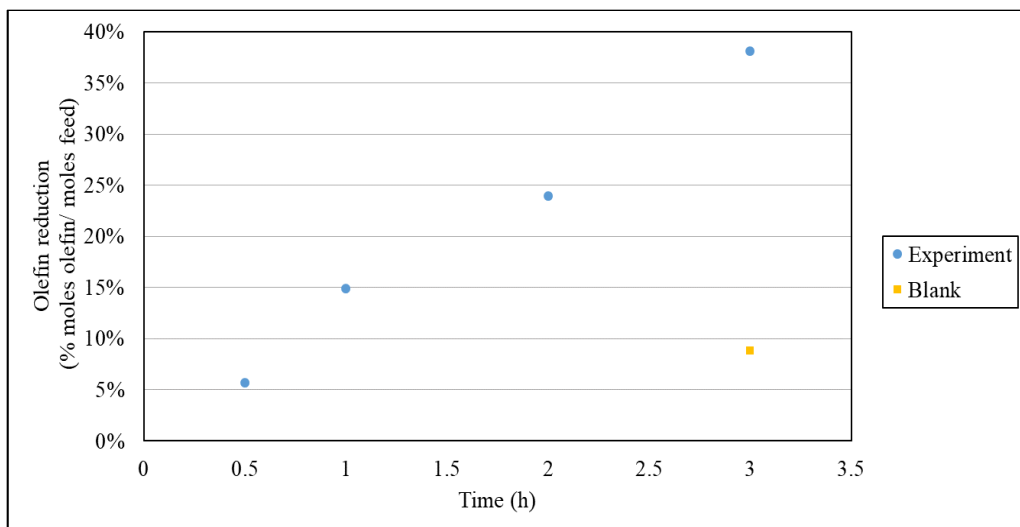


Figure 4.15 Effect of time on olefin reduction at 350 °C and 1:1 weight ratio of asphaltenes to 1-hexene

Similar to the trend observed in the study of effect of time at 250 °C (Figure 4.11), an increase in reaction time resulted in a rise in olefin reduction. However, in comparison to the reactions at 250 °C, the olefin reduction was much higher in reactions at 350 °C, with ~ 40 % at 3 h reaction time, while at 250 °C and 24 h reaction time, the olefin reduction was ~ 4.5%. The blank reaction of 1-hexene at 350 °C, 3 h and 7 MPa (Exp. 19) also resulted in a considerable olefin reduction capacity (~10 %). The effect of the reactor walls on the results from the blank experiment will be further discussed in Section 4.5.4.

From Table 4.9, the analysis of the product distribution showed that the conversion of 1-hexene and reduction in the olefin content was primarily due to the formation of *n*-hexane and C₁₂ olefins. In contrast to the previous experiments at 250 °C, the higher temperature and longer reaction times lead to a more varied product distribution; including the presence of heavier compounds with hydrocarbon chain lengths of C₁₂-C₃₆ (Exp. 15-18 in Table 4.10).

4.5.3 Effect of ratio of asphaltenes to 1-hexene

After the evaluation of the effect of temperature, the next parameter to study was the effect of weight ratio of asphaltenes to 1-hexene. The weight ratio of asphaltenes to 1-hexene was varied from 1:1, 2:1, 4:1 and 9:1 at 300 °C and 2 h reaction time. The results were obtained from experiments 6, 7, 8, 9 and 10, which are listed in Table 4.5. Figure 4.16 presents the olefin reduction for the different experiments. Increasing the weight ratio of asphaltenes to 1-hexene leads to an increase in olefin reduction. At 8:1 ratio, an olefin reduction of ~ 10 % was achieved.

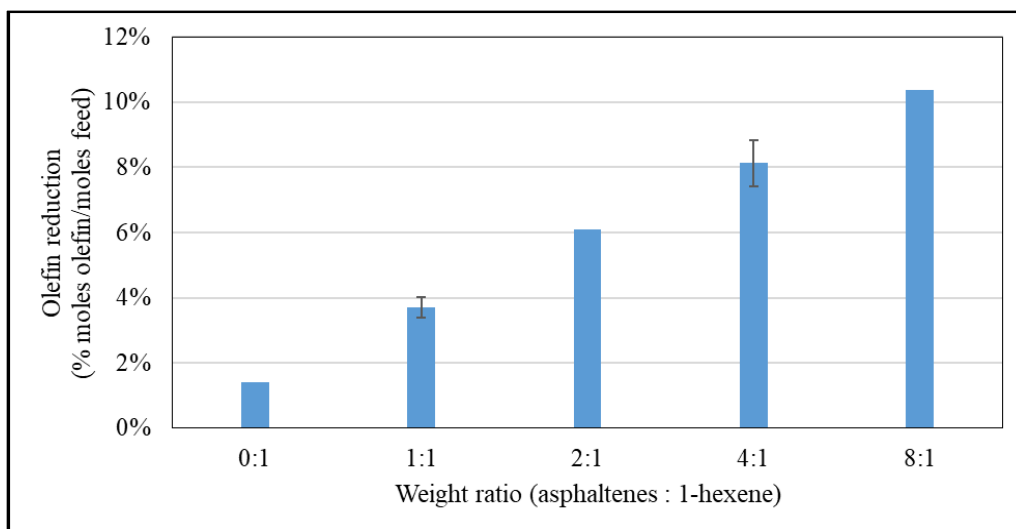


Figure 4.16 Effect of weight ratio of asphaltenes to 1-hexene on olefin reduction at 300 °C and 2 h

From Table 4.8, the conversion of 1-hexene increased when the ratio of asphaltenes to 1-hexene was higher (Exp. 6-9). The conversion of 1-hexene and olefin reduction was primarily due to the formation of *n*-hexane and C₁₂ alkanes and olefins (See Table 4.9). Addition of more asphaltenes favored the formation of more saturated compounds. Based on the results obtained from SimDist (Table 4.10), the higher amount of asphaltenes in the sample appears to suppress the formation of heavier compounds (compare Exp. 9 with Exp.7-8). This is even more visible when comparing results from a blank experiment (Exp.10: 1-hexene at 300 °C and 2 h reaction time) with Exp. 9

(8:1 weight ratio of asphaltenes to 1-hexene at 300 °C and 2 h reaction time). There is a higher weight percentage of C₆ in Exp. 9 (97 wt. %) than in the blank Exp. 10 (86 wt. %), where heavier compounds were formed (namely, C₂₂ with 11 wt. %).

4.5.4 Effect of reactor walls and asphaltene contribution to reaction with 1-hexene

Based on the results presented in Table 4.8, blank experiments, which are nothing else than the self-reaction of 1-hexene at different experimental conditions, led to an olefin reduction between ~1-9 % due to the formation of C₁₂ olefins (see Table 4.9 for more information on product selectivity). This contribution towards olefin reduction is not insignificant and needs to be taken into account when 1-hexene is reacted with asphaltenes to determine the actual effect of the asphaltenes in the reaction.

Product selectivity was re-calculated in terms of contribution of asphaltenes to product selectivity and the results are shown in Figure 4.17. The calculations to decouple the effect of the blank reactions from the experimental results can be found in Appendix F.

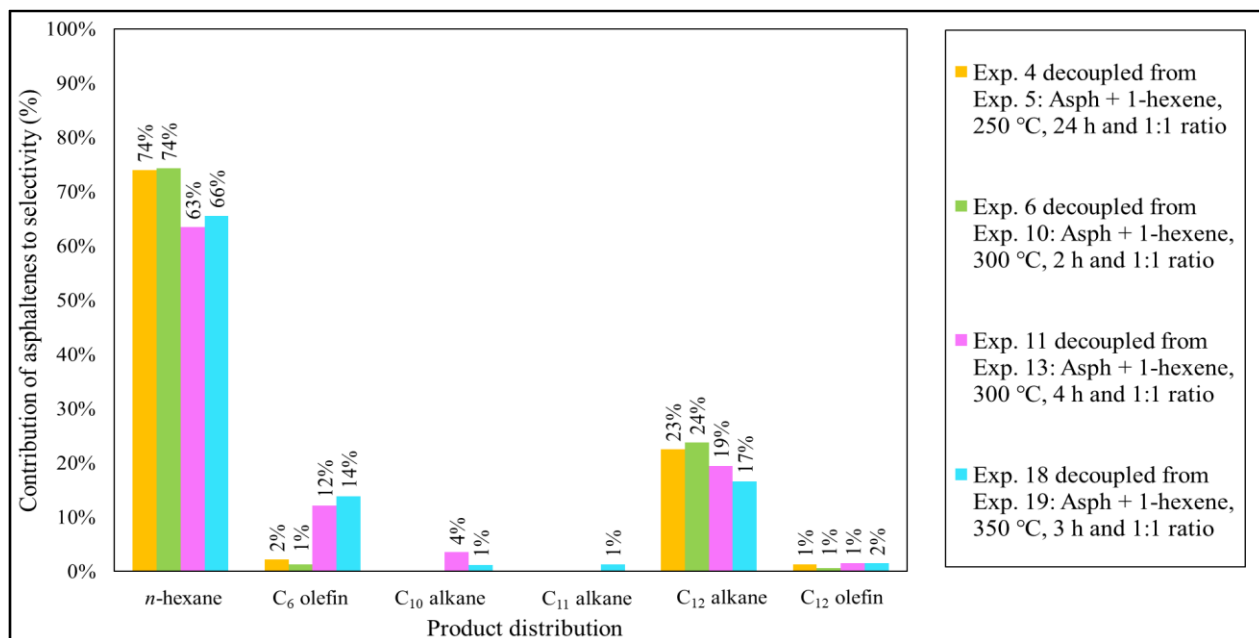


Figure 4.17 Contribution of asphaltenes to product selectivity (decoupling the effect of the reactor walls)

From Figure 4.17, the actual effect of the asphaltenes contributing towards olefin reduction is mainly via hydrogenation. It appears that the formation of C₁₂ olefins is mainly caused by the self-reaction of 1-hexene, and probably its interaction with the metallic walls of the reactors that can act as catalyst and lead to the oligomerization of the olefin. Once the hexene is oligomerized to form C₁₂, it is likely that the asphaltenes hydrogenated the C₁₂ olefins to form C₁₂ alkanes. As C₁₂ alkanes were not formed in the blank experiments, and only formed in the presence of asphaltenes in the reaction. Therefore, the actual contribution of asphaltenes for olefin reduction is by olefin hydrogenation and not by the formation of dimers. As a result, the main products associated solely with the reaction of asphaltenes and 1-hexene are the formation of *n*-hexane.

4.5.5 Chemistry for olefin reduction using asphaltenes

Olefin reduction was achieved in the experimental work by the formation of *n*-hexane. When 1,2-dihydronaphthalene was used as hydrogen donor in the preliminary study, it was shown that 1-hexene was capable of accepting hydrogens from 1,2-dihydronaphthalene to form *n*-hexane. The resulting production of *n*-hexane for all the cases shed light on the potential hydrogenation of olefins without the use of hydrogen or catalyst. As a result, the following reaction (Figure 4.18) takes place:

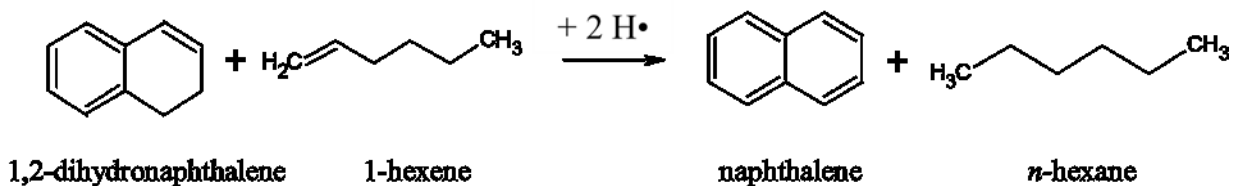


Figure 4.18 Reaction of 1,2-dihydronaphthalene and 1-hexene for *n*-hexane formation

However, when using industrial asphaltenes as hydrogen donor, olefin reduction was obtained by saturation of 1-hexene to form *n*-hexane. The production of alkanes results in the removal of the unsaturation, therefore, giving a direct reduction in olefin content. Figure 4.19 shows the proposed reactions to explain the observed products from the reactions of 1-hexene and asphaltenes, including the effect of the blank experiments that lead to the formation of C₁₂ olefins.

As seen in Figure 4.19, pathway 1 leads to the formation of *n*-hexane when 1-hexene reacts with the asphaltenes. However, pathway 2 occurs simultaneously and the catalytic effect of the reactor walls or presence of impurities leads to the formation of C₁₂ olefins. The competitive reaction between pathways 1 and 2 can be observed from the results in Table 4.9 (namely Exp. 9 and 10). The blank experiment (Exp. 10) resulted in ~ 67 % product selectivity towards C₁₂ olefins. When a high supply of asphaltenes was provided to the system (Exp. 9), pathway 1 was favored, resulting in ~ 50 % product selectivity towards the formation of *n*-hexane and only ~ 11 % in C₁₂ olefins. Therefore, the presence of asphaltenes “suppresses” the formation of C₁₂ olefins produced from the interaction of 1-hexene and the reactor walls/impurities. Furthermore, once the C₁₂ olefins are formed, the molecules of C₆ and C₁₂ olefins will compete for the available hydrogens provided by the asphaltenes to form either *n*-hexane or C₁₂ alkanes.

Different pathways could result in the formation of hexene isomers. Pathways 1 and 3 form C₆ olefins as side products. While the self-reaction of 1-hexene and its interaction with the reactor wall/impurities can also result in the formation of C₆ olefins. From Figure 4.17, it can be seen that C₆ olefins are formed from the self-reaction of 1-hexene and by the presence of the asphaltenes in the system. C₆ olefins are mainly formed during self-reaction of 1-hexene under milder conditions, such as at 250 °C, 24 h or 300 °C at 2 h reaction time. However, when the conditions were more severe, i.e., 300 °C at 4 h or at 350 °C at 3 h reaction time, hexene isomers were formed by the presence of asphaltenes in the system.

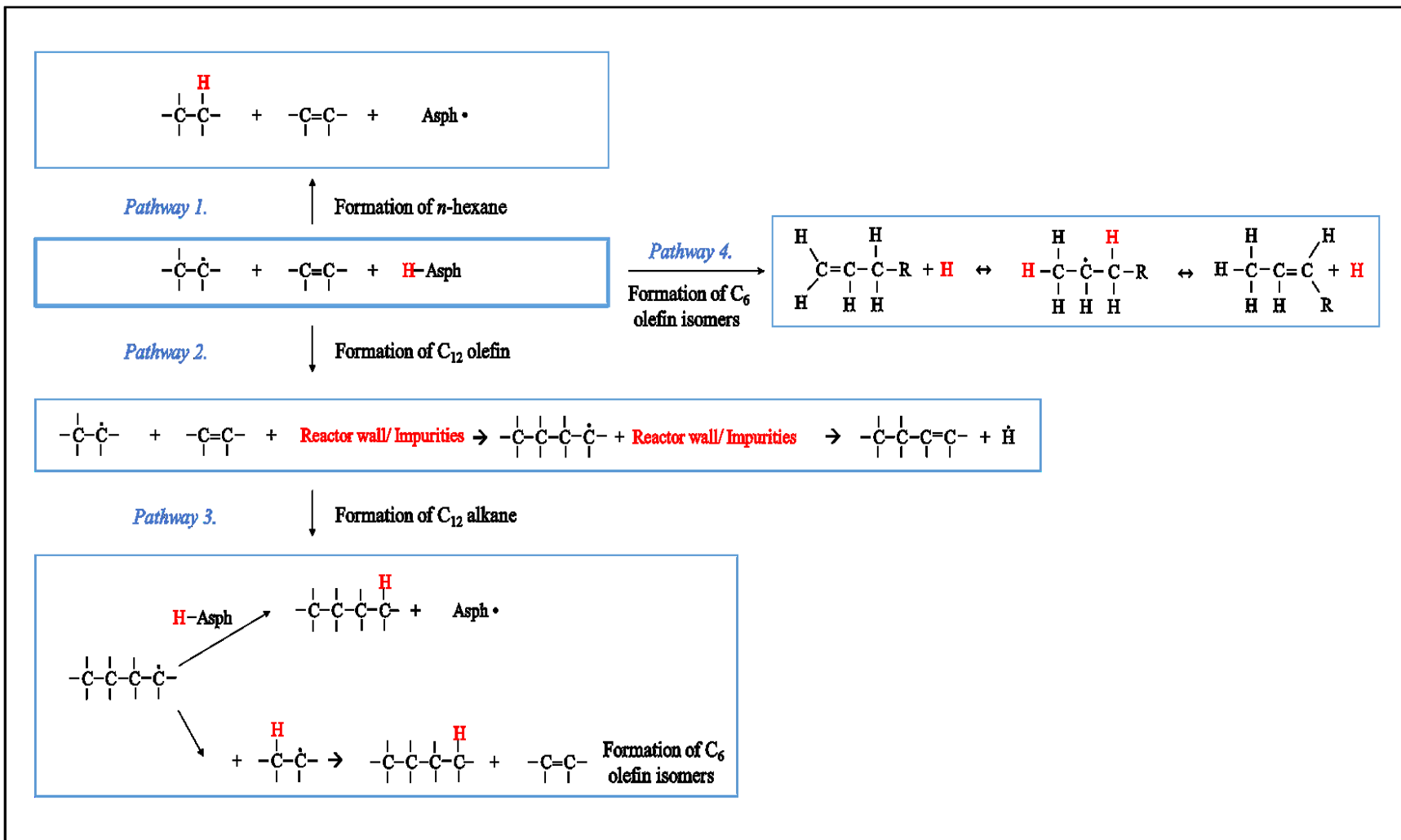


Figure 4.19 Proposed reactions of olefin with asphaltene

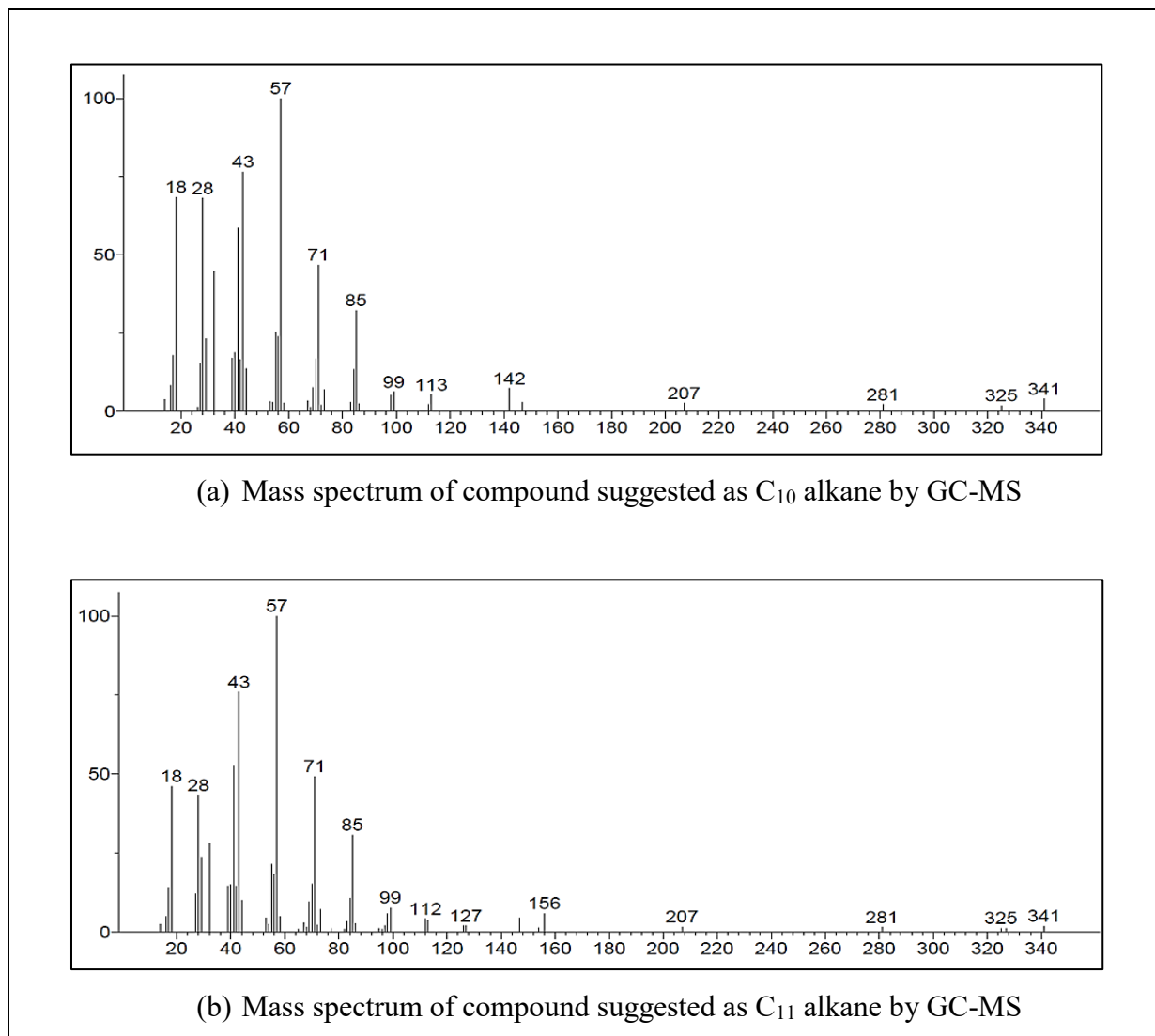


Figure 4.20 Mass spectra of compounds suggested as C₁₀ and C₁₁ alkane by GC-MS

Furthermore, the formation of C₁₀ and C₁₁ alkane was identified by GC-MS for certain experiments involving asphaltenes. From Table 4.9, C₁₀ alkanes were detected in the products of Exp. 8-9, 11-12, 14, and 16-18. C₁₁ alkanes, on the other hand, were detected in the products of Exp. 15-18. According to the mass spectra of both compounds (Figure 4.20), they are likely to be C₁₀ and C₁₁ alkane. The molecular ion peaks for C₁₀ and C₁₁ were 142 and 156, respectively, which corresponds to the molecular weight of these compounds. The characteristic mass fragments of 28,

43, 57, 71 and 85 m/z can be associated with the hydrocarbon fragments of C₂H₄, C₃H₇, C₄H₉, C₅H₁₁, and C₆H₁₃, respectively.

From Table 4.9, C₁₀ alkanes were formed for all experiments involving asphaltenes at 300 °C except Exp. 6 and 7. C₁₀ alkane was formed at high concentration of asphaltenes in the system (Exp. 8 and 9, 4:1 and 8:1 weight ratio of asphaltenes to 1-hexene respectively, at 2 h reaction time). Similarly, C₁₀ alkane was formed when reaction times were relatively long (Exp. 11 and 12, 1:1 weight ratio of asphaltenes to 1-hexene, at 4 h reaction time). Likewise, from Table 4.9, experiments using asphaltenes and conducted at 350 °C resulted in the detectable formation of C₁₀ and C₁₁ alkanes. Therefore, the formation of C₁₁ alkanes is likely favored by higher reaction temperatures like 350 °C, whereas C₁₀ alkanes are formed at 300 °C.

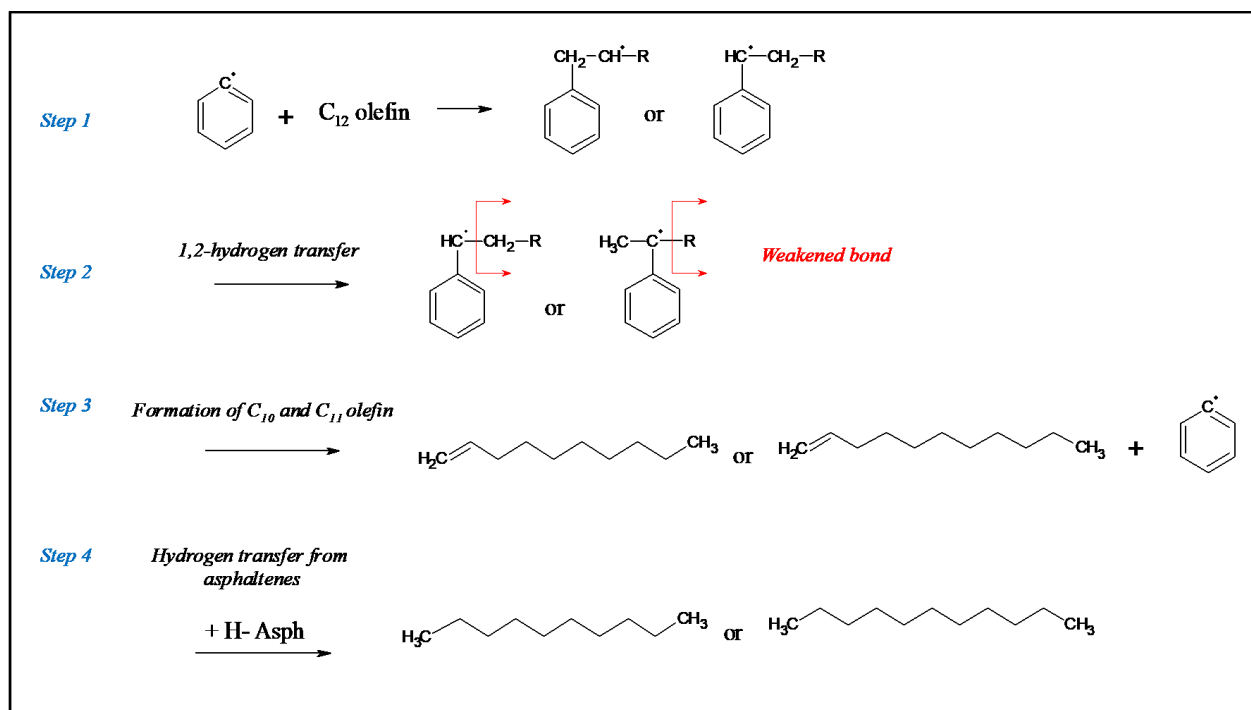


Figure 4.21 Proposed pathway for formation of C₁₀ and C₁₁ alkanes

A possible explanation for the formation of C₁₀ and C₁₁ alkanes can be associated with the presence of multinuclear aromatics in the asphaltenes that can naturally lead to persistent free radical carbon

stabilized by the aromatic/ multicyclic structures. As a result, the presence of an aromatic carbon radical, or carbon radical stabilized by resonance such as the molecule shown in *step 1* in Figure 4.21 can react with C₁₂ olefins present in the reaction products. As hydrogen transfer occurs in the system, it could result in 1,2-hydrogen transfer to form the products shown in *step 2*. Once the benzylic radical is formed, the C-C bond between the benzylic radical and the rest of the alkyl is weaker than the other C-C bonds. As a result, this leads to alkyl elimination to form C₁₀ and C₁₁ olefins. Because hydrogenation with asphaltenes occurs in the system, it can enable hydrogen transfer to form C₁₀ and C₁₁ alkanes.

4.5.6 Thermally cracked naphtha treated with asphaltenes

4.5.6.1 1-Hexene representation in thermally cracked naphtha

The main purpose of the preliminary study was to determine if a poor hydrogen acceptor such as 1-hexene was capable of accepting hydrogens from a hydrogen donor (model compound). 1-Hexene is by nature, a poor hydrogen acceptor because the possible interaction between the double bond and the hydrogen radical is either in the alpha or beta position. As a result, forming either a secondary or a primary radical. However, radicals are electron-deficient molecules and their stabilization is obtained by electron substituents pushing electron density towards the electron-deficient carbon.²⁰ Therefore, primary and secondary radicals are not stable radicals in comparison to a tertiary or aryl radical.²¹ Tertiary radicals are stabilized by the alkyl groups attached to the radical that provides a stabilizing effect through hyperconjugation.²² Aryl radicals, on the other hand, are stabilized by resonance stabilization.²¹ As a result, the instability of the radical affects the likelihood of the olefin accepting hydrogens via hydrogen transfer.²¹ Therefore, it was unlikely that 1-hexene can accept hydrogens from 1,2-dihydronaphthalene to produce a primary or secondary radical species.

Furthermore, the final application is intended for treating the olefins in the thermally cracked naphtha. It is known that the thermally cracked naphtha feed contains mainly olefins from C₅ to C₇ hydrocarbon chain length in the configurations of linear, branched and cyclic.⁹ As the formation of methyl radicals is not likely for C₅ to C₇ olefins, this leads to the alpha mono-olefins being the

worst olefin acceptor in the cracked naphtha. By evaluating the worst-case scenario for olefins in the thermally cracked naphtha as hydrogen acceptors, the study can then broadly consider the other olefins present in the naphtha. Therefore, the selection of 1-hexene is appropriate to represent the olefins in the thermally cracked naphtha.

4.5.6.2 Reactions of asphaltenes and thermally cracked naphtha

Olefin reduction was achieved by treating the thermally cracked naphtha with asphaltenes (Table 4.11). Approximately 14 % olefin reduction with respect to 1-hexene in the naphtha was obtained in Exp. 20 (350 °C, 3 h reaction time and 4:1 ratio of asphaltenes to 1-hexene). For Exp. 20, the conversion of 1-hexene in the naphtha was ~ 79 %. This result is similar to the conversion obtained for Exp. 21, where the conversion of 1-hexene was ~ 73 %. This leads to the idea that the reactivity of 1-hexene is not affected by the presence of the other components present in the naphtha, but the selectivity is affected.

The conversion of 1-hexene was not only due to the formation of the products presented in Table 4.12. The moles of 1-hexene in the naphtha that reacted was 0.095 % (see mol % of 1-hexene in Table 4.12). From the experiments performed with model compounds, it is known that the expected products formed from 1-hexene are mainly *n*-hexane and C₆ olefins. Yet, the sum of the mole percentage differences between *n*-hexane and the C₆ olefins (0.1090 %) was more than the amount of 1-hexene that reacted (0.095 %). This indicates that there were other sources of C₆ olefins in the naphtha, which can enable the formation of more C₆ olefins and the possible formation of *n*-hexane.

Furthermore, from Table 4.11, the olefin reduction with respect to 1-hexene in the naphtha (Exp. 20: ~14 %) was considerably lower than the reaction of 1-hexene under the same experimental conditions (Exp. 21: ~30 %). However, 1-hexene is under a competitive reaction for hydrogens with all the other components present in the naphtha, such as other olefins. A clear example of competition for hydrogens can be observed from Table 4.12, where there were reduction C₁₂ olefins, which indicate that these olefins are also competing for the hydrogens to form other C₁₂ saturated compounds.

Asphaltenes have a limited amount of transferable hydrogen to supply to the system,⁵ therefore, hydrogen supply is not unlimited. As a result, the more favorable hydrogen acceptors will most likely outcompete 1-hexene. 1-Hexene is a poor hydrogen acceptor as it could form either a primary or a secondary radical. Additionally, based on the characterization of the naphtha,⁹ it was found that most of the olefins present are branched. This means that they can either form a secondary or tertiary radical as intermediate. Thus, the branched olefins are more susceptible to receive hydrogens from the asphaltenes than the linear 1-hexene. Consequently, the actual olefin reduction in the naphtha, although not determined, it is estimated to be higher than 14 % mol. Therefore, the actual amount of olefins converted are more than 14 % mol of 1-hexene in feed/mol 1-hexene in naphtha.

Moreover, it is known that reaction of 1-hexene with a hydrogen donor forms *n*-hexane as main reaction product. As a result, a similar comparison can be done between the linear olefins from C₅ to C₇ (main hydrocarbon chain length of the olefins present in the naphtha)⁹ to view the differences in olefin reduction. Table 4.14 shows the area ratios calculated from the results obtained from the GC-FID between the mono-olefins and its corresponding alkanes. The ratios of olefin to alkane content in the naphtha decreased after treatment with asphaltenes. For all cases, the decrease in olefin content is in similar proportions (~ 20 % reduction). This indicates that the hydrocarbon chain length does not appear to affect the reactivity of the olefin for hydrogen transfer, but rather depends mainly on the stability of the intermediate radical that leads to the formation of an alkane.

21

Table 4.14 Comparison between ratios of linear alpha olefins to their corresponding hydrocarbon chain length linear alkane

	Area ratios		
	$\frac{1 - \text{pentene}}{n - \text{pentane}}$	$\frac{1 - \text{hexene}}{n - \text{hexane}}$	$\frac{1 - \text{heptene}}{n - \text{heptane}}$
Untreated spiked naphtha	0.1439	0.1429	0.1194
Spiked naphtha treated with asphaltenes	0.0310	0.0290	0.0284

Furthermore, after the treatment with asphaltenes, the treated naphtha remained with a similar boiling curve, without the formation of heavier compounds (Figure 4.10). This indicates that the treatment does not affect the shift of the naphtha cut towards the distillate cut. As a result, energy requirements downstream would not be affected as the naphtha remains with similar boiling conditions.

4.5.7 Industrial applications and cost evaluation

Currently, CNOOC's BituMax process uses olefin-aromatics alkylation to treat the olefins in the naphtha and distillate prior to mixing this stream with the heavier cuts to obtain partially upgraded bitumen.²³ Considering that the treatment of thermally cracked naphtha using asphaltenes to reduce the olefin content was feasible, the purpose of this section is to compare the equipment sizing and economics between these two types of processes. Three cases were considered: (1) olefins-aromatic alkylation process, (2) use of asphaltenes to treat the olefins at 250 °C, and (3) use of asphaltenes to treat the olefins at 350 °C. Note that the conditions with the highest olefin reduction at those temperatures (Exp. 4 and Exp. 18 in Table 4.8) were selected.

For more information related to the description and calculations for each process, see Appendix G.

4.5.7.1 CNOOC BituMax: Olefins-aromatic alkylation

The current option of olefins-aromatic alkylation (Figure 4.22) reduces the olefin content by alkylating the olefins in the feed with the aromatic compounds present in the naphtha with the use of an acid catalyst.²⁴ The current process reduces 50 % of the olefin content to fulfill pipeline specifications. The products formed from olefins-aromatic alkylation increases the formation of heavier compounds. Therefore, there will be a shift in the boiling curve of the treated naphtha towards the heavier end.

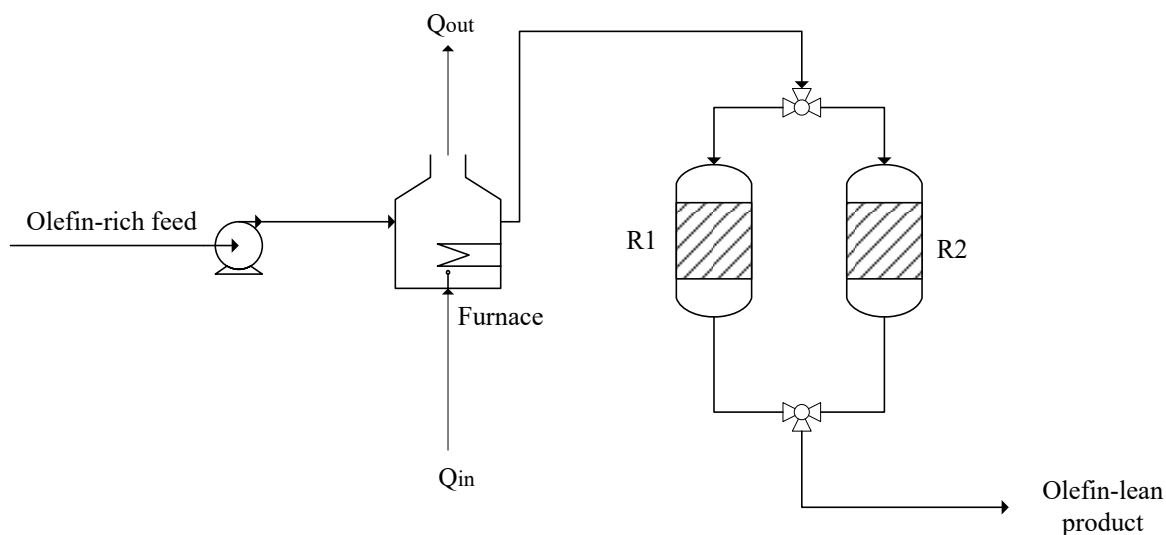


Figure 4.22 Process diagram of CNOOC olefin-aromatics alkylation plant

A simple cost and design evaluation using the Pré-Estime Method²⁵ was performed for the olefins-aromatic alkylation process and the summary is shown in Table 4.15.

Table 4.15 Summary of cost and design evaluation for Olefins-Aromatic Alkylation Process

Process:		Olefins-aromatics alkylation	
Total flowrate (kg/h)		10,000 (naphtha)	
Furnace		Reactor	
T_{in} (°C)	25	# of reactors	2
T_{out} (°C)	350	Residence time (h)	1
$Q_{required}$ (kJ/h)	9,332,000	Pressure (MPa)	6
		Volume (m ³)	13.12
Total cost of furnace (CAD)	807,000	Height (m)	5.50
		Radius (m)	0.87
		Wall thickness (mm)	87.90
		Cost of catalyst (CAD)/ kg feed	66
		Total cost of reactor (s) (CAD)	3,326,000
Total cost (CAD)^a			4,000,000

^a Cost calculations were performed with 2019 costing year and location at Fort McMurray, AB, Canada

4.5.7.2 Olefins treating with asphaltenes at 250 °C

At 250 °C, the use of a high-pressure steam heat exchanger can be considered to provide the required heat to heat the feed to the reaction temperature.²⁶ The advantage of using heat exchangers rather than a furnace is the considerable decrease in cost of the overall process. However, based on the experimental results (Figure 4.13), the olefin reduction obtained at 250 °C was relatively low. It required 24 h reaction time to obtain ~ 4 % olefin reduction. Therefore, it is expected that a vessel that can provide 24 h residence time will have considerably large dimensions. Thus, it is worth evaluating whether using heat exchangers to reduce the cost of a furnace, while using a larger vessel will be a viable alternative. A summary of the cost and design evaluation is presented for more information about the process (Table 4.16).

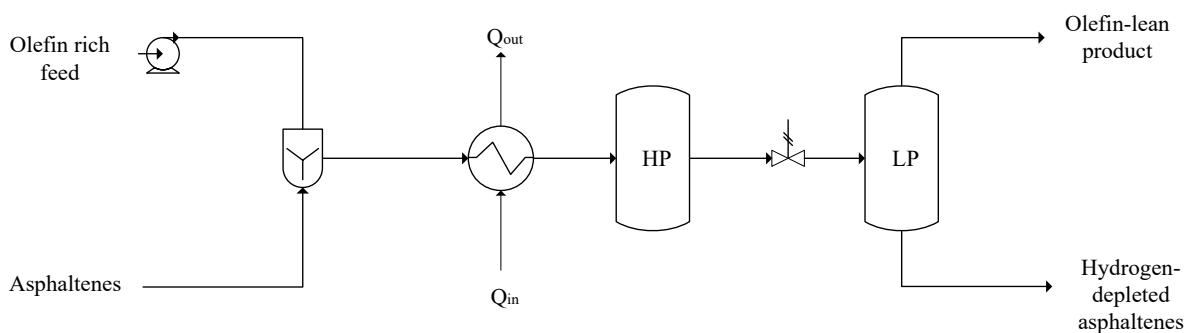


Figure 4.23 Process diagram for olefin treatment with asphaltenes at 250 °C

Table 4.16 Summary of cost and design evaluation for treatment plant using asphaltenes at 250 °C

Process:		Treatment with asphaltenes at 250 °C			
Total flowrate (kg/h):		10,495			
Naphtha flowrate (kg/h):		10,000			
Asphaltene flowrate (kg/h):		495			
Heat exchanger		Reactor		Flash	
T _{in} (°C)	25	# of reactors	1	Residence time (h)	0.33
T _{out} (°C)	250	Residence time (h)	24	Pressure (MPa)	0.44
Q _{required} (kJ/h)	6,607,000	Pressure (MPa)	6	Volume (m ³)	4.2
Area (m ²)	80	Volume (m ³)	305	Height (m)	3.7
		Height (m)	15.00	Radius (m)	0.6
Total cost of heat exchanger (CAD)	171,000	Radius (m)	2.50	Wall thickness (mm)	6.87
		Wall thickness (mm)	237.00		
		Total cost of reactor (s) (CAD)	10,678,000	Total cost of flash (CAD)	69,700
Total cost (CAD)^a					11,000,000

^a Cost calculations were performed with 2019 costing year and location at Fort McMurray, AB, Canada

4.5.7.3 Olefins treating with asphaltenes at 350 °C

At 350 °C, the process will require the construction/installation of an industrial furnace to provide the required heat to reach the reaction temperature (Figure 4.24). However, the olefin reduction capacity is much higher (~38 %). Therefore, the required vessel would be much smaller than the previous case at 250 °C, as it only requires 3 h residence time. A summary of the cost and design evaluation is presented for more information about the process (Table 4.17).

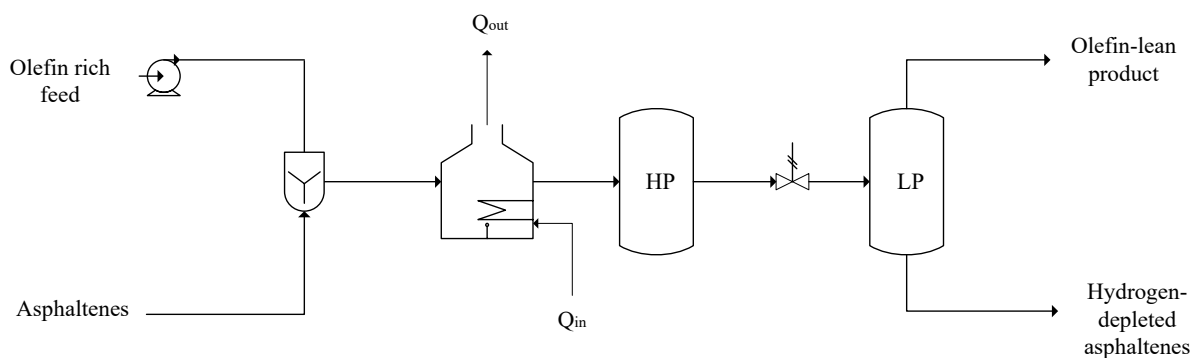


Figure 4.24 Process diagram for olefin treatment with asphaltenes at 350 °C

Table 4.17 Summary of cost and design evaluation for treatment plant using asphaltenes at 350 °C

Process:		Treatment with asphaltenes at 350 °C			
Total flowrate (kg/h):		10,615			
Naphtha flowrate (kg/h):		10,000			
Asphaltene flowrate (kg/h):		615			
Furnace		Reactor		Flash	
T _{in} (°C)	25	# of reactors	1	Residence time (h)	0.33
T _{out} (°C)	350	Residence time (h)	3		
Q _{required} (kJ/h)	9,600,000	Pressure (MPa)	7	Pressure (MPa)	0.44
		Volume (m ³)	40	Volume (m ³)	4.2
Total cost of furnace (CAD)	916,000	Height (m)	8.00	Height (m)	4
		Radius (m)	1.30	Radius (m)	0.6
		Wall thickness (mm)	148.00	Wall thickness (mm)	6.27
		Total cost of reactor (s) (CAD)	2,726,000	Total cost of flash (CAD)	74,500
Total cost (CAD)^a		4,000,000			

^a Cost calculations were performed with 2019 costing year and location at Fort McMurray, AB, Canada

4.5.7.4 Comparison of the different processes

By comparing these three cases, the process operating at 250 °C by asphaltene treatment resulted in the most expensive (~ 11 million CAD), while the asphaltene treatment operating at 350 °C resulted in the lowest capital cost. Due to the low olefin reduction capacity of the asphaltenes at 250 °C, the reaction vessel required large dimensions in order to provide 24 h residence time, while achieving the same olefin reduction as the other cases. Consequently, the reaction vessel represented the highest cost of the overall process.

As a result, the processes worth comparing are the olefins-aromatics alkylation with the treatment using asphaltenes at 350 °C. The process using asphaltenes at 350 °C resulted in a lower overall capital cost than the olefins-aromatic alkylation.

Additionally, the process using asphaltenes does not require the use of catalysts. Therefore, it represents a reduction in operational costs that can be significant in the end. However, a more detailed study is necessary to provide such conclusions. Furthermore, based on the simplified sizing calculations, the current furnace used for olefins-aromatic alkylation can be used to fulfill the heat requirement for the process with asphaltenes, as both heat requirements are similar (~ 9500 MJ/h).

The use of asphaltenes to treat the olefins in the thermally cracked naphtha can also be compared with the other processes currently used in the industry. The most common process for olefin treatment is hydrotreatment. This process can reach conversion levels of ~ 80-100 % at temperatures higher than 250 °C.²⁷ However, this process requires the use of catalysts during hydrogenation and for the production of hydrogen in situ. The production of hydrogenation also results in a considerable increase in operational cost (See Chapter 2 Literature Review).²⁸ Meanwhile, a process using asphaltenes for olefin reduction can be used in a plant that produces asphaltenes on-site, which is usually generated as waste; and avoids the need for hydrogen production. Nevertheless, in the absence of an operating cost estimate, although the process using asphaltenes has potential, the comparison between both processes cannot be conclusive without further studies.

4.6 Conclusions

It is known that asphaltenes have hydrogen donor properties, and it was questioned whether the asphaltenes can saturate olefins present in thermally cracked naphtha to decrease the olefin content. The following observations are derived from the experimental work:

- The preliminary study using 1,2-dihydronaphthalene as hydrogen donor, and 1-hexene as hydrogen acceptor at 300 °C resulted in the formation of *n*-hexane. Therefore, olefin conversion was possible by using model compounds.
- Asphaltenes can saturate 1-hexene via hydrogen transfer at 250 – 350 °C. Olefin reduction occurs mainly by two different and simultaneous chemistries: olefin saturation and olefin

dimerization. It was reasoned that dimerization was partly caused by the reaction of 1-hexene with the reactor's metallic walls/impurities because some dimerization was observed during control experiments with only 1-hexene. Hydrogenation of the olefins resulted from the addition of asphaltenes in the reaction.

- In the experimental condition range that was evaluated, olefin reduction is favored by the increase in temperature (250 – 350 °C), reaction time (0.5 – 24 h) and amount of asphaltenes provided in the reaction (1:1 – 8:1 weight ratio of asphaltenes to 1-hexene).
- Asphaltenes were capable of saturating olefins present in thermally cracked naphtha. Approximately 14 % (mol 1-hexene/ mol 1-hexene in naphtha) olefin reduction with respect to 1-hexene in the naphtha was achieved at 350 °C, 3 h reaction time and 4:1 weight ratio of asphaltenes to 1-hexene.
- A preliminary economic evaluation indicated that a process using asphaltenes to treat the olefins in the thermally cracked naphtha at 350 °C has a slightly lower capital cost than the currently used olefins-aromatic alkylation process for the BituMax Partial Upgrader. Operating costs were only qualitatively compared. The proposed process appears to have promise, but it is premature to draw definite conclusions.

References (Chapter 4)

- (1) Strausz, O.; Lown, E. *The Chemistry of Alberta Oil Sands, Bitumen and Heavy Oils*; Alberta Energy Research Institute: Calgary, 2003.
- (2) Gould, K. A.; Wiehe, I. A.; Briarwood, W.; Dri, V.; Heights, B.; Solutions, S.; Lane, L. Natural Hydrogen Donors in Petroleum Resids. *Energy Fuels* **2007**, *21* (3), 1199–1204.
- (3) Naghizada, N.; Prado, G. H. C.; de Klerk, A. Uncatalyzed Hydrogen Transfer during 100–250 ° C Conversion of Asphaltenes. *Energy & Fuels* **2017**, *31* (7), 6800–6811.
- (4) Myers, A. *Carbonized Asphaltene-Based Carbon-Carbon Fiber Composites*; Kansas City National Security Campus for Honeywell, Kansas City, 2017.
- (5) Naghizada, N. Uncatalyzed Hydrogen Transfer during 100–250 ° C Conversion of Asphaltenes, Master of Science Thesis, University of Alberta, Edmonton, AB, 2017.
- (6) Styles, Y.; Klerk, A. De. Sodium Conversion of Oilsands Bitumen-Derived Asphaltenes. *Energy Fuels* **2016**, *30* (7), 5214–5222
- (7) Paez, N. Identification, Conversion and Reactivity of Diolefins in Thermally Cracked Naphtha, Master of Science Thesis, University of Alberta, Edmonton, AB, 2016.
- (8) Uzcátegui, G.; Fong, S. Y.; De Klerk, A. Cracked Naphtha Reactivity: Effect of Free Radical Reactions. *Energy and Fuels* **2018**, *32* (5), 5812–5823.
- (9) Santiago, C.; Subramanya, A. S. *Olefin Characterization of Thermally Cracked Naphtha*; Edmonton, 2019.
- (10) Dietz, W. A. *Response Factors for Gas Chromatographic Analyses*; New Jersey, 1966.
- (11) ASTM Standard D7169-11. *Standard Test Method for Boiling Point Distribution of Samples with Residues Such as Crude Oils and Atmospheric and Vacuum Residues by High Temperature Gas Chromatography. ASTM D7169-11.*; American Society for Testing and Materials, West Conshohocken, PA, 2011.
- (12) Pradelle, F.; Braga, S. L.; Martins, A. R. F. A.; Turkovics, F.; Pradelle, R. N. C. Gum Formation in Gasoline and Its Blends: A Review. *Energy and Fuels* **2015**, *29* (12), 7753–7770.
- (13) Payan, F.; De Klerk, A. Hydrogen Transfer in Asphaltenes and Bitumen at 250 °c. *Energy and Fuels* **2018**, *32* (9), 9340–9348.
- (14) Hunt, I. Chapter 13: Spectroscopy, University of Calgary, Calgary, AB

- <http://www.chem.ucalgary.ca/courses/351/Carey5th/Ch13/ch13-ms-3.html>, (accessed Aug 10, 2019)
- (15) Alkhateeb, F. L.; Hayward, T. C.; Thurbide, K. B. A Novel Ultrashort Capillary Gas Chromatography Method Using On-Column Injection and Detection. *Can. J. Chem.* **2015**, *94* (4), 259–264.
 - (16) King, H.-H.; Stock, L. M. Hydrogen Transfer Reactions of Two Reactive Donors, 1,2- and 1,4-Dihydro- Naphthalene. *Fuel* **1981**, *60*, 80748–80749.
 - (17) Hirayama, F.; Lipsky, S. Fluorescence of Mono-Olefinic Hydrocarbons. *J. Chem. Phys.* **1975**, *62* (2), 576–583.
 - (18) Gonikberg, M. G.; Zhulin, V. M. Thermal Polymerization of Dimethylbutenes under High Pressures; *Russ. Chem. Bull.* **1957**, *7*, 1210-1219
 - (19) Moad, G.; Rizzardo, E.; Solomon, D. H. Other Initiating Systems. In *Comprehensive Polymer Science and Supplements*; Pergamon: Melbourne, 1989; pp 141–146.
 - (20) Parsons, A. F. *An Introduction to Free Radical Chemistry*; Blackwell Science: Oxford, 2000.
 - (21) Abell, P. I.; Benson, S. W.; Fischer, H.; Howard, A. J.; Kaplan, L.; Kice, J. L.; Kochi, J. K.; Martin, J. C.; Nelsen, S. F.; O’Neal, E. H.; et al. *Free Radicals: Volume II*; Kochi, J. K., Ed.; Wiley-Interscience Publication: New York, 1973.
 - (22) Solomons, G. T. W.; Fryhle, C. B. *Organic Chemistry*, 9th ed.; John Wiley & Sons, Inc.: Hoboken, NJ, 2008.
 - (23) De Klerk, A. *Annual Report 2016-2017 (Year 1), Progress Report on Industrial Research Chair Program Issued to NSERC, Nexen Energy ULC, and Alberta Innovates*; Edmonton, 2017.
 - (24) Zerpa, N.; De Klerk, A.; Xia, Y.; Omer, A. A. Olefins Reduction of a Hydrocarbon Feed Using Olefins-Aromatics Alkylation. Canadian Patent 2,916,767, 2015.
 - (25) Chauvel, A.; Fournier, G.; Raimbult, C.; Pigeyre, A. *Manual of Process Economic Evaluation*, 2nd Ed.; Editions Technip: Paris, 2003.
 - (26) Ulrich, G. D.; Vasudevan, P. T. *Chemical Engineering. Process Design and Economics. A Practical Guide.*, 2nd Ed.; Process Publishing: Durham, 2004.
 - (27) Xin, Q.; Alvarez-Majmutov, A.; Dettman, H.; Chen, J. Hydrogenation of Olefins in Bitumen-Derived Naphtha over a Commercial Hydrotreating Catalyst. *Energy & Fuels* **2018**, *32* (5), 6167–6175.

- (28) Murray, G. R. *Upgrading Oilsands Bitumen and Heavy Oil*; University of Alberta Press: Edmonton, 2015.
- (29) Ovalles, C. *Subsurface Upgrading of Heavy Crude Oils and Bitumen*; Taylor & Francis: Boca Raton, 2019.

CHAPTER 5 – CONCLUSIONS

5.1 Introduction

Olefin formation occurs when highly dense and viscous bitumen undergoes a thermal process to produce lighter products.¹ However, the presence of olefins in the product has been associated with fouling in the pipelines and equipment downstream.² As a result, these compounds have to be treated or removed prior to transporting and processing the cracked product to the market. Hydrotreating has been a commonly used technology to treat the olefins in the oil industry that are produced from different processes.³ However, hydrotreating involves costly operations and large space requirements, which can be a limitation for processes such as partial upgrading of bitumen. As a result, the research work was focused on evaluating alternative pathways to treat the olefins without the use of hydrogen.

The first proposal involves the study of reactive absorption of olefins by using phosphoric acid. The chemistry between olefins from C₅-C₇ hydrocarbon chain length and phosphoric acid was studied to determine the feasibility of this alternative.

The second proposal uses industrial asphaltenes to treat the olefins via hydrogen transfer. Different experimental conditions were evaluated to determine the olefin reduction by the use of asphaltenes.

The following sections will describe the major conclusions and suggested future work related to this research study.

5.2 Significance and major conclusions

5.2.1 Use of phosphoric acid

The present research work provides scientific contributions to fill a gap in the literature about the chemistry between olefins and phosphoric acid. It provides information and a better understanding

of the interaction of C₅-C₇ olefins with phosphoric acid. Previously, the literature was mainly focused on the use of phosphoric acid with olefins of C₂ - C₄ hydrocarbon chain length.

Major conclusions:

- Phosphoric acid is reactive with linear, branched and cyclic olefins with hydrocarbon chain length of C₅-C₇ at 50 °C. The resulting products were alkyl phosphoric acid esters.
- The alkyl phosphoric acid esters formed from C₅ olefins were found to be mainly soluble in the aqueous layer. However, the increase in hydrocarbon chain length to C₆-C₇ hydrocarbon chain length led to an increase in solubility in the organic phase.
- It is not viable to use phosphoric acid to remove the olefins in the thermally cracked naphtha via reactive absorption. The reaction rate is slow, the removal efficiency is low and the presence of six-membered cyclic compounds in the naphtha can lead to the formation of emulsion that can complicate the separation of the naphtha from the acid.

5.2.2 Use of asphaltenes

The successful results of the use of asphaltenes to treat the olefins in the thermally cracked naphtha open the opportunity to use a by-product with limited applications as a useful tool to potentially replace an energy and cost intensive process, such as hydrotreatment. This can likely offer operational cost reduction for the heavy oil industry, as asphaltenes are mainly present in the upgrading facilities, and the proposed process does not require the use of catalysts and hydrogen production on site.

Major conclusions:

- Asphaltenes are capable of transferring hydrogen to 1-hexene at 250 – 350 °C. Olefin reduction was obtained via two different and simultaneous pathways: olefin saturation and

olefin dimerization. Olefin saturation resulted from the addition of hydrogen from asphaltenes in the reaction.

- Olefin dimerization was partly associated with the interaction of 1-hexene with the reactor's metallic walls/ impurities, as these products were observed during control experiments of only 1-hexene.
- To study olefin reduction, experimental parameters such as reaction temperature, time and amount of asphaltenes in the system were varied. It was found that olefin reduction was favored with an increase in reaction temperature (250 – 350 °C), reaction time (0.5 – 24 h) and of the amount of asphaltenes added to the system (1:1 – 8:1 weight ratio of asphaltenes to 1-hexene).
- Asphaltenes can be used to hydrogenate the olefins in the thermally cracked naphtha. At 350 °C, 3 h reaction time and 4:1 weight ratio of asphaltenes to 1-hexene approximately 14 % (mol 1-hexene/ mol 1-hexene in naphtha) olefin reduction with respect to 1-hexene in the naphtha was achieved.

5.3 Suggested future work

5.3.1 Use of phosphoric acid

- The present study was focused on the use of liquid phosphoric acid to simplify the study of the chemistry between the olefins and the phosphoric acid. However, the leaching of alkyl phosphoric acid esters towards the organic phase could potentially be decreased by the use of solid phosphoric acid (SPA). Because the support of the SPA could provide additional surface interaction to maintain the alkyl phosphoric acid esters in the “aqueous phase” (surface of the catalyst). Therefore, it would be worth evaluating the use of solid phosphoric acid to treat the olefins in the thermally cracked naphtha.

- If the leaching of alkyl phosphoric acid esters can be decreased or eliminated, then it would be worth evaluating the process at different operational conditions that could lead to an increase in reaction rate. However, such a study would have to be accompanied by an evaluation of the thermal stability of the different alkyl phosphoric acid esters.
- Because most of the reactions involved long reaction times, such as 68 h, it would be worth performing all the experiments in pressurized batch reactors rather than a glass ball flask with condenser. The latter can have leakage in the system that can lead to considerable mass loss in comparison to a pressurized batch reactor.
- Other studies can be performed to analyze the feasibility of removing the alkyl phosphoric acid esters from the organic phase. If it were chemically viable, then it would be appropriate to perform a design and cost evaluation to compare this process with currently used processes for olefin treatment.

5.3.2 Use of asphaltenes

- As olefin reduction was achieved by treating the thermally cracked naphtha with the asphaltenes, it would be interesting to further evaluate the characteristics of the treated naphtha. For example, what are the impacts of favoring the chemistry of dimerization in the naphtha rather than saturating the olefin? Can this naphtha be used as diluent for the dilbit (diluted bitumen)? What are the other potential chemistries occurring between the other components present in the naphtha with the asphaltenes?
- Having knowledge about the source of transferrable hydrogens present in the asphaltenes, would this stream have an increase in economic value? Therefore, it could be worthwhile studying other applications using this information. How can the use of the hydrogen donor capacity of the asphaltenes be useful for the other processes in the oil industry?

- As the process using asphaltenes could potentially be used for olefin hydrogenation, does this process represent a positive impact on the environment? A cradle to grave study would be worth performing to understand the impact of the overall process in comparison to hydrotreatment or other processes used for olefin treatment. What will be the impact on greenhouse gas emissions? Will solid waste management be the same for usual asphaltenes in comparison to hydrogen-depleted asphaltenes?
- From recent research work,⁴ asphaltenes are used for carbon fiber production. During the process, hydrogen is removed from the asphaltenes during carbonization to achieve carbon bound carbon fiber composite. Therefore, the hydrogen-depleted asphaltenes can be used for future studies of carbon-fiber technology to further increase the value of the asphaltenes.

5.4 Presentations and publications

The following includes a list of the work to be published and presentations in conferences related to the work developed from this research project.

- Fong, S.Y; Montoya Sánchez, N; De Klerk, A. Alternative Technologies for Olefin Treatment in Thermally Cracked Naphtha: Use of Phosphoric Acid. *(Presented at the 257th ACS National Meeting, 2019, Orlando, FL, USA)*
- Fong, S.Y; Montoya Sánchez, N; De Klerk, A. Reaction of Pentenes, Hexenes, and Heptenes with Phosphoric Acid. *(Paper submitted for publication in Energy & Fuels on August, 2019).*

References (Chapter 5)

- (1) Murray, G. R. *Upgrading Oilsands Bitumen and Heavy Oil*; University of Alberta Press: Edmonton, 2015.
- (2) Nagpal, J. M.; Joshi, G. C.; Singh, J.; Rastogi, S. N.; Joshi, G. C.; Singh, J.; Gum, S. N. R. Gum Formation Olefinic Precursors in Motor Gasoline, a Model Compound. *Fuel Sci. Technol. Intl.* **1994**, *12* (6), 873–894.
- (3) Xin, Q.; Alvarez-Majmutov, A.; Dettman, H.; Chen, J. Hydrogenation of Olefins in Bitumen-Derived Naphtha over a Commercial Hydrotreating Catalyst. *Energy & Fuels* **2018**, *32* (5), 6167–6175.
- (4) Myers, A. *Carbonized Asphaltene-Based Carbon-Carbon Fiber Composites*; Kansas City National Security Campus for Honeywell, Kansas City, 2017.

REFERENCES

- Abell, P. I.; Benson, S. W.; Fischer, H.; Howard, A. J.; Kaplan, L.; Kice, J. L.; Kochi, J. K.; Martin, J. C.; Nelsen, S. F.; O'Neal, E. H.; et al. *Free Radicals: Volume II*; Kochi, J. K., Ed.; Wiley-Interscience Publication: New York, 1973.
- Aitani, A. M. Oil Refining and Products. In *Encyclopedia of Energy*, El Sevier, 2004, pp. 715–729.
- Alemán-Vázquez, L. O.; Torres-Mancera, P.; Ancheyta, J.; Ramírez-Salgado, J. Use of Hydrogen Donors for Partial Upgrading of Heavy Petroleum. *Energy and Fuels*, **2016**, *30* (11), 9050–9060.
- Alkhateeb, F. L.; Hayward, T. C.; Thurbide, K. B. A Novel Ultrashort Capillary Gas Chromatography Method Using On-Column Injection and Detection. *Can. J. Chem.* **2015**, *94* (4), 259–264.
- ASTM Standard D7169-11. Standard Test Method for Boiling Point Distribution of Samples with Residues Such as Crude Oils and Atmospheric and Vacuum Residues by High Temperature Gas Chromatography. ASTM D7169-11.; American Society for Testing and Materials, West Conshohocken, PA, 2011.
- Bellefon, C. De; Schweich, D. Kinetics of α -Methylstyrene Hydrogenation on Pd / Al₂O₃. *Ind. Eng. Chem. Res.* **2002**, *41* (7), 1711–1715.
- Buglass, A. J.; Lee, S. H. Sequential Analysis of Malic Acid and Both Enantiomers of Lactic Acid in Wine Using a High-Performance Liquid Chromatographic Column-Switching Procedure. *J. of Chrom. Sci.* **2001**, *39* (11), 453–458.
- Chauvel, A.; Fournier, G.; Raimbult, C.; Pigeyre, A. *Manual of Process Economic Evaluation*, 2nd Ed.; Editions Technip: Paris, 2003.
- Chen, T.; Hsiao, C.; Huang, S.; Huang, J. The Nearest-Neighbor Effect on Random-Coil NMR Chemical Shifts Demonstrated Using a Low-Complexity Amino-Acid Sequence. *Prot. & Pept. Let.* **2016**, *23* (11), 967–975.
- Chilingarian, G. V.; Yen, T. F. Introduction to Asphaltenes and Asphalts. In *Asphaltenes and Asphalts, Volume 2*; El Sevier Science, 2000; pp 1–5.

- De Filippis, P. A Simple Test Method for Distinguishing Straight-Run from Thermal (Visbreaker) Residues or Bitumens. *Fuel* **1995**, *74* (10), 1537–1539.
- De Klerk, A. Annual Report 2016-2017 (Year 1), Progress Report on Industrial Research Chair Program Issued to NSERC, Nexen Energy ULC, and Alberta Innovates; Edmonton, 2017.
- De Klerk, A. Key Catalyst Types for the Efficient Refining of Fischer-Tropsch Syncrude: Alumina and Phosphoric Acid. In *Catalysis: Volume 23*; 2011; pp 1–49.
- De Klerk, A. Reactivity Differences of Octenes over Solid Phosphoric Acid. *Ind. Eng. Chem. Res.* **2006**, *45* (2), 578–584.
- De Klerk, A. CHE 522 Lecture on Utilities Part I: Off-gas treating. Presented at University of Alberta, Edmonton, AB, 2018.
- Dietz, W. A. Response Factors for Gas Chromatographic Analyses; Esso Research and Engineering Company, Linden, NJ, 1966.
- E. Cady, W.; F. Marschner, R.; P. Cropper, W. Composition of Virgin, Thermal, and Catalytic Naphthas from Mid-Continent Petroleum. *Ind. Eng. Chem.* **1952**, *44* (8), 1859–1864.
- Elsayed, H. A.; Menoufy, M. F.; Shaban, S. A.; Ahmed, H. S.; Heakal, B. H. Optimization of the Reaction Parameters of Heavy Naphtha Reforming Process Using Pt-Re / Al₂O₃ Catalyst System. *Egypt. J. Pet.* **2017**, *26* (4), 885–893.
- Enbridge Quality Pooling. Enbridge: Quality Pooling Specification Package; Edmonton, 2018. (Accessed on Jun. 28, 2019)
- Farrar, T. C.; Schwartz, J. L.; Rodriguez, S. pH, Temperature, and Concentration Dependence of the Chemical Shift and Scalar Coupling Constants in disodium hydrogen phosphite and disodium fluorophosphate. *J. Phys. Chem.* **1993**, *97* (28), 7201–7207.
- Fellows, G. K.; Mansell, R.; Schlenker, R.; Winter, J. Public-Interest Benefit Evaluation of Partial-Upgrading Technology; Calgary, Vol. 10, 2017.
- Gibian, M. J.; Corley, R. C. Organic Radical-Radical Reactions. Disproportionation vs. Combination. *Chem. Rev.* **1973**, *73* (5), 441–464.
- Gieseeman, J.; Brasier, R. S. Bitumen Partial Upgrading 2018 Whitepaper; Jacobs Consultancy, Edmonton, AB, 2018.

- Gonikberg, M. G.; Zhulin, V. M. Thermal Polymerization of Dimethylbutenes under High Pressures; *Russ. Chem. Bull*, **1957**, 7, 1210-1219
- Gorenstein, D. G. *Phosphorus-31 Chemical Shifts: Principles and Empirical Observations. In Phosphorus 31 NMR: Principles and Applications*; Academic Press Inc., Publishers: Orlando, 1984; pp 7–36.
- Gould, K. A.; Wiehe, I. A.; Briarwood, W.; Dri, V.; Heights, B.; Solutions, S.; Lane, L. Natural Hydrogen Donors in Petroleum Resids. *Energy Fuels*, **2007**, 21 (3), 1199–1204.
- Gray, M. R.; McCaffrey, W. C. Role of Chain Reactions and Olefin Formation in Cracking, Hydroconversion, and Coking of Petroleum and Bitumen Fractions. *Energy Fuels*, **2002**, 16 (3) 756–766.
- Gross, L.; Mullins, O. C.; Schuler, B.; Meyer, G.; Peña, D. Unraveling the Molecular Structures of Asphaltenes by Atomic Force Microscopy. *J. Am. Chem. Soc.* **2015**, 137 (31), 9870–9876.
- Hardy, C. J. Analysis of Alkyl Esters of Phosphoric Acid by Gas Chromatography. *J. Chromatogr.* **1964**, 13, 372–376.
- Häring, H.W. *Industrial Gases Processing*; Wiley-VCH: Weinheim, 2008.
- Hirayama, F.; Lipsky, S. Fluorescence of Mono-Olefinic Hydrocarbons. *J. Chem. Phys.* **1975**, 62 (2), 576–583.
- Howell, B. A.; Daniel, Y. G. Thermal Degradation of Phosphorus Esters Derived from Isosorbide and 10-Undecenoic Acid. *J. Therm. Anal. Calorim.* **2015**, 121 (1), 411–419.
- Hunt, I. Chapter 13: Spectroscopy, University of Calgary, Calgary, AB, <http://www.chem.ucalgary.ca/courses/351/Carey5th/Ch13/ch13-ms-3.html>. (Accessed on Aug 10, 2019)
- Hupfer, M.; Ru, B.; Berlin, D.-; Schmieder, P. Origin and Diagenesis of Polyphosphate in Lake Sediments : A 31 P-NMR Study. *Limnol. Oceanogr.* **2004**, 49 (1), 1–10.
- Ipatieff, V. N. Catalytic Polymerization of Gaseous Olefins by Liquid Phosphoric Acid: I. Propylene. *Ind. Eng. Chem.* **1935**, 27 (9), 1067–1069.
- Ipatieff, V. N. *Catalytic Reactions at High Pressures and Temperatures*; The Macmillan Company: New York, 1937.
- Jameson, R. F. The Composition of the “Strong” Phosphoric Acids. *J. Chem. Soc.* **1959**, 0, 752–759.

- King, H.-H.; Stock, L. M. Hydrogen Transfer Reactions of Two Reactive Donors, 1,2- and 1,4-Dihydro- Naphthalene. *Fuel* **1981**, *60*, 80748–80749.
- Kosting, P. R.; Heins, C. Corrosion of Metals by Phosphoric Acid. *Ind. Eng. Chem.* **1930**, *23* (2), 140–150.
- Leprince, P. *Petroleum Refining Vol. 3 Conversion Processes*; Editions Technip: Paris, 2001.
- Levitt, M.; Perutz, M. F. Aromatic Rings Act as Hydrogen Bond Acceptors. *J. Mol. Biol.* **1988**, *201* (4), 751–754.
- Maples, R. *Petroleum Refinery Process Economics*; PennWell: Tulsa, 1993.
- March, J. *Advanced Organic Chemistry*, 3rd ed.; Wiley: New York, 1985.
- Masliyah, J. H.; Czarnecki, J.; Xu, Z. *Handbook on Theory and Practice of Bitumen Recovery from Athasbasca Oil Sands. Volume I: Theoretical Basis*; Kingsley Knowledge Publishing Canada, 2011.
- Moad, G.; Rizzardo, E.; Solomon, D. H. *Other Initiating Systems. Comprehensive Polymer Science and Supplements*; Pergamon: Melbourne, 1989; pp 141–146.
- Moad, G.; Solomon, D. H. *The Chemistry of Radical Polymerization*, 1st ed.; El Sevier: Oxford, 2006.
- Müller, A. Über Die Absorption Des Äthylens Durch Ortho', Pyro' Und Metaphosphorsäure. *Eur. J. Inorg. Chem.* **1925**, *58* (9), 2105–2110.
- Murray, G. R. *Upgrading Oilsands Bitumen and Heavy Oil*; University of Alberta Press: Edmonton, 2015.
- Myers, A. *Carbonized Asphaltene-Based Carbon-Carbon Fiber Composites*; Kansas City National Security Campus for Honeywell, Kansas City, 2017.
- Naghizada, N. *Uncatalyzed Hydrogen Transfer during 100-250 °C Conversion of Asphaltenes*, Master of Science, University of Alberta, Edmonton, AB, 2017.
- Naghizada, N.; Prado, G. H. C.; de Klerk, A. Uncatalyzed Hydrogen Transfer during 100-250 ° C Conversion of Asphaltenes. *Energy & Fuels* **2017**, *31* (7), 6800–6811.
- Nagpal, J. M.; Joshi, G. C.; Singh, J.; Rastogi, S. N.; Joshi, G. C.; Singh, J.; Gum, S. N. R. Gum Formation Olefinic Precursors in Motor Gasoline, a Model Compound. *Fuel Sci. Technol. Intl.* **1994**, *12* (6), 873–894.

- Nicholas, C. P. Applications of Light Olefin Oligomerization to the Production of Fuels and Chemicals. *Appl. Catal. A Gen.* **2017**, *543* (3), 82–97.
- Nimana, B.; Canter, C.; Kumar, A. Energy Consumption and Greenhouse Gas Emissions in Upgrading and Refining of Canada’s Oil Sands Products. *Energy* **2015**, *83* (1), 65–79.
- Nonhebel, D. C.; Walton, J. C. *Free-Radical Chemistry*; Cambridge University Press: London, 1974.
- Ovalles, C. *Subsurface Upgrading of Heavy Crude Oils and Bitumen*; Taylor & Francis: Boca Raton, 2019.
- Paez, N. Identification, Conversion and Reactivity of Diolefins in Thermally Cracked Naphtha, Master of Science Thesis, University of Alberta, Edmonton, AB, 2016.
- Parsons, A. F. *An Introduction to Free Radical Chemistry*; Blackwell Science: Oxford, 2000.
- Payan, F.; De Klerk, A. Hydrogen Transfer in Asphaltenes and Bitumen at 250 °C. *Energy and Fuels* **2018**, *32* (9), 9340–9348.
- Pradelle, F.; Braga, S. L.; Martins, A. R. F. A.; Turkovics, F.; Pradelle, R. N. C. Gum Formation in Gasoline and Its Blends: A Review. *Energy and Fuels* **2015**, *29* (12), 7753–7770.
- Pretsch, E.; Clerc, T.; Seibl, J.; Simon, W. *¹H NMR in Tables of Spectral Data for Structure Determination of Organic Compounds*; Berlin: Springer-Verlag: Berlin, 1983; pp 104–177.
- Quintana, J. B.; Rodil, R.; Reemtsma, T. Determination of Phosphoric Acid Mono- and Diesters in Municipal Wastewater by Solid-Phase Extraction and Ion-Pair Liquid Chromatography-Tandem Mass Spectrometry. *Anal. Chem.* **2006**, *78* (5), 1644–1650.
- Ramnas, O.; Ostermark, U.; Petersson, G; Characterization of Sixty Alkenes in a Cat-Cracked Gasoline Naphtha by Gas Chromatography. *Chromat.* **1994**, *38* (3-4), 222–226.
- Ruchardt, C.; Gerst, M.; Nolke, M. The Uncatalyzed Transfer Hydrogenation of α -Methylstyrene by Dihydroanthracene or Xanthene - a Radical Reaction. *Angew. Chem. Int. Ed. Engl.* **1992**, *31* (11), 1523–1525.
- Santiago, C.; Subramanya, A. S. Olefin Characterization of Thermally Cracked Naphtha; University of Alberta, Edmonton, AB, (unpublished work), 2019.
- Schmerling, L.; Ipatieff, V. N. The Mechanism of the Polymerization of Alkenes. *Adv. Catal.* **1950**, *2*, 21–80.

- Sheu, E. Y.; Mullins, O. C. *Asphaltenes Fundamentals and Applications*; Plenum Press: New York, 1995.
- Silverstein, R. M.; Webster, F. X. *Spectrometric Identification of Organic Compounds*, 6th ed; John Wiley & Sons, Inc.: New York, 1998.
- Solomons, G. T. W.; Fryhle, C. B. *Organic Chemistry*, 9th ed.; John Wiley & Sons, Inc.: Hoboken, NJ, 2008.
- Strausz, O.; Lown, E. *The Chemistry of Alberta Oil Sands, Bitumen and Heavy Oils*; Alberta Energy Research Institute: Calgary, 2003.
- Styles, Y.; Klerk, A. De. Sodium Conversion of Oilsands Bitumen-Derived Asphaltenes. *Energy & Fuels*, **2016**, *30* (7), 5214-5222.
- Tempesti, T. C.; Pierini, A. B.; Baumgartner, M. T. Steric Effects of Nucleophile-Radical Coupling Reaction. Determination of Rate Constants for the Reaction of Aryl Radicals with 2-Naphthoxide Anion. *New J. Chem.* **2009**, *33* (7), 1523–1528.
- Ulrich, G. D.; Vasudevan, P. T. *Chemical Engineering. Process Design and Economics. A Practical Guide*, 2nd Ed.; Process Publishing: Durham, 2004.
- Uzcátegui, G.; Fong, S. Y.; De Klerk, A. Cracked Naphtha Reactivity: Effect of Free Radical Reactions. *Energy and Fuels* **2018**, *32* (5), 5812–5823.
- Waggaman, W. H. *Phosphoric Acid, Phosphates, and Phosphatic Fertilizers*, 2nd ed.; Reinhold: New York, 1952.
- Woodstock, A. H. The Alkyl Esters of Phosphoric Acid. *Chem. Ind.* **1942**, *51*, 516–521, 557.
- Xin, Q.; Alvarez-Majmutov, A.; Dettman, H.; Chen, J. Hydrogenation of Olefins in Bitumen-Derived Naphtha over a Commercial Hydrotreating Catalyst. *Energy & Fuels* **2018**, *32* (5), 6167–6175.
- Zabrocki, K.; Schaupp, K. Emulsifier Composition. U.S. Patent No. 4,360,452, 1982.
- Zachariah, A.; De Klerk, A. Partial Upgrading of Bitumen: Impact of Solvent Deasphalting and Visbreaking Sequence. *Energy and Fuels* **2017**, *31* (9), 9374–9380.
- Zerpa, N.; De Klerk, A.; Xia, Y.; Omer, A. A. Olefins Reduction of a Hydrocarbon Feed Using Olefins-Aromatics Alkylation. Canadian Patent No. 2,916,767, 2015.

APPENDIX A

Additional chromatograms from GC-MS

Chromatograms of the products from the control experiments obtained from GC-MS and mentioned in Chapter 4, Table 4.4 are shown. The first blank experiment (Exp. 0.4) is the reaction of 1,2-dihydronaphthalene with *n*-hexane at 300 °C, 2 h and 1:1 weight ratio of 1,2-dihydronaphthalene to *n*-hexane (Figure A.1). Followed by the chromatogram of the blank experiment of 1,2-dihydronaphthalene at 300 °C and 2 h reaction time (Exp. 0.5, Figure A.2). Later on, the chromatogram of the blank experiment of *n*-hexane at 300 °C and 2 h reaction time is shown (Exp. 0.6, Figure A.3). Finally, a chromatogram of the material feed of 1-hexene is shown in Figure A.4.

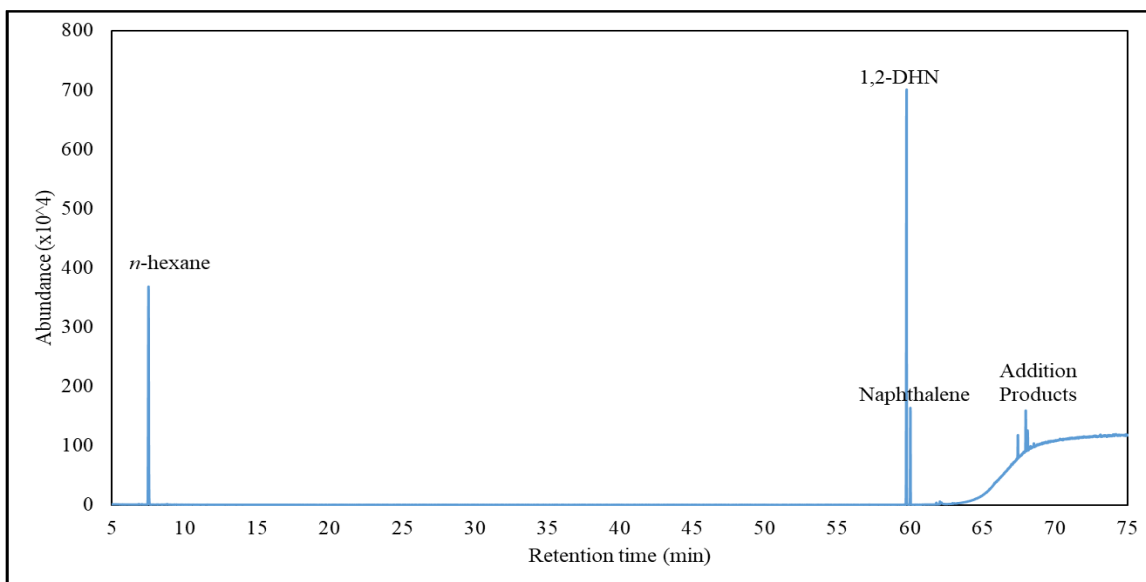


Figure A.1 Product distribution from reactions of 1,2-dihydronaphthalene and *n*-hexane at 300 °C, 2 h and 1:1 ratio (chromatogram obtained from GC-MS)

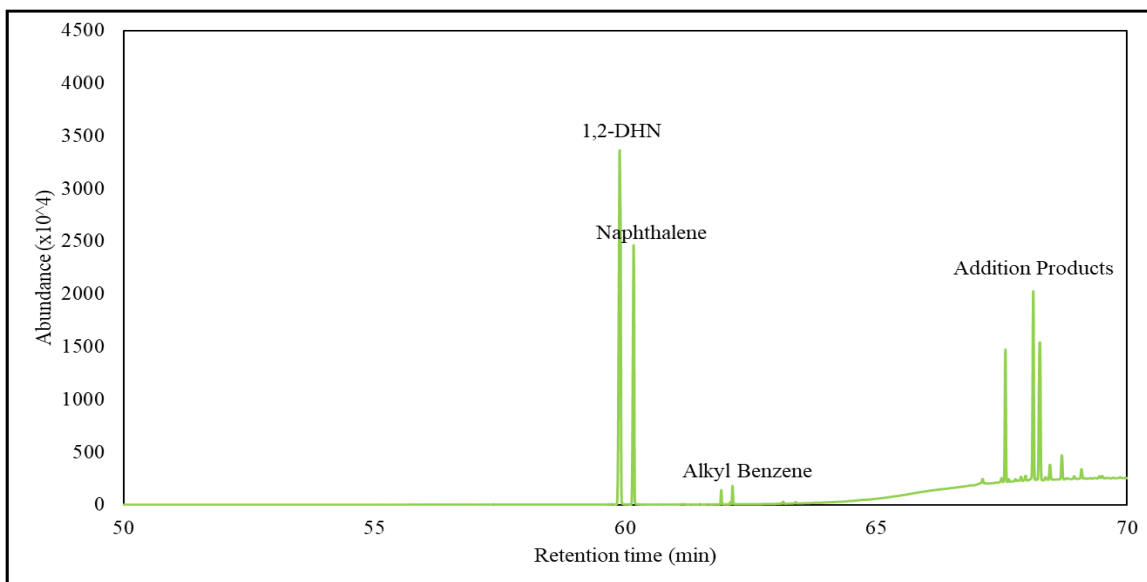


Figure A.2 Product distribution from reactions of 1,2-dihydronaphthalene at 300 °C and 2 h (chromatogram obtained from GC-MS)

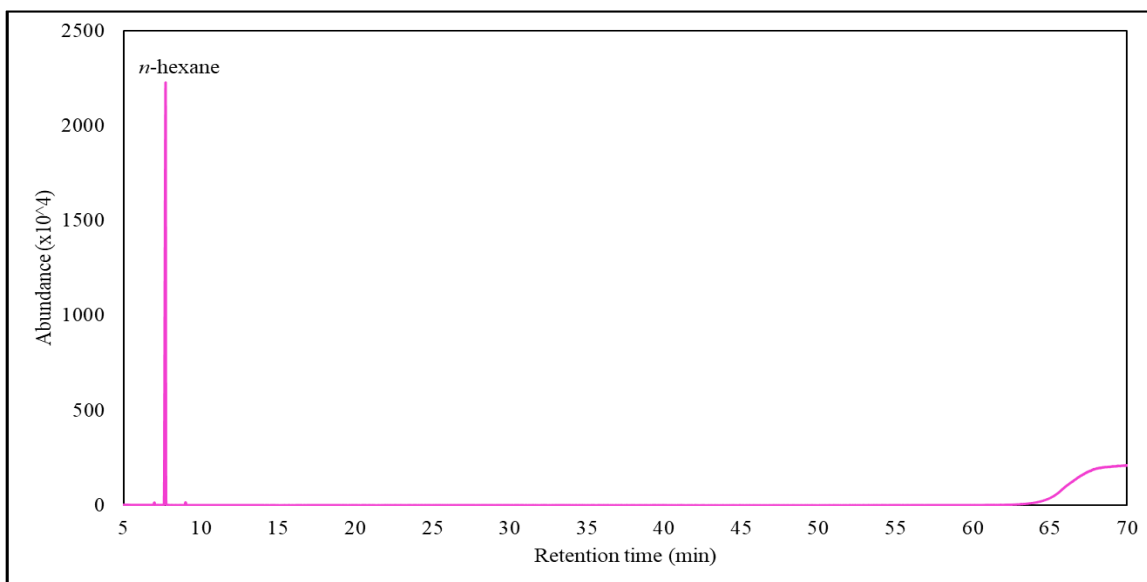


Figure A.3 Product distribution from reactions of n-hexane at 300 °C and 2 h (chromatogram obtained from GC-MS)

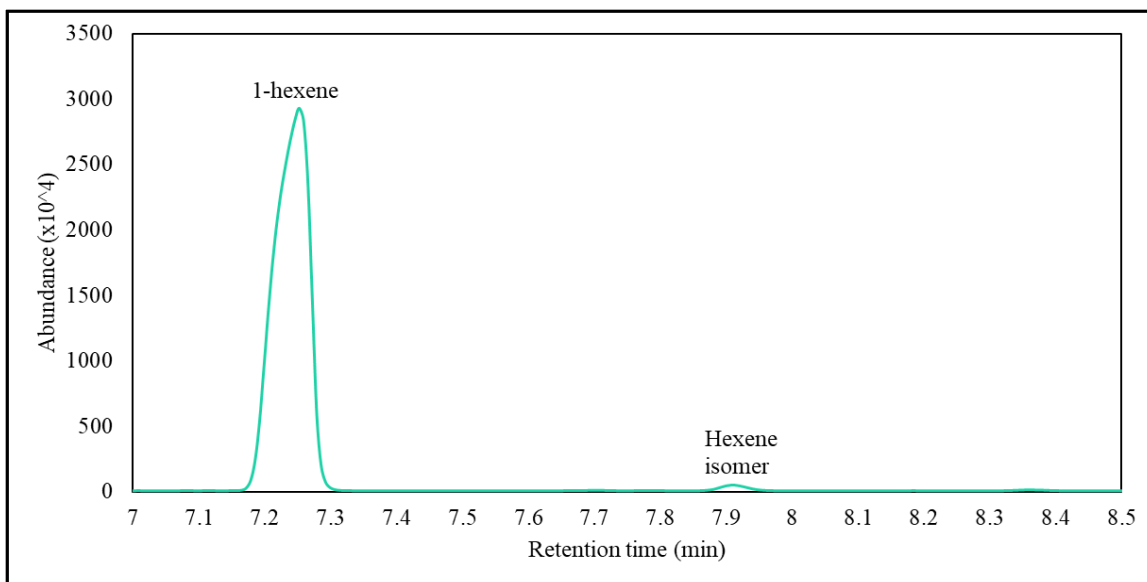


Figure A.4 GC-MS chromatogram of 1-hexene (feed material)

APPENDIX B

Measured masses of asphaltenes and 1-hexene

Table B.1 Experimental conditions for the reactions of asphaltenes as hydrogen donor and 1-hexene as hydrogen acceptor

Exp.	Weight ratio asphaltenes: 1-hexene	Temperature [°C]	Time [h]	Repetition	g asph.	g 1-hexene
1	1:1	250	1	1.1	1.503	1.502
				1.2	1.500	1.500
2	1:1	250	2	2.1	1.513	1.510
				2.2	1.504	1.504
3	1:1	250	4	3.1	1.501	1.512
				3.2	1.504	1.507
4	1:1	250	24	4.1	1.500	1.504
				4.2	1.500	1.512
				4.3	1.507	1.513
5	0:1 ^a	250	24	5	0	3.028
6	1:1	300	2	6.1	1.503	1.509
				6.2	1.499	1.503
				6.3	1.509	1.506
7	2:1	300	2	7	2.001	1.008
8	4:1	300	2	8.1	7.211	1.833
				8.2	7.178	1.815
				8.3	7.239	1.811
9	8:1	300	2	9.1	8.004	1.006
				9.2	8.003	1.005
10	0:1 ^a	300	2	10	0	3.0092
11	1:1	300	4	11	1.505	1.514
12	2:1	300	4	12.1	1.999	1.000
				12.2	2.002	1.008
13	0:1 ^a	300	4	13	0	3.016
14	1:1	325	2	14.1	1.503	1.507
				14.2	1.503	1.506
				14.3	1.503	1.506
15	1:1	350	0.5	15.1	1.512	1.510
				15.2	1.503	1.513
16	1:1	350	1	16.1	1.506	1.504
				16.2	1.501	1.502
17	1:1	350	2	17.1	1.509	1.512
				17.2	1.502	1.500
18	1:1	350	3	18.1	1.505	1.501
				18.2	1.515	1.515
19	0:1 ^a	350	3	19.1	0	1.014
				19.2	0	1.006
				19.3	0	1.015

^a Control experiments. The control experiments were performed to determine which products are formed from 1-hexene under the experimental conditions without the presence of asphaltenes.

Table B.1 contains the measured masses of reactants used for the reactions of asphaltenes and 1-hexene at different experimental conditions.

APPENDIX C

Comparison between recovered and filtered samples: Reactions of asphaltenes and 1-hexene

C.1 Chromatograms of recovered and filtered samples

For simplification, the calculations determined for reactions involving 1-hexene and asphaltenes were done by using only the GC-FID results of the recovered product. Hence, the liquid product adsorbed into the solids inside the vial was not taken into consideration for the calculations. This assumption was done after verifying that the composition/ concentration of the liquid product adsorbed into the solids was the same as the composition/ concentration of the recovered liquid (outside the vial after reaction).

As a result, the following chromatograms (Figure C.1 and C.2) were taken, as an example to highlight, the compounds in the recovered product were the same as the liquid products adsorbed in asphaltenes. The liquid adsorbed into the asphaltenes was obtained via methanol extraction, which is explained in more detail in Section 4.2.2.3 in Chapter 4.

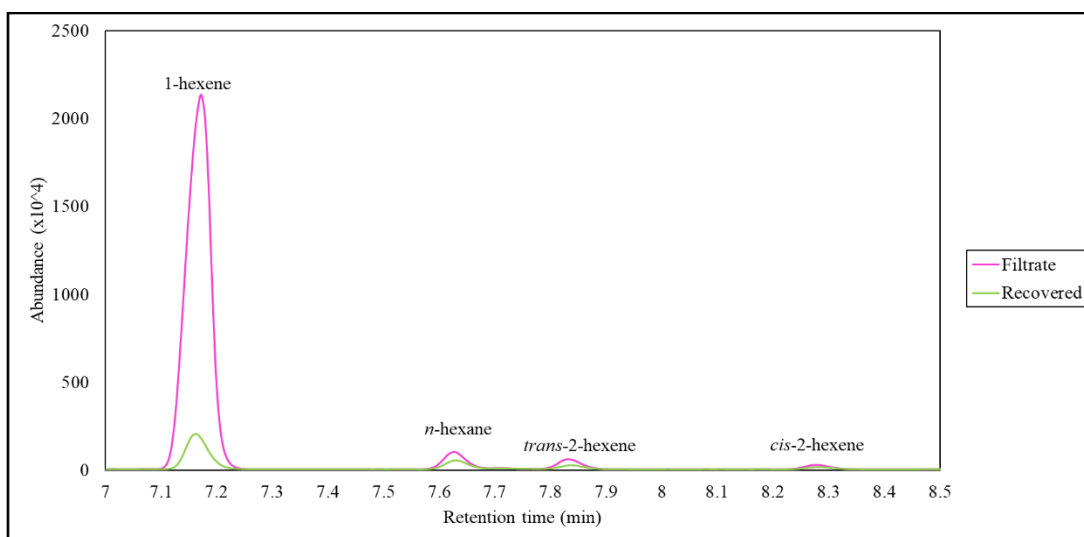


Figure C.1 Light product distribution from reactions of 1-hexene and asphaltenes at 350 °C, 0.5 h, 7 MPa, 1:1 weight ratio (chromatogram obtained from GC-MS)

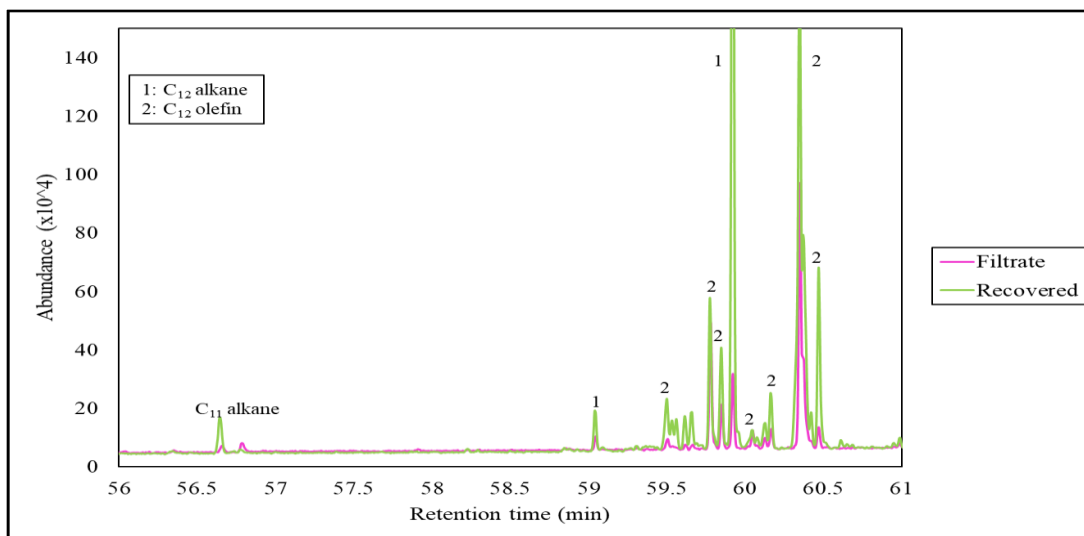


Figure C.2 Heavier product distribution from reactions of 1-hexene and asphaltenes at 350 °C, 0.5 h, 7 MPa, 1:1 weight ratio (chromatogram obtained from GC-MS)

The concentration of the recovered and filtrate products was compared. This was done by comparing the ratios of sum of the peak areas of each compound group by the area of the peak corresponding to the internal standard (ISTD). In this case, biphenyl was selected as internal standard as its retention time in the GC-FID is different from the products of interest and it is soluble in methanol. Retrospectively, a better approach would have been using a compound with a more similar structure to the analytes in order to have a relative response factor of approximately 1.¹ Therefore, the use of an olefin or paraffin with similar hydrocarbon chain length and structure as the analytes would have been a better fit as internal standard.

Table C.1 shows a summary of the areas obtained by GC-FID analyses of each compound group, the ratio between the area of the compound group and area of the internal standard, and the corrected ratio by using the extraction efficiency determined in Section C.2. According to the area ratios with extraction efficiency (filtrate product) and the area compound group/ area of internal standard (recovered product), these values have similar magnitudes. All except for the relative concentration of C₁₂ alkanes, which resulted, lower in the recovered product.

Table C.1 Comparison between the concentrations of filtrate and recovered product of reaction of asphaltenes and 1-hexene at 350 °C, 0.5 h, 7 MPa, 1:1 weight ratio

Compound	Filtrate product			Recovered product	
	Area	Area compound group/ Area ISTD	With extraction efficiency	Area	Area compound group/ Area ISTD
1-hexene	12.565	0.051	0.141	165.061	0.698
<i>n</i> -hexane	2.751	0.011	0.063	4.126	0.017
C ₆ olefins	4.263	0.017	0.048	16.639	0.070
C ₁₁ alkane	0.344	0.001	0.002	0.367	0.002
C ₁₂ olefins	7.422	0.030	0.041	4.129	0.017
C ₁₂ alkane	3.956	0.016	0.022	0.407	0.002
ISTD	248.120	1.000	-	236.637	1.000

Calculations were more accurate if the olefin reduction and conversion of 1-hexene were determined based on concentration than by mass because it was difficult to track all the potential mass losses during the reaction process. Therefore, based on the results and reasons previously explained, the assumption that the recovered and filtrate product had similar composition and concentration was taken into consideration for the calculations.

C.2 Extraction efficiency of methanol

Extraction was necessary in order to analyze the lighter compounds that are absorbed into the asphaltenes. In order to protect the integrity of the chromatographic columns of the GC-MS and GC-FID, it was important to use a solvent that did not dissolve the asphaltenes but would rather extract the products of interest from the asphaltenes.

As this is an important step in terms of how much product can be recovered, control experiments were performed in order to determine the extraction efficiency of methanol with the products of

interest. According to the results obtained from GC-MS, the products of interest consisted mainly of C₆ and C₁₂ hydrocarbons. Therefore, the following set of experiments was performed at 1:1 mass ratio of total hydrogen donor to products of interest Table C.1, with the use of 1-hexene, *n*-hexane, and *n*-dodecane as representative model compounds.

Table C.2 Control experiments to determine product recovery by using methanol extraction

Experiment	Hydrogen donor	Products of Interest
1	Asphaltenes	1-hexene
2	Asphaltenes	1-hexene and <i>n</i> -hexane
3	Asphaltenes	1-hexene, <i>n</i> -hexane, and <i>n</i> -dodecane

The experiments were performed by mixing the products of interest and asphaltenes in a glass vial. The mixture was left to sit for 3 h to simulate the contact time as the reaction experiments. The samples were later extracted with methanol and filtered according to the procedure in Chapter 4, Section 4.2.2.2. Similarly, the samples were analyzed with GC-FID for quantification of 1-hexene, *n*-hexane, and *n*-dodecane in the product filtrate. All experiments were performed in duplicate.

- *Sample Calculations for Extraction Efficiency*

Using the calibration curve created in Section C.3, it was possible to determine the weight percentage of each compound of interest in the sample prepared for GC-FID analysis. Therefore, following the subsequent steps, it is possible to calculate the extraction efficiency:

- 1) Calculate the amount of each compound in the sample used for GC-FID analysis. The wt. % of each compound is reported by the GC-FID.

g of 1 – hexene in the GC – FID sample =

$$\text{wt. \% of 1 – hexene} \left[\frac{\text{g of 1 – hexene}}{\text{g of sample used for GC – FID}} \right] \times \text{g of sample used GC – FID}$$

(Eq. 1)

- 2) Calculate the amount of each compound in the total amount of filtrate obtained from the methanol extraction.

g of 1 – hexene in the total filtrate =

$$\text{g of 1 – hexene in the GC – FID sample} \times \left(\frac{\text{g of total amount of filtrate}}{\text{g of sample used for GC – FID}} \right)$$

(Eq. 2)

- 3) Calculate the extraction efficiency:

$$\begin{aligned} \% \text{ Extraction efficiency of 1 – hexene} \\ = \frac{\text{Initial g of 1 – hexene in the mixture}}{\text{g of 1 – hexene in the total filtrate}} \times 100\% \end{aligned}$$

(Eq. 3)

Similarly, the same should be repeated if *n*-hexane and *n*-dodecane are used in the extraction experiment. The results obtained for each experiment are shown in Table C.3.

Table C.3 Results for control experiments for product recovery with methanol without heating

Experiment	% Extraction efficiency \pm standard deviation		
	1-hexene	<i>n</i> -hexane	<i>n</i> -dodecane
1	10.52 \pm 0.05	-	-
2	25.95 \pm 3.84	12.93 \pm 4.05	-
3	35.95 \pm 0.05	17.71 \pm 1.02	72.61 \pm 10.57

C.3 Calibration curve for quantification

To quantify the amount of unreacted 1-hexene and possible formation of *n*-hexane in the reaction products, the creation of calibration curves was necessary. The calibration curves for 1-hexene and *n*-hexane were obtained from the GC-FID. A calibration curve was also made for *n*-dodecane in order to quantify this compound for the calculation of the extraction efficiency.

For all the calibrations curves, biphenyl was used as internal standard. However, as previously explained, the use of a similar compound with hydrocarbon chain length and structure as the analytes would have been a better fit as internal standard.

Initially, due to the unknown range of how much 1-hexene could be present in the filtrate product, a wide range of data points were made for this compound. The calibration curve for 1-hexene consists of eight different levels of concentration (0.003, 0.005, 0.007, 0.01, 0.15, 0.02, 0.025, 0.03 g/mL) with a known concentration of biphenyl (0.01 g/mL). As *n*-hexane and *n*-dodecane are potential products, it was expected that the filtrate will have lower a lower concentration than 1-hexene, therefore, the calibration curve range was smaller. A total of five different concentration levels were made for *n*-hexane and *n*-dodecane (0.0001, 0.0005, 0.001, 0.005 and 0.01 g/mL), and similarly, with a known amount of biphenyl as internal standard (0.01 g/mL).

The different solutions were injected in triplicate in the GC-FID, and each point on the calibration curve represents an average value. All curves are plotted by area ratio (area of the peak of the compound reported in the GC-FID divided by the area of the peak of the biphenyl) versus the

amount ratio (concentration of the compound reported in the GC-FID divided by the concentration of the biphenyl). The calibration curves showed a regression line coefficient of $R^2 > 0.99$.

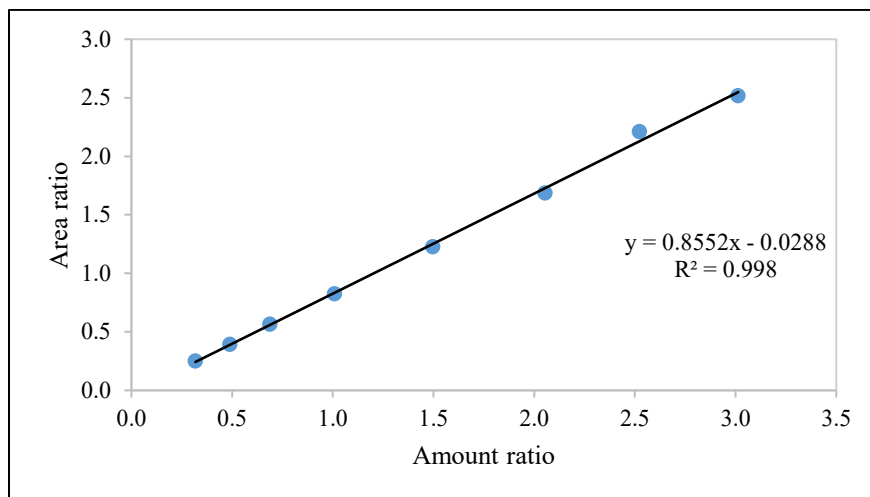


Figure C.3 Calibration curve for 1-hexene obtained from GC-FID by using biphenyl as internal standard.

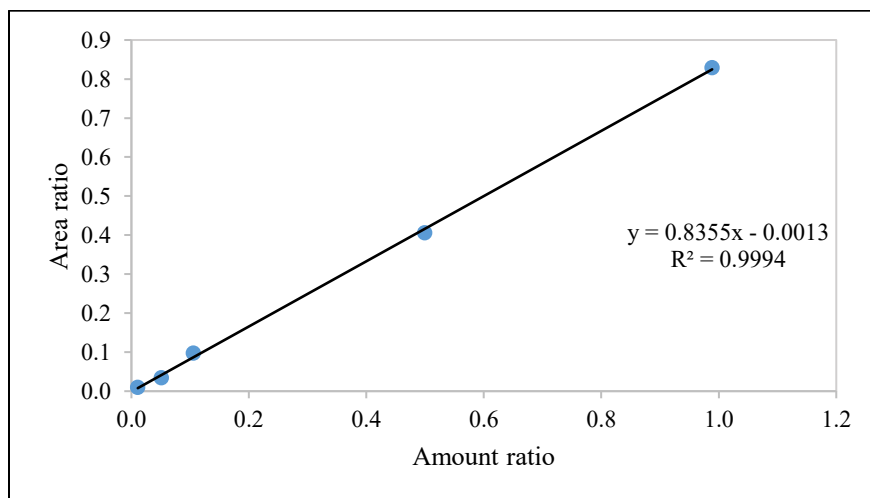


Figure C.4 Calibration curve for n-hexane obtained from GC-FID by using biphenyl as internal standard.

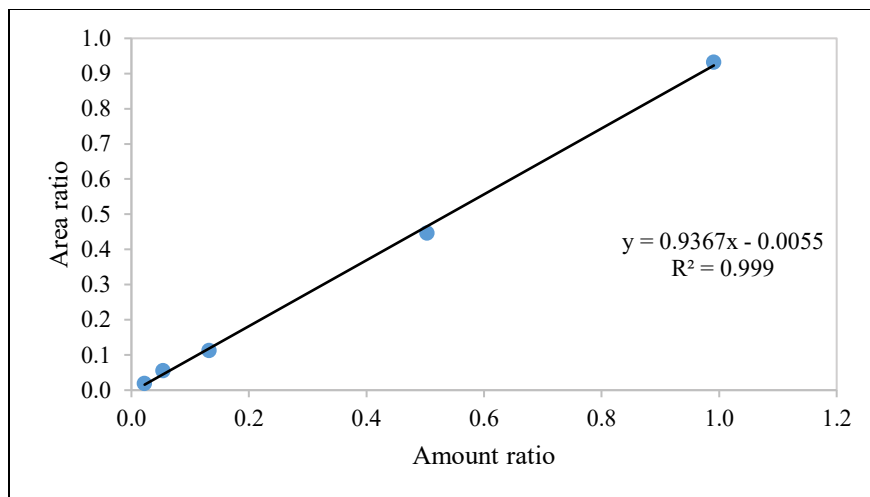


Figure C.5 Calibration curve for n-dodecane obtained from GC-FID by using biphenyl as internal standard.

References (Appendix C)

- (1) Scanlon, J. T. Calculation Using Effective Carbon Number. *J. Chromatogr. Sci.* **1985**, *23*, 333–340.

APPENDIX D

Calculations for conversion and selectivity of reactions with 1,2-dihydronaphthalene as hydrogen donor

The following steps describe the calculations to determine the conversions of 1-hexene and 1,2-dihydronaphthalene and the product selectivity of the reactions at different experimental conditions. The reactions of 1,2-dihydronaphthalene as hydrogen donor and 1-hexene as hydrogen acceptor at 250 °C, 1 h reaction time and 300 °C, 2 h reaction time were analyzed by GC-FID. Similarly, a blank reaction of 1,2-dihydronaphthalene at 300 °C and 2 h reaction time was also analyzed for comparison. The areas obtained from the analyses are summarized and classified by compound groups and shown in Table D.1. The identification of the peaks was done by GC-MS.

Table D.1 Peak areas from GC-FID analyses of reactions using 1,2-dihydronaphthalene as hydrogen donor

	Area in FID		
	1,2-DHN +1-hexene 250 °C, 1 h	1,2-DHN + 1-hexene 300 °C, 2 h	1,2-DHN (blank) 300 °C, 2 h
P-1: 1-hexene	123.98872	90.97478	0
P-2: <i>n</i> -hexane	0	0.929254	0
P-3: <i>trans</i> -3-hexene	0	0	0
P-4: <i>cis</i> -2-hexene	0.634372	0.910698	0
P-5: <i>trans</i> -2-hexene	0.649198	0.351048	0
P-6: C ₁₂ olefin	0.278013	0	0
P-7: 1,2-DHN	105.70532	67.47829	46.20582
P-8: naphthalene	2.4679	21.68602	18.94077
P-9: not identified	0.703805		0.624917
P-10: tetralin + oxygen	0.931593	1.890821	0.86195
P-11: not identified	0.557259	0.561669	0
P-12: addition products	0	8.302305	0
P-13: C ₁₂ olefin	0	0.415222	0

For each experiment, the following equations were used to determine the conversions and product selectivity:

- ***Conversion of 1-hexene***

$$\text{Conversion of 1-hexene} = 1 - \frac{\text{Area of 1-hexene}}{\sum \text{all the areas} - \text{Area of 1,2DHN}}$$

(Eq. 1)

- ***Conversion of 1,2-dihydronaphthalene***

$$\text{Conversion of 1,2-dihydronaphthalene} = 1 - \frac{\text{Area of 1,2 DHN}}{\sum \text{all the areas} - \text{Area of 1-hexene}}$$

(Eq. 2)

- ***Product selectivity***

$$\text{Selectivity}_i = \frac{\text{Area of compound group } i}{\sum \text{all the areas} - \text{Area of 1-hexene} - \text{Area of 1,2 DHN}} \times 100 \%$$

APPENDIX E

Conversion of SimDist boiling curve to weight percentage of carbon number

E.1 Boiling points of the linear paraffins in the standard

Table E.1 Boiling points of the linear paraffins in the calibration standard used for SimDist analyses

Carbon Name	Boling Point (°C)	Carbon Name	Boling Point (°C)
C ₅	36	C ₄₈	566
C ₆	69	C ₅₀	575
C ₇	98	C ₅₂	584
C ₈	126	C ₅₄	592
C ₉	151	C ₅₆	600
C ₁₀	174	C ₅₈	608
C ₁₁	196	C ₆₀	615
C ₁₂	216	C ₆₂	622
C ₁₄	254	C ₆₄	629
C ₁₅	271	C ₆₆	635
C ₁₆	287	C ₆₈	641
C ₁₇	302	C ₇₀	647
C ₁₈	316	C ₇₂	653
C ₂₀	344	C ₇₄	658
C ₂₂	369	C ₇₆	664
C ₂₄	391	C ₇₈	670
C ₂₆	412	C ₈₀	675
C ₂₈	431	C ₈₂	681
C ₃₀	449	C ₈₄	686
C ₃₂	466	C ₈₆	691
C ₃₄	481	C ₈₈	695
C ₃₆	496	C ₉₀	700
C ₃₈	509	C ₉₂	704
C ₄₀	522	C ₉₄	708
C ₄₂	534	C ₉₆	712
C ₄₄	545	C ₉₈	716
C ₄₆	556	C ₁₀₀	720

SimDist analyses were performed on the experimental products involving asphaltenes in the reaction feed. SimDist analyses provide the boiling point distribution curve of the sample by comparing it against a standard. The calibration standard used for SimDist analyses contains a mixture of known concentrations of linear paraffins. The list of the boiling point of each paraffin in the standard can be found in the report obtained from the SimDist analysis, as a matter of illustration, the list is shown in Table E.1.

E.2 Determining the weight percentage of carbon number

Once the samples are analyzed by SimDist, a boiling curve distribution report can be obtained from the software of the instrument. The report provides a list of boiling points in °C and a corresponding list of weight percentage. The boiling curve distribution is obtained by plotting the boiling point (*y*-axis) versus the weight percentage of sample boiled at that temperature (*x*-axis). To convert the boiling curve data into weight percentage per carbon number, the boiling points are compared to the boiling points of the standard in Table E.1.

As a matter of example, the reaction product of asphaltenes and 1-hexene at 300 °C, 2 h reaction time, 4:1 weight ratio of asphaltenes to 1-hexene at 6 MPa (Exp. 8) has the following SimDist results (shown in Table E.2):

Table E.2 Boiling points of the linear paraffins in the calibration standard used for SimDist analyses

% Off	BP (°C)	% Off	BP (°C)	% Off	BP (°C)	% Off	BP (°C)
1	57.91	26	67.28	51	68.32	76	69.9
2	59.47	27	67.54	52	68.32	77	70.11
3	60.51	28	67.54	53	68.32	78	70.31
4	61.55	29	67.54	54	68.32	79	70.52
5	62.59	30	67.54	55	68.32	80	70.94
6	63.63	31	67.54	56	68.32	81	71.15
7	64.41	32	67.54	57	68.32	82	71.36
8	65.19	33	67.8	58	68.58	83	71.78
9	65.98	34	67.8	59	68.58	84	71.99
10	66.24	35	67.8	60	68.58	85	72.41
11	66.24	36	67.8	61	68.58	86	73.04
12	66.5	37	67.8	62	68.58	87	75.14
13	66.5	38	67.8	63	68.58	88	206.67
14	66.76	39	67.8	64	68.84	89	209.93
15	66.76	40	68.06	65	68.84	90	209.93
16	66.76	41	68.06	66	68.84	91	209.93
17	67.02	42	68.06	67	68.84	92	209.93
18	67.02	43	68.06	68	69.06	93	209.93
19	67.02	44	68.06	69	69.06	94	209.93
20	67.02	45	68.06	70	69.06	95	209.93
21	67.28	46	68.06	71	69.27	96	209.93
22	67.28	47	68.06	72	69.27	97	209.93
23	67.28	48	68.06	73	69.48	98	209.93
24	67.28	49	68.32	74	69.69	99	209.93
25	67.28	50	68.32	75	69.69	100	209.93

Based on the results shown in Table E.2, the sample contains approximately 87 wt. % of hydrocarbons with a chain length of C₆ as 57-75 °C is closest to 69 °C, corresponding to the boiling point of linear paraffin C₆. The sample additionally has 13 wt. % of C₁₂ material as 88 – 100 wt. % resulted in a boiling point of ~ 210 °C. At 210 °C, the boiling point is closest to C₁₁ and C₁₂ linear paraffin boiling points (196 and 216 °C, respectively). However, based on the observations from the analyses obtained from GC-MS, most of the heavier compounds formed from this experiment were identified as C₁₂ olefins and alkanes. Therefore, it is most likely that most of the remaining 13 wt. % of sample corresponds to C₁₂ hydrocarbons.

A similar procedure was done to the other experiments, where the boiling point distribution curve from the SimDist results was converted to weight percentage of carbon number. Due to time constraints, samples that were performed in duplicates and triplicates, SimDist analysis was performed to only one sample randomly chosen from the batch.

APPENDIX F

Calculations to decouple the effect of blanks on reactions of asphaltenes and 1-hexene

The following steps describe the calculations to decouple the effect of the blank reactions on the reactions of asphaltenes and 1-hexene. This was done because the blank reactions of 1-hexene at the different experimental conditions resulted in the formation of C₆ and C₁₂ olefins. The contribution of these products was noticeable, and therefore, decoupling the blank from the selectivity was necessary to determine the actual contribution of asphaltenes to olefin reduction.

For all cases, the product distribution was classified into the following compound groups: *n*-hexane, C₆ olefins (isomers of 1-hexene), C₁₀ alkanes, C₁₁ alkanes, C₁₂ alkanes, and C₁₂ olefins. According to the results obtained by GC-MS, the compounds formed from the blank reactions are C₆ and C₁₂ olefins. Therefore, these were the only compounds decoupled from the reactions involving asphaltenes. Additionally, the calculations were performed only on the experiments that have a corresponding blank. This means a blank that is representative of its experimental conditions. These experiments were Exp. 4, 6, 11 and 18 shown in Table 4.5 from Chapter 4. The blanks that were representative are Exp. 5, 10, 13 and 19 respectively.

As a matter of illustration, the calculation for Exp. 6 (asphaltenes and 1-hexene at 300 °C, 2 h reaction time and 1:1 ratio) and its corresponding blank Exp. 10 (1-hexene at 300 °C, 2 h reaction time) are described.

1. Selectivity of C₆ and C₁₂ olefins for each reaction and their corresponding blank must be corrected by using the conversion of 1-hexene determined for each case (Eq.1). Similar steps were done to determine the contribution of asphaltenes towards selectivity of C₁₂ olefins at the experimental conditions.

$$\begin{aligned}
& \text{Contribution of asphaltenes towards selectivity of } C_6 \text{ olefins at } 300\text{ }^\circ\text{C, } 2\text{ h} \\
& = (\text{Selectivity } C_6 \text{ olefins}_{Exp.6} \times \text{Conversion of } 1 - \text{hexene}_{Exp.6}) \\
& - (\text{Selectivity } C_6 \text{ olefins}_{Exp.10} \times \text{Conversion of } 1 - \text{hexene}_{Exp.10}) \\
& \text{(Eq. 1)}
\end{aligned}$$

2. The selectivity for *n*-hexane, C₁₀ alkane, C₁₁ alkane, and C₁₂ alkane remains the same for all cases (calculations shown in Section 4.2.4.4 from Chapter 4).
3. Because it is more common to represent selectivity on a 100 % basis. The selectivity of each compound group was normalized with respect to the sum of all the contributions of asphaltenes towards selectivity of compound group *i*.

APPENDIX G

Cost and design evaluation for olefin reduction processes

G.1 Current and proposed processes for olefin reduction

G.1.1 CNOOC BituMax: Olefins-aromatic alkylation

The current design for CNOOC's BituMax project for olefin treatment is via olefins-aromatic alkylation (Figure G.1). This process reduces the amount of olefins in the feed by alkylating the olefins with the aromatics present in the hydrocarbon feed, with the use of an acid catalyst.¹ The olefin-rich feed, such as the naphtha, is pressurized at 6 MPa and then heated to 350 °C before entering the packed bed reactor. Two reactors are required as it is a swing operation as catalyst regeneration is required. Each reactor requires a weight hour space velocity (WHSV) of approximately 1 h⁻¹ to achieve required conversion to fulfill pipeline specifications.

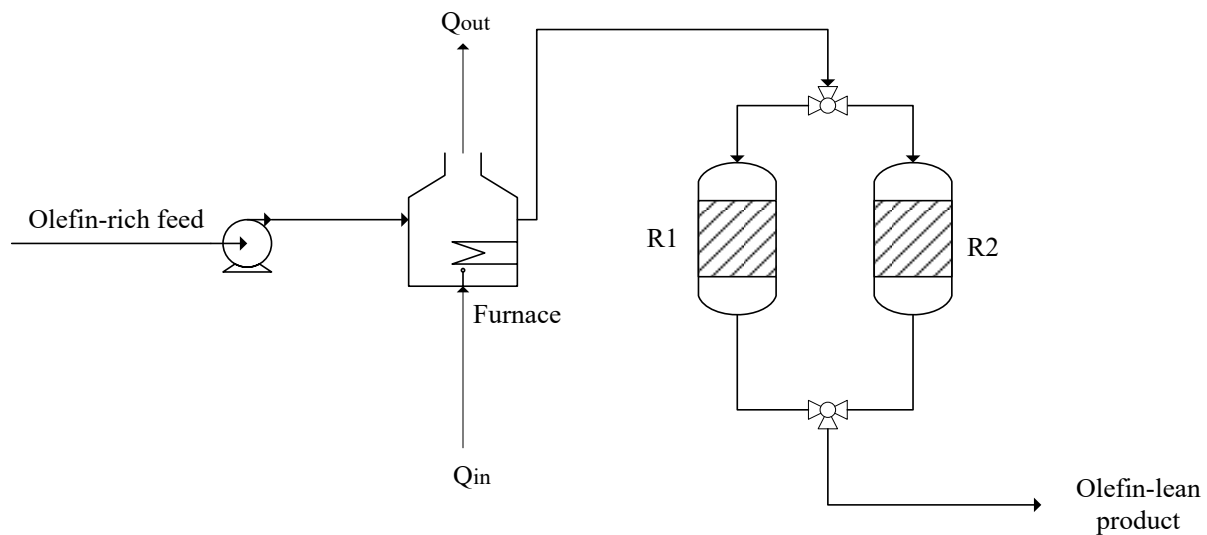


Figure G.1 Process diagram of CNOOC olefin alkylation plant

G.1.2 Olefins treating with asphaltenes at 250 °C

As the expense associated with the construction and installation of a furnace may considerably increase the overall cost of a process, the possibility of operating at 250 °C was evaluated. The experimental results selected for evaluation were Exp. 4 from Table 4.5 in Chapter 4, as it gave the highest olefin reduction at 250 °C. The size and cost of the equipment required for operations at 250 °C were calculated in order to compare this proposal with the olefins-aromatic alkylation plant. For this process, an olefin rich feed, such as the naphtha, is mixed with a stream of hot asphaltenes at 6 MPa (Figure G.2). This mixture is then heated with a high-pressure-steam heat exchanger to 250 °C. The reactants are placed in contact inside a vessel for a residence time of 24 h. After reaction, the pressure will be dropped to 0.44 MPa, which will lead to the flash separation of the naphtha and a stream of hydrogen-depleted asphaltenes.

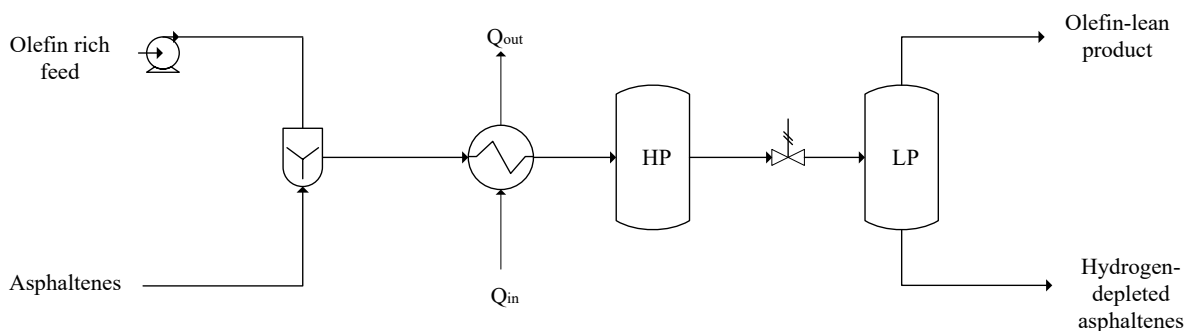


Figure G.2 Process diagram for olefin treatment with asphaltenes at 250 °C

G.1.3 Olefins treating with asphaltenes at 350 °C

The second alternative evaluated is similar to the process at 250 °C (See scheme at Figure G.3). However, the reaction temperature is at 350 °C, which will require the construction and installation of a furnace. However, the required residence time is 3 h, which is considerably lower than 24 h, as the experimental results indicated that at 350 °C the olefin reduction was significantly higher.

The experiment selected for evaluation was Exp. 18 from Table 4.5 in Chapter 4, as it resulted in the highest olefin reduction at 350 °C.

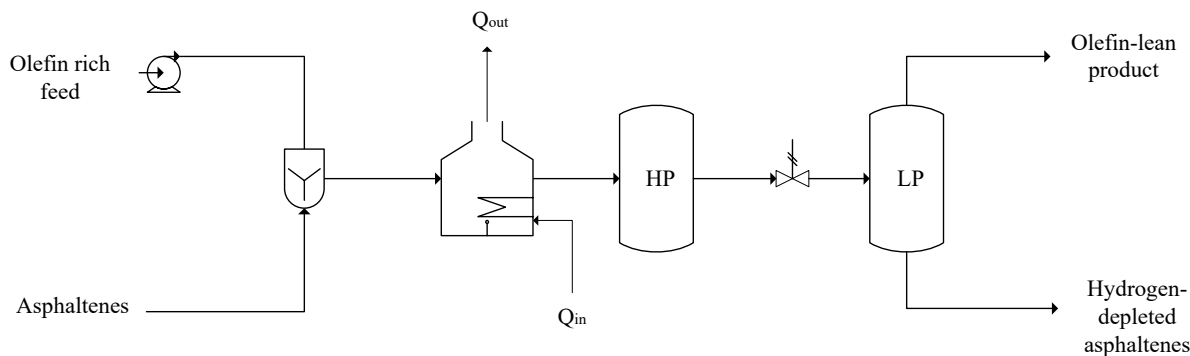


Figure G.3 Process diagram for olefin treatment with asphaltenes at 350 °C

G.2 Calculations for equipment sizing and cost estimation

The calculations follow the Pré-Estime Method,² which provides a rapid and simple equipment sizing. The purpose of these calculations is to have a rough economic estimate and comparison between the currently used olefins-aromatic alkylation and the new alternatives by using asphaltenes as hydrogen donors.

G.2.1 Furnace

Furnace is required for the process of olefins-aromatic alkylation and the treatment with asphaltenes at 350 °C. The following equation includes the cost calculation of the furnace and its respective correction factors suggested by the Pré-Estime Method (type, material, and pressure), in addition to the factors to correct by installation, location, currency and inflation.

Corrected price =

$$\text{base price} \cdot (1 + f_d + f_m + f_p) \cdot f_{inst} \cdot f_{loc} \cdot f_{cur} \cdot \left(\frac{\text{Present value of Cost Index}}{\text{Historical value of Cost Index}} \right)$$

(Eq. 28)

Where the correction factors are for:

f_d : type of furnace^a

f_m : material^a

f_p : pressure^a

f_{inst} : installation^a

f_{loc} : location^a

f_{cur} : currency exchange^a

Present value of Cost Index: Cost Index^b of the present year

Historical value of Cost Index: Cost Index^b of the year of the base price

^a Value can be found in reference ²⁻⁵

^b The cost indices adjust for the difference in the cost of goods and services at two different points in time. The present value should be as recent as possible. For plant costs, the Chemical Engineering (CE) Index can be used.

- **Determining the base price**

To determine the base price, the required heating power has to be known beforehand. In the case of the naphtha, it does not evaporate at the operational conditions. Therefore, the required heat can be calculated in the following manner:

$$\dot{Q} \left[\frac{\text{kcal}}{\text{h}} \right] = \frac{\dot{m} \cdot C_p \cdot (T_{out} - T_{ent})}{\eta}$$

(Eq. 29)

Where:

$\dot{Q} \left[\frac{\text{kcal}}{\text{h}} \right]$: Required heating power (to be determined)

\dot{m} : Total mass flow rate in the feed = 10,000 kg/h of naphtha + mass of required asphaltenes if applicable (to be determined)

C_p : Specific heat capacity of the fluid⁶ (to be determined)

T_{out} : Temperature of the fluid at the outlet of the equipment = 350 °C

T_{ent} : Temperature of the fluid at the inlet of the equipment = 25 °C

η : Efficiency of the heat transfer⁷ = 70 %

- **Calculating the required amount of asphaltenes**

The amount of asphaltenes required directly depends on the amount of olefins to be reduced from the stream. It is known from the naphtha characterization performed by Santiago and Subramanya⁸ that the naphtha feed contains ~ 10 wt. % of olefins, mainly in the C₅-C₇ hydrocarbon chain length. Therefore, to convert this value into olefin molar content, approximate molecular weight of the olefins was determined by the following manner:

Molecular weight of olefins in naphtha

$$= \frac{MW_{1-pentene} + MW_{1-hexene} + MW_{1-heptene}}{3} = 84.16 \text{ g/mol}$$

(Eq. 30)

Therefore,

$$\text{Olefin molar content} = 0.10 \frac{\text{g olefins}}{\text{g naphtha}} \cdot \frac{1 \text{ mol olefin}}{84 \text{ g olefin}} = 1.19 \cdot 10^{-3} \frac{\text{moles olefin}}{\text{g naphtha}}$$

(Eq. 31)

In order to achieve pipeline specifications, the BituMax process requires a reduction of 50 mol % (approximate value) of the olefin content.

$$\text{Required olefin reduction} = 1.19 \cdot 10^{-3} \frac{\text{moles olefin}}{\text{g naphtha}} \cdot 50\% = 5.95 \cdot 10^{-4} \frac{\text{moles olefin}}{\text{g naphtha}}$$

(Eq. 32)

For calculations, the naphtha feed was assumed as 10,000 kg/h.

Required olefin reduction in the feed

$$= 5.95 \cdot 10^{-4} \frac{\text{moles olefin}}{\text{g naphtha}} \cdot 10,000 \cdot 10^3 \frac{\text{g naphtha}}{\text{h}} = 5940 \frac{\text{moles olefin}}{\text{h}}$$

(Eq. 33)

Based on the experimental results, the overall olefin reduction at 350 °C, 3 h reaction time, 7 MPa and 1:1 weight ratio of asphaltenes to 1-hexene (1.5 g each) was 38.1 % (Table 4.8 in Chapter 4). As a result, the olefin reduction capacity under these experimental conditions can be calculated.

$$\text{Olefin reduction capacity} = \frac{\text{moles olefin feed} - \text{moles olefin product}}{1.5 \text{ g asphaltenes}}$$

(Eq. 34)

Where:

$$\text{moles olefin feed} = 1.5 \text{ g 1-hexene} \cdot \frac{1}{MW_{1\text{-hexene}}} = 0.0178 \text{ moles 1-hexene}$$

From the results obtained from Eq. 8 in Chapter 4, the moles of olefin in the product can be calculated as follow:

moles olefin product

$$= \sum \% \text{ moles of olefin} \left[\frac{\text{moles olefin product}}{\text{moles feed}} \right] \cdot \text{moles olefin feed}$$

(Eq. 35)

As a result:

$$\text{Olefin reduction capacity at 350 °C} = 3.22 \cdot 10^{-3} \frac{\text{moles olefin reduced}}{\text{g asphaltenes} \cdot \text{h}}$$

(Eq. 36)

Therefore, the required amount of asphaltenes can be determined:

$$\begin{aligned}
 & \text{Required amount of asphaltenes} \\
 &= 5940 \frac{\text{moles olefin}}{h} \cdot \frac{g \text{ asphaltenes}}{3.22 \cdot 10^{-3} \text{ moles olefin reduced}} \\
 &= 615 \frac{kg \text{ asphaltenes}}{h}
 \end{aligned}$$

(Eq. 37)

- **Calculating the specific heat capacity of a mixture**

For process using asphaltenes in the feed, the following equation and values were used to calculate the specific heat of the mixture:

$$C_p = \frac{m_{naphtha}}{m_{naphtha} + m_{asphaltenes}} \cdot C_{p \text{ naphtha}} + \frac{m_{asphaltenes}}{m_{naphtha} + m_{asphaltenes}} \cdot C_{p \text{ asphaltenes}}$$

(Eq. 38)

Where:

$C_{p \text{ naphtha}}$: Specific heat of the naphtha (approximated to kerosene)⁶ $\approx 0.48 \frac{kcal}{kg \cdot ^\circ C}$

$C_{p \text{ asphaltenes}}$: Specific heat of the asphaltenes (approximated to asphalt)⁹ $\approx 0.22 \frac{kcal}{kg \cdot ^\circ C}$

Once the required amount of asphaltenes and specific heat are calculated, the base price can be determined by reading directly Figure G.4.²

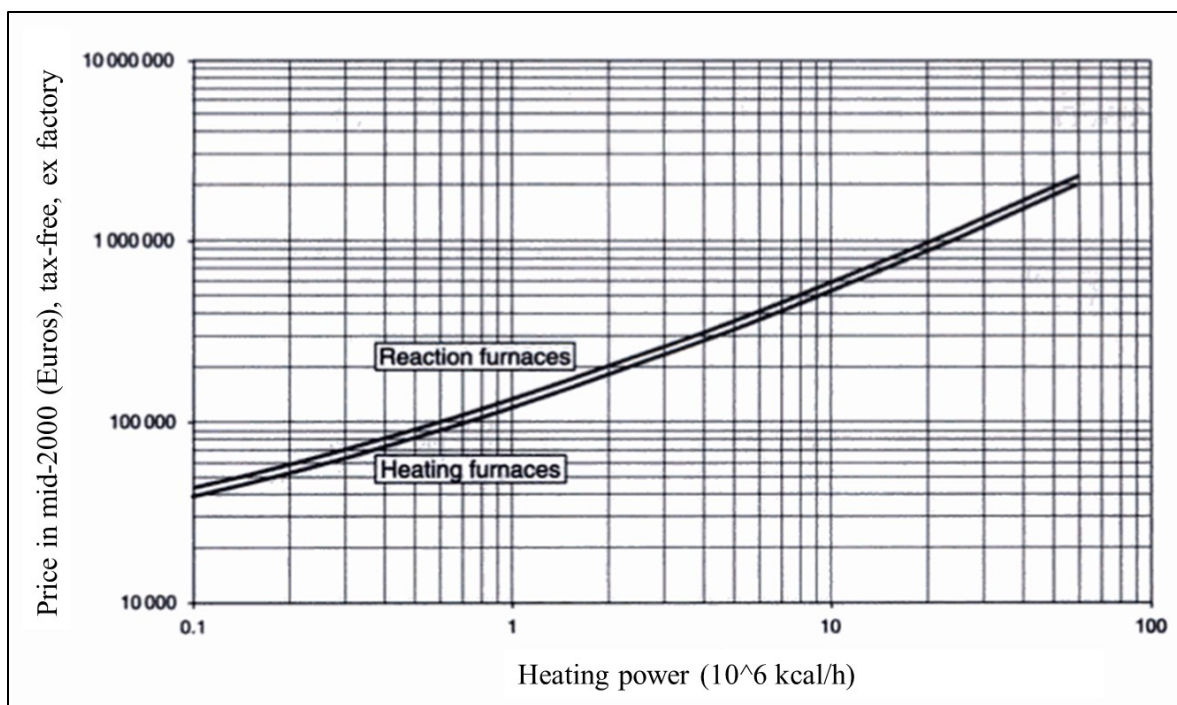


Figure G.4 Furnace prices²

For the correction factors, the values were read directly from the literature^{2-5,7} according to the conditions for the processes.

Table G.1 Correction factors used for calculations of the furnace

Correction factor		Olefins-aromatic alkylation / Treatment with asphaltenes at 350 °C	
Description	Factor	Description	Factor
Type of furnace	f_d	Cylindrical	0.00 ²
Material	f_m	Stainless steel	0.75 ²
Pressure	f_p	6 – 7 MPa ^a	0.10 ²
Installation	f_{int}	Furnace	1.3 ⁴
Location	f_{loc}	Ft. McMurray, AB, Canada	1.6 ³
Currency exchange	f_{cur}	EUR to CAD	0.68 ⁵
Present value cost index	-	CE index 2018	603.1 ¹⁰
Historical value cost index	-	CE index 2000	394.1 ¹⁰

^a Olefins-aromatic alkylation at 6 MPa and treatment with asphaltenes at 350 °C at 7 MPa

G.2.2 Heat exchanger

The heat exchanger is evaluated for the process using asphaltenes at 250 °C. The corrected cost can be determined from the base price including correction factors found in the literature^{2-5,7}:

$$\begin{aligned} & \text{Corrected price} \\ & = \text{base price} \cdot f_d \cdot f_l \cdot f_{np} \cdot f_p \cdot f_t \cdot f_m \cdot f_{inst} \cdot f_{loc} \cdot f_{cur} \cdot \left(\frac{\text{Present value of Cost Index}}{\text{Historical value of Cost Index}} \right) \end{aligned}$$

(Eq. 39)

Where the correction factors are:

f_d : factor characteristic of the type of exchanger^a

f_l : tube length^a

f_{np} : number of tube passes^a

f_p : pressure in the shell and tubes^a

f_t : temperature^a

f_m : kinds of material used^a

f_{int} : installation^a

f_{loc} : location^a

f_{cur} : currency exchange^a

Present value of Cost Index: Cost Index^b of the present year

Historical value of Cost Index: Cost Index^b of the year of the base price

^a Value can be found in reference ²⁻⁵

^b The cost indices adjust for the difference in the cost of goods and services at two different points in time. The present value should be as recent as possible. For plant costs, the Chemical Engineering (CE) Index can be used.

- **Determining the base price**

To calculate the base price, the required heat exchanger surface has to be determined previously.

The required area can be calculated from:

$$\text{Exchanger surface [m}^2\text{]} = \frac{Q}{U \cdot (T_{out} - T_{ent})}$$

(Eq. 40)

Where:

\dot{Q} : Required heating power (Calculated with (Eq. 29) following similar procedure)

U : Overall heat transfer coefficient = 88 kcal/ (h. m². °C) (for steam in tube side and naphtha in shell side, assuming that the presence of asphaltenes does not affect the coefficient)²

T_{out} : Temperature of the fluid at the outlet of the equipment = 250 °C

T_{ent} : Temperature of the fluid at the inlet of the equipment = 25 °C

With the value of required area, the base price of the heat exchanger can be found directly from Figure G.5.

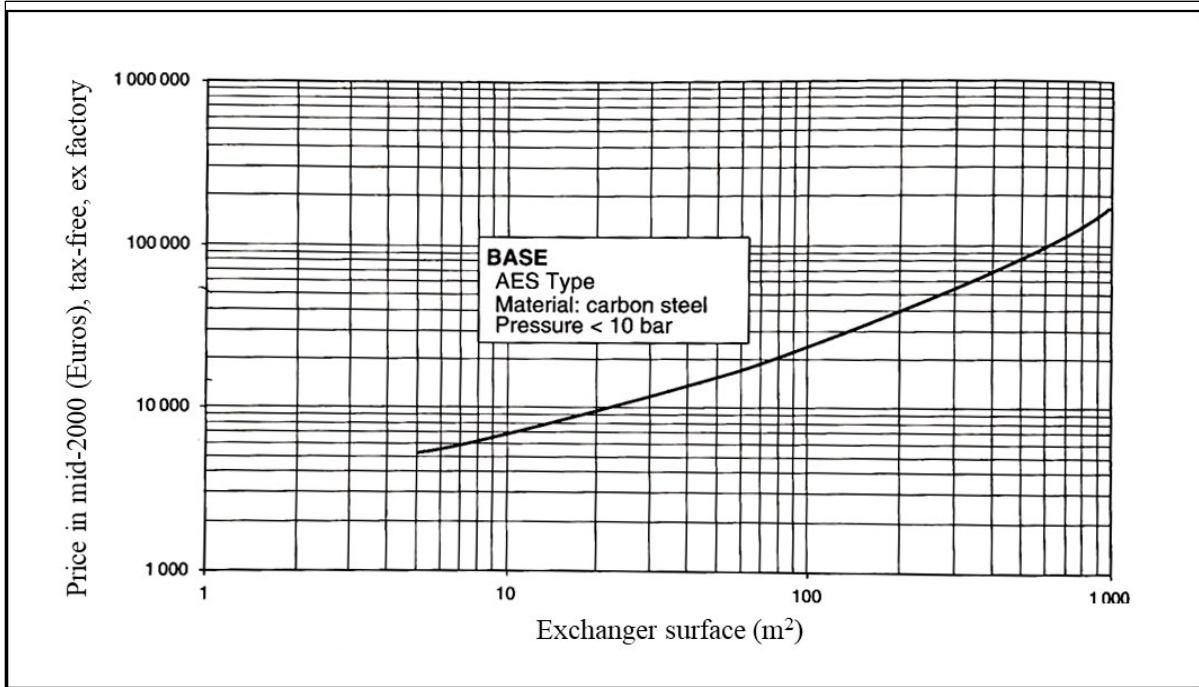


Figure G. 5 Price of tube-type exchangers²

Finally, the corrected price can be determined by adding the corresponding correction factors that can be found in the literature.^{2-5,7}

Table G. 2 Correction factors used for calculations of the heat exchanger

Correction factor		Treatment with asphaltenes at 250 °C	
Description	Factor	Description	Factor
Type of exchanger	f_d	AFT	1.08^2
Tube length	f_m	4.87 ft	1.00^2
Number of tube passes	f_{np}	2	1.00^2
Pressure in the shell and tubes	f_p	6 MPa	1.81^2
Temperature	f_t	T < 350 °C	1.00^2
Material	f_m	Carbon steel (shell)/ Copper (tubes)	1.30^2
Installation	f_{int}	Heat exchanger, Carbon steel (shell)/ Copper (tubes)	2.0^4
Location	f_{loc}	Ft. McMurray, AB, Canada	1.6^3
Currency exchange	f_{cur}	EUR to CAD	0.68^5
Present value cost index	-	CE index 2018	603.1^{10}
Historical value cost index	-	CE index 2000	394.1^{10}

G.2.3 Reactor and flash separator (pressurized vessels)

The reactors and flash separator can be designed as a pressurized vessel. Therefore, the following steps can be used in all three cases.

- **Calculating the correct price of the vessel**

The corrected price of the vessel can be calculated as:

Corrected price of vessel

$$\begin{aligned} &= (\text{Price shell and ends} \\ &+ \text{accessories}) \cdot f_{inst} \cdot f_{loc} \cdot f_{cur} \cdot \left(\frac{\text{Present value of Cost Index}}{\text{Historical value of Cost Index}} \right) \end{aligned}$$

(Eq. 41)

Where:

$$\text{Price of shell and ends} = \left(\frac{\text{EUR}}{\text{kg}} \right) \cdot (\text{kg shell} + \text{vessel ends} \cdot f_f) \cdot f_e \cdot f_m$$

(Eq. 42)

f_f : Correction for shell diameter (depending on the diameter, see reference²)

f_e : Correction for wall thickness (to be determined)

f_m : Correction for material² = 3.2

And:

$$\text{Price of accessories} = \text{base price} \cdot f_{am}$$

(Eq. 43)

f_{am} : Correction for material² = 3.0

- **Calculating the thickness of the vessel wall**

The total thickness of the vessel wall can be calculated as²:

$$e = \frac{P \cdot R}{\alpha \cdot t - 0.6 P} + se$$

(Eq. 44)

Where values can be determined from the literature² or from the operational conditions (values used for calculations are shown in Table G.3:

se: Extra thickness = 3 mm

P: Relative operating pressure (bar)

R: Radius of the vessel (mm) (to be determined)

t: Maximum allowable stress (bar)^a

α : welding coefficient = 1.00

^a Value can be found in reference²⁻⁵

- **Calculating the radius of the vessel**

The radius of the vessel was calculated by assuming a cylindrical volume:

$$\text{Volume of vessel (m}^3\text{)} = \frac{\text{Reaction time [h]}}{\text{Volumetric flow rate } \left[\frac{\text{m}^3}{\text{h}}\right]} = \frac{\pi \cdot R^2}{H}$$

(Eq. 45)

Where the usual ratio of $H/(2.R) = 3$.¹¹ Therefore, the height of the vessel was selected until the ratio was ~ 3 .

- **Calculating the weight of the shell and vessel ends**

The weight of the shell can be calculated as:²

$$\text{shell weight (kg)} = 24.7 \cdot D' \cdot H \cdot e$$

(Eq. 46)

Where:

D': Diameter of the shell (m)

H: Height of the shell (m)

e: Thickness of the shell and bottoms (mm)

To calculate the weight of the top and bottom of the vessel ends:

$$\text{weight of vessel ends (kg)} = \text{unit weight} \left(\frac{\text{kg}}{\text{mm}} \right) \cdot \text{thickness (e)(mm)}$$

(Eq. 47)

Where the unit weight can be read directly from Figure G.6 by using the diameter of the shell.

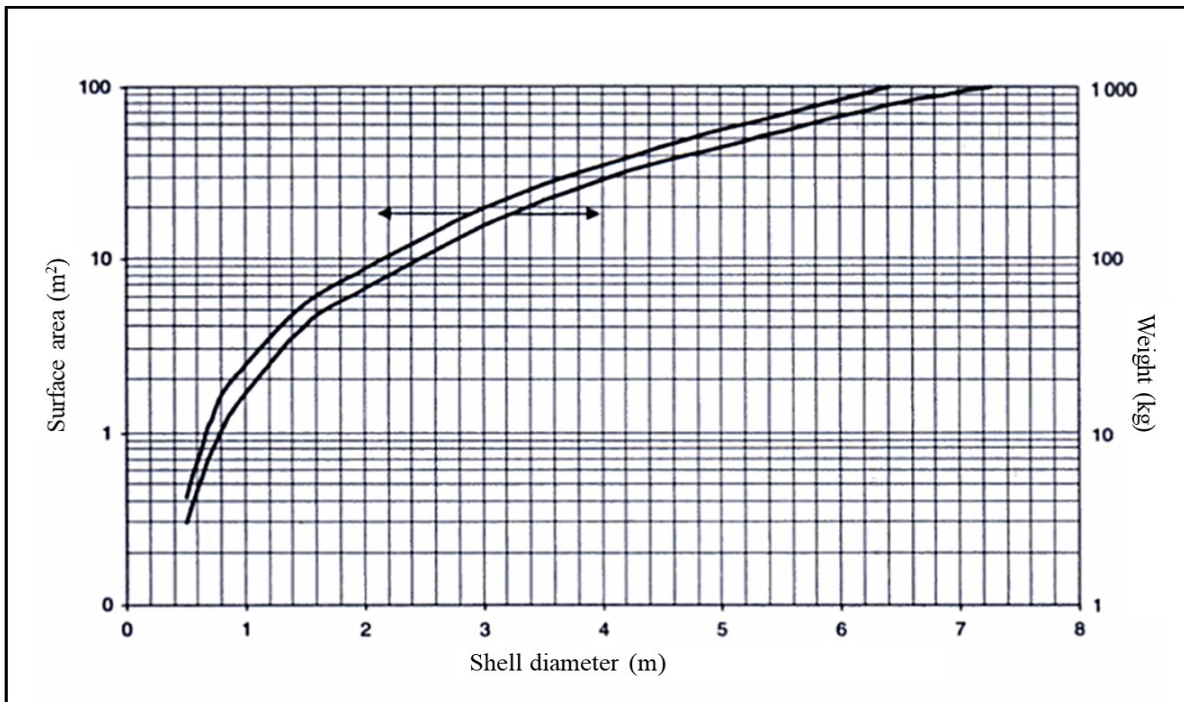


Figure G.6 Determination of surface area and weight for two bottoms²

- **Calculating the cost of the shell and vessel ends**

The cost of shell and ends to solve (Eq. 42) can be read directly from Figure G.7.

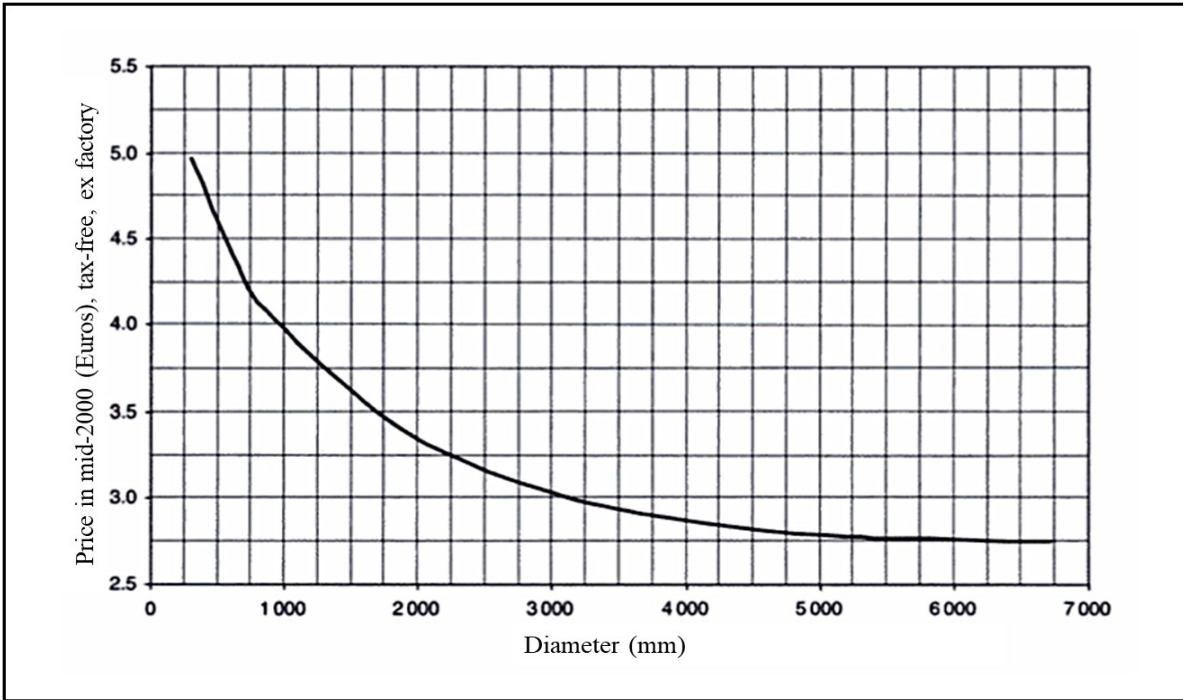


Figure G.7 Determination of base price for shell and bottoms²

The thickness correction factor to solve (Eq. 42) was determined from Figure G.8.

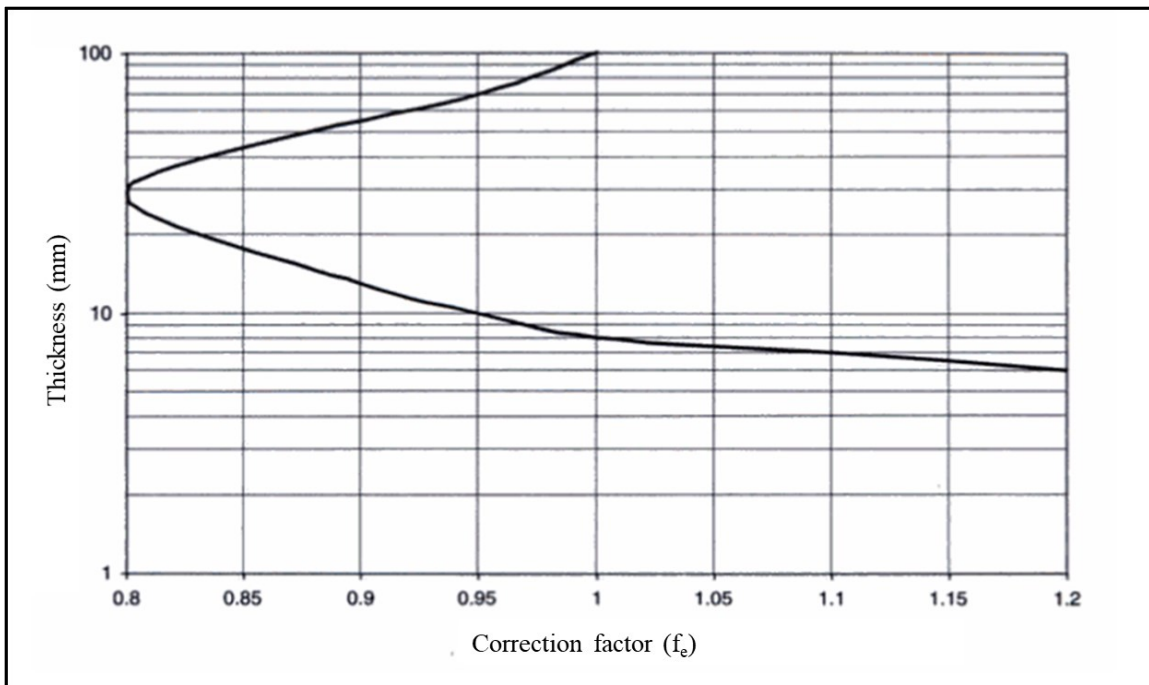


Figure G.8 Determination of thickness correction factor f_e ²

- **Calculating the cost of accessories**

The base price for the cost of accessories can be directly determined from Figure G.9.

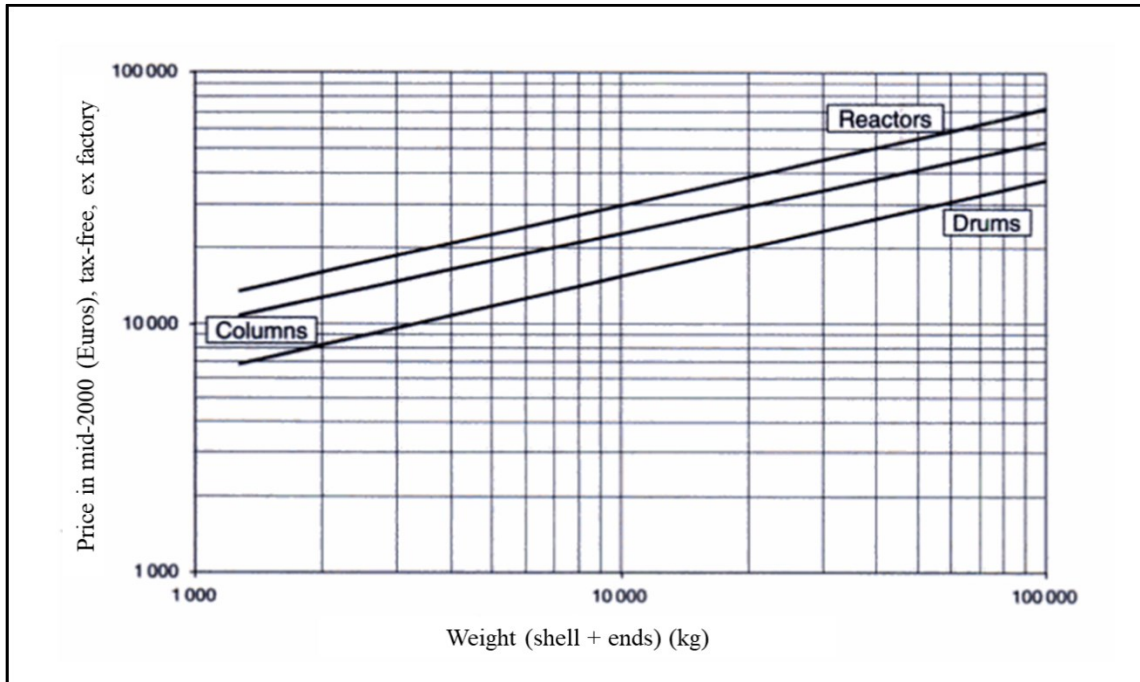


Figure G.9 Determination of prices of accessories for reactors, columns, and drums²

Finally, Table G.3 contains the correction factors that were used for calculations of the vessels.

Table G.3 Correction factors and parameters used for calculations of the pressurized vessels

Correction factor			
Description	Factor	Description	Factor
Shell diameter	f_f	Varies depending on shell diameter	1.5-2.5 ²
Wall thickness	f_e	Varies depending on wall thickness	0.98-1.2 ²
Material of shell and ends	f_m	SA 240 – 316 L	3.2 ²
Material of accessories	f_{am}	SA 240-316	1.81 ²
Installation	f_{int}	Pressurized vessel (stainless steel)	1.7 ⁴
Location	f_{loc}	Ft. McMurray, AB, Canada	1.6 ³
Currency exchange	f_{cur}	EUR to CAD	0.68 ⁵
Present value cost index	-	CE index 2018	603.1 ¹⁰
Historical value cost index	-	CE index 2000	394.1 ¹⁰

The results for cost and design evaluation for each process are summarized in the following tables (Table G.4-G.6).

Table G.4 Summary of cost and design evaluation for Olefins-Aromatic Alkylation Process

Process:		Olefins-aromatic alkylation	
Total flowrate (kg/h)		10,000 (naphtha)	
Furnace		Reactor	
T _{in} (°C)	25	# of reactors	2
T _{out} (°C)	350	Residence time (h)	1
Q _{required} (kJ/h)	9,332,000	Pressure (MPa)	6
Total cost of furnace (CAD) 807,000		Volume (m ³)	13.12
		Height (m)	5.50
		Radius (m)	0.87
		Wall thickness (mm)	87.90
		Cost of catalyst (CAD)/ kg feed	66
		Total cost of reactor (s) (CAD)	3,326,000
Total cost (CAD)^a		4,000,000	

^a Cost calculated at year 2019 and Fort McMurray, AB, Canada for location

Table G.5 Summary of cost and design evaluation for treatment plant using asphaltenes at 250 °C

Process:		Treatment with asphaltenes at 250 °C			
Total flowrate (kg/h):		10,495			
Naphtha flowrate (kg/h):		10,000			
Asphaltene flowrate (kg/h):		495			
Heat exchanger		Reactor		Flash	
T _{in} (°C)	25	# of reactors	1	Residence time (h)	0.33
T _{out} (°C)	250	Residence time (h)	24		
Q _{required} (kJ/h)	6,607,000	Pressure (MPa)	6	Pressure (MPa)	0.44
Area (m ²)	80	Volume (m ³)	305	Volume (m ³)	4.2
Total cost of heat exchanger (CAD) 171,000		Height (m)	15.00	Height (m)	3.7
		Radius (m)	2.50	Radius (m)	0.6
		Wall thickness (mm)	237.00	Wall thickness (mm)	6.87
		Total cost of reactor (s) (CAD)	10,678,000	Total cost of flash (CAD)	69,700
		Total cost (CAD)^a		11,000,000	

^a Cost calculated at year 2019 and Fort McMurray, AB, Canada for location

Table G.1 Summary of cost and design evaluation for treatment plant using asphaltenes at 350 °C

Process:		Treatment with asphaltenes at 350 °C			
Total flowrate (kg/h):		10,615			
Naphtha flowrate (kg/h):		10,000			
Asphaltene flowrate (kg/h):		615			
Furnace		Reactor		Flash	
T _{in} (°C)	25	# of reactors	1	Residence time (h)	0.33
T _{out} (°C)	350	Residence time (h)	3	Pressure (MPa)	0.44
Q _{required} (kJ/h)	9,600,000	Pressure (MPa)	7	Volume (m ³)	4.2
Total cost of furnace (CAD)	916,000	Volume (m ³)	40	Height (m)	4
		Height (m)	8.00	Radius (m)	0.6
		Radius (m)	1.30	Wall thickness (mm)	6.27
		Wall thickness (mm)	148.00		
		Total cost of reactor (s) (CAD)	2,726,000	Total cost of flash (CAD)	74,500
Total cost (CAD)^a		4,000,000			

^a Cost calculated at year 2019 and Fort McMurray, AB, Canada for location